

Design, Synthesis and Application of 1,2-Dihydropyridines, Dibenzoxazepines and Diindolylmethanes

**THESIS SUBMITTED TO AcSIR FOR THE AWARD OF THE DEGREE
OF DOCTOR OF PHILOSOPHY
IN CHEMICAL SCIENCES**



By

JAMSHEENA V.

Register Number: 10CC14J39003

Under the guidance of

Dr. Ravi Shankar Lankalapalli



Organic Chemistry Section

Chemical Sciences and Technology Division

CSIR–National Institute for Interdisciplinary Science and Technology

(CSIR–NIIST)

Thiruvananthapuram-695 019, Kerala

July 2019

Dedicated to My Parents,
Family Members and
Teachers

DECLARATION

I hereby declare that the Ph.D. thesis entitled “**Design, Synthesis and Application of 1,2-Dihydropyridines, Dibenzoxazepines and Diindolymethanes**” is an independent work carried out by me under the supervision of **Dr. Ravi Shankar Lankalapalli** at the Organic Chemistry Section, CSTD, CSIR-NIIST, Thiruvananthapuram and it has not been submitted anywhere else for any other degree or diploma.

In keeping the general practice of reporting scientific observations, due acknowledgement has been made wherever the work described is based on the findings of other investigators.


24/01/19
Jamsheena V.

NATIONAL INSTITUTE FOR INTERDISCIPLINARY SCIENCE AND TECHNOLOGY
Council for Scientific and Innovative Research (CSIR)
Industrial Estate P.O., Pappanamcode, Thiruvananthapuram-695019
Kerala, India



Dr. Ravi Shankar Lankalapalli
Senior Scientist, Organic Chemistry Section
Chemical Sciences and Technology Division

Tel: 91- 471- 2515317
E-mail: ravishankar@niist.res.in

CERTIFICATE

This is to certify that the work incorporated in this Ph.D. thesis entitled “**Design, Synthesis and Application of 1,2-Dihydropyridines, Dibenzoxazepines and Diindolylmethanes**” submitted by **Ms. Jamsheena V.** to Academy of Scientific and Innovative Research (AcSIR) in fulfillment of the requirements for the award of the Degree of Doctor of Philosophy in Chemical Sciences, embodies original research work under my supervision/guidance. I further certify that this work has not been submitted to any other University or Institution in part or full for the award of any degree or diploma. Research material obtained from other sources has been duly acknowledged in the thesis. Any text, illustration, table, etc. used in the thesis from other sources have been duly cited and acknowledged.


24/07/19
Jamsheena V

(Student)


24/07/19
Dr. Ravi Shankar Lankalapalli

(Thesis Supervisor)

Thiruvananthapuram

July, 2019

ACKNOWLEDGEMENTS

*First and foremost, I take immense pleasure and privilege to express my heartfelt gratitude to my research supervisor **Dr. Ravi Shankar Lankalapalli**, Chemical Science and Technology Division, CSIR-National Institute for Interdisciplinary Science and Technology (NIIST), Trivandrum, who has been a true inspiration. Throughout my period of work at NIIST, he provided encouragement, sound advice, and full freedom to work. He was the embodiment of patience and diligence and I consider myself extremely fortunate to have him as my guide.*

I am grateful to Dr. A. Ajayaghosh, Director, CSIR-NIIST and former Directors Dr. Suresh Das and Dr. Gangan Prathap for providing the laboratory facilities to carry out the research work.

It is my privilege to place on record my gratitude towards Dr. P. Sujatha Devi (present), Dr. R. Luxmi Varma (former) Head, Chemical Sciences and Technology Division for allowing me to freely use the available facilities at the division and for all the timely help and advice provided.

My special thanks to our collaborators, Dr. P. Jayamurthy, Dr. S. Priya, Dr. Dileep Kumar B. S. of APT division for biological evaluation of the synthesized molecules and Dr. Rakesh K. Mishra for helping me with photophysical characterization of the compounds.

My research work would have been incomplete if it were not for the timely advice and criticism given by Dr. R. Luxmi Varma, Dr. K. V. Radhakrishnan and Dr. K. G. Raghu who formed the Doctoral Advisory Committee (DAC).

I would like to acknowledge Dr. C. H. Suresh (present), Dr. R. Luxmi Varma (former) and Dr. Mangalam S. Nair (former), AcSIR programme coordinators at CSIR-NIIST for their timely help and advice for the academic procedures of AcSIR.

I would like to acknowledge Dr. K. V. Radhakrishnan, Dr. A. Kumaran, Dr. Kaustabh Kumar Maiti, Dr. B. S. Sasidhar, Dr. Sunil Varughese and Dr. D. Shridevi, Scientists of Organic Chemistry Section for the encouragement and support.

I thank Dr. A. Sundaresan, Mr. M. M. Sreekumar, Dr. B. S. Dileep Kumar and Dr. K. G. Raghu for their necessary help and for allowing me to carry out my work at the Agro-processing and Technology Division.

I like to thank and Dr. Jubi John of organic section for his fruitful discussion and Dr. Nibin. M. Joy for his help in conducting some of the reactions.

I would like to acknowledge Dr. Aneesh E. M. and Anoopkumar A. N., Communicable Disease Research Laboratory, St. Joseph's College of Irinjalakuda for their support and help in completion of CSIR-800 project.

I express my thanks to Dr. S. Sini, Dr. R. Dhanya, Dr. G. Shilpa, Taniya M. S., A. R. S. Jesmina and Gopika V. K., for their help and support for the biological study.

I would like to extend special thanks to Dr. G. Jaggaiah Naidu, Dr. C. H. Chandrasekhar, my seniors and Ms. Veena K. S., Ms. Jaice Raveendran, Mr. Arun Kumar T., Mr. Mahesha C. K., Mr. Krishnakumar K. A., Ms. Geethanjali, Mr. Vikas for their enormous love and affection during my stay at NIIST and also for their assistance in conducting some of the reactions.

I would like to thank Dr. Sunil Varughese, for providing X-ray crystal structures. I thank Ms. Saumini Mathew, Mr. Saran P. Raveendran, Mr. Syam and Mr. Rakesh Gokul for recording NMR spectra. Thanks are also due to Ms. S. Viji and Ms. Aathira for mass spectral analysis.

I would like to thank all the scientific, administrative and supporting staff and other members of the NIIST family for their help, co-operation and facilities provided.

I would like to extend my thanks to Dr. Shyni G. L., Mr. Syam Nath, Ms. Habeeba, Ms. Jubi Jacob, Dr. Sithara Thomas, Ms. Anagha of APT division for their companionship and great support. I like to thank Sumitha Paul, Afeefa Ummer, Dr. Greeshma Gopalan, Dr. Fathimath Salfeena, Ms. Sreedevi, Ms. Alisha of CSTD for their companionship. I would like to thank our lab M.Sc project students Ms. Nissy, Ms. Shruthi and Ms. Kalyani for their active involvement in completion of some of my projects.

The JRF and SRF fellowship received from Council of Scientific & Industrial Research (CSIR), New Delhi, India is duly acknowledged and appreciated. Academy of Scientific and Innovative Research (AcSIR), India, is duly acknowledged for enrolling me into their PhD programme.

I would like to extend my sincere thanks to all my friends at CSIR-NIIST who made me to smile every day and also for sharing my happy moments.

Last but not least I am most thankful for my family members and teachers for their encouragement and unconditional love and support. I thank my mother (Beevi kutty), father (Mohammed kutty), husband (Ishaque M), sisters, brother, in-laws and all my family members for their unquestionable faith and trust.

Jamsheena V

CONTENTS

	Page No.
DECLARATION	i
CERTIFICATE	iii
AKNOWLEDGEMENT	v
CONTENTS	vii
List of Figures	x
List of Schemes	xii
List of Tables	xiii
Abbreviations	xiv
Chapter-1: Introduction	1
1.1 A brief introduction to heterocyclic compounds	1
1.1.1 Application of heterocyclic compounds	3
1.1.1A Biological importance	4
1.1.1Aa. Antibacterial activity	4
1.1.1Ab. Antifungal activity	5
1.1.1Ac. Analgesic and Anti-inflammatory activity	6
1.1.1Ad. Heterocycles against parasitic diseases	7
1.1.1Ae. Antiviral agents	8
1.1.1Af. Anticancer agents	9
1.1.1Ag. Heterocycle used to cure brain and heart related problems	10
1.1.1B. Agricultural importance	10
1.1.1C. Heterocycles in industry and technology	11
1.2. A brief history of 1,2-dihydropyridines	11
1.2.1. Importance of dihydropyridines	13
1.2.1A. 1,4-DHP	13
1.2.1B. 1,2-DHP	14
1.2.2. Synthetic routes to 1,2-DHP	17
1.3. A brief history of dibenzoxazepines and dibenzoxazepinones	29
1.3.1. Importance of dibenzoxazepines and dibenzoxazepinones	30
1.3.2. Synthetic routes to dibenzoxazepines and dibenzoxazepinones	32
1.4. A brief history of Diindolylmethanes (DIMs)	37
1.4.1 Importance of DIMs	37
1.3.2. Synthetic routes to DIMs	40
1.5. Conclusion and present work	45
1.6. References	46
Chapter-2: New 1,2-Dihydropyridine Based Fluorophores and Their Applications as Fluorescent Probes	75
2.1. Abstract	75
2.2. Introduction	75
2.3. Results and discussions	78

2.3.1. Synthesis	78
2.3.2. Photophysical properties	82
2.3.3. Application	85
2.4. Conclusion	92
2.5. Experimental section	92
2.5.1. General experimental methods	92
2.5.2. General procedure for the synthesis of 1,2-DHP 4a-4i	93
2.5.3. General procedure for the synthesis of hydrazone	
2.5.4. General procedure for the synthesis of 1,2-DHPs 5a-5g	93
2.5.5. Procedure for the synthesis of 1,2-DHP 5h	94
2.5.6. Procedure for the synthesis of 1,2-DHP 5h'	94
2.5.7. Procedure for the synthesis of 1,2-DHP 5j	95
2.5.8. Cellular studies	95
2.5.8A. Cell culture and treatment	95
2.5.8B. Cell viability study of 1,2 DHPs 5h and 5h' on L6 myoblast	95
2.5.8C. Preparation of cell lysate	96
2.5.8D. Cell viability on HeLa Cell	96
2.5.8E. Co-Localization study of 1,2-DHPs with MitoTracker CMXRos	96
2.5.9. Spectral details of products	96
2.6. References	108
Chapter-3: Metal-Free Diaryl Etherification of Tertiary Amines by <i>Ortho</i> -C(sp ²)-H Functionalization for Synthesis of Dibenzoxazepines and -ones	113
3.1. Abstract	113
3.2. Introduction	113
3.3. Results and discussions	117
3.4. Conclusion	126
3.5. Experimental section	126
3.5.1. General information	126
3.5.2. General procedure for the synthesis of tertiary amine 1b	127
3.5.3. General procedure for the synthesis of dibenzoxazepine 3b	127
3.5.4. General procedure for the synthesis of dibenzoxazepinone 4c	128
3.5.5. 10-(2-methoxy-5-nitrobenzyl)-7-methyl-10,11-dihydrodibenzo[b,f][1,4]oxazepine (3al')	128
3.5.6. N-(tert-butyl)-7,10-dimethyl-2-nitro-10,11-dihydrodibenzo[b,f][1,4]oxazepine-11-carboxamide (23)	128
3.5.7. 2-(5-formyl-2-(methylamino)phenoxy)-5-nitrobenzaldehyde (24)	129
3.5.8. 2-((2-hydroxy-4-methylphenyl)(methyl)amino)-5-nitrobenzaldehyde (25)	129
3.5.9. 2-(methyl(4-methyl-3,6-dioxocyclohexa-1,4-dien-1-yl)amino)-5-nitrobenzaldehyde (26)	129
3.5.10. 2,10-dimethyl-7-nitro-9,10-dihydroacridin-4-ol (27)	130
3.5.11. 7-ethyl-10-methyl-5-tosyl-10,11-dihydro-5H-dibenzo[b,e][1,4]diazepine (29)	130
3.5.12. Spectral details of products	130

3.6. References	155
Chapter-4: Design, Synthesis and Cytotoxicity Evaluation of Diindolylmethane Conjugates of Biaryls and Diaryl ethers	161
4.1. Abstract	161
4.2. Introduction	161
4.3. Results and discussions	166
4.3.1. Synthesis of DIM-ortho-biaryls (DIM) 2a-2l	166
4.3.2. Cytotoxic effects of DIM- 2a-2l	167
4.3.3. Morphological analysis by phase contrast microscopy	168
4.3.4. Synthesis of diindolylmethane conjugates of biaryl/diaryl ethers	171
4.3.5. Antiproliferative activity of DIM conjugates of biaryl/diaryl ethers 3a-3o and 4a-4p	174
4.4. Conclusions	178
4.5. Experimental section	178
4.5.1. General information	178
4.5.2. Procedure for the synthesis of di(1H-indol-3-yl)methane (1)	179
4.5.3. General procedure for the synthesis of biaryl conjugated DIM (2a-2l)	179
4.5.4. General procedure for the synthesis of biaryl conjugated DIM (3a-3o)	179
4.5.4A. 4-Hydroxycinnamaldehyde (5)	179
4.5.4B. 4-Acetylcinnamaldehyde (6)	179
4.5.4C. Diethyl 4'-acetoxyl-6-formyl-[1,1'-biphenyl]-2,4-dicarboxylate (7)	180
4.5.4D. Diethyl 6-formyl-4'-hydroxy-[1,1'-biphenyl]-2,4-dicarboxylate (8)	180
4.5.4E. Diethyl 6-(di(1H-indol-3-yl)methyl)-4'-hydroxy-[1,1'-biphenyl]-2,4-dicarboxylate (3a-3o)	180
4.5.5. Diethyl 4'-(2-((tert-butoxycarbonyl)amino)ethoxy)-6-(di(1H-indol-3-yl)methyl)-[1,1'-biphenyl]-2,4-dicarboxylate (9)	180
4.5.6. Diethyl 4'-(2-aminoethoxy)-6-(di(1H-indol-3-yl)methyl)-[1,1'-biphenyl]-2,4-dicarboxylate (3aa)	181
4.5.7. N-benzyl-2-(2-(di(1H-indol-3-yl)methyl)phenoxy)-4-fluoroaniline (12)	181
4.5.8. 2-(2-(di(1H-indol-3-yl)methyl)phenoxy)-4-fluoroaniline (4)	181
4.5.9. Cell Culture and Cytotoxicity Studies	181
4.5.10. Morphological analysis by phase contrast microscopy	182
4.5.11. Spectral details of products	183
4.6. References	204
Summary and conclusion	211
List of publications	214

List of Figures

Sl. No		Page No.
1	Figure 1.1A. Examples of aliphatic and aromatic heterocycles	1
2	Figure 1.1B. History of heterocyclic chemistry	3
3	Figure 1.1C. Examples of marketed antibacterial drugs	5
4	Figure 1.1D. Representative examples of antifungal drugs in current use	6
5	Figure 1.1E. Examples of analgesic and anti-inflammatory drugs	7
6	Figure 1.1F. Some of the heterocyclic molecules having anti-parasitic activity	8
7	Figure 1.1G. Examples of antiviral drugs	8
8	Figure 1.1H. Examples of anticancer drugs	9
9	Figure 1.1I. Examples of drugs used for brain and heart related problems	10
10	Figure 1.1J. Some of the currently marketed agrochemicals	11
11	Figure 1.1K. Heterocycles used in industry and technology	12
12	Figure 1.2A. Reductive cofactor NADH (26), antihypertensive drug nifedipine (27) and possible isomeric structures of DHP (28-32)	13
14	Figure 1.2B. 1,4-DHP containing calcium channel blockers available in the market	14
15	Figure 1.3A. a) benzene fused seven-membered heterocyclic scaffolds. b) Isosteric replacement of phenothiazine.	30
16	Figure 1.3B. Isomeric forms and pharmacologically active dibenzoxazepines	32
17	Figure 1.4A. Structure of DIM, I3C along with biologically active DIM derivatives	39
18	Figure 1.4B. DIM isolated from natural sources	40
19	Figure 2.1. The design of 1,2-dihydropyridine based fluorophore	75
20	Figure 2.2A. Examples of 1,2- and 1,4-DHP fluorescent molecules	76
21	Figure 2.2B. Design strategy of the <i>N</i> -benzylideneamine appended 1,2-DHP based fluorophore	77
22	Figure 2.3A. Absorption and emission ($\lambda_{ex} = 430$ nm) spectra of 1,2-DHPs in MeOH at room temperature. a) 5a , b) 5b , c) 5c , and d) 5d	84
23	Figure 2.3B. Absorption and emission ($\lambda_{ex} = 430$ nm) spectra of 1,2-DHPs in MeOH at room temperature. e) 5e , f) 5f , and g) 5g .	85
24	Figure 2.3C. Cytotoxicity assessed by MTT assay in HeLa cells.	86
25	Figure 2.3D. Fluorescent images of HeLa cells a) treated with 1,2-DHPs 5b , 5d and 5g for 10 min, b) MitoTracker red CMXRos	86
26	Figure 2.3E. Absorption and emission spectral profile (normalized) of a) 1,2-DHP 5h and b) 1,2-DHP 5h' in methanol and Hepes buffer	88
27	Figure 2.3F. Energy minimized structure	88
28	Figure 2.3G. Photostability of 1,2-DHP 5h' .	89
29	Figure 2.3H. a) Cytotoxicity of 1,2-DHPs 5h and 5h' in L6 myoblast by MTT assay at different concentrations.	90
30	Figure 2.3I. Changes in the fluorescence intensity of 1,2-DHP 5h in presence various biologically important metal ions	91
31	Figure 2.3J. Changes in the fluorescence intensity of 1,2-DHP 5h' (10 μ M) at different pH (5 to 8).	91

32	Figure 2.5A. ¹ H and ¹³ C NMR Spectra of 4b	98
33	Figure 2.5B. ¹ H and ¹³ C NMR Spectra of 5a	102
34	Figure 2.5C. ¹ H and ¹³ C NMR spectrum of 1,2-DHP 5h	105
35	Figure 2.5D. ¹ H and ¹³ C NMR spectrum of 1,2-DHP 5h'	106
36	Figure 2.5E. ³¹ P NMR spectrum of 1,2-DHP 5h'	107
37	Figure 3.1A. Synthesis of diaryl ether from tertiary amine	113
38	Figure 3.2A. Pharmacologically active dibenzoxazepines	114
39	Figure 3.3A. ORTEP diagram of diaryl ether 2a	119
40	Figure 3.5A. ¹ H and ¹³ C-NMR of diaryl ether 2a	131
41	Figure 3.5B. ¹ H and ¹³ C-NMR of 3b	132
42	Figure 3.5C. ¹ H and ¹³ C-NMR of 4c	144
43	Figure 3.5D. ¹ H and ¹³ C-NMR of 23	147
44	Figure 3.5E. ¹ H and ¹³ C-NMR of 24	148
45	Figure 3.5F. ¹ H and ¹³ C-NMR of 25	149
46	Figure 3.5G. ¹ H and ¹³ C-NMR of 26	152
47	Figure 3.5H. ¹ H and ¹³ C-NMR of 27	153
48	Figure 3.5I. ¹ H and ¹³ C-NMR of 29	154
49	Figure 4.2A. Molecular targets of DIM-1	162
50	Figure 4.2B. Representative biaryl structural motifs	164
51	Figure 4.2C. Basic skeleton of DIM biaryl motifs	165
52	Figure 4.3A. Structures of DIM- <i>ortho</i> -biaryls (DIM) 2a-2l	166
53	Figure 4.3B. Morphology of HeLa and H9C2 cells treated with DIM- 2a and 2d	169
54	Figure 4.3C. Morphology of MDA-MB-231 and H9C2 cells treated with DIM- 2a and 2d	170
55	Figure 4.3D. Basic skeleton of the biaryl and diaryl ether conjugated DIMs	171
56	Figure 4.3E. Structures of biaryl conjugated DIMs 3a-3o	173
57	Figure 4.3F. Structures of diaryl ether conjugated DIMs 4a-4p .	175
58	Figure 4.3G. Morphology of MDA-MB-231 and L6 cells treated with DIM- 3aa	178
59	Figure 4.5A. ¹ H and ¹³ C-NMR of DIM-1	183
60	Figure 4.5B. ¹ H and ¹³ C-NMR of DIM-2a	184
61	Figure 4.5C. ¹ H and ¹³ C-NMR of DIM-2d	186
62	Figure 4.5D. ¹ H and ¹³ C-NMR of DIM-3a	191
63	Figure 4.5E. ¹ H and ¹³ C-NMR of DIM-3aa	197
64	Figure 4.5F. ¹ H and ¹³ C-NMR of DIM-4a	198

List of Schemes

Sl. No		Page No.
1	Scheme 1.2.1. Transformation of 1,2-DHP to pyridine, piperidine, pyridones and its utility	15
2	Scheme 1.2.2. Transformation of 1,2-DHP to azepines and 1,2-DHP in D-A synthesis of isoquinuclidine and its utility	16
3	Scheme 1.2.3. Synthesis of pyridocarbazole alkaloids (olivacine and guatambuine), (\pm)-elaeokanine A and R-(-)-coniine using 1,2-DHP derivatives	17
4	Scheme 1.2.4. Synthetic routes to 1,2-DHP 51-62	18
5	Scheme 1.2.5. Synthetic routes to DHP 63-72	20
6	Scheme 1.2.6. Synthetic routes to DHP 75-84	21
7	Scheme 1.2.7. Synthetic routes to 1,2-DHP 86-96	22
8	Scheme 1.2.8. Synthetic routes to 1,2-DHP 99-108	23
9	Scheme 1.2.9. Synthetic routes to 1,2-DHP 110-119	24
10	Scheme 1.2.10. Synthetic routes to 1,2-DHP 121-132	26
11	Scheme 1.2.11. Synthetic routes to 1,2-DHP 134-147	27
12	Scheme 1.2.12. Synthetic routes to 1,2-DHP 151-171	29
13	Scheme 1.3.1. Synthetic routes to dibenzoxazepines 182-191	33
14	Scheme 1.3.2. Synthetic routes to dibenzoxazepines 194-201	34
15	Scheme 1.3.3. Synthetic routes to dibenzoxazepines 204-211	35
16	Scheme 1.3.4. Synthetic routes to dibenzoxazepines 215-218'	36
17	Scheme 1.4.1. Synthetic routes to DIM 231-241	41
18	Scheme 1.4.2. Synthetic routes to DIM 244-252	42
19	Scheme 1.4.3. Synthetic routes to DIM 255-264	43
20	Scheme 1.4.4. Synthetic routes to DIM 267-279	44
21	Scheme 2.3.1. Synthesis of <i>N</i> -phenyl (4) and <i>N</i> -benzylideneamine (5) appended 1,2-DHP	79
22	Scheme 2.3.2. Synthesis and ORTEP diagram of 4-nitrophenyl ester of 1,2-DHP 5j	79
23	Scheme 2.3.3. Synthesis of tetracyclic 1,2-DHP 4j' and synthesis of 1,2-DHP 5h'	82
24	Scheme 3.2.1. Strategies for dibenzoxazepinone	115
25	Scheme 3.2.2. HIR mediated intramolecular cyclisation and diaryl etherification	116
26	Scheme 3.3.1. Control experiments	123
27	Scheme 3.3.2. Plausible mechanistic pathway	124
28	Scheme 3.3.3. Demonstration of applicability of methodology	125
29	Scheme 3.5.1. Synthesis of tertiary amines via double reductive amination	127
30	Scheme 4.2.1. Formation of DIM-1 from I3C	162
31	Scheme 4.3.1. Synthesis of biaryl conjugated DIMs 3a-3o and DIM- 3aa	172
32	Scheme 4.3.2. Synthesis of diaryl ether conjugated DIMs 4a-4p	174

List of Tables

Sl. No		Page No.
1	Table 2.3.1. <i>N</i> -benzylideneamine appended 1,2-DHP fluorophores 5a-5h' by four-component condensation reaction ^a	80
2	Table 2.3.2. <i>N</i> -phenyl 1,2-DHP fluorophores 4a-4h' by three-component condensation reaction	81
3	Table 2.3.3. Photophysical characterization of <i>N</i> -phenyl 1,2-DHPs 4a-4j'	82
4	Table 2.3.4. Photophysical characterization of 1,2-DHP 5a-5h'	83
5	Table 3.3.1. Optimization of reaction conditions	118
6	Table 3.3.2. Substrate scope for dibenzoxazepine	120
7	Table 3.3.3. Substrate scope for dibenzoxazepinone	122
8	Table 4.3A. Evaluation of cytotoxicity of DIM- 2a-2l in HeLa, MDA-MB-231 and H9C2	168
9	Table 4.3B. Cytotoxic activity of DIM derivatives on MDA-MB-231 cell line	176
10	Table 4.3C. Cytotoxic activity of DIM derivatives on L6 cell line	177

ABBREVIATIONS

^1H NMR	Proton nuclear magnetic resonance
^{13}C NMR	Carbon-13 nuclear magnetic resonance
4CR	Four-Component Reaction
Å	Angstrom
Ac	Acetyl
AIDS	Acquired Immune Deficiency Syndrome
AM	Alloxan monohydrate
ANO	Ammonium niobium oxalate
aq	aqueous
Ar	Aryl
AuCl	Gold(I) chloride
BCA	Bicinchoninic acid
BINAM	1,1'-Bi(2-naphthylamine)
Bn	Benzyl
BnOCOCI	Benzyl chloroformate
Boc	<i>t</i> -Butoxycarbonyl
calcd	Calculated
Cat	Catalytic
CCDC	The Cambridge Crystallographic Data Centre
CNS	Central nervous system
CO	Carbon monoxide
COX	Cyclooxygenase
d	doublet
DBU	1,8-Diazabicyclo[5.4.0]undec-7-ene
DCE	Dichloethane
DCM	Dichloromethane
dd	doublet of doublet
DDQ	2,3-Dichloro 5,6-dicyano 1,4-benzoquinone
DFT	Density Functional Theory
DHP	Dihydropyridine
DIM	Diindolylmethane
DMA	Dimethylacetamide
DMAP	4-(Dimethylamino) pyridine
DMAPh	4-(Dimethylamine)-4-phenyl
DME	Dimethoxyethane
DMEM	Dulbecco's Modified Eagle's Medium
DMF	Dimethylformamide
DMP	Dess-Martin periodinane
DMSO	Dimethyl sulfoxide
DNA	Deoxyribonucleic acid
dppp	1,3-Bis(diphenylphosphino)propane

e.g	example
EDG	Electron donating group
equiv	equivalent
ESI	Electrospray ionization
Et	Ethyl
EtOAc	Ethyl Acetate
EtOH	Ethanol
GI ₅₀	Growth inhibition of 50 percentage of cells
GLUT4	Glucose transporter type 4
h	hour
HCl	Hydrochloric acid
HDAC	Histone Deacetylases
HFIP	1,1,1,3,3,3-hexafluoro-2-propanol
HIR	Hypervalent Iodine Reagent
HIV	Human immunodeficiency virus
HMBC	Heteronuclear multiple bond correlation spectroscopy
HRMS	High resolution mass spectrometry
I3C	Indole-3-carbinol
IBX	2-Iodoxybenzoic acid
IC ₅₀	Inhibition concentration 50%
ICT	Intramolecular charge transfer
IUPAC	International Union for Pure and Applied Chemistry
KHMDS	Potassium bis(trimethylsilyl)amide
m	multiplet
<i>m/z</i>	Mass to charge ratio
<i>m</i> -CPBA	<i>meta</i> -Chloroperoxybenzoic acid
Me	Methyl
MeOH	Methanol
MHz	Megahertz
mM	Millimolar
mmol	Millimole
MS	Molecular sieves
MsCl	Methanesulfonyl chloride
MTT	3-(4,5-Dimethylthiazol-2-yl)-2,5-diphenyltetrazolium bromide
MW	Microwave
n.d	not detected
NADH	Nicotinamide adenine dinucleotide
NBS	N-Bromosuccinimide
NIS	<i>N</i> -Iodosuccinimide
nm	nanometer
NMR	Nuclear magnetic resonance
NSAIDs	Non-steroidal anti-inflammatory drugs
OLED	Organic light-emitting diodes

OMe	Methoxy
PCC	Pyridinium chlorochromate
Ph	Phenyl
PIDA	Phenyliodine diacetate
ppm	Parts per million
PTA	Phosphotungstic Acid
PTPs	Protein tyrosine phosphatases
<i>p</i> -TsOH	<i>p</i> -Toluenesulfonic acid
q	quartet
R _f	Retention factors
RNA	Ribonucleic acid
rt	room temperature
s	singlet
SAR	Structure–activity relationship
S _N Ar	Nucleophilic aromatic substitution
t	triplet
TBHP	Tert-butyl hydroperoxide
<i>t</i> -Bu	Tert-butyl
TCAs	Tricyclic antidepressant drugs
TCSPC	Time-correlated single photon counting
td	triplet of doublet
TEMPO	(2,2,6,6-Tetramethylpiperidin-1-yl)oxyl
TFA	Trifluoroacetic acid
TFAA	Trifluoroacetic anhydride
THF	Tetrahydrofuran
TLC	Thin layer chromatography
TMEDA	Tetramethylethylenediamine
TMS	Trimethylsilyl
TNBC	Triple-negative breast cancer
Tp ^{Br3}	hydrotrispyrazolylborate ligand
TRPA1	Transient receptor potential ankyrin 1
Ts	Tosyl
U-4CR	Ugi four-component reaction
UV	Ultraviolet

Chapter-1

Introduction

1.1 A brief introduction to heterocyclic compounds

Heterocyclic compounds, generally called heterocycles, are a major class of organic compounds in which one of the constituent members should be heteroatom and the IUPAC Gold Book describes them as “Cyclic compounds having as ring member atoms of at least two different elements, e.g., quinoline, 1,2-thiazole, bicyclo[3.3.1]tetrasiloxane”.¹ The prefix hetero- (from Greek heteros, meaning “other” or “different”) refers to the non-carbon atoms, or heteroatoms, in the ring, while the cyclic part (from Greek kyklos, meaning “circle”) of a heterocycle indicates that at least one ring structure is present in such a compound.² Nitrogen, oxygen, and sulfur are the most common heteroatoms present, but heterocycles with other heteroatoms are also widely reported. Heterocyclic compounds can be broadly classified into aliphatic and aromatic heterocycles. The aliphatic heterocycles are analogues of amines, ethers, thioethers, amides, *etc.* and the presence of ring strain mainly influences their properties. Aziridine **1**, oxirane **2**, thiirane **3**, azetidine **4**, oxetane **5**, thietane **6**, pyrrolidine **7**, tetrahydrofuran **8**, tetrahydrothiophene **9**, piperidine **10**, *etc.* are the common aliphatic heterocycles (Figure 1.1A). One of the rules governing the aromaticity of a heterocycle is Huckel's rule according to which any cyclic planar conjugated system having $4n+2$ π electrons are aromatic. Some of the examples include pyrrole **11**, furan **12**, thiophene **13**, imidazole **14**, pyrazole **15**, *etc.* (Figure 1.1A). According to the heteroatom present in the ring, heterocycles can also be classified as oxygen, nitrogen or sulphur based and within each class compounds are organized based on the size of the ring.

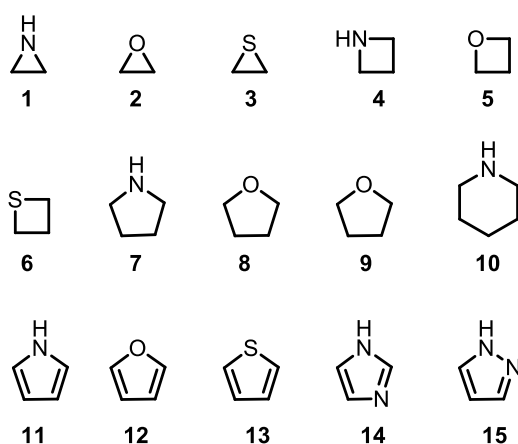


Figure 1.1A. Examples of aliphatic and aromatic heterocycles.

Heterocyclic chemistry is the branch of chemistry that deals exclusively with synthesis, properties and applications of heterocycles especially with those vital to drug design and accounts for nearly one third of the current publications in organic chemistry. In fact, two-thirds of organic compounds are heterocyclic in nature. Heterocyclic compounds are widely distributed in our nature and they are the major components of biological molecules essential to life; they play a crucial role in the metabolism of all living cells. Nucleotides, the building blocks of RNA and our genetic material DNA are also the derivatives of heterocyclic bases namely pyrimidines (adenine and guanine) and purines (cytosine, thymine, and uracil). Chlorophyll, the pigment required for photosynthesis and heme, the oxygen carrier in plants and animals are derivatives of the porphyrin ring. Essential diet ingredients such as thiamin (vitamin B1), riboflavin (vitamin B2), nicotinamide (vitamin B3), pyridoxine (vitamin B6) and ascorbic acid (vitamin C), *etc.* are heterocyclic compounds as well. Moreover, a large number of heterocyclic compounds, both synthetic and natural, are pharmacologically active and are in clinical use.

The history of heterocyclic chemistry started along with the development of organic chemistry in the early 1800s (Figure 1.1B). Compounds with aromatic heterocyclic rings are reported in the initial studies of organic chemistry. For example, Alloxan **16** was isolated by Brugnatelli from uric acid **17** in 1818.³ The other derivatives of uric acid, purines **18** and pyrimidines **19** were described in 1838 by Wöhler and Liebig, but the laboratory synthesis was reported only in the late 19th century.^{3,4} Meanwhile, furan **12** derivative, furfural **20** was isolated by Dobereiner in 1821 (published in 1832) by treating starch with sulphuric acid. Later in 1870, Perkin synthesized benzofuran **21** from coumarin **22**.³ The most commonly known nitrogen heterocycles, pyrrole **11** and pyridine **23** were discovered in 1850s in an oily mixture formed by strong heating of bones. At the same time, chemistry of the well-known benzopyrrole, Indole **24** began to develop along with the study of indigo dye **25**. Thiophene **13**, a frequent contaminant of the benzene was first discovered during the purification of benzene in 1882. In 1951, the role of heterocyclic compounds (purines **18** and pyrimidines **19**) in the genetic code was described by Chargaff's rules.

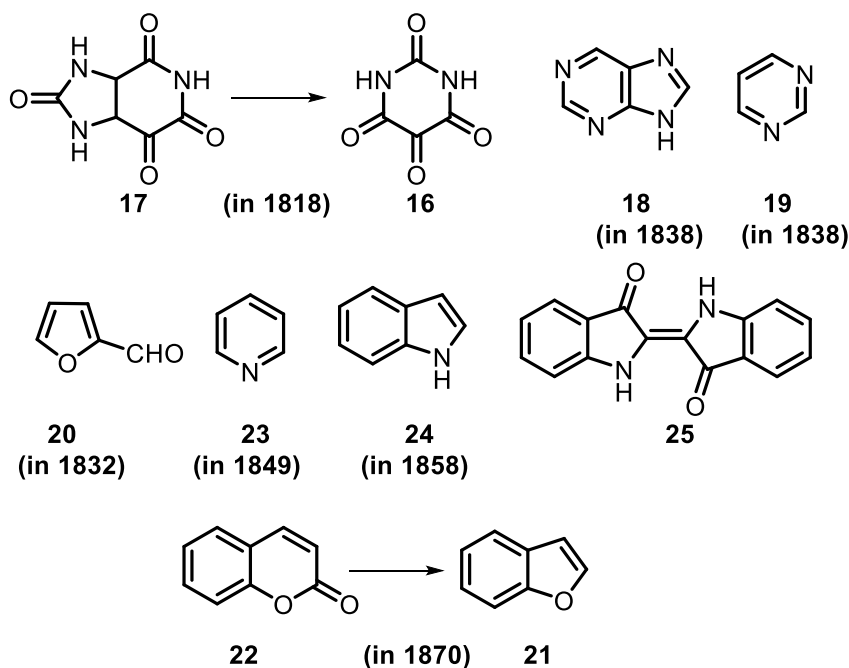


Figure 1.1B. History of heterocyclic chemistry.

1.1.1 Application of heterocyclic compounds

Heterocycles are one of the vital classes of organic compounds, and are present in wide varieties of drugs, vitamins, biomolecules, many natural products, and compounds with biological activities like antitumor, antibiotic, anti-inflammatory, antidepressant, antimalarial, *etc.*⁵ Also, they have been commonly found as a key structural unit in synthetic pharmaceuticals and agrochemicals. Most of the heterocycles possess important applications in materials science such as fluorescent sensor, brightening agents, dyestuff, information storage, plastics, analytical reagents, photographic materials and recorders of information. In addition, they have applications in supramolecular and polymer chemistry, especially in conjugated polymers. They are also used in food and cosmetic industry. Moreover, they act as organic conductors, semiconductors, molecular wires, photovoltaic cells, organic light-emitting diodes (OLEDs), light harvesting systems, optical data carriers, chemically controllable switches, and liquid crystalline compounds. Heterocycles are also of considerable interest because of their synthetic utility as synthetic intermediates, protecting groups, chiral auxiliaries, organocatalysts, and metal ligands in asymmetric synthesis, *etc.* Because of the enormous pharmacological and biological properties, substantial attention has been paid to develop new efficient methods to synthesize heterocycles.

1.1.1A Biological importance

For thousands of years, people extracted medicine from ‘nature’s own drugstore’, comprising sources such as leaves, fruits, barks, and herbs for curing diseases. It was later realized that the successful traditional treatments of this type were triggered by various heterocyclic compounds present in the extracts derived from plants, animals, and insects. Nowadays heterocycles are common structural units in many of the marketed drugs and medicinal chemistry targets in the drug discovery process.

In the recent years there has been growing interest in synthesizing heterocyclic compounds with excellent biological activity.^{5h,5i} Most of the heterocyclic compounds such as benzimidazole, quinazolines show potent anti-tumor activity, and some of them are pharmacologically active against life-threatening infections caused by pathogenic fungi on the immune system like cancer, AIDS, Ebola, *etc.* Heterocyclic compounds find wide variety of applications as therapeutic agents, especially as antibacterial and antifungal agents which show activity against certain viruses such as HIV. In addition, they also function as anticancer, antiulcer, antiallergic agents, *etc.*

1.1.1Aa. Antibacterial activity

Antibacterial drugs or antibiotics are substances that are active against bacteria and may either kill or suppress the growth of these organisms. They are either produced by microorganisms (antibiotics) or by chemical synthesis. In the late 19th century, Louis Pasteur commented on the observed antagonism between some bacteria, and suggested that it would offer great hope for therapeutics.⁶ The utilization of antibacterial agents in treating ailments started with the discovery of synthetic antibiotics derived from dyes.⁷ In 1907, Paul Ehrlich discovered a medicinally useful drug, the first synthetic antibacterial, salvarsan (arsphenamine) by screening hundreds of dyes against various organisms which was used to treat syphilis in the first half of the 20th century.⁸ Later in 1928, the first natural antibiotic penicillin was discovered by Alexander Fleming, and was successfully used to treat *Streptococcus* infection from 1942. The discovery of the first sulphonamide antibacterial drug, prontosil by the German pathologist Gerhard Domagk in 1932, opened the era of antibacterials.⁹

Heterocycles play a tremendous role in the development of potent antibacterial agents from the discovery of the first natural antibiotic penicillin, which is composed of a five-

membered thiazolidine ring and a four-membered azetidene nucleus in the form of β -lactam. It was found that the lack of the β -lactam ring structure can destroy the antibacterial activity of penicillin.¹⁰ Modifications on the penicillin nucleus led to the discovery of more successful drugs like imipenem, aztreonam, *etc.*¹¹ Moreover, the intensive research work demonstrated that modification on the first sulphonamide heterocyclic drug prontosil with the introduction of heterocyclic substituents markedly enhanced their biological activity. Later, a large number of antibacterial drugs came to the market which are of either natural origin or semi-synthetic derivatives or purely synthetic which includes quinolines, oxadiazoles, isoxazoles, thiazines, nitrofurans, *etc.*¹² Some of the representative antibacterial drugs are listed in the figure 1.1C.

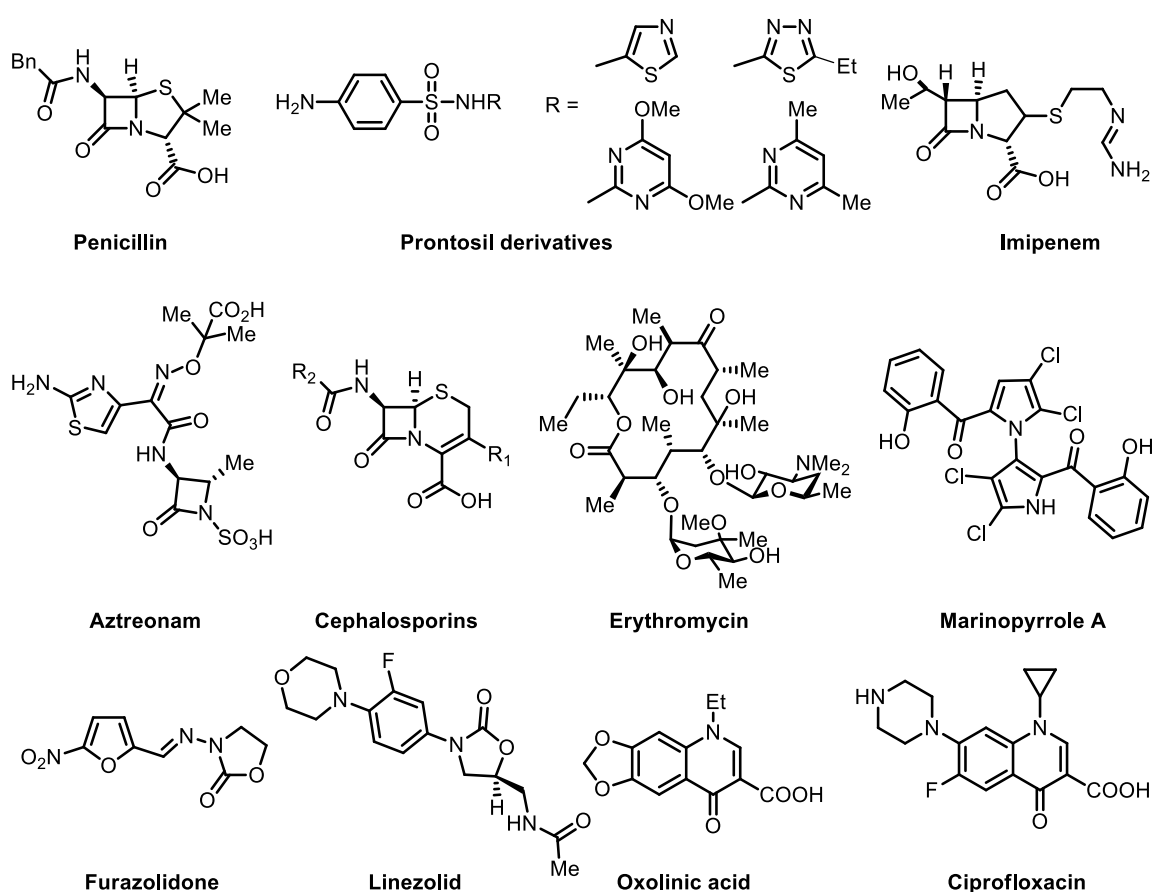


Figure 1.1C. Examples of marketed antibacterial drugs.

1.1.1Ab. Antifungal activity

Invasive, life-threatening fungal infections are devastating, particularly for immunocompromised patients. The antifungal drug discovery started with the use of Amphotericin B, a polyene, in 1958.¹³ Later, many heterocyclic compounds such as

polyenes, azoles, echinocandins, *etc.* emerged as potent antifungal drugs.¹⁴ Imidazole and 1,2,4-triazole are also one of the most important representative drug groups used as antifungal agents and some of them are listed in figure 1.1D.

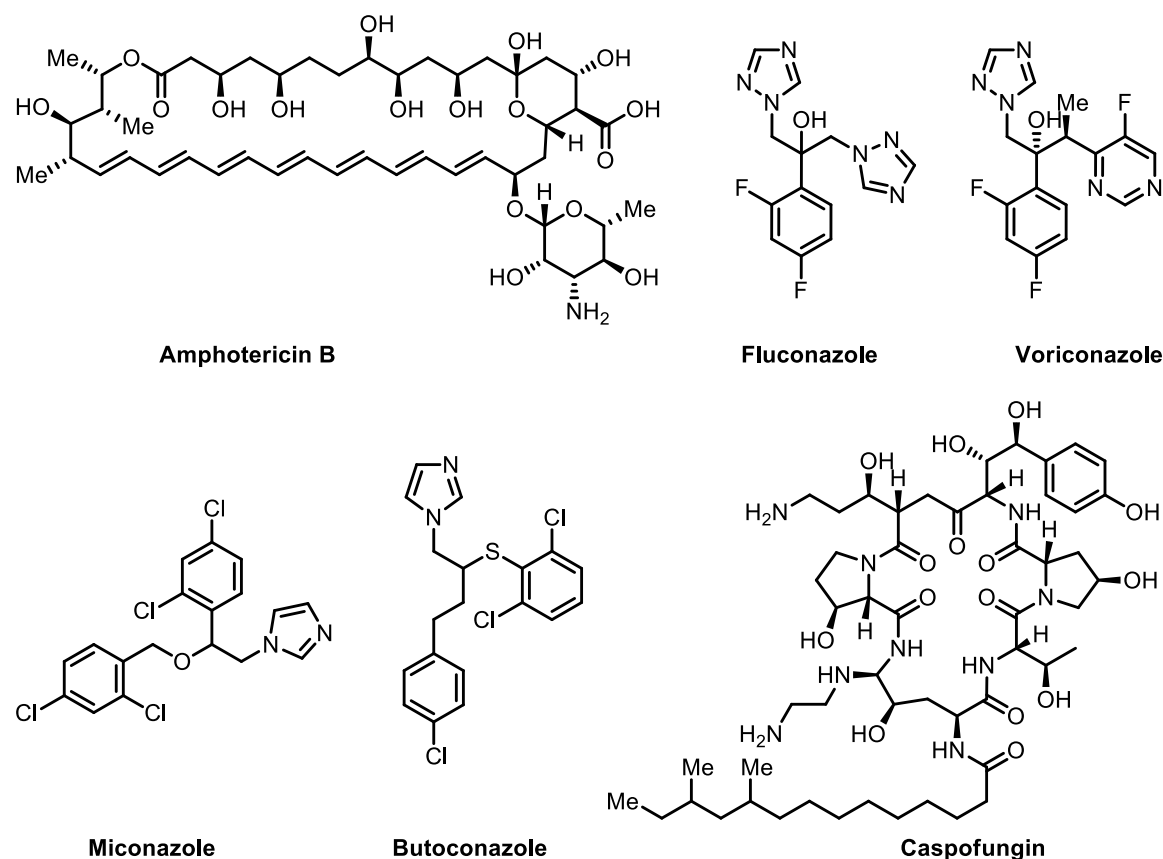


Figure 1.1D. Representative examples of antifungal drugs in current use.

1.1.1Ac. Analgesic and Anti-inflammatory activity

The anti-inflammatory nature is the property of a substance or treatment that reduces inflammation or swelling, and half of the anti-inflammatory drugs belong to the family of analgesics, remedying pain by reducing inflammation. They can be further classified into steroidal and non-steroidal anti-inflammatory drugs (NSAIDs), and the action of NSAIDs is to alleviate pain by counteracting the cyclooxygenase (COX) enzyme, either in a selective or non-selective manner. A number of NSAIDs such as indomethacin, ibuprofen, phenylbutazone, oxyphenbutazone, diclofenac, fenoprofen, carprofen, benoxaprofen, sulindac, and aspirin, *etc.* are available in the market. Heterocycles such as pyrimidine, pyridine, thiazole, triazole, *etc.* are well explored as anti-inflammatory agents, and they act either in a non-selective or selective manner.¹⁵ Analgesics are another

class of drugs that relieve pain. They can be divided into opioid and non-opioid drugs depending on the involvement of the opioid receptors located in the central nervous system. Majority of the recently introduced analgesic and anti-inflammatory drugs belongs to heterocyclic family and some of them are listed below (Figure 1.1E).¹⁶

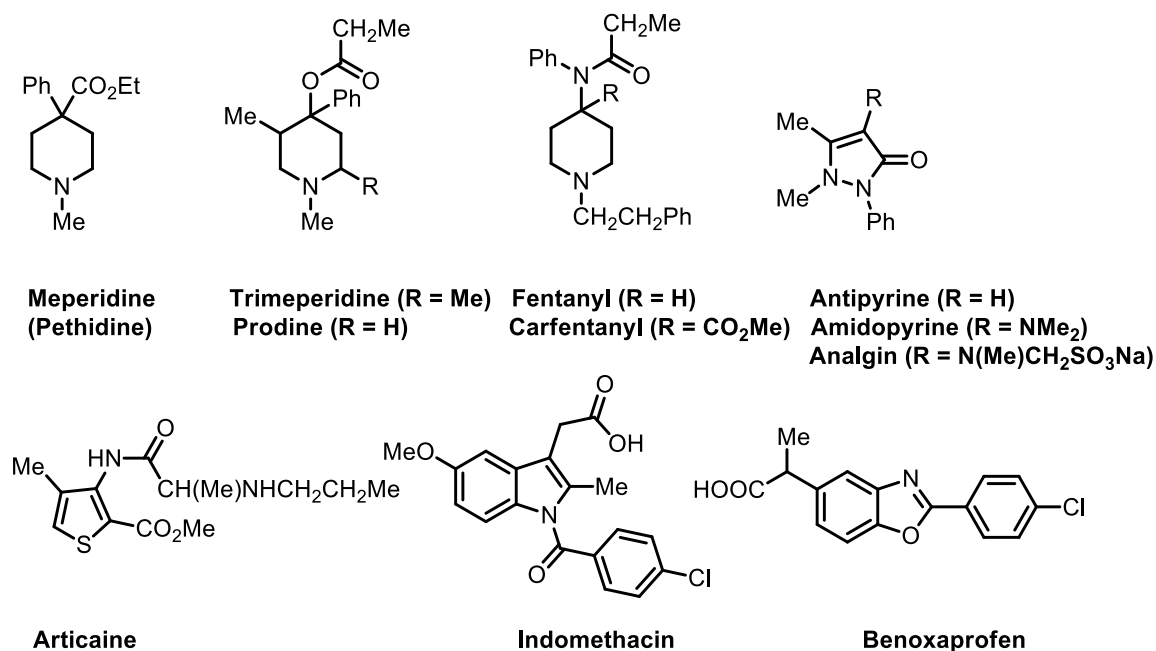


Figure 1.1E. Examples of analgesic and anti-inflammatory drugs.

1.1.1Ad. Heterocycles against parasitic diseases

Parasitic disease is an infectious disease which affects millions of people with a high mortality rate. Malaria, trypanosomiasis, leishmaniasis and chronic diarrhoea are the major parasitic diseases which pose an increasing threat to human health and welfare. These are caused by *Plasmodium*, *Trypanosoma*, *Leishmania*, and intestinal protozoa.¹⁷ The disclosure of the anti-malarial activity of quinines opened up a greater scope for the drug discovery against these parasites. Chloroquine, a quinine derivative is considered to be the third largest drug produced and consumed in the world. Nowadays the development of the genomic sequencing of parasitic organisms has helped in discovering new drug targets, which in turn has helped to design better, safer and effective drugs. Many heterocyclic compounds with different modifications are explored to have potential activity against parasites and some of them are listed in figure 1.1F.¹⁸

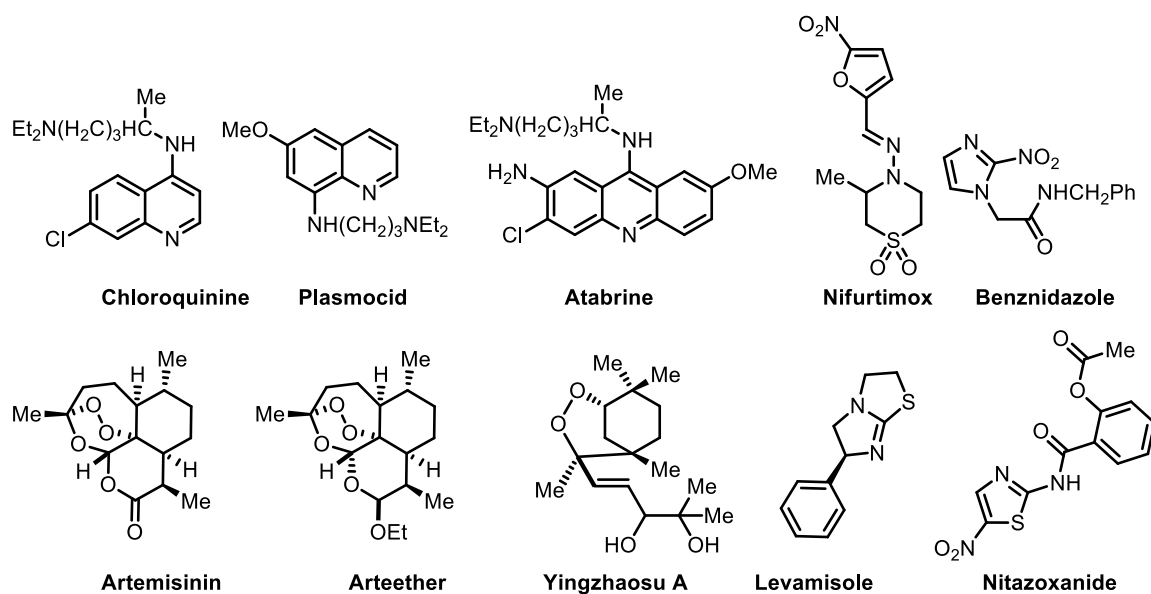


Figure 1.1F. Some of the heterocyclic molecules having anti-parasitic activity.

1.1.1Ae. Antiviral agents

Enormous scientific efforts have been devoted in finding potential and efficient drugs for treating life-threatening viral infections like HIV, herpes viruses, the hepatitis B and C viruses, and influenza A and B viruses. The evolution of knowledge in the field of genetic and molecular function of organisms has greatly helped in developing antiviral drugs. A number of heterocyclic compounds are being utilized to fight viral infections, and some of them are listed below (Figure 1.1G).^{5a}

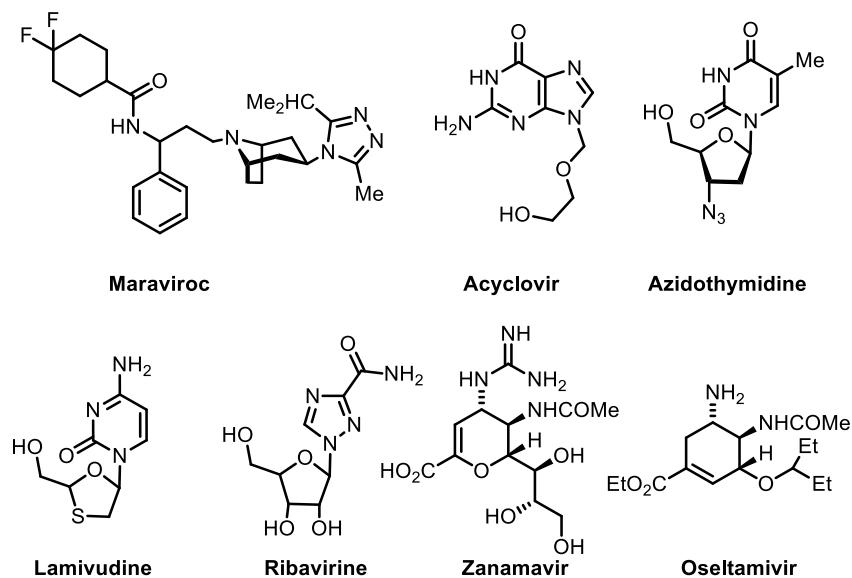


Figure 1.1G. Examples of antiviral drugs.

1.1.1Af. Anticancer agents

Heterocyclic compounds are the true corner stones of medicinal chemistry as they represent most of the currently marketed pharmaceuticals, along with their intrinsic versatility and unique physicochemical properties. Apart from the already marketed drugs, numerous other heterocyclic compounds are being examined for their promising activities.^{5a,19} Moreover, the development of anticancer drugs has been a principal focus for several decades. There are many naturally occurring heterocyclic compounds, namely the alkaloids, taxols and synthetic heterocycles which display potent anticancer activity, few of them are listed in Figure 1.1H.²⁰

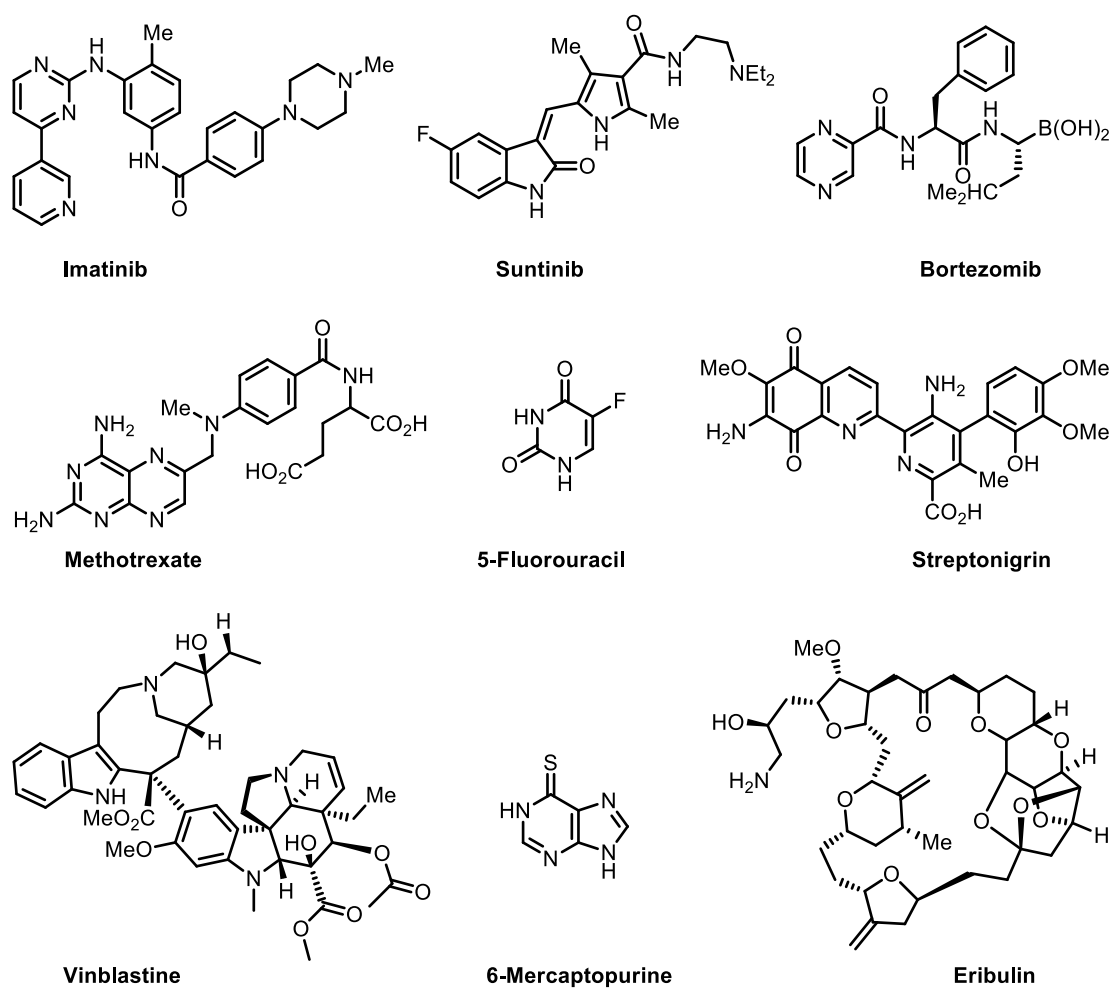


Figure 1.1H. Examples of anticancer drugs.

1.1.1Ag. Heterocycle used to cure brain and heart related problems

A large class of heterocyclic drugs are employed for the treatment of brain and heart related problem such as antihypertensive, antianginal, antidepressant, *etc.* 1,4-dihydropyridine, azines and azoles, heteroaromatic compounds, *etc.* are explored as effective cardiovascular agents, while a number of thiazepine and diazepine derivatives are successfully used for the treatment of brain disorders (Figure 1.1I).^{5a}

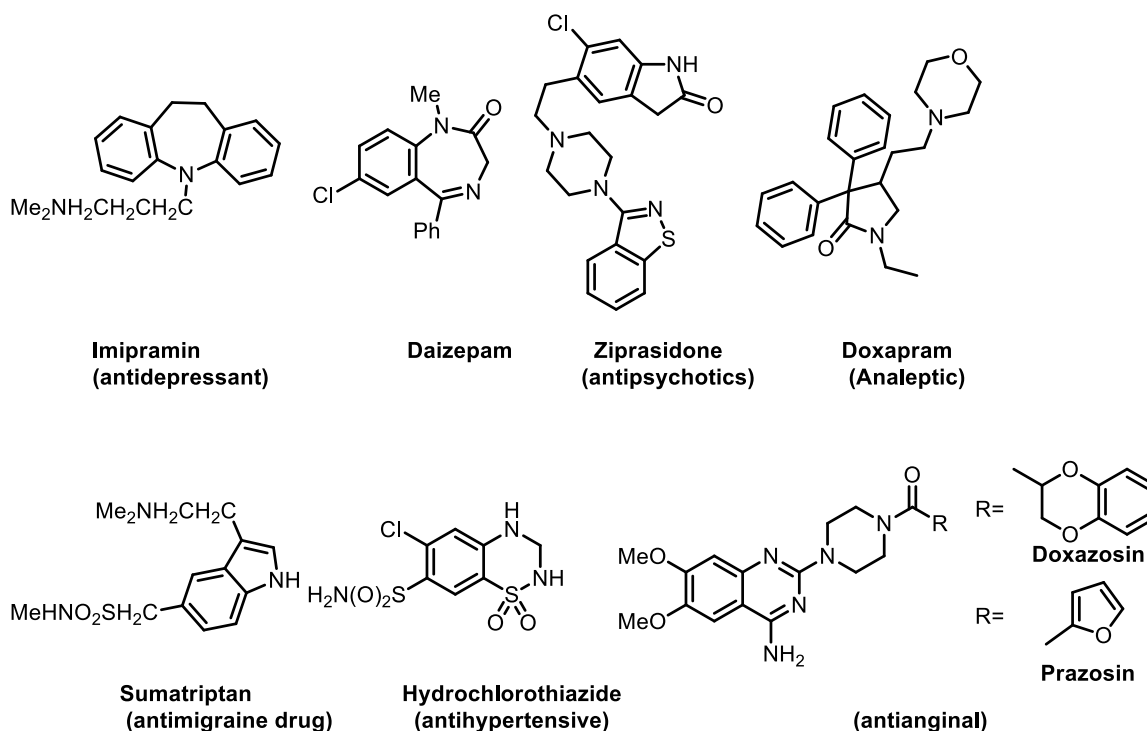


Figure 1.1I. Examples of drugs used for brain and heart related problems.

1.1.1B. Agricultural importance

During the last decades, exhaustive efforts have been undertaken to discover safer, environment friendly and active chemicals that help to stimulate or regulate the growth and development of plants, and for the specific control of weeds, bugs, and fungal infections.^{5a,21} Approximately 70% of chemicals that have been utilized in agriculture within the last 20 years bear at least one heterocyclic ring. Heterocyclic compounds, especially azoles, thiaziazole, isoxazole, benzimidazole, dihydropyrimidinones, azines, and benzodiazepine derivatives are frequently employed as pesticides. Other heterocycles such as sulfonyleureas and indole derivatives are of great help in the growth and

development of plants. Some of the agrochemicals that are currently in the market are listed below (Figure 1.1J).

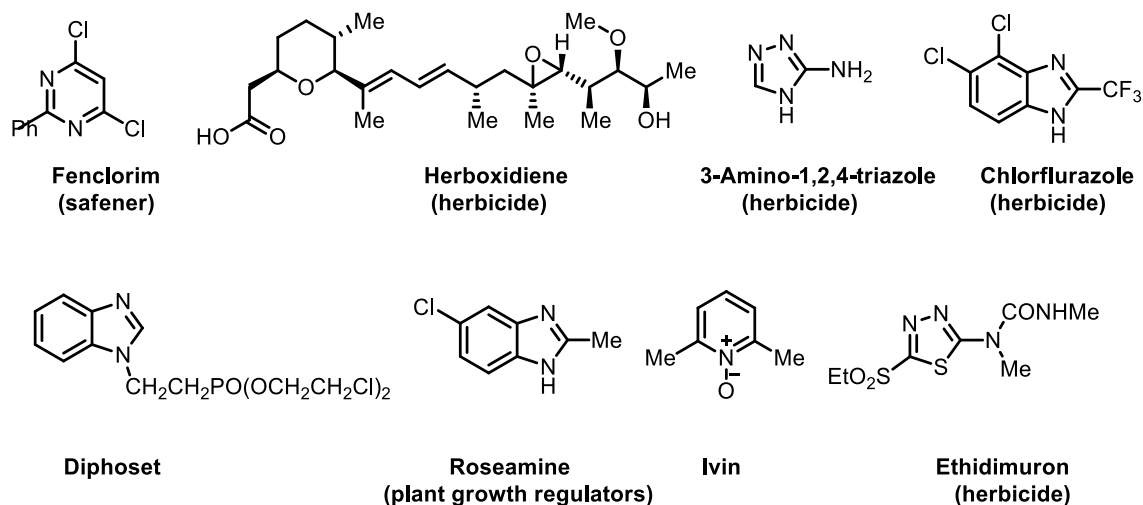


Figure 1.1J. Some of the currently marketed agrochemicals.

1.1.1C. Heterocycles in industry and technology

Heterocycles possess vital applications and have become indispensable in the development of industry and technology including the biomedical sciences, electronics, communications, and aerospace technology. They remain enormously important both in modern and traditional branches of industry such as the dye industry, food industry, *etc.* Nowadays heterocycles find applications as fluorescent sensors, brightening agents, dyestuff, information storage, plastics, analytical reagents, photographic materials and recorders of information. In addition, they have applications in the food industry as food additives and in the modern market of cosmetics and perfumery products. They also occupy an essential place in the field of analytical chemistry for the determination of various metal ions and compounds. Moreover, they act as organic conductors, semiconductors, molecular wires, photovoltaic cells, organic light-emitting diodes (OLEDs), light harvesting systems, optical data carriers, chemically controllable switches, and liquid crystalline compounds (Figure 1.1K).^{5a}

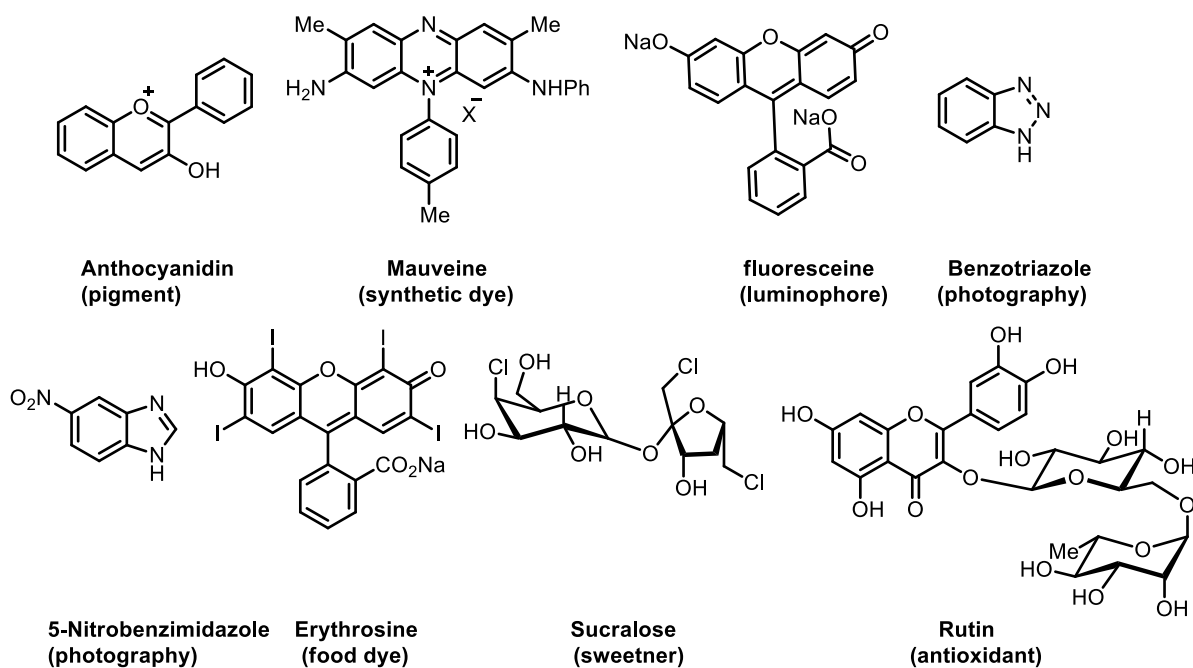


Figure 1.1K. Heterocycles used in industry and technology.

Due to their enormous importance in pharmaceutical industry, medicinal industry and various drug development areas, enough concerns have been given for the design, synthesis and application of heterocycles. Also, heterocycles in modern drug design serve as a useful tool to manipulate lipophilicity, polarity and hydrogen bonding capacity of molecules, which may lead to improved pharmacological, pharmacokinetics, toxicological and physicochemical properties of drug candidates and ultimately drugs. Based on the above studies, researchers are being focussing mainly on the design and synthesis of heterocycles.

1.2. A brief history of 1,2-dihydropyridines

Dihydropyridines (DHPs) represent a group of organic compounds based on a pyridine core which serve as important intermediates in the synthesis of pyridine derivatives and are endowed with a broad range of synthetic and biological interests.²² The chemistry of DHPs, started in 1882 when Hantzsch disclosed the first synthesis of these compounds.²³ During his attempt, he observed the formation of 1,4-dihydropyridines (1,4-DHPs) as isolable intermediates that can be oxidised to pyridine derivatives. The isolation of reductive cofactor, nicotinamide adenine dinucleotide (NADH **26**, Figure 1.2A) and the attention gathered by Hantzsch DHPs such as nifedipine (**27**) as antihypertensive drug

stimulated the interest of DHP chemistry. Eventhough, theoretically five isomeric DHPs 1,2-, 1,4-, 2,3-, 3,4-, and 2,5-dihydro types are possible (Figure 1.2A), the most known DHPs are either the 1,2-DHP **28** or the 1,4-DHP **29** in structure, due to the involvement of the nitrogen lone pair in the stabilisation of enamines.^{22a,24}

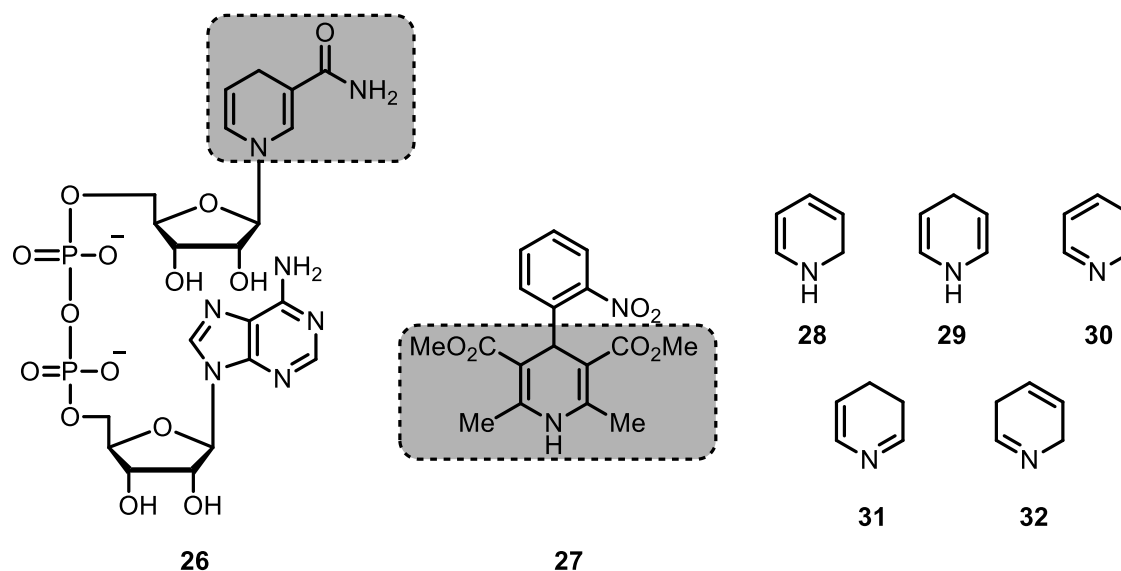


Figure 1.2A. Reductive cofactor NADH (**26**), antihypertensive drug nifedipine (**27**) and possible isomeric structures of DHP (**28-32**).

1.2.1. Importance of dihydropyridines

1.2.1A. 1,4-DHP

Hantzsch 1,4-DHP synthesis in 1882 marks the inception of a heterocyclic system endowed with a broad range of synthetic and biological interests.²³ 1,4-DHP is a key intermediate in the synthesis of other heterocycles, it mimics the functions of NADH, an oxidoreductase co-enzyme in biological systems and possesses a vast spectrum of pharmacological properties. 1,4-DHPs have been used as calcium-channel modulating agents in the treatment of cardiovascular diseases (e.g. Amlodipine, Felodipine, Nicardipine, Nisoldipine, Nitrendipine, and Nimodipine, Figure 1.2B), and also explored as multidrug-resistance-reversing agents in cancer chemotherapy, antimycobacterial and anticonvulsant agent.²⁵

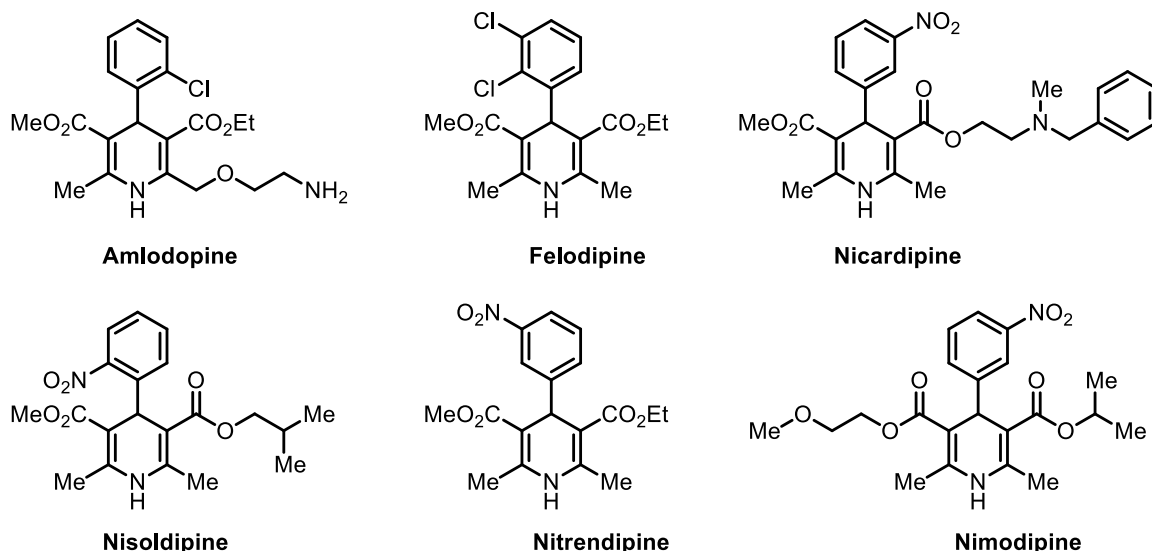
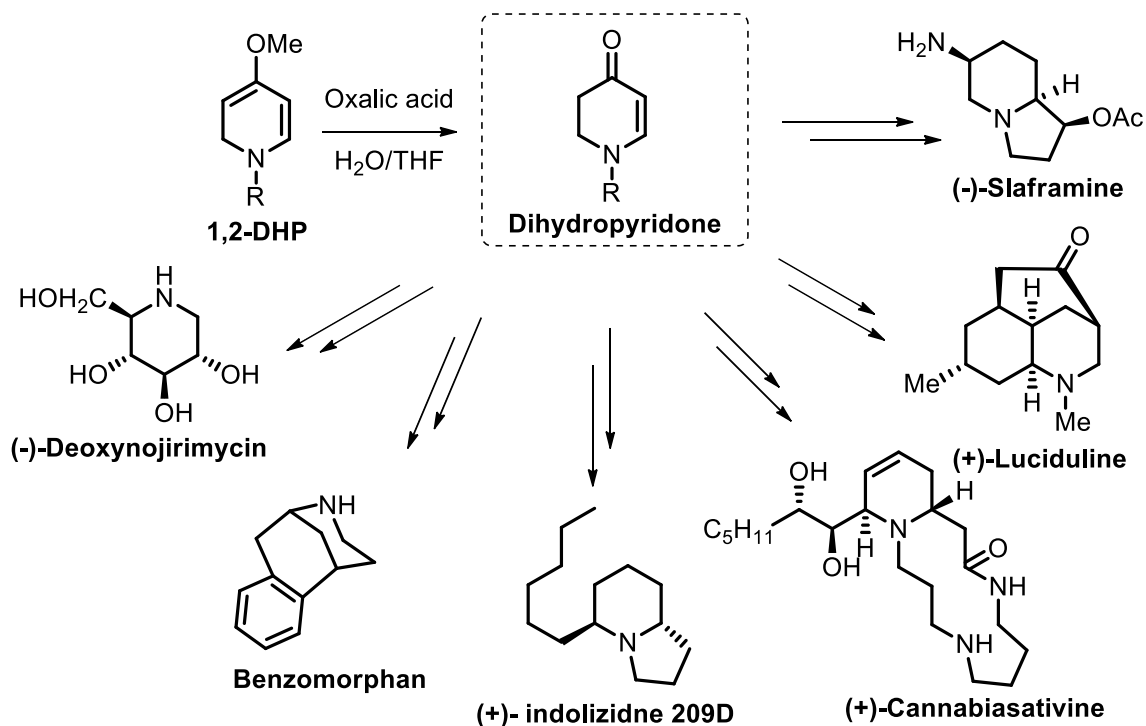
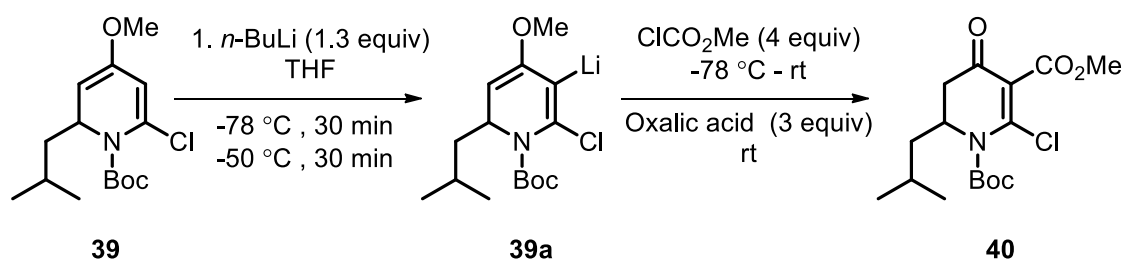
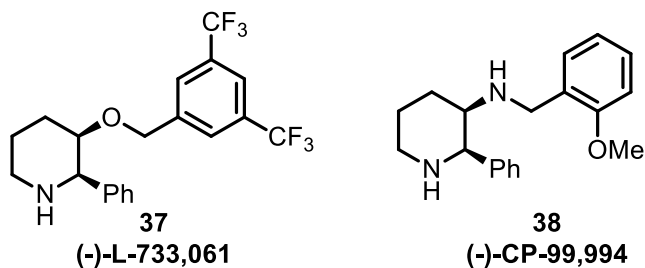
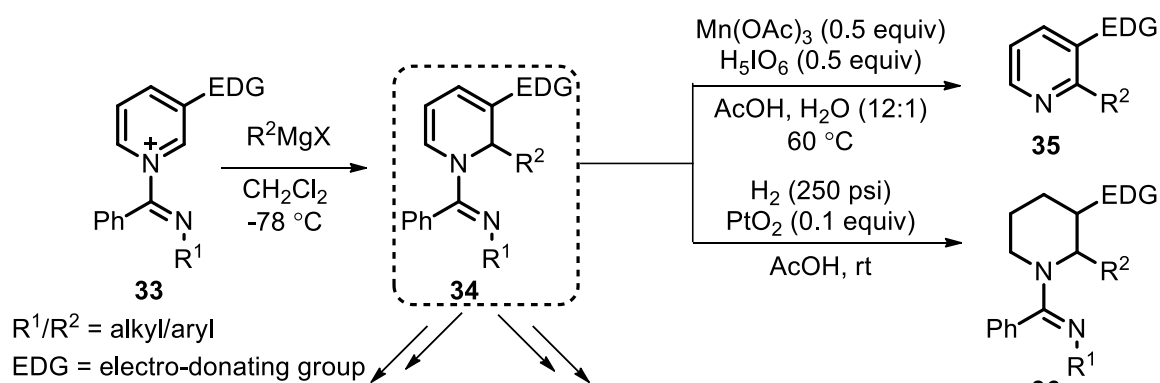


Figure 1.2B. 1,4-DHP containing calcium channel blockers available in the market.

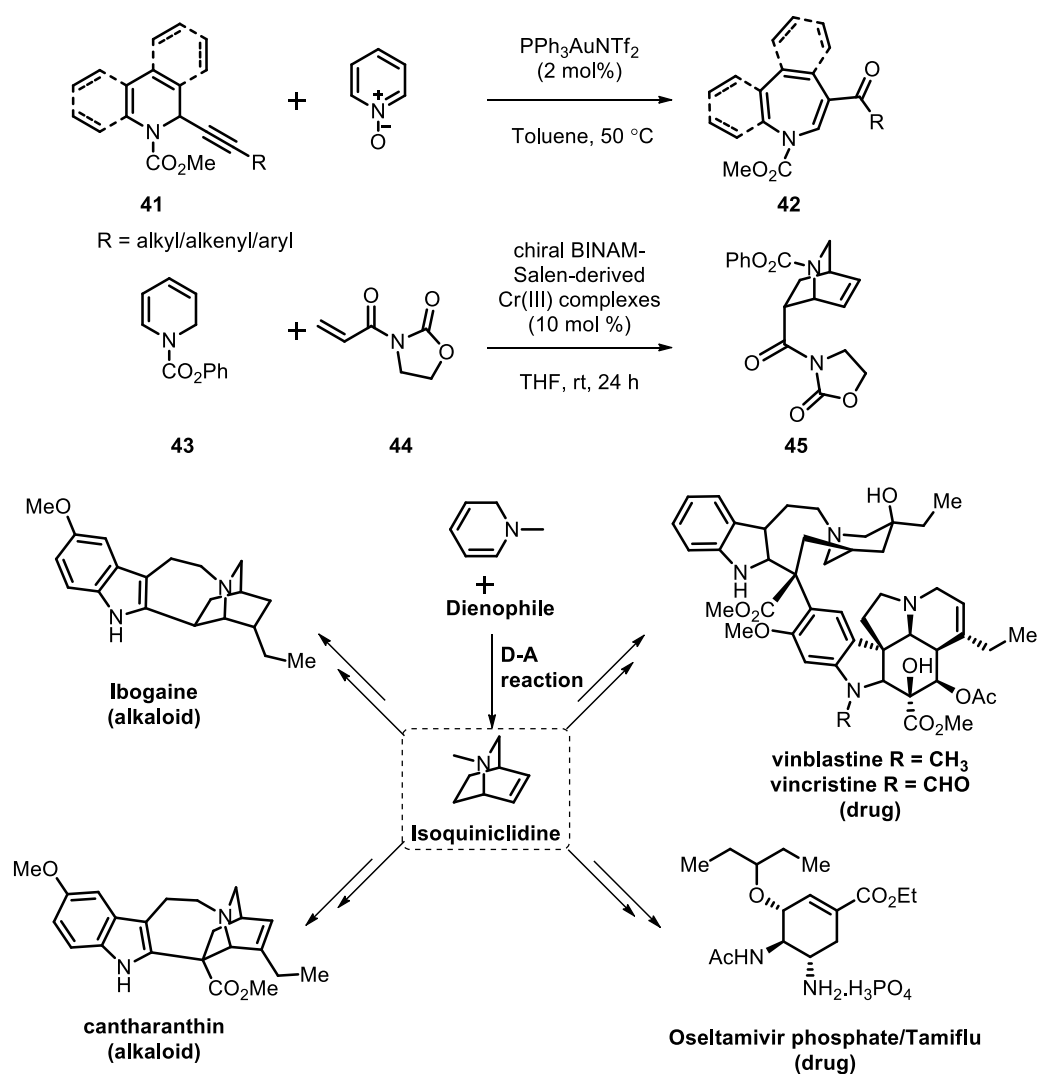
1.2.1B. 1,2-DHP

1,2-DHPs have not been explored in detail for their biological properties as that of 1,4-DHPs, however, they are widely used as precursor scaffold for the preparation of many biologically active compounds.^{22c,26} In 1993, Ezer *et al.* reported the potential anti-ulcer property of 1,2-DHP derivatives with significant antisecretory action and cytoprotective effect.²⁷ Very recently, Wang *et al.* investigated the neuroprotective effect of 2-disubstituted 1,2-DHP on neurotoxin-induced differentiated PC12 cells and indeed it has exhibited good neuroprotective effect *via* the mitochondrial apoptosis pathway.²⁸ 1,2-DHP is considered as an important intermediate in the synthesis of pyridines and piperidines.²⁹ For example, Charette *et al.* reported the conversion of 2,3-disubstituted 1,2-DHP intermediate **34** synthesized from the 3-substituted pyridinium salts **33** to the corresponding pyridine **35** and piperidine **36** under oxidation and reduction conditions, respectively (Scheme 1.2.1).^{29c} They successfully applied this methodology for the synthesis of (-)-L-733,061 (**37**) and (-)-CP-99,994 (**38**), two members of a highly potent, nonpeptide, Substance P antagonists (Scheme 1.2.1). Comins *et al.* applied the sequential tandem directed lithiation/electrophilic substitution strategy on *N*-Boc-4-methoxy-1,2-DHP **39** to access the corresponding dihydropyridone **40** *via* intermediate **39a** (Scheme 1.2.1).³⁰ These dihydropyridones have proficiently served as precursors for diversely functionalised piperidine based systems like indolizidines, phenanthroindolizidines, polyamine alkaloids, lycopodium alkaloids, benzomorphan, *etc* (Scheme 1.2.1).³¹



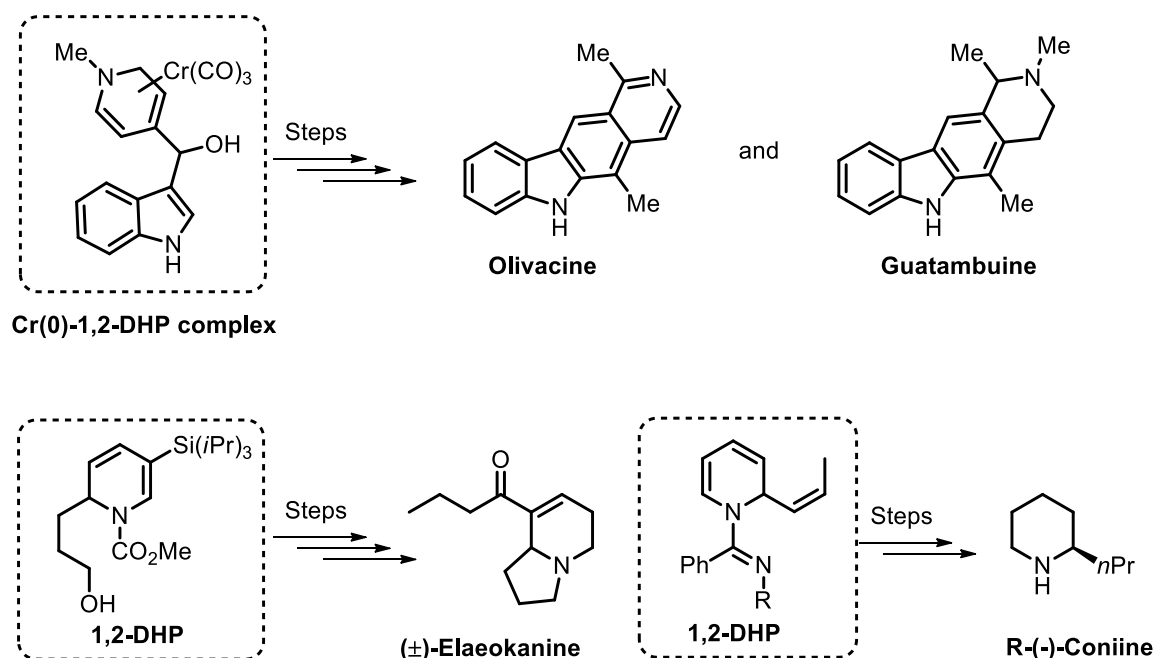
Scheme 1.2.1. Transformation of 1,2-DHP to pyridine, piperidine, pyridones and its utility.

Recently, Li *et al.* reported the gold-catalyzed oxidative ring expansion of 2-alkynyl substituted 1,2-DHP **41** and its analogues to functionalized azepines **42** in the presence of pyridine *N*-oxide oxidant (Scheme 1.2.2).³² Moreover 1,2-DHPs have also found a wide application as a preferred cyclic aza-diene precursor scaffolds in the Diels-Alder reaction especially in the preparation of isoquinuclidine ring systems,³³ which is a key intermediate in the synthesis of some alkaloids, such as ibogaine, cantharanthin, isoquinuclidine drugs, namely vinblastine and vincristine, and an anti-influenza drug Oseltamivir phosphate (Scheme 1.2.2).³⁴ For instance, Rawal *et al.* developed a catalytic enantioselective version of the Diels-Alder reaction between 1,2-DHP **43** and 3-acryloyloxazolidin-2-one **44** using chiral BINAM-Salen-derived Cr(III) complexes, to yield isoquinuclidine **45** (Scheme 1.2.2).³⁵



Scheme 1.2.2. Transformation of 1,2-DHP to azepines and 1,2-DHP in D-A synthesis of isoquinuclidine and its utility.

1,2-DHP also finds application as a synthetic intermediate in the synthesis of many natural products such as pyridocarbazole alkaloids (olivacine and guatambuine), (\pm)-elaekanine A, R(-)-coniine, *etc* (Scheme 1.2.3).³⁶

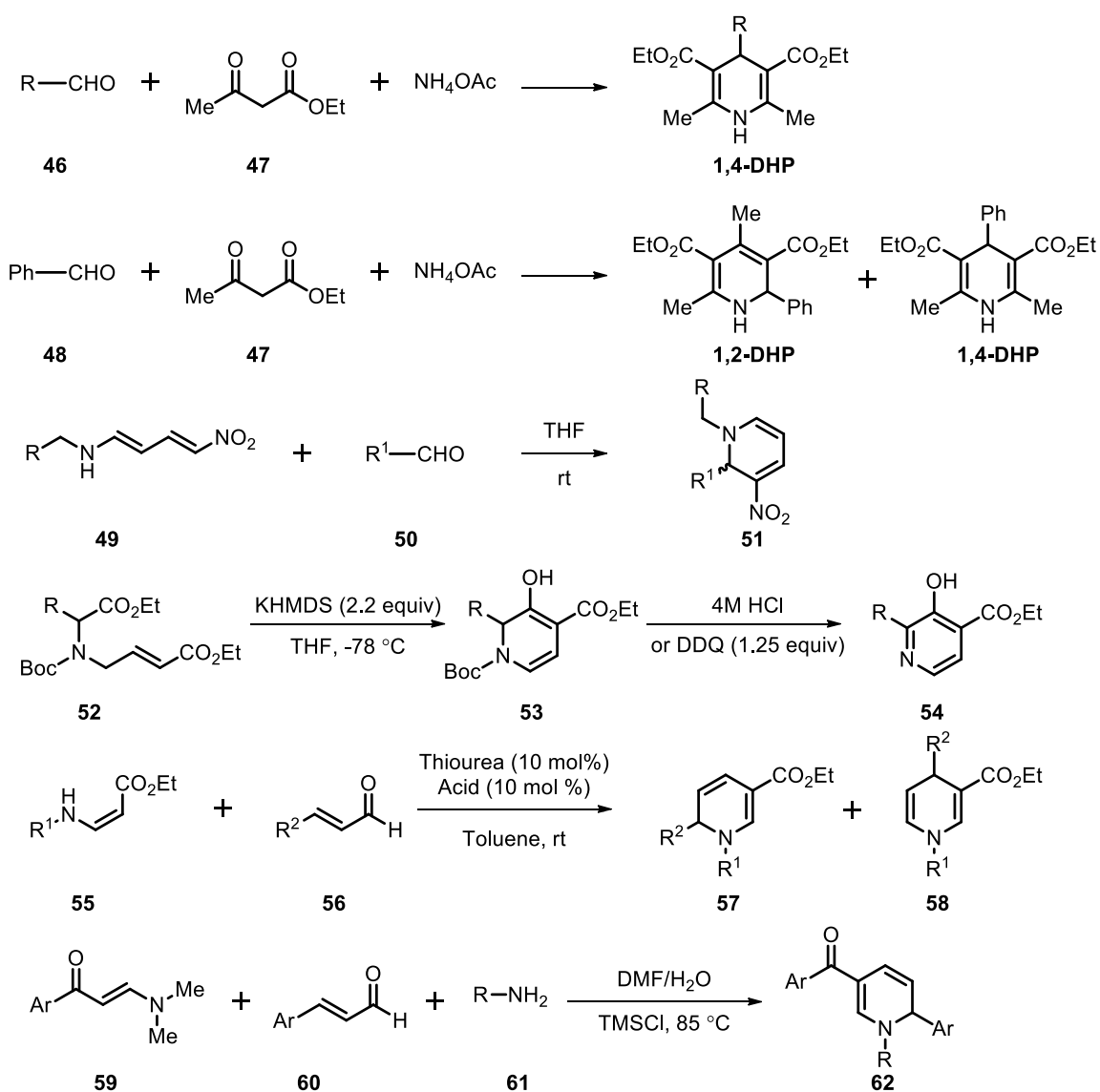


Scheme 1.2.3. Synthesis of pyridocarbazole alkaloids (olivacine and guatambuine), (\pm)-elaekanine A and R(-)-coniine using 1,2-DHP derivatives.

1.2.2. Synthetic routes to 1,2-DHP

Cyclization reactions (Hantzsch ring closure), reduction or nucleophilic addition of pyridinium ions and pericyclic reactions are the most common methods employed for the synthesis of substituted 1,2-DHPs. The early development in the chemistry of 1,2-DHP until 1982 had covered the reviews of Eisner and Kuthan, and Stout and Meyers.^{22a,b} Later, Lavilla in 2002, Silva *et al.* in 2013 and more recently Sharma *et al.* in 2017 also compiled the literature for the synthesis of DHPs.^{22c,d,26}

Numerous research groups have revisited the Hantzsch 1,4-DHP synthesis which proceeds through a one-pot multicomponent condensation reaction of an aldehyde **46**, ethyl acetoacetate **47** and ammonium acetate over the years (Scheme 1.2.4). In 2009, Shen *et al.* observed the formation of 1,2-DHP, when aromatic aldehyde **48** instead of aliphatic aldehyde reacted with ethyl acetoacetate **47** and ammonium acetate under solvent, catalyst and heat-free (at room temperature) conditions, which on air oxidation for 72 hours yielded 2-arylpyridines (Scheme 1.2.4).³⁷

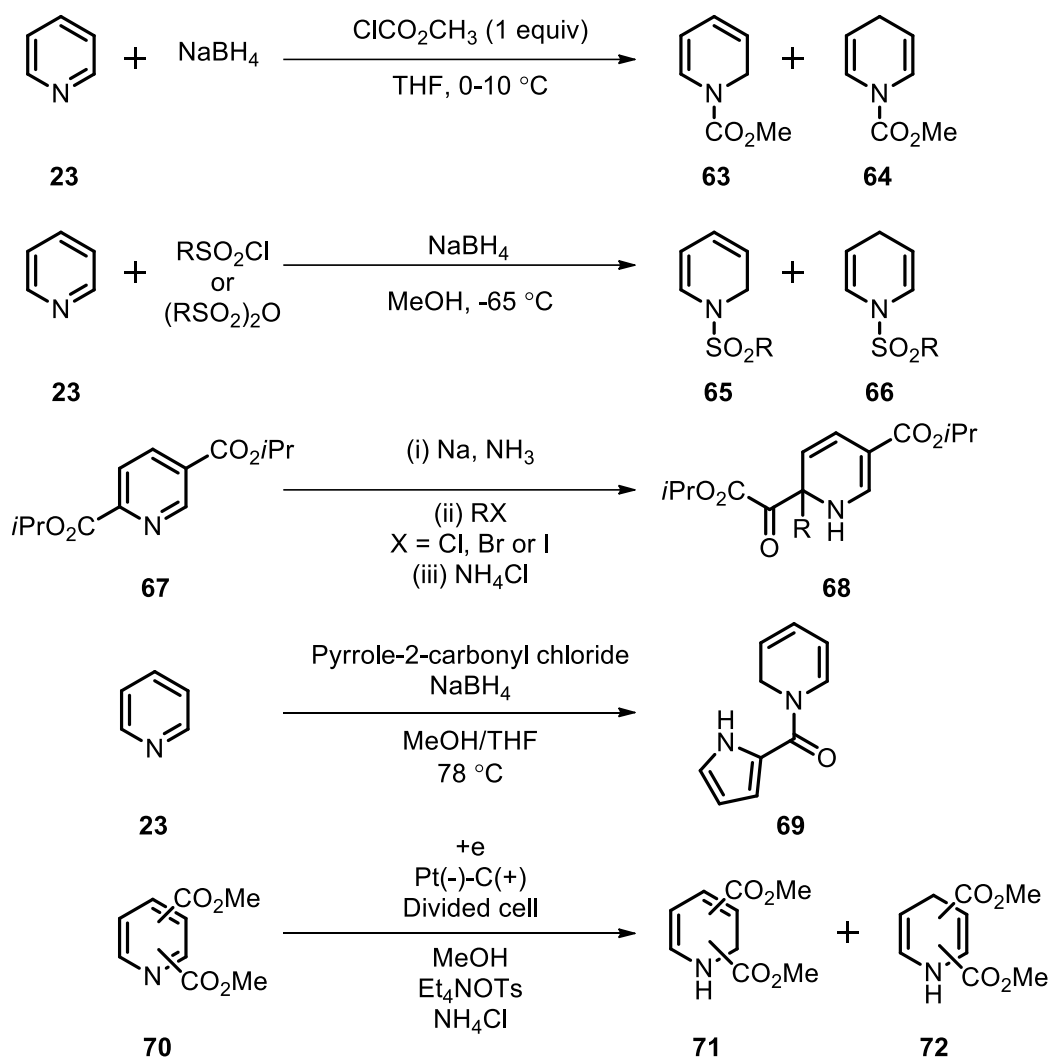


Scheme 1.2.4. Synthetic routes to 1,2-DHP **51-62**.

Koike *et al.* reported an efficient heterocyclic annulation reaction of *sec*-nitrodienamine **49** with aldehyde **50** for the synthesis of 2-methyl-3-nitro-1,2-DHPs **51** (Scheme 1.2.4).³⁸ A unique method for the synthesis of chiral 1,2-DHPs **53** by Dieckmann condensation of α -amino acid derivatives **52** was achieved by Kawabata *et al.*. Further, they have extended this methodology for the synthesis of trisubstituted pyridine derivatives **54** by oxidation with 4M hydrochloric acid solution or 2,3-dichloro-5,6-dicyano-1,4-quinone (DDQ) (Scheme 1.2.4).³⁹ A bronsted acid and thiourea co-catalyzed asymmetric synthesis of functionalized 1,2- and 1,4-DHPs (**57** and **58**) was reported by Yoshida *et al.* in 2010. In this synthesis, a bronsted acid–thiourea catalyst was used to catalyze the asymmetric cycloadditions of β -enamino esters **55** to α,β -unsaturated aldehydes **56** (Scheme 1.2.4).⁴⁰

Wan *et al.* in 2009 reported a three-component sequential reaction of enaminones **59**, α,β -unsaturated aldehydes **60**, and amines **61** for the regioselective synthesis of 1,2-DHPs **62**. The observed regioselectivity was controlled by both steric and electronic effects of the amine component (Scheme 1.2.4).⁴¹

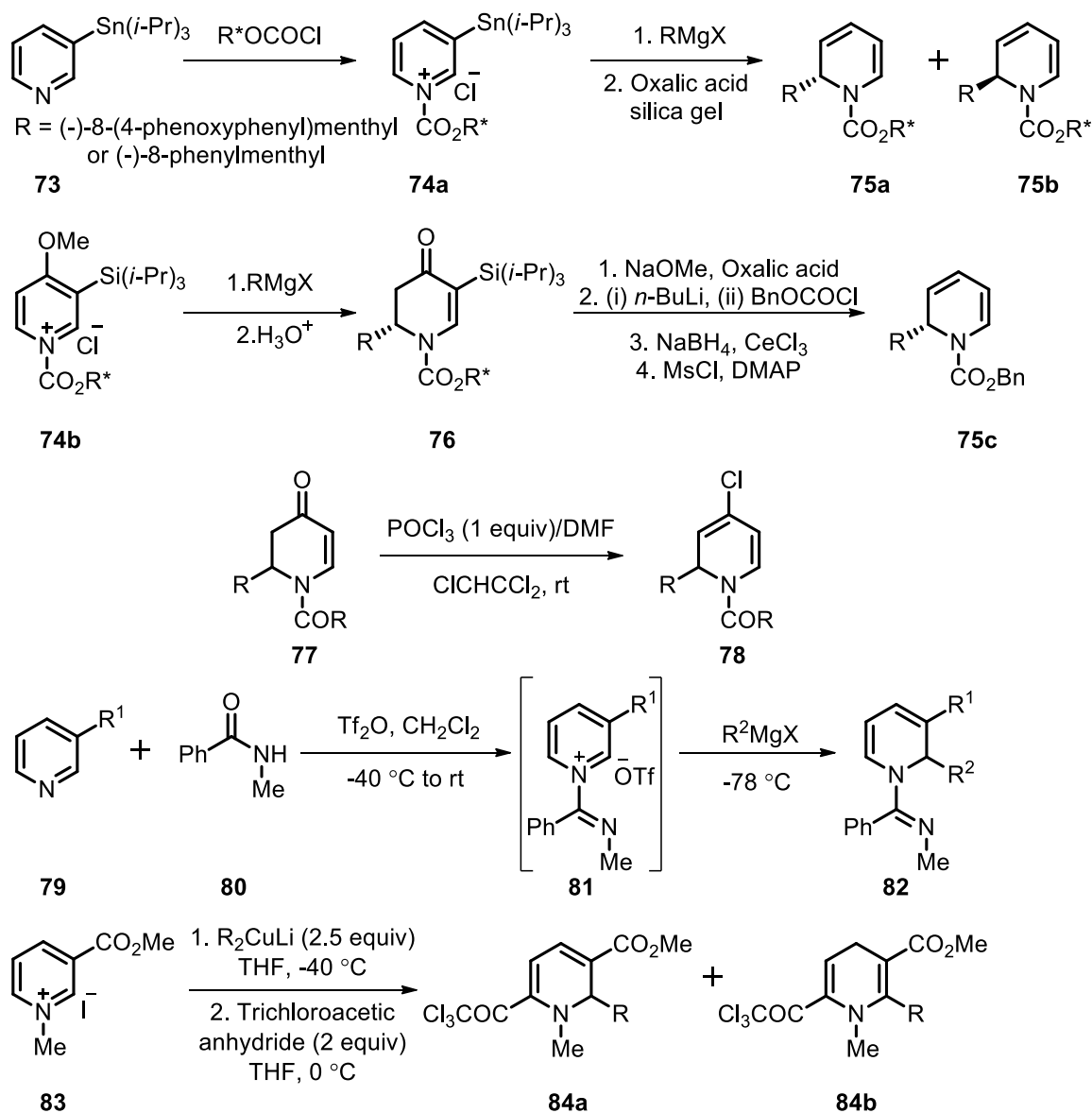
Reduction of pyridine or pyridinium salt through dearomatizing transformation is an attractive strategy for the synthesis of substituted 1,2-DHPs. One of the pioneering work in this area was exemplified by Fowler in 1972, who carried out the NaBH₄ reduction of *in situ* generated *N*-(alkoxycarbonyl)pyridinium chloride from a pyridine **23** and a chloroformate ester to form 1,2-(**63**) and 1,4-DHPs (**64**) (Scheme 1.2.5).⁴² Later, in 1986 Sundberg *et al.* performed a detailed study on the Fowler reduction of 3-substituted pyridines.⁴³ In 1975, Booker *et al.* reported the reduction of 3,5-disubstituted pyridine to 1,2- and 1,4-DHPs using diborane and sodium cyanoborohydride, respectively.⁴⁴ A solvent and temperature dependent reduction of *in situ* generated *N*-sulfonyl pyridinium salt to corresponding 1,2- and 1,4-DHPs was published by Knaus and Redda in 1977.⁴⁵ It involves the reaction of sulfonyl chlorides and sulfonic acid anhydrides with pyridine **23** in the presence of sodium borohydride to form *N*-sulfonyl-1,2 (**65**) and 1,4-DHP (**66**) (Scheme 1.2.5). A controlled reduction of 4-methyl-3-ethylpyridinium iodide to corresponding 1,2-DHPs was established by Kutney *et al.* in 1979 by complexation with tricarbonylchromium(0).⁴⁶ Later, Davies *et al.* also showed that the usage of tricarbonyl(η -pyridine)chromium(0) complexes as a stable synthetic precursor for the synthesis of 1,2-DHPs.⁴⁷ Donohoe *et al.* investigated the partial reduction of electron deficient pyridines **67** to 1,2-DHPs **68** using both Birch reduction conditions and sodium/naphthalene in THF (Scheme 1.2.5).⁴⁸ The same group later employed this methodology for the synthesis of dihydropyridones and natural product alkaloids.⁴⁹ Direct preparation of *N*-acyl-1,2-DHPs **69** was reported from pyridine **23** and pyrrole-2-carbonyl chloride by the single step reduction with borohydride by Schroif-Gregoire *et al.* in 2006 (Scheme 1.2.5).⁵⁰ This strategy has been used in the synthesis of pyrrole-2-aminoimidazole marine metabolites. Moreover, the electroreductive hydrogenation of pyridine dicarboxylic acid derivatives **70** in methanol to 1,2- (**71**) and 1,4-DHPs (**72**) was accomplished using a divided cell containing a platinum plate as the cathode and a carbon rod as the anode (Scheme 1.2.5).⁵¹



Scheme 1.2.5. Synthetic routes to DHP **63-72**.

Nucleophilic additions to *N*-activated pyridine derivatives were well explored in the synthesis of 1,2-DHP.⁵² Comins *et al.* reported efficient chiral auxiliary mediated asymmetric syntheses of *N*-acyl-2-alkyl-1,2-DHPs **75**. The first reaction involves the addition of Grignard reagent to an *in situ* generated chiral *N*-acylpyridinium salt **74a** from pyridine **73**, and the limitation of this was the removal of chiral auxiliary. They also demonstrated a second asymmetric synthesis of 1,2-DHP **75c** through the formation of dihydropyridone **76** from chiral *N*-acylpyridinium salt **74b** (Scheme 1.2.6).⁵³ The conversion of *N*-acyl-2,3-dihydro-4-pyridones **77** to 4-chloro-1,2-dihydropyridines **78** using the Vilsmeier reagent was also developed by the same group (Scheme 1.2.6).⁵⁴ Wanner *et al.* developed an efficient methodology to generate chiral *N*-acylpyridinium ions and used them to access the 1,2-DHPs.⁵⁵ The addition of Grignard reagent to 3-substituted-*N*-imidoylpyridinium salts **81** formed from 3-substitute pyridine **79** and amide

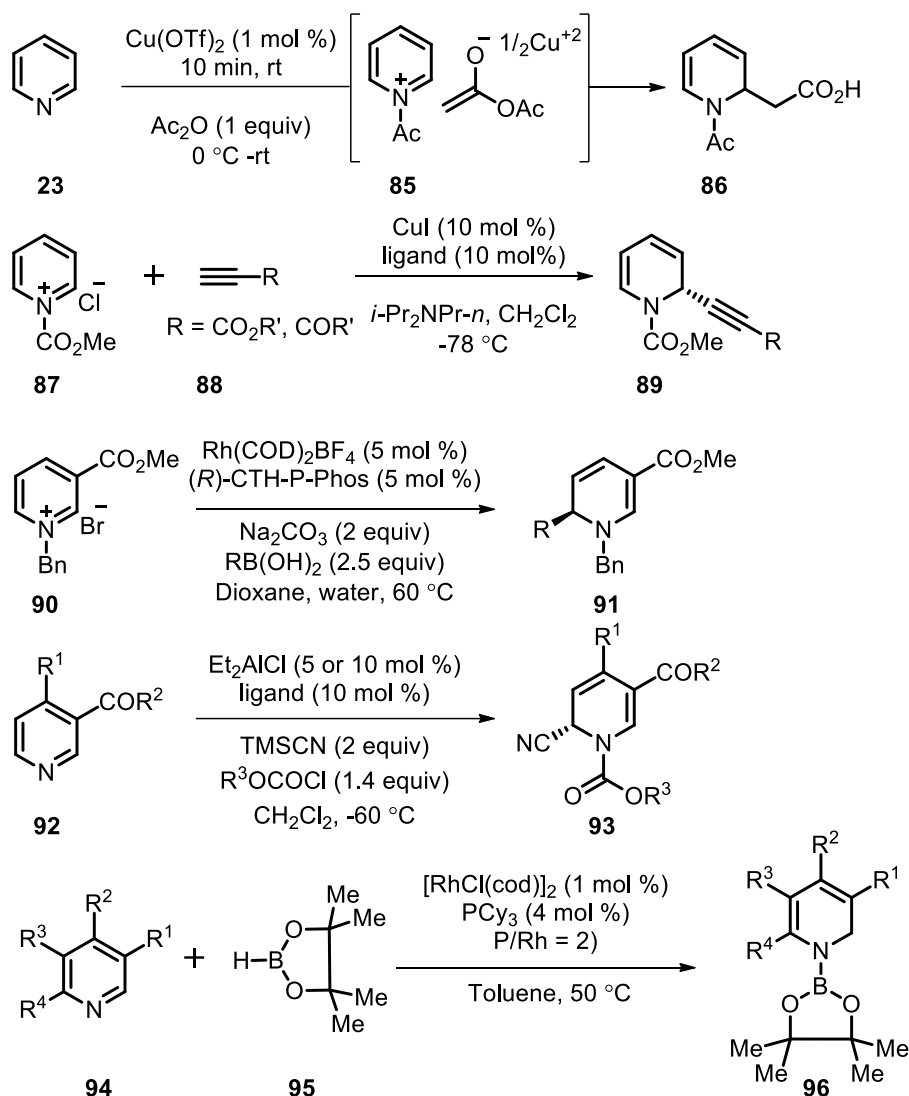
80 bearing an electron donating group (EDG) has been studied by Charette *et al.*. The approach resulted in a highly regioselective formation of 2,3-substituted 1,2-dihydropyridines **82** (Scheme 1.2.6).^{29a,36c} Addition of organometallic reagents to *N*-alkylpyridinium salts **83** to access polysubstituted DHPs **84** was reported by Bennasar *et al.* (Scheme 1.2.6).⁵⁶ Phase-transfer-catalysed nucleophilic addition to *N*-alkylpyridinium salt was performed by Lavilla *et al.*⁵⁷



Scheme 1.2.6. Synthetic routes to DHP **75-84**.

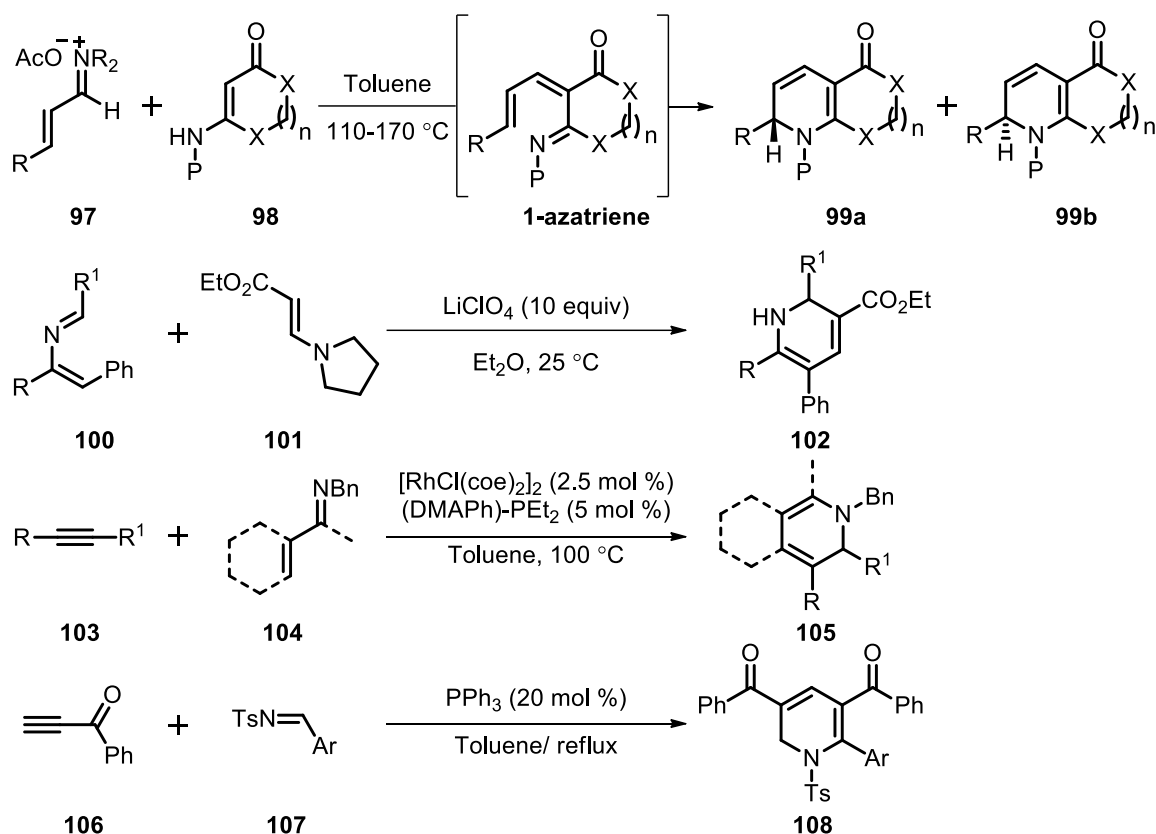
Crotti *et al.* have accomplished a regioselective introduction of methoxycarbonyl methyl group at the C-2 position of an unsubstituted pyridine **23** to access the *N*-acetyl-1,2-dihydropyridyl acetic acid methyl ester **86**, a valuable building block for piperidines. The reaction proceeded through the activation of acetic anhydride using catalytic amounts of

copper (II) triflate and subsequent addition of the copper enolate to *N*-acetyl pyridiniumion **85** under mild conditions (Scheme 1.2.7).⁵⁸ Other organometallic reagents like zinc, indium, *etc.* were also reported as an efficient reagent for the C-2 alkylation of the acylpyridinium salts.⁵⁹ Copper-catalyzed enantioselective addition of terminal alkyne **88** to *N*-acylpyridinium salt **87** to furnish 1,2-DHP **89** was reported by Sun *et al.* (Scheme 1.2.7).⁶⁰ A similar kind of reaction was also reported by Black *et al.*⁶¹ Later, Christian *et al.* demonstrated rhodium-catalyzed highly enantioselective asymmetric method for the addition of aryl and alkenyl boronic acids to *N*-benzylpyridinium salt **90** to form corresponding 1,2-DHPs **91** (Scheme 1.2.7).⁶² A catalytic enantioselective Reissert reaction of pyridine derivatives **92** was reported by Ichikawa *et al.*.



Scheme 1.2.7. Synthetic routes to 1,2-DHP **86-96**.

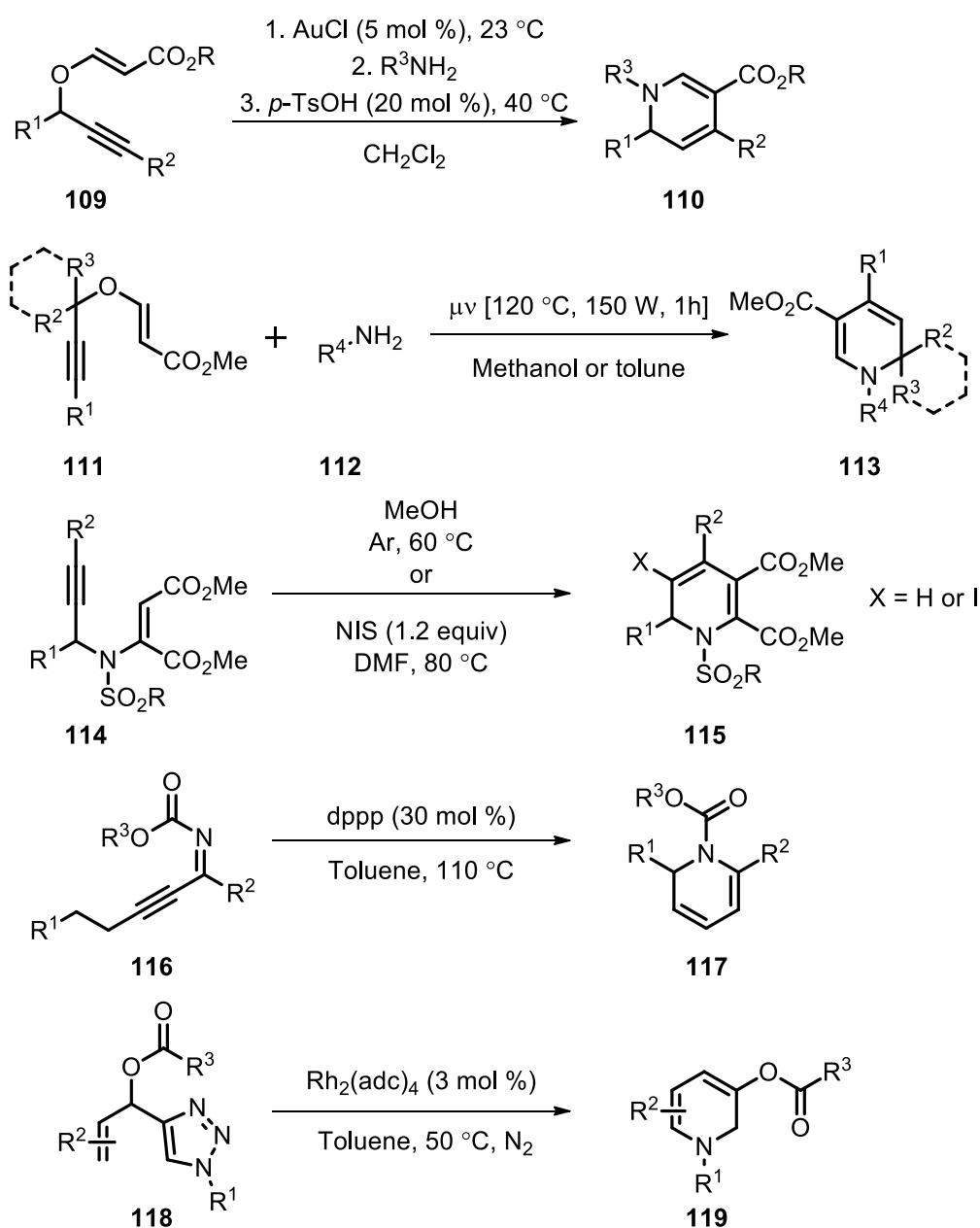
This transformation resulted in the formation of 1,2-DHP **93** through the development of new Lewis acid-Lewis base asymmetric bifunctional catalysts (Scheme 1.2.7).⁶³ Suginome *et al.* performed rhodium-catalyzed hydroboration of pyridines **94** with pinacolborane **95** at 50 °C. They have isolated the desired *N*-boryl 1,2-DHP **96** in high yields with regioselectivity (Scheme 1.2.7).⁶⁴



Scheme 1.2.8. Synthetic routes to 1,2-DHP **99-108**.

The 6π -electrocyclization of 1-azatrienes is one of the well-known concerted pericyclic reaction approaches for the synthesis of 1,2-DHPs. One of the pioneering works in this area was reported by Okamura *et al.*, suggesting that the introduction of either an electron donating or a withdrawing group at the 1-azatriene may accelerate the cyclization.⁶⁵ Katsumara and co-workers also studied the acceleration of 6π -azaelectrocyclization.⁶⁶ The first highly stereoselective [3+3] cycloaddition reactions of chiral vinylogous amides **97** with α,β -unsaturated iminiums **98** for the synthesis of 1,2-DHPs **99** was developed by Hsung *et al.* (Scheme 1.2.8).⁶⁷ Palacios *et al.* has reported the synthesis of 1,2-DHP **102** from enamines **100** and 2-azadienes **101** (readily prepared by aza-Wittig reactions) via [4+2] cycloaddition reaction (Scheme 1.2.8).⁶⁸ Metal-catalyzed C-H activation and

subsequent cyclization reactions were well explored in the synthesis of 1,2-DHP. For example, Ellman *et al.* reported a rhodium-catalyzed cascade C-H alkenylation and 6π -electrocyclization between alkyne **103** and α,β -unsaturated imine **104** to synthesize 1,2-DHP **105** in the presence of a special phosphine ligand (Scheme 1.2.8).⁶⁹ The groups of Yoshikai and Petit independently demonstrated that low valent cobalt species were capable of promoting the same reaction in good yields (Scheme 1.2.8).⁷⁰ Tong *et al.* developed the synthesis of highly substituted 1,2-DHPs **108** comprised of triphenylphosphine catalysed [2+2+2] annulation between 1-phenylpropynones **106** and aryl *N*-tosylimines **107** (Scheme 1.2.8).⁷¹

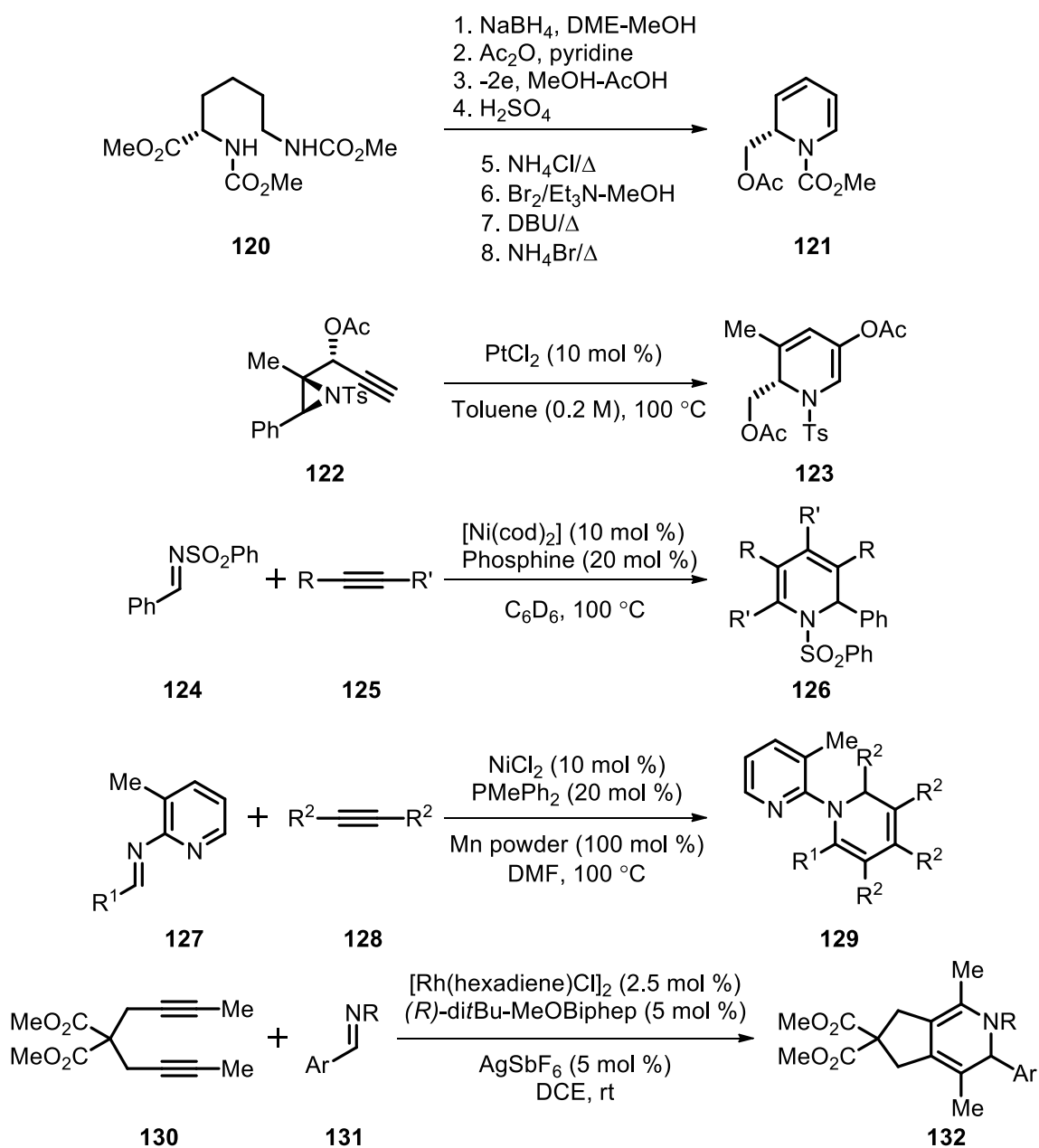


Scheme 1.2.9. Synthetic routes to 1,2-DHP **110-119**.

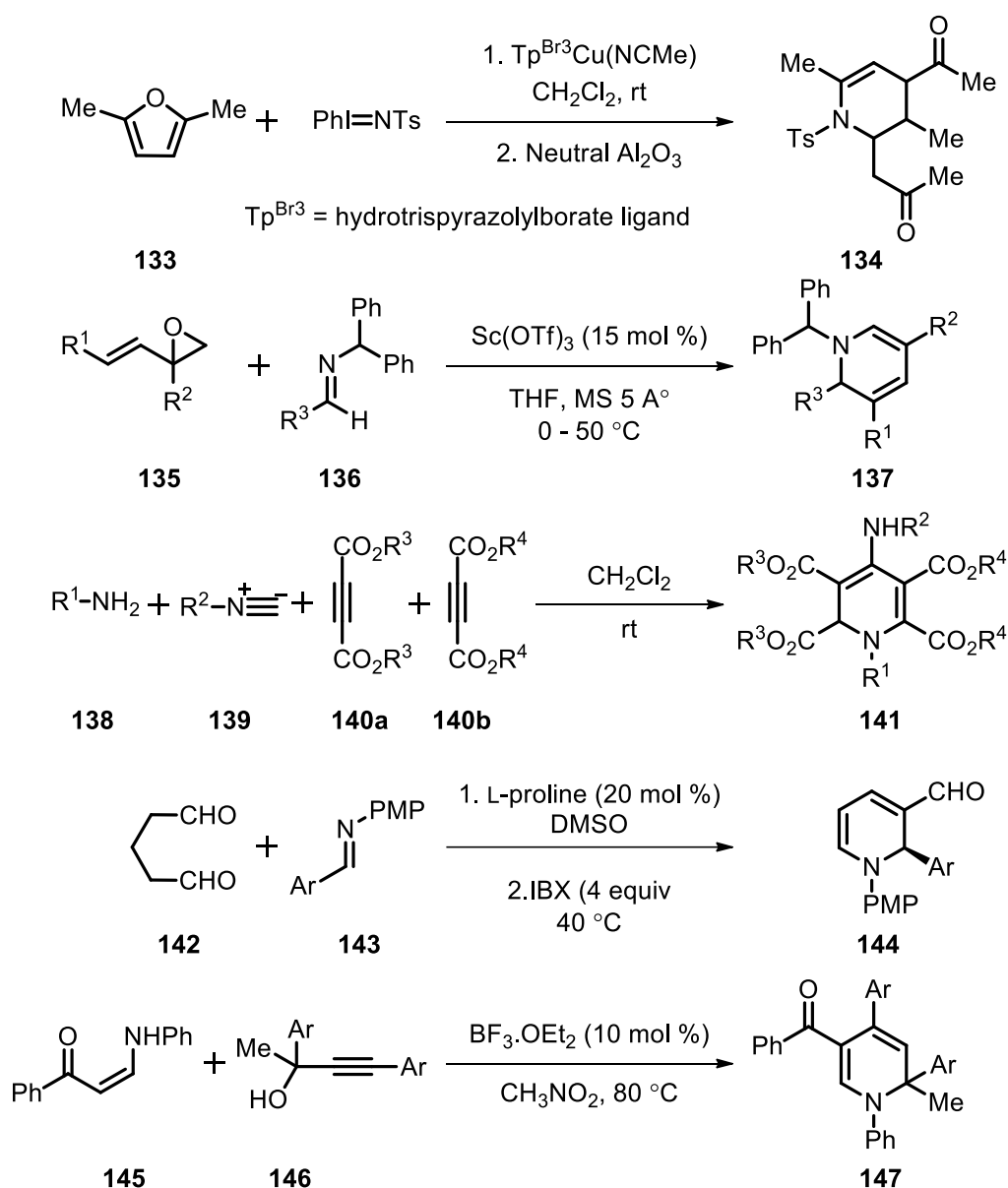
Kirsch *et al.* demonstrated that the use of propargyl vinyl ethers **109** are viable substrates for the synthesis of 1,2-DHPs **110**. The reaction involves a gold-catalyzed propargyl-Claisen rearrangement, condensation, and a Brønsted acid-catalyzed heterocyclisation (Scheme 1.2.9).⁷² Similarly different research groups have developed direct protocols toward 1,2-DHPs from propargyl vinyl ethers which undergo propargyl Claisen rearrangement to directly deliver the 2,4-dienals, then react with primary amine to deliver the 6π -aza-electrocyclization substrate 1-azatrienes (Scheme 1.2.9).⁷³ Tejedor *et al.* reported a general and practical protocol for the synthesis of 1,2-DHP **113** with mono, di and spiro substitution at sp^3 carbon. It involves microwave assisted domino reaction of propargyl vinyl ethers **111** and aliphatic or aromatic amines **112** in toluene or methanol solvent (Scheme 1.2.9).^{73c} The use of 3-aza-1,5-enynes **114** as a versatile substrate for selective synthesis of 1,2-DHPs **115** *via* metal free cyclization or NIS-induced electrophilic iodocyclization was studied by the Wan research group.⁷⁴ Trost *et al.* devised a phosphine catalyzed redox cycloisomerization approach for the synthesis of 2,6-disubstituted 1,2-DHP **117**. In this reaction, the starting substrate propargylidene carbamate **116** undergoes a one-pot alkyne isomerization and electrocyclization sequence to afford 1,2-DHP **117** in good yields (Scheme 1.2.9).⁷⁵ Further, they have extended this methodology for the synthesis of histamine H₃ receptor agonists. Very recently, Li *et al.* observed a rhodium-catalyzed tandem reaction of 4-(1-acetoxyallyl)-1-sulfonyl-1,2,3-triazole **118** through the formation of α -imino rhodium carbene, followed by 1,2-migration of an acetoxy group and six electron electrocyclic ring closure to access the corresponding 1,2-DHP **119** in moderate to good yields (Scheme 1.2.9).⁷⁶

Matsumura *et al.* reported the synthesis of enantiomerically pure 1,2-DHP **121** from L-lysine **120** by employing anodic oxidation as a key step (Scheme 1.2.10).⁷⁷ A novel Pt(II)-catalyzed cycloisomerization of aziridinyl propargylic esters **122** for the synthesis of 1,2-DHPs **123** was accomplished by Sarpong *et al.* (Scheme 1.2.10).⁷⁸ Ogoshi *et al.* demonstrated an oxidative cyclization of an imine **124** and two equivalent of alkyne **125** with nickel (0) undergo a sequential reaction to yield 1,2-DHPs **126** (Scheme 1.2.10).⁷⁹ A similar kind of reaction was also reported using rhodium as a catalyst.⁸⁰ A nickel-catalyzed [2+2+2] cycloaddition of *N*-pyridylimine **127** and alkyne **128** was the strategy developed by Adak *et al.* for the synthesis of 1,2-DHP derivatives **129** (Scheme 1.2.10).⁸¹ Asymmetric rhodium-catalysed [2+2+2] cycloaddition of diynes **130** with sulfonimines

131 to furnish enantioenriched 1,2-DHPs **132** was reported by Amatore *et al.* (Scheme 1.2.10).⁸²



Scheme 1.2.10. Synthetic routes to 1,2-DHP **121-132**.

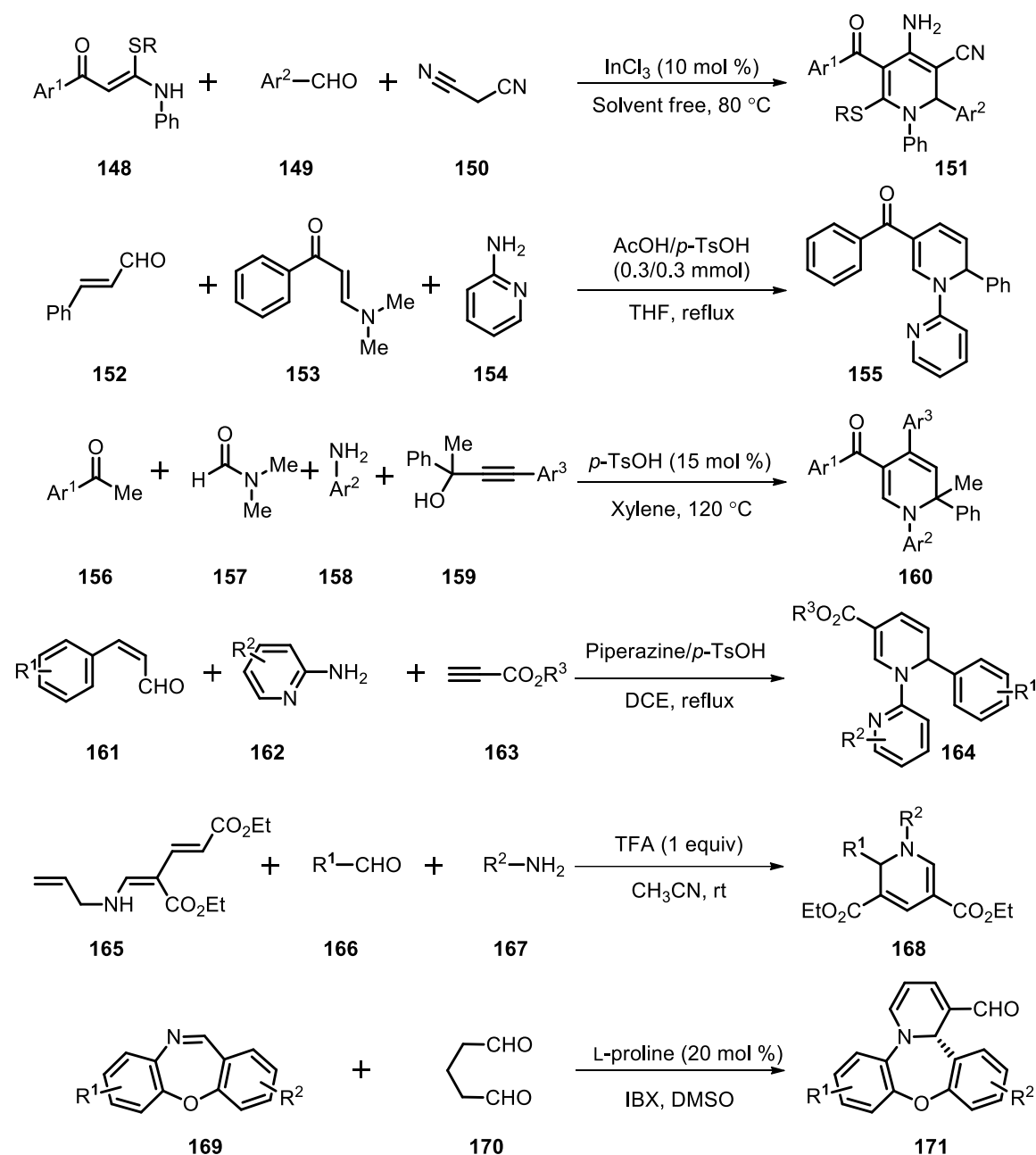


Scheme 1.2.11. Synthetic routes to 1,2-DHP **134-147**.

A novel conversion of mono- or dialkyl-substituted furans **133** into 1,2-DHPs **134** upon reaction with $\text{PhI}=\text{NTs}$ was demonstrated by Fructos *et al.* in 2010 (Scheme 1.2.11).⁸³ Brunner *et al.* reported the use of vinyloxiranes **135** as masked dienolates in vinylogous imino-aldol reactions with aldimine **136** that resulted in the formation of 1,2-DHPs **137** (Scheme 1.2.11).⁸⁴ Yavari *et al.* accomplished a one-pot synthesis of highly functionalized 1,2-DHPs **141** from primary alkylamines **138**, alkyl isocyanides **139**, and acetylenic esters **140** (Scheme 1.2.11).⁸⁵ Ramaraju *et al.* developed an enantioselective synthesis of 1,2-DHP **144** from glutaraldehyde **142** and *N*-PMP protected imine **143** by a L-proline-catalyzed [4+2] cycloaddition reaction (Scheme 1.2.11).⁸⁶ The mechanism

involves amino catalytic direct Mannich reaction/cyclization followed by IBX mediated selective oxidation to afford 1,2-DHP **144** in high yields and enantioselectivities. Shao *et al.* developed a Lewis acid catalysed cyclisation of enaminones **145** with propargylic alcohols **146** to generate multisubstituted 1,2-DHPs **147** (Scheme 1.2.11).⁸⁷ This regioselective reaction needed a catalytic amount of BF₃.OEt₂ to provide **147** in good to excellent yields and the proposed mechanism involves an allenyl/propargylic cation intermediate. Liu *et al.* later reported a similar reaction catalysed by iron tribromide.⁸⁸

Considerably, very few reports are available in the literature for the synthesis of 1,2-DHPs by multicomponent approach. Koley *et al.* reported a Lewis acid catalyzed highly convergent and regioselective three-component coupling of α -oxoketene-*N,S*-arylaminoacetals **148**, aldehydes **149**, and malononitrile **150** to synthesise 4-amino-1,2-DHPs **151** (Scheme 1.2.12).⁸⁹ The reaction involves InCl₃ catalyzed cascade Knoevenagel condensation/Michaeladdition/cyclization sequence leading to the formation of three consecutive new bonds and one ring. Cao *et al.* described a simple *p*-TsOH/AcOH catalyzed three-component assembly of enals **152**, *N,N*-disubstituted enaminones **153**, and 2-aminopyridines **154** to access the corresponding 1,2-DHP **155** in a regioselective manner (Scheme 1.2.12).⁹⁰ This reaction exhibited broad substrate scope and provided the products in moderate to good yields. Recently, Xie *et al.* devised a metal-free *p*-TsOH catalysed four-component reaction (4CR) of aromatic ketones **156**, DMF **157**, amine **158** and propargylic alcohols **159** to construct the functionalized 1,2-DHP **160** in moderate to good yields (Scheme 1.2.12).⁹¹ This reaction utilises DMF **157** as a one carbon synthon in the formation of **160**. In 2014, Wan *et al.* developed a tunable three-component reactions of enals **161**, electron deficient alkynes **162**, and primary amines **163** for selective synthesis of 1,2-DHPs **164** (Scheme 1.2.12).⁹² In 2017, Our group also has developed a convenient synthesis of 1,2-DHPs **168** from dienaminodioate **165** and an *in situ* generated imine, from aldehyde **166** and amine **167** by TFA in a one-pot cascade synthesis (Scheme 1.2.12).⁹³ The advantages associated with this transformation include metal-free reactions and heat-free conditions. More recently an asymmetric synthesis of chiral tetracyclic dibenzo[*b,f*][1,4]oxazepine fused 1,2-DHPs **171** was reported by Choudhary *et al.*. This reaction involves L-proline-catalyzed direct Mannich/cyclization of dibenzo[*b,f*][1,4]-oxazepine-imines **169** with aqueous glutaraldehyde **170**, followed by IBX-mediated dehydrogenative oxidation (Scheme 1.2.12).⁹⁴



Scheme 1.2.12. Synthetic routes to 1,2-DHP **151-171**.

1.3. A brief history of dibenzoxazepines and dibenzoxazepinones

Dibenzoxazepine and dibenzoxazepinones belong to a class of seven-member heterocyclic compounds fused with two benzene rings. The “benzo” prefix indicates that the benzene ring is fused into the oxazepine or oxazepinone ring. There are several benzene fused seven-membered heterocyclic compounds that differ in the position, number and type of heteroatom present. They are considered as privileged heterocyclic scaffolds in virtue of their ability to provide useful ligands to a number of biological

receptors (Figure 1.3A).⁹⁵ They have attracted considerable attention from chemists since the early 1950s due to the introduction of tricyclic antidepressant drugs (TCAs) by the isosteric replacement of ‘phenothiazines’ ‘S’ with a ‘C-C’ (Figure 1.3A). The broad spectrum of biological properties exhibited by this class of compounds evoked considerable interest in the synthesis and exploration of the psychopharmacological properties of seven-membered tricyclic compounds.

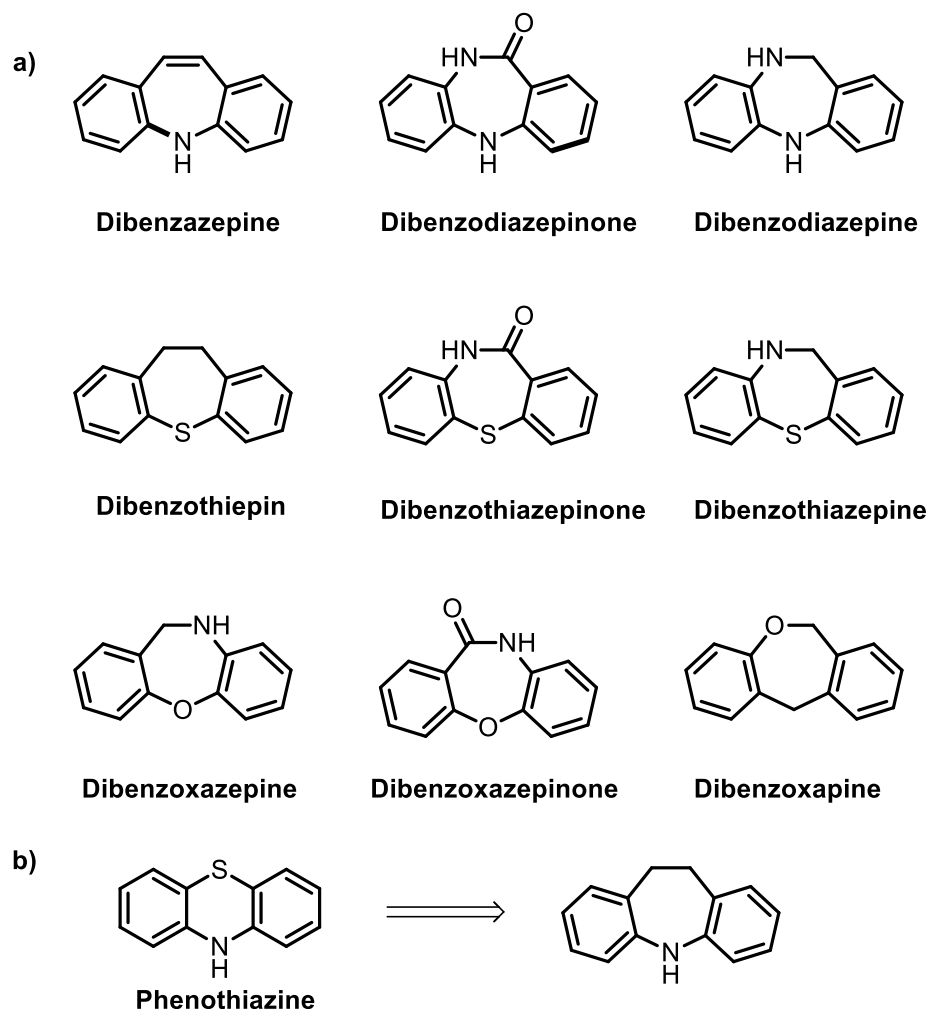


Figure 1.3A a) benzene fused seven-membered heterocyclic scaffolds. b) Isosteric replacement of phenothiazine.

1.3.1. Importance of dibenzoxazepines and dibenzoxazepinones

Even-though three isomeric forms of dibenzoxazepine systems **172-174** are possible, depending on the position of -O- and -N- atom present, the tricyclic isomer **172** is of particular interest because of their presence in many biologically active compounds. They

possess a broad range of biological activities such as anti-HIV, antitumor, antioxidant, oral contraceptive, TRPA1 agonist, sodium channel blocker, CNS depressant, *etc.* For instance, Loxapine and amoxapine are two well known antidepressant drugs currently in market.⁹⁶ The simple dibenzoxazepine, commonly known CR gas is an incapacitating and a lachrymatory agent and is used by defence forces around the world. Gijsen *et al.* reported that the analogues of dibenzoxazepines are extremely potent activators of the human transient receptor potential ankyrin 1 (TRPA1) channel.⁹⁷ This can help to advance the development of treatments for conditions like asthma and pain. The PGE₂ antagonist property of 8-chlorodibenzoxazepine-10-carboxylic acid derivatives **175** was studied by Hallinan *et al.*⁹⁸ In 2006, Smits *et al.* studied the ability of dibenzoxazepines derivatives to probe the binding site of the histamine H₄ receptor (H₄R).⁹⁹ Their study led to the discovery of (*E*)-7-chloro-11-(4-methylpiperazin-1-yl)dibenzoxazepine **176** as a potent H₄R agonist. Dols *et al.* explored the progesterone receptor agonist property of 2,3,4,14b-tetrahydro-1*H*-dibenzopyrido-[1,2-*d*][1,4]oxazepines **177**.¹⁰⁰ Their structure activity relationship (SAR) study led to the identification of potent progesterone agonists up to 1 nM activity. In addition, dibenzoxazepines are also explored for their antipsychotic activity, mineralocorticoid receptor antagonist property and as sodium channel blockers by different research groups.¹⁰¹ Moreover, dibenzoxazepine derivatives are valuable synthons that can be used in the preparation of other fused ring compounds.¹⁰²

Dibenzoxazepinones are pharmaceutically relevant molecules present in antidepressants and antipsychotics. Researchers have extensively studied the pharmacological properties of various dibenzoxazepinone derivatives. Sintamil is a tricyclic antidepressant dibenzoxazepinone which is currently available.¹⁰³ In 1987, Chakrabarti and Hicks studied the anti-inflammatory property of dibenzoxazepinone derivatives and found that 2-[10,11-dihydro-11-oxodibenz[*b,f*][1,4]oxazepin-7 or 8-yl] propanoic acids **178** possess potential anti-inflammatory properties.¹⁰⁴ The HIV inhibitory activity of the dibenzoxazepinones was reported by Klunder *et al.*, and this led to the discovery of a potent HIV inhibitor of up to 19 nM activity.¹⁰⁵ Binaschi *et al.* explored the antitumor activity of dibenzoxazepinones **179**, found that they can inhibit the histone deacetylase (HDAC) proteins, a promising target for the development of antitumor agents.¹⁰⁶

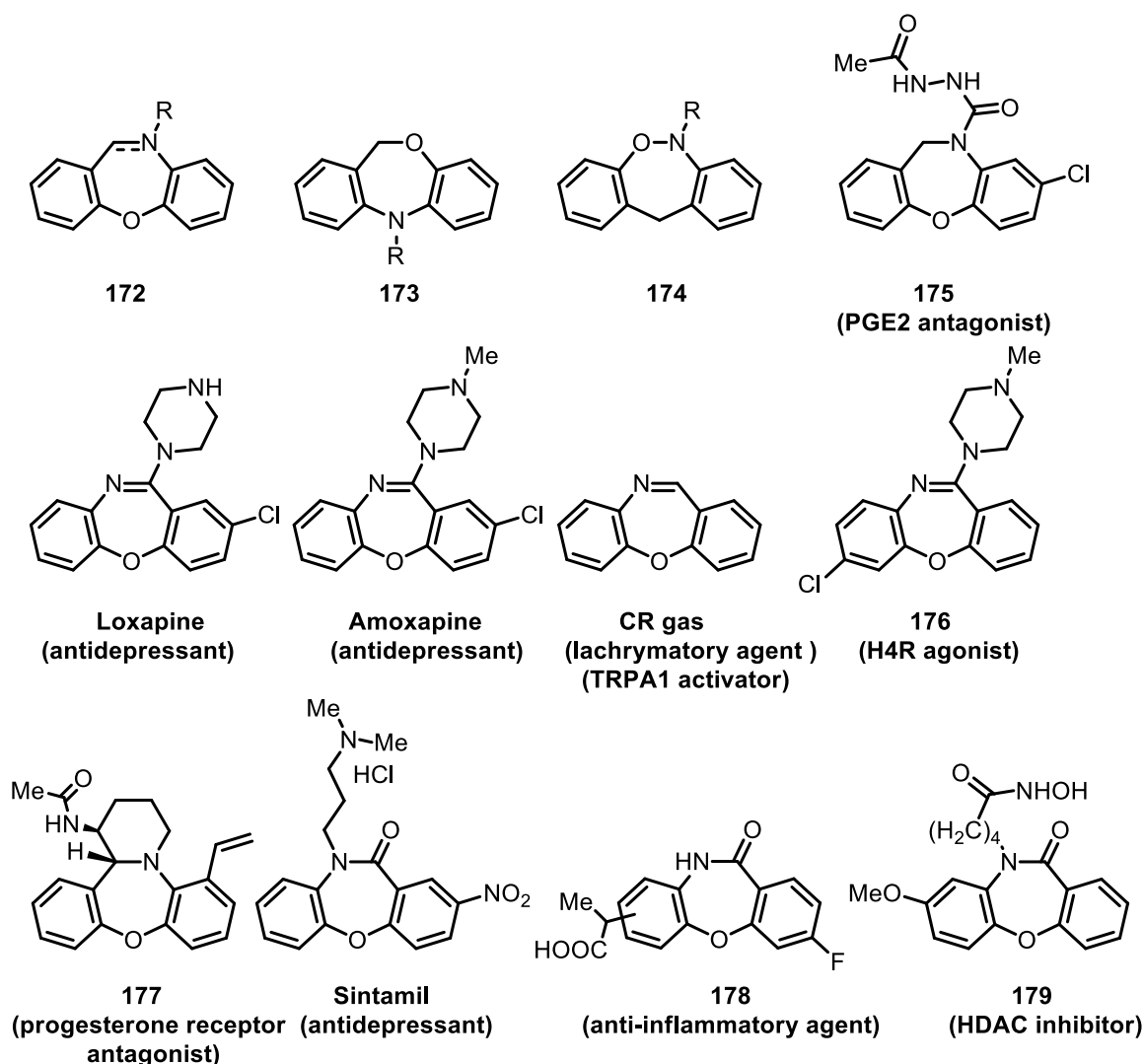
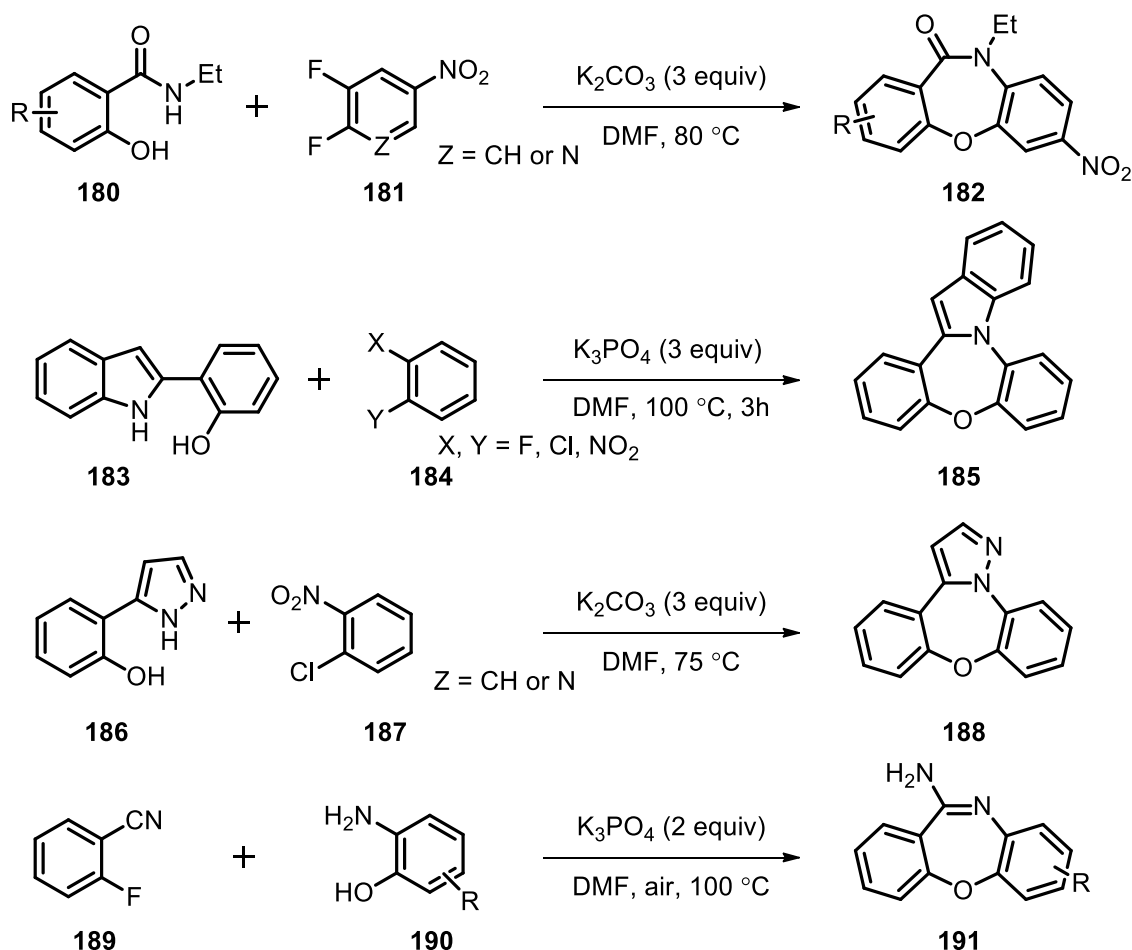


Figure 1.3B. Isomeric forms and pharmacologically active dibenzoxazepines.

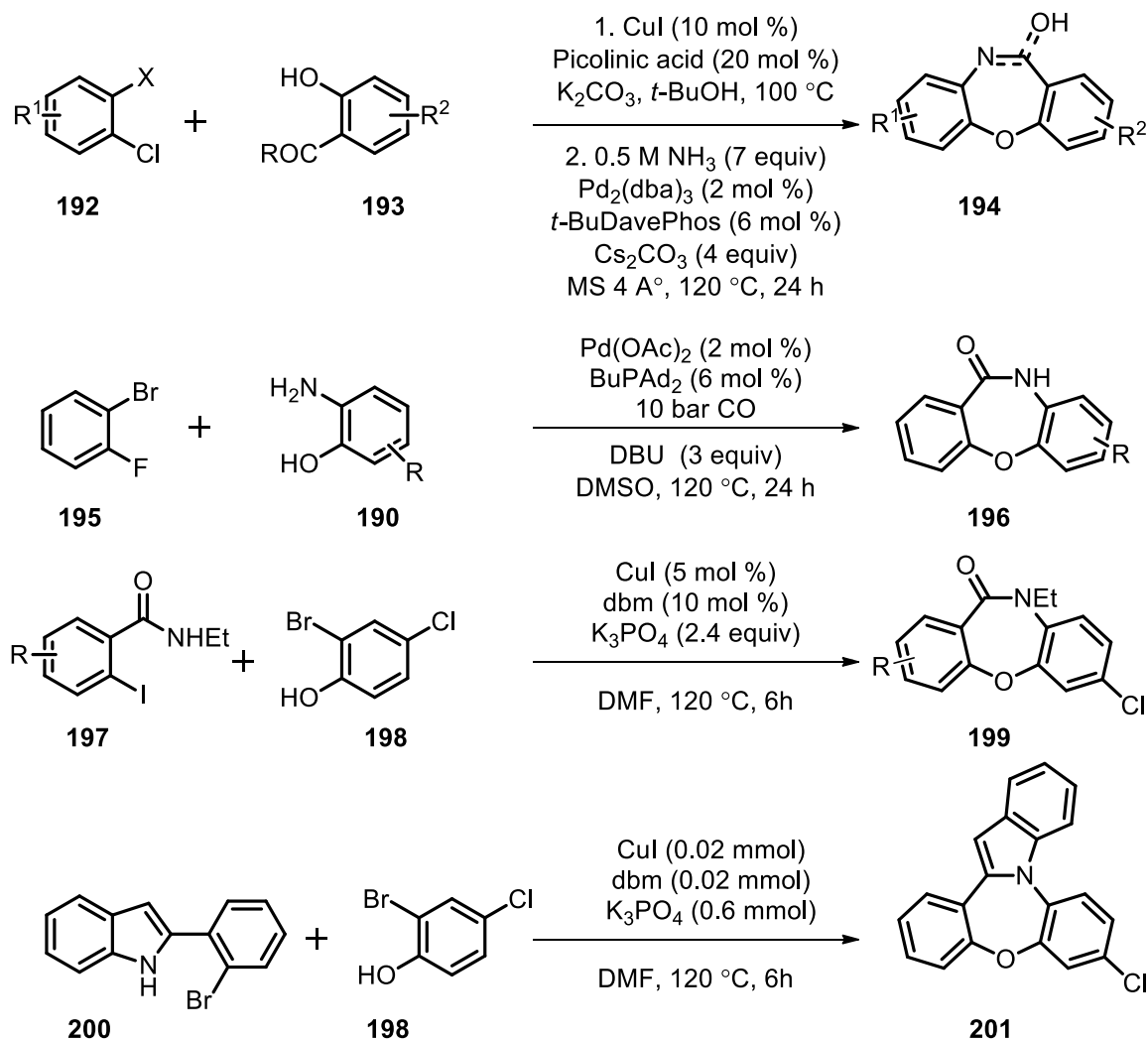
1.3.2. Synthetic routes to dibenzoxazepines and dibenzoxazepinones

Over the years, various approaches have been developed for the synthesis of dibenzoxazepine core skeleton. Base promoted nucleophilic aromatic substitution (S_NAr) is a classical method employed for the construction of the seven-membered ring *via* Smiles rearrangement of suitable substrates by a domino C-O and C-N bond formation. For instance, Ma *et al.* reported a convenient and facile methodology for the regioselective synthesis of fused oxazepinone scaffolds **182** in 2011.¹⁰⁷ This process involved an efficient construction of the oxazepinone scaffold **182** by a one-pot coupling/Smiles rearrangement/cyclization approach from commercially available *N*-substituted salicylamides **180** and substituted benzenes/pyridines **181** (Scheme 1.3.1). Later in 2016, the same group established a K_3PO_4 promoted approach for the synthesis

of indole-fused dibenzo[*b,f*][1,4]oxazepine derivatives **185** via Smiles rearrangement from 2-(1*H*-indol-2-yl)phenol **183** and 1,2-dihalobenzenes/2-halonnitroarenes **184** (Scheme 1.3.1).¹⁰⁸ Aromatic nucleophilic substitution–Smiles rearrangement–denitrocyclization process was the strategy used by Sapegin *et al.* for the synthesis of dibenzo[*b,f*]pyrazolo[1,5-*d*][1,4]oxazepines **188**.¹⁰⁹ The approach involves condensation of 2-(1*H*-pyrazol-5-yl)phenols **186** with 1-chloro-2-nitrobenzenes **187** under basic conditions in DMF (Scheme 1.3.1). Feng *et al.* developed a base-promoted green protocol for the synthesis of dibenzo[*b,f*][1,4]oxazepin-11-amines **191** from 2-aminophenols **189** and 2-fluorobenzonitriles **190**.¹¹⁰ The reaction proceeds via K_3PO_4 mediated S_NAr with a concomitant addition reaction (Scheme 1.3.1). A base mediated solid phase synthesis of dibenzoxazepinones was reported by Hone *et al.* in 2003 where as Samet *et al.* reported an intramolecular nitro group displacement of polynitroaromatic compounds.¹¹¹



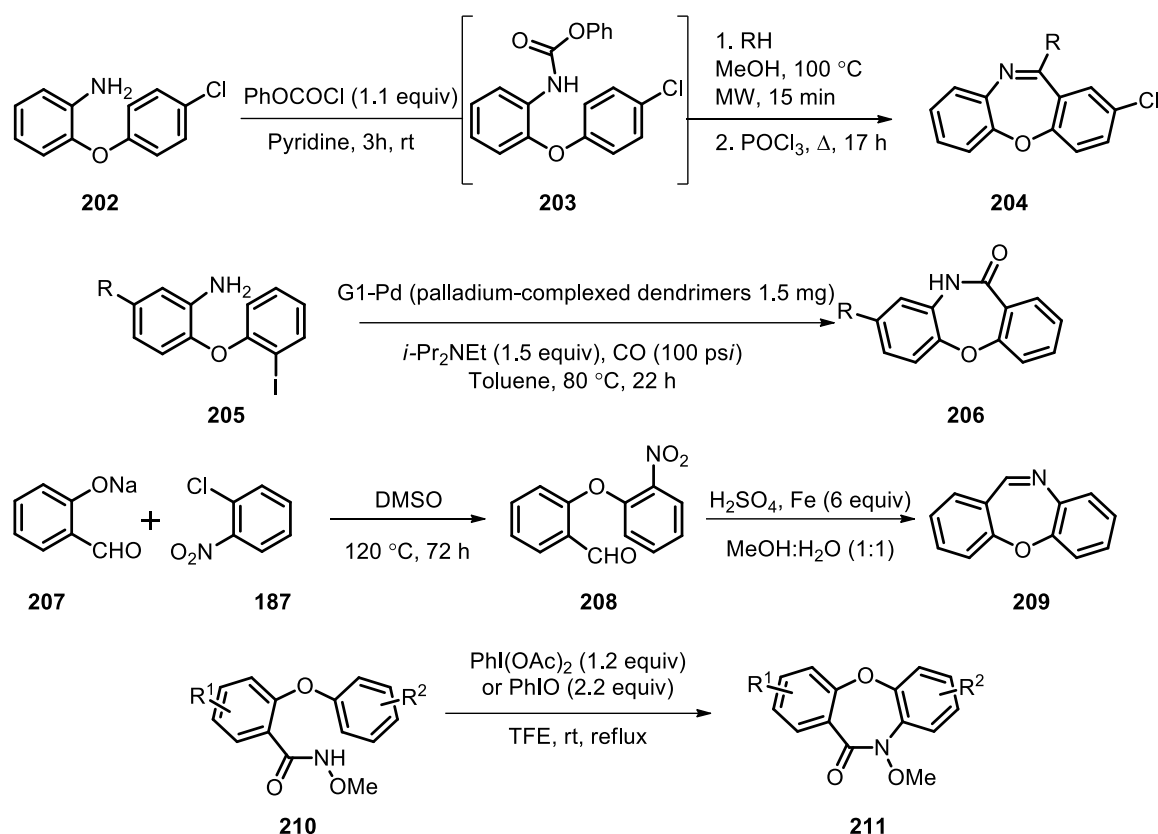
Scheme 1.3.1. Synthetic routes to dibenzoxazepines **182-191**.



Scheme 1.3.2. Synthetic routes to dibenzoxazepines **194-201**.

In recent years, metal-catalyzed C-O and C-N bond coupling reaction has also found application in the synthesis of dibenzoxazepine core. For instance, Buchwald and Tselikhovsky developed a novel sequence of Ullmann etherification of 2-hydroxyaryl ketones/carboxylates **193** with 1,2-dihaloarenes **192** and palladium-catalyzed amination using ammonia solution followed by intramolecular imine/amide formation to afford dibenzoxazepines/ones **194** (Scheme 1.3.2).¹¹² Shen *et al.* reported a one-pot palladium-catalyzed aminocarbonylation/ $\text{S}_{\text{N}}\text{Ar}$ sequence for the synthesis of dibenzo[*b,e*][1,4]oxazepin-11(5*H*)-ones **196** from 2-aminophenols **190** and 2-bromofluorobenzenes **195** (Scheme 1.3.2).¹¹³ Kitching *et al.* covered an efficient copper-initiated domino synthesis of dibenzoxazepinones **199** from 2-iodobenzamides **197** and 2-bromophenols **198** (Scheme 1.3.2).¹¹⁴ Later Ma and Zhu independently reported a directing group-assisted synthesis of dibenzoxazepinones.¹¹⁵ Moreover, Sang *et al.* established a copper (I) catalyzed highly efficient protocol for the synthesis of indole

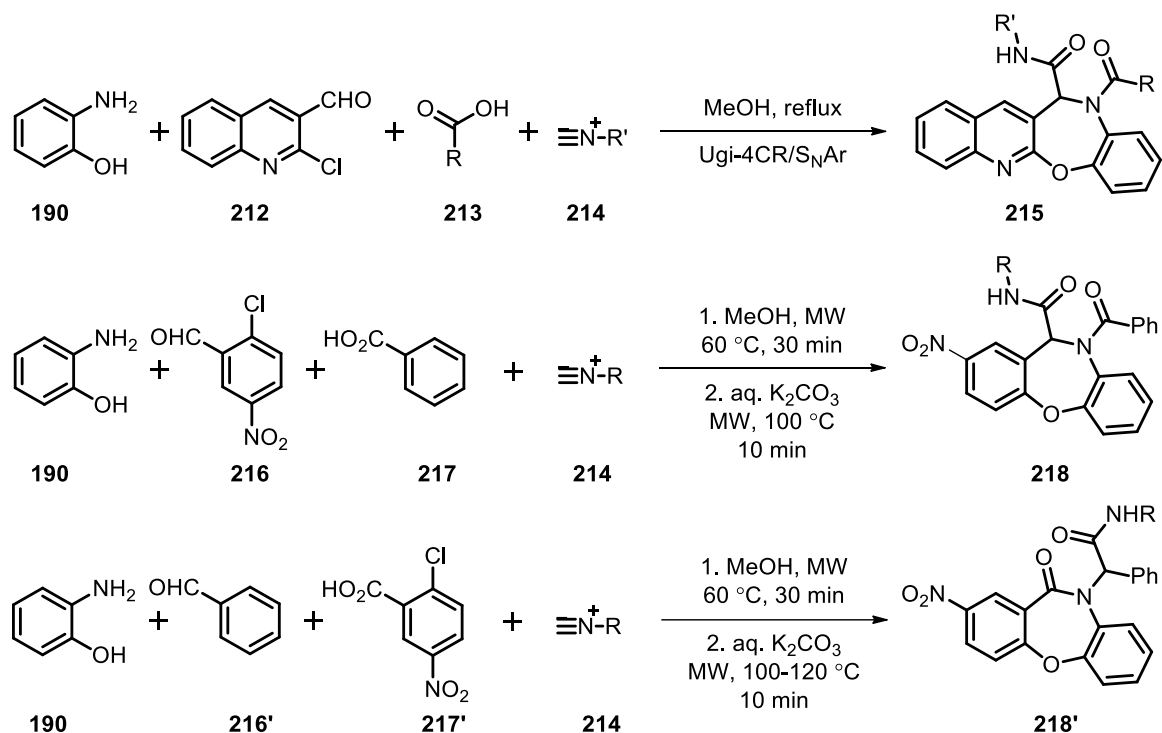
fused dibenzo[*b,f*][1,4]oxazepines **201**. This transformation involves Ullmann coupling of 2-(2-halophenyl)-1*H*-indoles **200** and 2-halophenols **198** and subsequent Smiles rearrangement to generate **201** (Scheme 1.3.2).¹¹⁶ Metal-catalyzed coupling and subsequent transformation were employed efficiently by Mitra's research group.¹¹⁷



Scheme 1.3.3. Synthetic routes to dibenzoxazepines **204-211**.

Key precursor formed from the diaryl etherification methodology served as a suitable substrate for various intramolecular transformations. Zaware *et al.* developed a novel protocol for the synthesis of 11-substituted dibenzo[*b,f*][1,4]oxazepines **204** from diaryl ether **202**. The key transformations include generation of a carbamate intermediate **203**, microwave assisted conversion of carbamate and subsequent cyclocondensation.¹¹⁸ A palladium-complexed dendrimers supported on silica has served as an efficient catalyst for the intramolecular cyclocarbonylation of substituted 2-(2-iodophenoxy)anilines **205**, a series of substituted dibenzo[*b,f*][1,4]oxazepin-11(10*H*)-ones **206** were prepared by Alper *et al.*¹¹⁹ Diaryl ether was also used as a suitable substrate for the reductive cyclization reaction.¹²⁰ Fakhraian *et al.* used etherification/reduction cyclization of sodium salt of salicylaldehyde **207** with 1-chloro-2-nitrobenzene **187** to furnish the corresponding benzoxazepine scaffolds **209** *via* the formation of diaryl ether **208**.^{120a} While a reduction

lactamisation sequence of diaryl ether was the approach followed by Bunce *et al.*^{120b} Microwave-assisted etherification and subsequent cyclocondensation were also employed by various research groups for the synthesis of dibenzoxazepines.¹²¹ Guo *et al.* reported a hypervalent iodine(III)-mediated oxidative cyclization of 2-(aryloxy)benzamides **210** under mild reaction conditions resulted in the formation of dibenzoxazepinone scaffolds **211**.¹²²



Scheme 1.3.4. Synthetic routes to dibenzoxazepines **215-218'**.

Post Ugi annulation was another interesting strategy used for the generation of dibenzoxazepine scaffolds.¹²³ Gandhi *et al.* developed a convenient and facile one-pot tandem Ugi-four component reaction (U-4CR)/S_NAr approach for the synthesis of highly functionalized diverse quino[2,3-*b*][1,5]benzoxazepines **215**. This involves the one-pot U-4CR of 2-chloroquinoline-3-carbaldehyde **212**, 2-aminophenol **190**, carboxylic acid **213** and isocyanide **214** which undergoes a tandem base-free S_NAr cyclization.^{123a} Microwave-assisted one-pot U-4CR and intramolecular *O*-arylation was developed by Xing *et al.* in 2006 for the synthesis of dibenzoxazepine scaffolds **218**. By reacting the functionalized benzaldehydes **216/216'** and benzoic acids **217/217'** along with aminophenol **190** and isocyanide **214**, the U-4CR products without isolation were treated with aqueous K₂CO₃ to promote the intramolecular S_NAr, leading to the formation of

benzoxazepine derivatives **218** and **218'** respectively.^{123b} Later they had employed microwave-assisted intramolecular Ullmann etherification as the post-Ugi annulation strategy for the efficient generation of a dibenz[*b,f*][1,4]oxazepine scaffold from suitably substituted aldehydes and benzoic acids.^{123c}

1.4. A brief history of Diindolymethanes (DIMs)

Indole, a nitrogen-containing heterocycle is ubiquitous in agrochemicals, pharmaceuticals and natural products with a plethora of biological activities. Disubstituted methane with two indole units commonly known as bis(indolyl)methane/diindolymethane (DIM) **219** is present in various natural products and pharmaceuticals. DIM is an active metabolite of indole-3-carbinol (I3C) **220**, a glucosinolate conjugate present in various *cruciferous* vegetables such as cabbage, broccoli, brussels sprouts, *etc* (Figure 1.4A). It is generally suggested that DIM mediates beneficial and functional activities of I3C.

1.4.1 Importance of DIMs

DIMs are ubiquitous heterocycles present in a variety of natural products and pharmaceutical ingredients and are considered as an important scaffold for drug discovery. Furthermore, DIMs and their analogues show a wide range of biological and pharmacological activities such as antioxidant, anti-inflammatory, antifungal, antibacterial, antibiotic, antiangiogenic and analgesic properties (Figure 1.4A).¹²⁴ For instance, Damodiran *et al.* synthesized a class of 1,4-disubstituted 1,2,3-bis-triazoles **221** from DIMs and found them active against *Staphylococcus aureus* and *Candida albicans*.^{124f} Kamal *et al.* reported an Al(OTf)₃ mediated synthesis of DIMs and found that the nitrofuryl BIM **222** showed a potent antifungal and antibacterial property.^{124e} Moreover, the antioxidant function of DIMs was studied by Li *et al.* and they demonstrated that these could effectively inhibit the NF-κB with corresponding reduction of oxidative stress.¹²⁴ⁱ The potent radical scavenging activity of 6-OMe substituted DIM **223** was reported by Benabadji *et al.* and was shown to be more potent than that of reference compound Vitamin E.^{124j} Cho *et al.* demonstrated the anti-inflammatory effect of DIM by the inhibition of lipopolysaccharide-induced release of proinflammatory mediators in murine macrophages.^{124h} Pillaiyaret *al.* evaluated the GPR84 agonist property of a class of synthesised DIMs and found that di-(5-fluoro-1*H*-indole-3-yl)methane **224** and di-(5,7-difluoro-1*H*-indole-3-yl)methane **225** displayed the highest activity in cAMP assays.^{124k}

In addition, they are also known to exhibit a broad spectrum of antiproliferative effects on various tumours by targeting a wide spectrum of signalling pathways with effective concentrations in the range of 1–100 μM .¹²⁵ The compound has been evaluated recently for phase II clinical trial for stage I/II prostate cancer, and has also been assessed for phase III clinical study for cervical dysplasia.^{126,127} The synergistic effect of DIM with paclitaxel can effectively promote the apoptosis in human breast cancer cells through G2M phase cell-cycle arrest.¹²⁸ The anticancer potential of I3C, DIM, and its derivatives were reviewed by various research groups.^{125e-j} For example Safe and his research group extensively studied the anticancer effect of DIM derivatives in different cell lines. In 2007, they reported that DIM and 1,1-bis(3'-indolyl)-1-(*p*-substitutedphenyl)methanes(C-DIMs), such as *p-t*-butyl derivative(DIM-C-*p*Ph*t*Bu) **226** inhibit the growth of Panc-1 and Panc-28 pancreatic cancer cells through endoplasmic reticulum stress-dependent upregulation of death receptor DR5.^{125o} Another C-DIM analog, bromophenyl derivative (DIM-C-*p*PhBr) **227** was reported to induce apoptosis and endoplasmic reticulum stress in pancreatic and colon cancer cells.^{125k-n} The study on antiandrogenic activity of dihalo DIMs **228** suggest that it may become the basis for the development of novel agents for clinical treatment against hormone-sensitive prostate cancer.^{125p} C-DIMs were effectively tested against different cancer lines and have shown potent activity.¹²⁹

The effect of I3C and DIM on type 2 diabetes mellitus was also studied by different research groups.¹³⁰ Lee *et al.* in 2017 examined the effect of DIMs on adipogenesis using 3T3-L1 adipocytes and *Caenorhabditis elegans* and found that DIM suppressed adipogenesis using AMPK α -dependent mechanism.¹³¹ More recently Choi *et al.* reported that DIM enhanced glucose uptake through upregulation of insulin signalling pathway, has resulted in greater glucose transporter 4 (GLUT4) expression.¹³² Also, DIM and its derivatives are good plant growth promoters¹³³ and potent inhibitors of *Leishmania donovani* topoisomerase I.¹³⁴

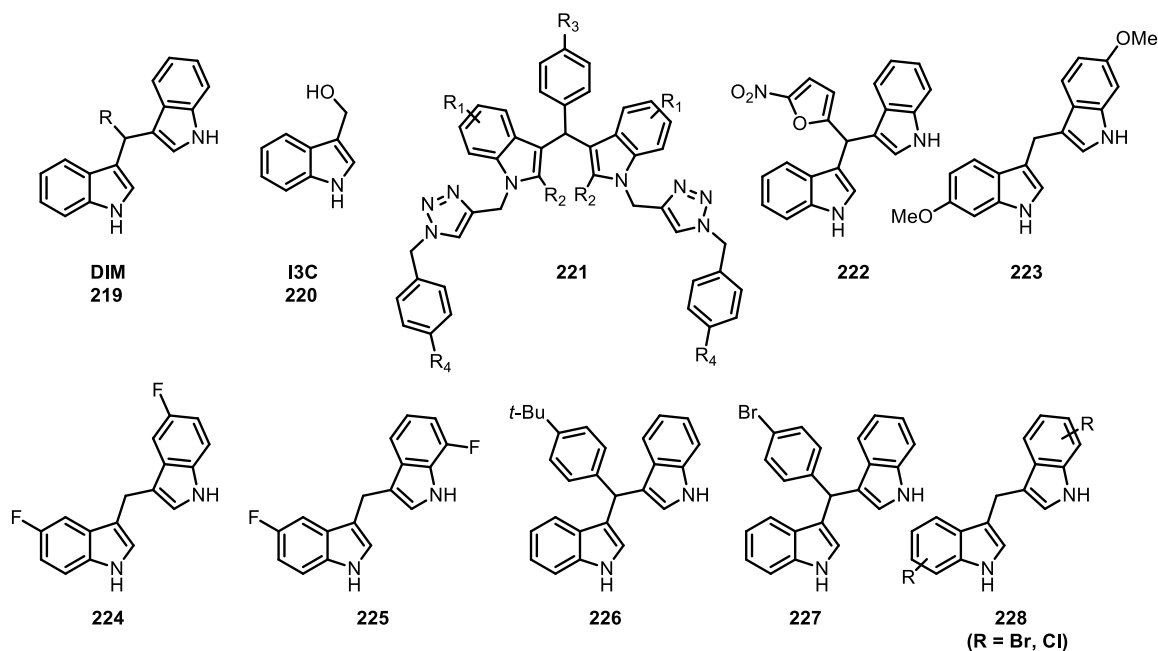


Figure 1.4A. Structure of DIM, I3C along with biologically active DIM derivatives.

Natural derivatives of DIM were also isolated and reported for biological activities.¹³⁵ For example, vibrindole A, isolated from marine bacterium *Vibrio parahaemolyticus* showed antimicrobial and hemolytic activities.^{135b} Kobayashi *et al.* reported another antibiotic DIM derivative trisindoline, isolated from *Vibrio sp.*, which was in turn separated from a marine sponge *Hyrtios altum*.^{135c} In 1994, Khuzhaev *et al.* reported the isolation of the dimeric alkaloid arundine from the roots of *Arundo donax*.^{135d} Later in 2003 Veluri *et al.* reported the isolation of 1,1,3-tris(3-indolyl)butane, along with arundine and tris(1*H*-indol-3-yl)methane from a North Sea bacterium *Vibrio parahaemolyticus*.^{135e} Cai *et al.* isolated the two indole alkaloids, arsendolines A and B from a marine-derived bacterium strain of *Aeromonas sp.*, and arsendoline B showed cytotoxicity against A-549 cell lines with an IC₅₀ value of 22.6 μM.^{135f} Osawa and Namiki reported the isolation and structural elucidation of streptindole, a novel genotoxic metabolite isolated from intestinal bacteria *Streptococcus faecium*.^{135g}

Moreover, A class of Indole-carbazoles was reported as a glass-forming high triplet energy material (2.97–2.99 eV) by Kirkus *et al.*,¹³⁶ Whereas He *et al.* and Martínez *et al.* independently reported the use of oxidized BIMs as selective colorimetric sensors.¹³⁷ More recently Lafzi *et al.* reported the efficiency of tetraphenylethene conjugated DIMs as an aggregation induced emissive material.¹³⁸

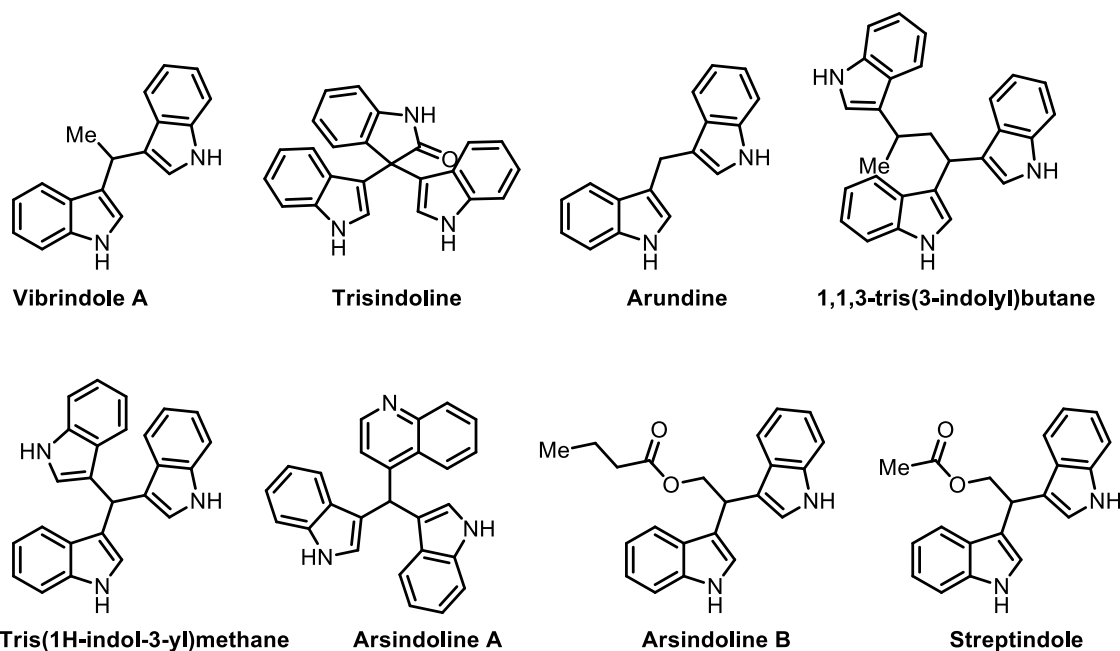
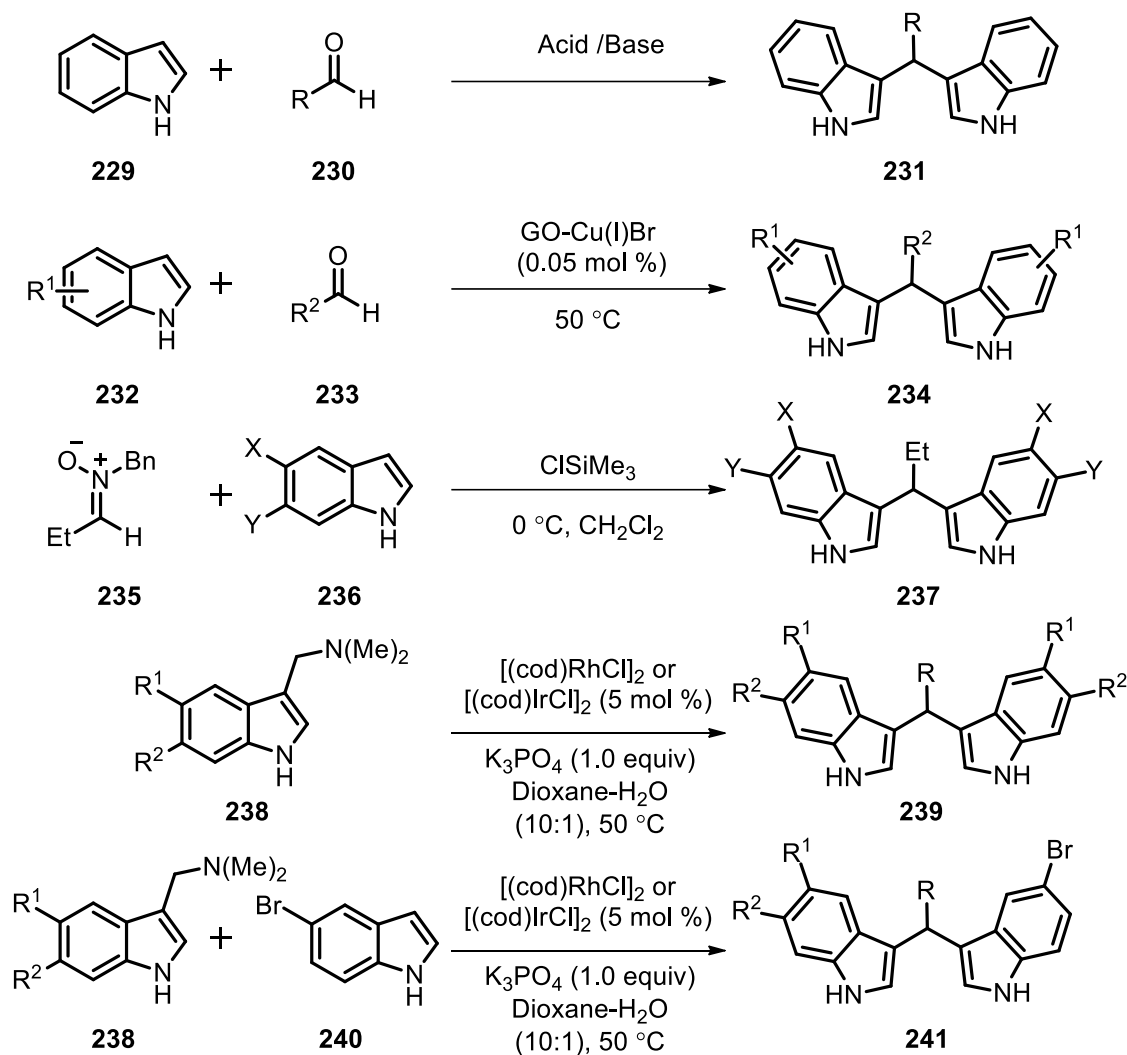


Figure 1.4B. DIM isolated from natural sources.

1.3.2. Synthetic routes to DIMs

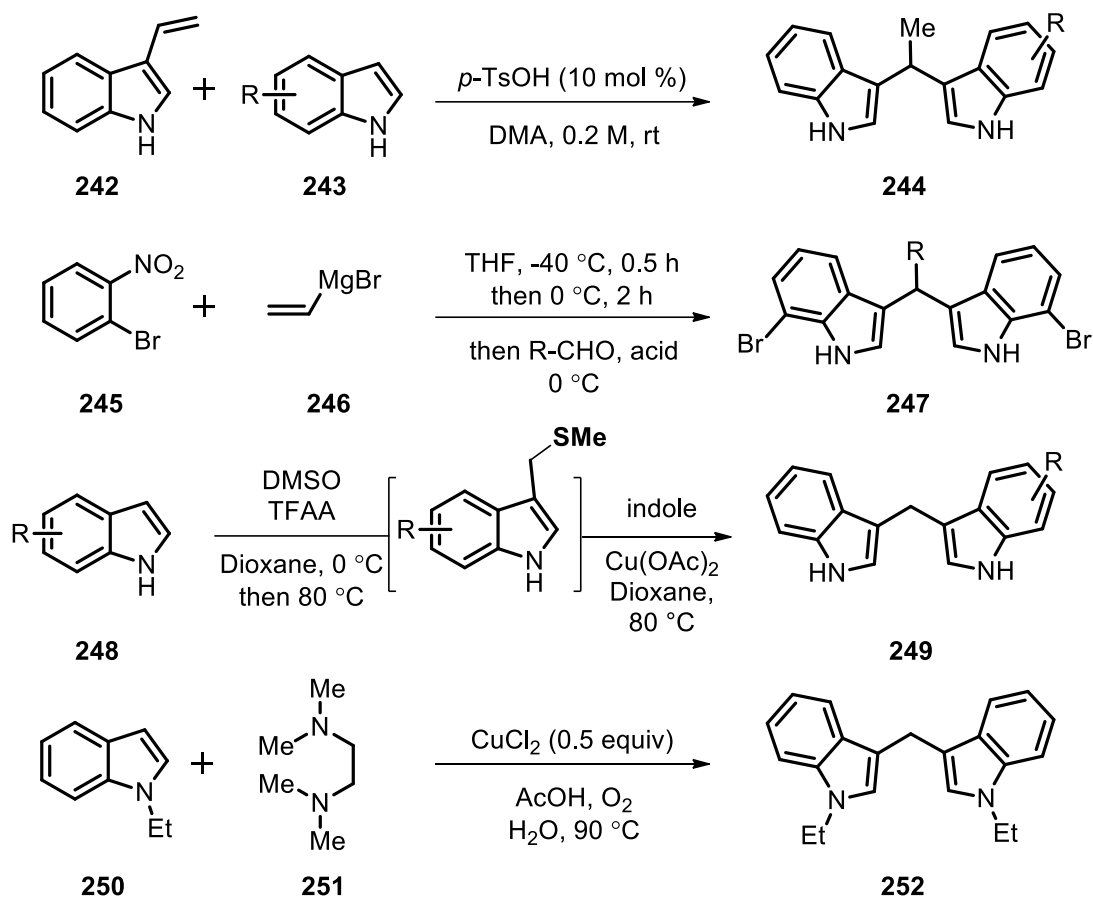
Owing to its wide occurrence in biological compounds, many approaches have been developed for the preparation of DIMs. The classical and simple method for the synthesis of symmetrical DIM **231** is the condensation of indole **229** with aldehyde or ketones **230** in the presence of acids or bases.¹³⁹ A variety of protic or Lewis acid catalysts and catalytic reagents are used for mediating this synthesis and this have been reviewed by Shiri *et al.* in 2010.¹⁴⁰ Various acids like acetic acid (AcOH), silica-supported sodium hydrogen sulphate (NaHSO₄.SiO₂), trifluoroacetic acid (TFA), zeolite, iron(III)chloride (FeCl₃.6H₂O), lanthanide triflate, *etc.* were successfully utilized for the synthesis of DIMs. Ionic liquids and other catalysts like tetrabutylammonium hydrogen sulphate, phase transfer catalyst, graphene oxide decorated with Cu(I)Br nanoparticles, triethylborane, Fe/Al pillared clay, *etc.* were also employed for the synthesis of DIMs.¹⁴¹ For instance, Srivastava *et al.* successfully applied graphene oxide decorated with Cu(I)Br (GO-Cu(I)Br) nanoparticles for the synthesis of symmetric DIM **234** from substituted indole **232** and aldehyde **233** (Scheme 1.4.1).^{141e} The synthesised DIMs **234** have been screened for the anti-HIV activity. Mendes *et al.* developed a green and efficient method for the synthesis of DIM **234** using ammonium niobium oxalate (ANO) NH₄[NbO(C₂O₄)₂(H₂O)_x].nH₂O as a catalyst.¹⁴²



Scheme 1.4.1. Synthetic routes to DIM **231-241**.

In addition to the simple condensation method of indole and aldehyde/ketone, several other approaches are also reported in the literature.¹⁴³ Chalaye-Mauger *et al.* in 2000 reported the utilisation of nitrones for the synthesis of DIM. According to their approach, nitrones **235** can react with substituted indoles **236** in the presence of ClSiMe₃ to furnish substituted DIMs **237**.^{143b} de la Herrán *et al.* demonstrated the rhodium or iridium complex-catalyzed reaction of gramines (3-aminomethylindoles) **238** to form the symmetric DIM **239**. The reaction of gramines **238** with 5-bromoindole **240** under the same condition yielded unsymmetrical DIM **241** (Scheme 1.4.1).^{143c} Pathak *et al.* reported a *p*-TsOH catalysed hydroarylation of vinyl indoles **242** with exogenous nucleophile like substituted indole **243** to access biologically relevant DIM derivatives **244** (Scheme 1.4.2).^{143d} Abe *et al.* developed a one pot approach for the synthesis of DIM **247** through the Bartoli indole reaction of nitrobenzene **245** with vinyl magnesium bromide **246**

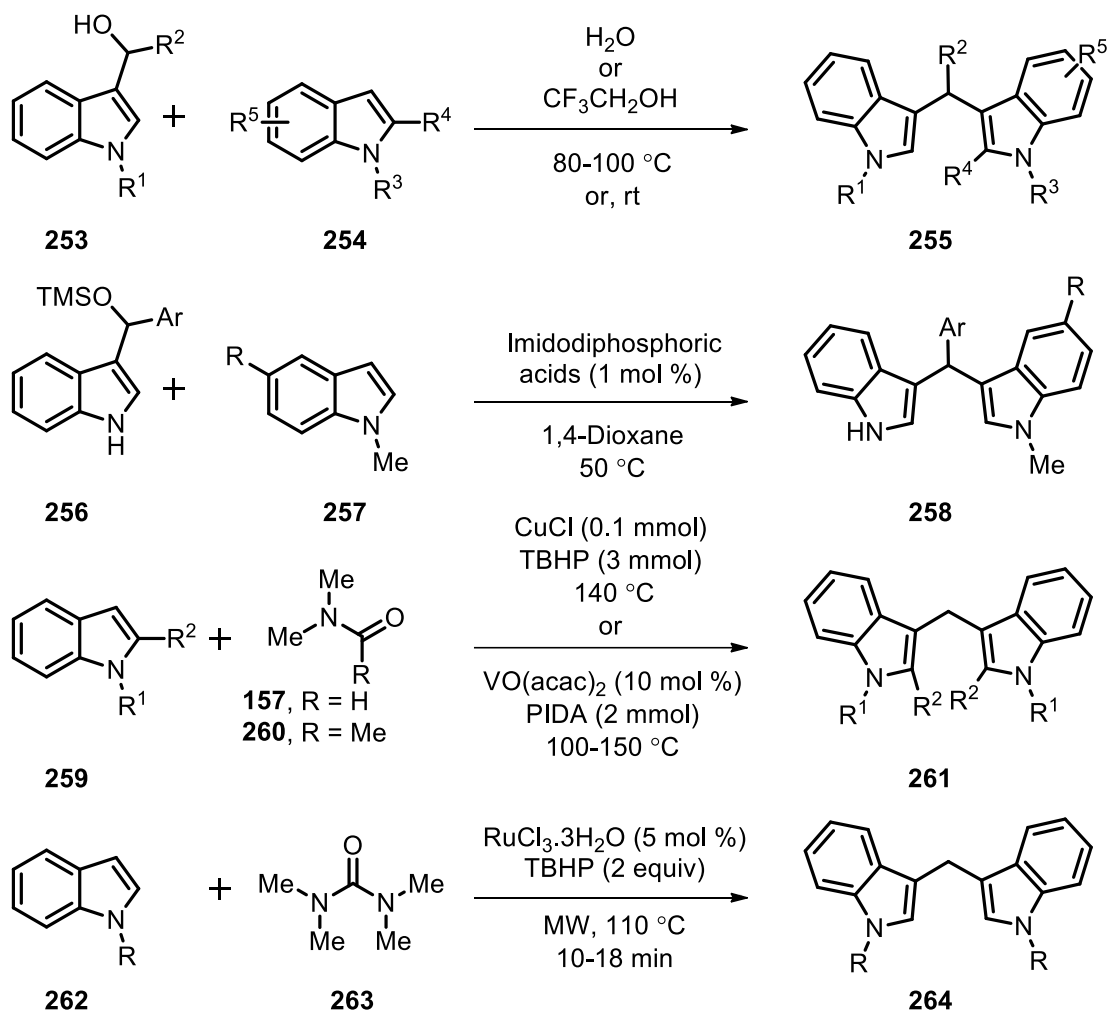
(Scheme 1.4.2).^{143f} The same group developed another one pot synthesis of DIM **249** via the intermolecular Pummerer reaction of indole **248** in the presence of DMSO and trifluoroacetic acid in 2014 (Scheme 1.4.2).^{143e} A green, simple, and efficient protocol for the selective methylenation of indoles **250** by using tetramethylethylenediamine **251** (TMEDA) as a carbon source in water was reported by Zhao *et al.* in 2013. The reaction involves a copper (II)-catalyzed C–H (sp³) bond oxidation and C–N bond cleavage to yield a series of DIMs **252** (Scheme 1.4.2).^{143g}



Scheme 1.4.2. Synthetic routes to DIM **244-252**.

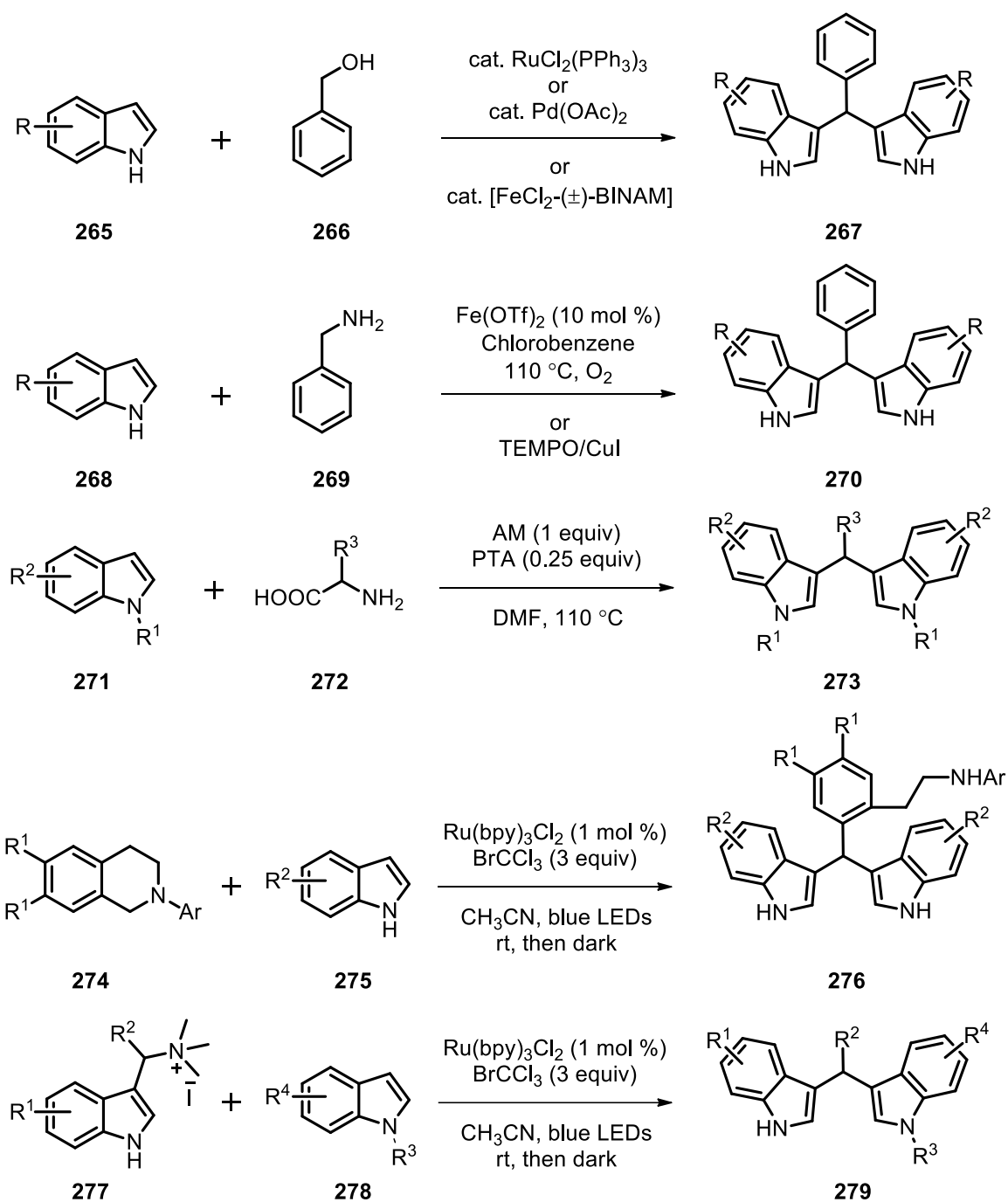
Recently, Xiao *et al.* reported a catalyst-free, environmental benign dehydrative S_N¹-type reaction of indolyl alcohols **253** with indole nucleophile **254** both on water and trifluoroethanol for the synthesis of DIMs **255** (Scheme 1.4.3).¹⁴⁴ Interestingly, the first enantioselective synthesis of DIM **258** was accomplished by Zhuo *et al.* in 2014. Their approach involved chiral imidodiphosphoric acids catalyzed Friedel–Crafts reaction of indole **257** with trimethylsilyl protected 3-arylindolylmethanol **256** (Scheme 1.4.3).¹⁴⁵ Pu *et al.* and Kaswan *et al.* independently reported the transition metal-catalyzed DIM **261**

synthesis using DMF **157** and dimethylacetamide **260** (DMA) as methylene sources respectively from substituted indole **259** (Scheme 1.4.3).¹⁴⁶ Later in 2016, Deb *et al.* demonstrated the effective utilisation of tetramethylurea **263** as methylene precursor under microwave-assisted ruthenium-catalyzed cross dehydrogenative coupling of indoles **262** to DIM **264** (Scheme 1.4.3).¹⁴⁷



Scheme 1.4.3. Synthetic routes to DIM **255-264**.

Apart from these alcohols, amines, amino acids, *etc.* were successfully employed for the synthesis of DIMs. Various groups successfully attempted the alkylation of indoles **265** with primary alcohols **266** in the presence of transition metal catalysts to furnish substituted DIMs **267** (Scheme 1.4.4).¹⁴⁸



Scheme 1.4.4. Synthetic routes to DIM **267-279**.

A novel approach for synthesis of DIMs **270** has been developed by Gopalaiah *et al.* under iron-catalysed oxidative coupling of benzylamines **269** and indoles **268** (Scheme 1.4.4).¹⁴⁹ Whereas Liao *et al.* recently reported the same reaction catalysed by TEMPO/CuI.¹⁵⁰ A decarboxylative deaminative coupling reaction of amino acids **272** with indoles **271** was reported for the efficient synthesis of DIMs **273** by Xiang *et al.* in 2015 (Scheme 1.4.4). The reaction is mediated by alloxan monohydrate (AM) as additive and catalysed by phosphotungstic acid, 44-hydrate (PTA).¹⁵¹ In addition, visible light

induced ring opening functionalization of tetrahydroisoquinolines **274** with indoles **275** was developed recently by Chen *et al.* in 2017 for the synthesis of biologically active DIM derivatives **276** (Scheme 1.4.4).¹⁵² More recently, Pillaiyar *et al.* reported a general synthetic approach for unsymmetrical azaDIMs **279**.¹⁵³ The strategy involves the reaction of readily accessible (3-indolylmethyl)trimethylammonium iodides **277** with azaindole **278** in water (Scheme 1.4.4).

1.5. Conclusion and present work

Nowadays heterocycles are common structural units in many of the marketed drugs and medicinal chemistry targets in the drug discovery process. In the recent years there has been growing interest in synthesis of heterocyclic compounds with excellent biological activity. 1,2-dihydropyridines (1,2-DHP), dibenzoxazepines and diindolylmethanes (DIM) are three commonly known heterocycles. Nevertheless, the biological and photophysical properties of 1,2-DHP, a well known synthetic intermediate, is not explored as that of its analogue 1,4-DHP. Dibenzoxazepines are well explored for their biological properties; however, studies on the synthetic methods under metal-free conditions are not much reported. The anticancer and antimicrobial properties of diindolylmethane were well reported, however, the structure-activity relationship studies on the derivatives of DIM are also important, which will assist to develop a DIM derivative with improved activity. In this context, my thesis work involve the design and synthesis of three types of heterocycles *viz.* 1,2-dihydropyridines, dibenzoxazepines and diindolylmethanes, and exploration of their biological activity and related aspects. **Chapter 2** comprise design, synthesis and application of new 1,2-DHP based fluorophores. A four-component condensation reaction using dienaminodioate, aldehyde, an *in situ* generated hydrazone in presence of trifluoroacetic acid, modification of our previous report, was employed for the synthesis. The design offers various sites for appendage to bioactives or functionalities required for conjugation. The photophysical properties of 1,2-DHPs were studied in detail, and demonstrated its application as mitochondria staining and sensing of protein tyrosin phosphatases. **Chapter 3** focuses on the development of an unprecedented one-pot method for the synthesis of dibenzoxazepines from tertiary amines mediated by hypervalent iodine reagent. Tertiary amines with suitably substituted *ortho*-hydroxybenzyl and phenyl groups is exploited to facilitate *ortho*-C(sp²)-H functionalization to afford diaryl ethers in presence of phenyliodine diacetate. The methodology was further extended to synthesise a number of molecular motifs. Whereas,

Chapter 4 deals with structure activity relationship study of diindolylmethane derivatives. The design and synthesis of three libraries of DIM was based on the conjugation of DIM with biaryl and diaryl ethers and substituents on indole and biaryl.

1.6. References

- (1) Moss, G. P.; Smith, P. A. S.; Tavernier, D. Glossary of class names of organic compounds and reactive intermediates based on structure. *Pure Appl. Chem.* **1995**, *67*, 1307–1375.
- (2) Katritzky, A. R.; Denisko, O. V. Heterocyclic compound, general aspects of heterocyclic compounds. *Encyclopædia Britannica, inc.*; 2014; pp 1–31.
- (3) Campaigne, E. Contemporary history series: Adrien albert and the rationalization of heterocyclic chemistry. *J. Chem. Educ.* **1986**, *63*, 860–863.
- (4) Lagoja, I. M. Pyrimidine as constituent of natural biologically active compounds. *Chem. Biodivers.* **2005**, *2*, 1–50.
- (5) (a) Pozharskii, A. F.; Soldatenkov, A. T.; Katritzky, A. R. *Heterocycles in Life and Society: An Introduction to Heterocyclic Chemistry, Biochemistry and Applications*; 2011. (b) Saini, M. S.; Kumar, A.; Dwivedi, J.; Singh, R. A review : Biological significance of heterocyclic compounds. *Int. J. Pharma Sci. Res.* **2013**, *4*, 66–77. (c) Dua, R.; Shrivastava, S.; Sonwane, S. K.; Srivastava, S. K. Pharmacological significance of synthetic heterocycles scaffold: A review. *Adv. Biol. Res.* **2011**, *5*, 120–144. (d) Hote, S. V; Bhojar, S. P. Heterocyclic compound- A review. *IOSR J. Appl. Chem.* **2014**, *2014*, 43–46. (e) Arora, P.; Arora, V.; Lamba, H. S.; Wadhwa, D. Importance of heterocyclic chemistry: A review. *Int. J. Pharm. Sci. Res.* **2012**, *3*, 2947–2954. (f) Asif, M. A mini review: Biological significances of nitrogen hetero atom containing heterocyclic compounds. *Int. J. Bioorganic Chem.* **2017**, *2*, 146–152. (g) De, S.; Babu, N. M.; Babu, S. T.; Sree, B. R.; Kiran, S. A.; Reddy, K. S. K. A review article on importance of heterocyclic compounds. *Mintage J. Pharm. Med. Sci.* **2016**, *5*, 18–27. (h) Taylor, A. P.; Robinson, R. P.; Fobian, Y. M.; Blakemore, D. C.; Jones, L. H.; Fadeyi, O. Modern advances in heterocyclic chemistry in drug discovery. *Org. Biomol. Chem.*

- 2016**, *14*, 6611–6637. (i) Gandhi, D.; Priyanka, K.; Agarwal, S. Synthetic aspects and biological studies of some heterocycles. *Chem. Biol. Interface* **2017**, *7*, 79–101.
- (6) Kingston, W. Irish contributions to the origins of antibiotics. *Ir. J. Med. Sci.* **2008**, *177*, 87–92.
- (7) Bosch, F.; Rosich, L. The contributions of Paul Ehrlich to pharmacology: a tribute on the occasion of the centenary of his nobel prize. *Pharmacology* **2008**, *82*, 171–179.
- (8) Williams, K. The introduction of ‘chemotherapy’ using arsphenamine – the first magic bullet. *J. R. Soc. Med.* **2009**, *102*, 343–348.
- (9) (a) Aminov, R. I. A brief history of the antibiotic era: lessons learned and challenges for the future. *Front. Microbiol.* **2010**, *1*, 1–7. (b) Wright, P. M.; Seiple, I. B.; Myers, A. G. The evolving role of chemical synthesis in antibacterial drug discovery. *Angew. Chemie - Int. Ed.* **2014**, *53*, 8840–8869.
- (10) Pan, X.; He, Y.; Chen, T.; Chan, K. F.; Zhao, Y. Modified penicillin molecule with carbapenem-like stereochemistry specifically inhibits Class C β -lactamases. *Antimicrob. Agents Chemother.* **2017**, *61*, 1–16.
- (11) (a) Kesado, T.; Hashizume, T.; Asahi, Y. Antibacterial activities of a new stabilized thienamycin, *N*-formimidoyl thienamycin, in comparison with other antibiotics. *Antimicrob. Agents Chemother.* **1980**, *17*, 912–917. (b) Karlowsky, J. A.; Lob, S. H.; Kazmierczak, K.; Badal, R. E.; Young, K.; Motyl, M. R.; Sahm, D. F. *In vitro* activity of imipenem against Carbapenemase-Positive *Enterobacteriaceae* isolates collected by the SMART global surveillance program from 2008 to 2014. *J. Clin. Microbiol.* **2017**, *55*, 1638–1649. (c) Chen, P.; Seth, A. K.; Abercrombie, J. J.; Mustoe, T. A.; Leung, K. P. Activity of imipenem against *Klebsiella pneumoniae* biofilms *in vitro* and *in vivo*. *Antimicrob. Agents Chemother.* **2014**, *58*, 1208–1213.
- (12) (a) Duarte, Y.; Arevalo, B.; Martinez, G.; Matus, F.; Poblete, T.; Gutierrez, M.; Amigo, J.; Vallejos, G.; Astudillo, L. Nitrogen heterocycles as potential antibacterial agents. *Proc. 17th Int. Electron. Conf. Synth. Org. Chem.* **2013**, a035.

- (b) Sharma, P. K. A review: Antimicrobial agents based on nitrogen and sulfur containing heterocycles. *Asian J. Pharm. Clin. Res.* **2017**, *10*, 47–49.
- (13) (a) Butts, A.; Krysan, D. J. Antifungal drug discovery: something old and something new. *PLoS Pathog.* **2012**, *8*, e1002870. (b) Roemer, T.; Krysan, D. J. Antifungal drug development: challenges, unmet clinical needs, and new approaches. *Cold Spring Harb. Perspect. Med.* **2014**, *4*, a019703.
- (14) Blondelle, S.; Nefzi, A.; Ostresh, J. M.; Houghten, R. A. Novel antifungal compounds derived from heterocyclic positional scanning combinatorial libraries. *Pure Appl. Chem.* **1998**, *70*, 2141.
- (15) (a) Sondhi, S. M.; Dinodia, M.; Singh, J.; Rani, R. Heterocyclic compounds as anti-inflammatory agents. *Curr. Bioact. Compd.* **2007**, *3*, 91–108. (b) Sondhi, S. M.; Singhal, N.; Johar, M.; Reddy, B. S. N.; Lown, J. W. Heterocyclic compounds as inflammation inhibitors. *Curr. Med. Chem.* **2002**, *9*, 1045–1074. (c) Cristina, A.; Leonte, D.; Vlase, L.; Bencze, L. C.; Imre, S.; Marc, G.; Apan, B.; Mogosan, C.; Zaharia, V. Heterocycles 48. Synthesis, characterization and biological evaluation of imidazo[2,1-*b*][1,3,4]thiadiazole derivatives as anti-inflammatory agents. *Molecules* **2018**, *23*, 2425.
- (16) Kuo, S.; Huang, L.-J.; Nakamura, H. Studies on heterocyclic compounds. 6. Synthesis and analgesic and antiinflammatory activities of 3,4-dimethylpyrano[2,3-*c*]pyrazol-6-one derivatives. *J. Med. Chem.* **1984**, *27*, 539–544.
- (17) Fairlamb, A. H.; Ridley, R. G.; Vial, H. J. *Drugs against parasitic diseases: R&D methodologies and issues Discoveries and drug development*; 2003.
- (18) (a) Azam, A.; Peerzada, M. N.; Ahmad, K. Parasitic diarrheal disease: drug development and targets. *Front. Microbiol.* **2015**, *6*, 1183. (b) Debnath, A.; McKerrow, J. H. Editorial: drug development for parasite-induced diarrheal diseases. *Front. Microbiol.* **2017**, *8*, 577–579.
- (19) Martins, P.; Jesus, J.; Santos, S.; Raposo, L. R.; Roma-Rodrigues, C.; Baptista, P. V.; Fernandes, A. R. Heterocyclic anticancer compounds: recent advances and the paradigm shift towards the use of nanomedicine's tool box. *Molecules* **2015**, *20*, 16852–16891.

- (20) Rajesh, E.; Sankari, L.; Malathi, L.; Krupaa, J. Naturally occurring products in cancer therapy. *J. Pharm. Bioallied Sci.* **2015**, *7*, S181.
- (21) (a) Lamberth, C. Pyrazole chemistry in crop protection. *Heterocycles* **2007**, *71*, 1467–1502. (b) Lamberth, C. Heterocyclic chemistry in crop protection. *Pest Manag. Sci.* **2013**, *69*, 1106–1114. (c) Suvarna Arunkumar, S. A review on synthetic heterocyclic compounds in agricultural and other applications. *Int. J. PharmTech Res.* **2015**, *8*, 170–179.
- (22) (a) Eisner, U.; Kuthan, J. The chemistry of dihydropyridines. *Chem. Rev.* **1972**, *72*, 1–42. (b) Stout, D. M.; Meyers, A. I. Recent advances in the chemistry of dihydropyridines. *Chem. Rev.* **1982**, *82*, 223–243. (c) Lavilla, R. Recent developments in the chemistry of dihydropyridines. *J. Chem. Soc. Perkin 1* **2002**, *2*, 1141–1156. (d) Silva, E. M. P.; Varandas, P. A. M. M.; Silva, A. M. S. Developments in the synthesis of 1,2-dihydropyridines. *Synthesis* **2013**, *45*, 3053–3089.
- (23) Hantzsch, A. Ueber die synthese pyridinartiger verbindungen aus acetessigäther und aldehydammoniak. *Justus Liebig's Ann. der Chemie* **1882**, *215*, 1–82.
- (24) Kuthan, J.; Kurfürst, A. Development in dihydropyridine chemistry. *Ind. Eng. Chem. Prod. Res. Dev.* **1982**, *21*, 191–261.
- (25) (a) Safak, C.; Simsek, R. Fused 1,4-dihydropyridines as potential calcium modulatory compounds. *Mini-Reviews Med. Chem.* **2006**, *6*, 747–755. (b) Wang, A. L.; Iadecola, C.; Wang, G. New generations of dihydropyridines for treatment of hypertension. *J. Geriatr. Cardiol.* **2017**, *14*, 67–72. (c) Drapak, I.; Perekhoda, L.; Tsapko, T.; Berezniakova, N.; Tsapko, Y. Cardiovascular calcium channel blockers: historical overview, development and new approaches in design. *J. Heterocycl. Chem.* **2017**, *54*, 2117–2128. (d) Bandyopadhyay, D.; Salazar, T.; Gonzalez, A. Dihydropyridines as calcium channel blockers: An overview. *J. Anal. Pharm. Res.* **2017**, *5*, 3–6. (e) Edraki, N.; Mehdipour, A. R.; Khoshneviszadeh, M.; Miri, R. Dihydropyridines: evaluation of their current and future pharmacological applications. *Drug Discov. Today* **2009**, *14*, 1058–1066. (f) Zarrin, A.; Mehdipour, A. R.; Miri, R. Dihydropyridines and multidrug resistance: previous attempts, present state, and future trends. *Chem. Biol. Drug Des.* **2010**, *76*, 369–381.

- (26) Sharma, V. K.; Singh, S. K. Synthesis, utility and medicinal importance of 1,2- & 1,4-dihydropyridines. *RSC Adv.* **2017**, *7*, 2682–2732.
- (27) Domány, G.; Matúz, J.; Sághy, K.; Ezer, E. 1,2-dihydropyridine derivatives as potential antiulcer agents. *Eur. J. Med. Chem.* **1993**, *28*, 633–636.
- (28) Wang, D.; Hu, S.; Zhang, J.; Li, Q.; Liu, X.; Li, Y. Investigation of the neuroprotective effects of a novel synthetic compound *via* the mitochondrial pathway. *Mol. Med. Rep.* **2017**, *16*, 1133–1138.
- (29) (a) Sales, M.; Charette, A. B. A Diels–Alder approach to the stereoselective synthesis of 2,3,5,6-tetra- and 2,3,4,5,6-pentasubstituted piperidines. *Org. Lett.* **2005**, *7*, 5773–5776. (b) Regio- and stereoselective 1,2-dihydropyridine alkylation/addition sequence for the synthesis of piperidines with quaternary centers. *Angew. Chemie - Int. Ed.* **2014**, *53*, 3877–3880. (c) Lemire, A.; Grenon, M.; Pourashraf, M.; Charette, A. B. Nucleophilic addition to 3-substituted pyridinium salts: expedient syntheses of (–)-L-733,061 and (–)-CP-99,994. *Org. Lett.* **2004**, *6*, 3517–3520. (d) Pelletier, G.; Constantineau-Forget, L.; Charette, A. B. Directed functionalization of 1,2-dihydropyridines: stereoselective synthesis of 2,6-disubstituted piperidines. *Chem. Commun.* **2014**, *50*, 6883–6885.
- (30) Young, D. W.; Comins, D. L.; Carolina, N. Tandem directed lithiations of *N*-Boc-1,2-dihydropyridines toward highly functionalized 2,3-dihydro-4-pyridones. *Org. Lett.* **2005**, *7*, 5661–5664.
- (31) (a) Comins, D. L.; Zhang, Y. M. Anionic cyclizations of chiral 2,3-dihydro-4-pyridones: a five-step, asymmetric synthesis of indolizidine 209D. *J. Am. Chem. Soc.* **1996**, *118*, 12248–12249. (b) Comins, D. L.; Joseph, S. P.; Zhang, Y. M. Regio- and stereoselective intramolecular Heck reactions of *N*-acyl-2,3-dihydro-4-pyridones. *Tetrahedron Lett.* **1996**, *37*, 793–796. (c) Comins, D. L.; Lamunyon, D. H.; Chen, X. Enantiopure *N*-acyldihydropyridones as synthetic intermediates: asymmetric syntheses of indolizidine alkaloids (–)-205A, (–)-207A, and (–)-235B. *J. Org. Chem.* **1997**, *62*, 8182–8187. (d) Comins, D. L.; Chen, X.; Morgan, L. A. Enantiopure *N*-acyldihydropyridones as synthetic intermediates: asymmetric synthesis of (–)-septicine and (–)-tylophorine. *J. Org. Chem.* **1997**, *62*, 7435–7438. (e) Comins, D. L.; Zhang, Y. M.; Zheng, X. Photochemical reactions of chiral 2,3-

- dihydro-4(1*H*)-pyridones: asymmetric synthesis of (-)-perhydrohistrionicotoxin. *Chem. Commun.* **1998**, *4*, 2509–2510. (f) Comins, D. L.; Green, G. M. Asymmetric synthesis of dienomyacin C. *Tetrahedron Lett.* **1999**, *40*, 217–218. (g) Kuethe, J. T.; Comins, D. L.; Carolina, N. The Mukaiyama-Michael reaction of *N*-acyl-2,3-dihydro-4-pyridones: regio- and stereoselective synthesis of *cis*-2,6-disubstituted 1,2,5,6-tetrahydropyridines. *Org. Lett.* **1999**, *1*, 1031–1033. (h) Comins, D. L.; Fulp, A. B. Enantiopure *N*-acyldihydropyridones as synthetic intermediates: asymmetric synthesis of (-)-slaframine. *Org. Lett.* **1999**, *1*, 1941–1943. (i) Comins, D. L.; Brooks, C. A.; Al-awar, R. S.; Goehring, R. R. IMDA/retro-Mannich approach to *cis*-perhydroquinoline lycopodium alkaloids: asymmetric synthesis of (+)-luciduline. *Org. Lett.* **1999**, *1*, 229–231. (j) Comins, D. L.; Zhang, Y. M.; Joseph, S. P. Enantiopure *N*-acyldihydropyridones as synthetic intermediates: asymmetric synthesis of benzomorphans. *Org. Lett.* **1999**, *1*, 657–659. (k) Kuethe, J. T.; Comins, D. L. Addition of metallo enolates to chiral 1-acylpyridinium salts: total synthesis of (+)-cannabisativine. *Org. Lett.* **2000**, *2*, 855–857. (l) Comins, D. L.; Sandelier, M. J.; Grillo, T. A. Asymmetric synthesis of (+)-deoxoprosopinine. *J. Org. Chem.* **2001**, *66*, 6829–6832. (m) Comins, D. L.; Huang, S.; McArdle, C. L.; Ingalls, C. L. Enantiopure 2,3-dihydro-4-pyridones as synthetic intermediates: a concise asymmetric synthesis of (+)-allopumiliotoxin 267A. *Org. Lett.* **2001**, *3*, 469–471.
- (32) Chen, M.; Chen, Y.; Sun, N.; Zhao, J.; Liu, Y.; Li, Y. Gold-catalyzed oxidative ring expansion of 2-alkynyl-1,2-dihydropyridines or -quinolines: highly efficient synthesis of functionalized azepine or benzazepine scaffolds. *Angew. Chemie - Int. Ed.* **2015**, *54*, 1200–1204.
- (33) (a) Silva, E. M. P.; Rocha, D. H. A.; Silva, A. M. S. Diels-Alder reactions of 1,2-dihydropyridines: an efficient tool for the synthesis of isoquinuclidines. *Synthesis* **2018**, *50*, 1773–1782. (b) Martin, R. M.; Bergman, R. G.; Ellman, J. A. Synthesis of isoquinuclidines from highly substituted dihydropyridines *via* the Diels-Alder reaction. *Org. Lett.* **2013**, *15*, 444–447. (c) Krow, G. R.; Huang, Q.; Szczepanski, S. W.; Hausheer, F. H.; Carroll, P. J. Stereoselectivity in Diels-Alder reactions of diene-substituted *N*-alkoxycarbonyl-1,2-dihydropyridines. *J. Org. Chem.* **2006**, *68*, 2571–2578. (d) Nakano, H.; Osone, K.; Takeshita, M.; Kwon, E.; Seki, C.; Matsuyama, H.; Takano, N.; Kohari, Y. A novel chiral oxazolidine organocatalyst

- for the synthesis of an oseltamivir intermediate using a highly enantioselective Diels-Alder reaction of 1,2-dihydropyridine. *Chem. Commun.* **2010**, *46*, 4827–4829.
- (34) (a) Kabouche, A.; Kabouche, Z. Bioactive diterpenoids of *Salvia* species. *Stud. Nat. Prod. Chem.* **2008**, *35*, 753–833. (b) Jana, G. K.; Sinha, S. Total synthesis of ibogaine, epiibogaine and their analogues. *Tetrahedron* **2012**, *68*, 7155–7165. (c) Sundberg, R. J.; Hong, J.; Smith, S. Q.; Sabat, M.; Tabakovic, I. Synthesis and oxidative fragmentation of catharanthine analogs. Comparison to the fragmentation - coupling of catharanthine and vindoline. *Tetrahedron* **1998**, *54*, 6259–6292. (d) Satoh, N.; Akiba, T.; Yokoshima, S.; Fukuyama, T. A practical synthesis of (–)-oseltamivir. *Angew. Chemie - Int. Ed.* **2007**, *46*, 5734–5736.
- (35) Takenaka, N.; Huang, Y.; Rawal, V. H. The first catalytic enantioselective Diels-Alder reactions of 1,2-dihydropyridine: efficient syntheses of optically active 2-azabicyclo[2.2.2]octanes with chiral BINAM derived Cr(III) salen complexes. *Tetrahedron* **2002**, *58*, 8299–8305.
- (36) (a) Kutney, J. P.; Noda, M.; Lewis, N. G.; Monteiro, B.; Mostowicz, D.; Worth, B. R. Dihydropyridines in synthesis and biosynthesis. V. synthesis of pyridocarbazole alkaloids: olivacine and (±)-guatambuine. *Can. J. Chem.* **1982**, *60*, 2426–2430. (b) Comins, D. L.; Myoung, Y. C. Synthesis and synthetic utility of 1-acyl-5-(trialkylsilyl)-1,2-dihydropyridines. Synthesis of (±)-elaekanine A. *J. Org. Chem.* **1990**, *55*, 292–298. (c) Charette, A. B.; Grenon, M.; Lemire, A.; Pourashraf, M.; Martel, J. Practical and highly regio- and stereoselective synthesis of 2-substituted dihydropyridines and piperidines: application to the synthesis of (–)-coniine. *J. Am. Chem. Soc.* **2001**, *123*, 11829–11830.
- (37) Shen, L.; Cao, S.; Wu, J.; Zhang, J.; Li, H.; Liu, N.; Qian, X. A revisit to the Hantzsch reaction: unexpected products beyond 1,4-dihydropyridines. *Green Chem.* **2009**, *11*, 1414–1420.
- (38) Koike, T.; Shinohara, Y.; Ishibashi, N.; Takeuchi, N.; Tobinaga, S. Synthesis of 2-substituted 3-nitro-1,2-dihydropyridines by heterocyclic annulation reactions of a *sec*-nitrodienamine with aldehyde compounds. *Chem. Pharm. Bull.* **2000**, *48*, 436–439.

- (39) Monguchi, D.; Majundar, S.; Kawabata, T. Synthesis of chiral 1,2-dihydropyridines and 2,3,4-trisubstituted pyridines from α -amino acids. *Heterocycles* **2006**, *68*, 2571–2578.
- (40) Yoshida, K.; Inokuma, T.; Takasu, K.; Takemoto, Y. Brønsted acid-thiourea co-catalysis: asymmetric synthesis of functionalized 1,4-dihydropyridines from β -enamino esters and α,β -unsaturated aldehydes. *Synlett* **2010**, *2010*, 1865–1869.
- (41) Wan, J.; Gan, S.; Sun, G.; Pan, Y. Novel regioselectivity: three-component cascade synthesis of unsymmetrical 1,4- and 1,2-dihydropyridines. *J. Org. Chem.* **2009**, *74*, 2862–2865.
- (42) Fowler, F. W. Synthesis of 1,2- and 1,4-dihydropyridines. *J. Org. Chem.* **1972**, *37*, 1321–1323.
- (43) Sundberg, R. J.; Hamilton, G.; Trindle, C. Synthesis and Diels-Alder reactions of *N*-carbalkoxydihydropyridines. Substituent effects on the regiochemistry of reduction of *N*-carbalkoxy-pyridinium ions. *J. Org. Chem.* **1986**, *51*, 3672–3679.
- (44) Booker, E.; Eisner, U. Reduction of 3,5-disubstituted pyridines to dihydropyridine. *J. Chem. Soc., Perkin Trans. 1* **1975**, 929–931.
- (45) Knaus, E. E.; Redda, K. The sodium borohydride reduction of *N*-sulfonylpyridinium salts. Synthesis of *N*-sulfonyl- 1,4- (1,2-) dihydropyridines. *Can. J. Chem.* **1977**, *55*, 1788–1791.
- (46) Kutney, J. P.; Badger, R. A.; Cullen, W. R.; Greenhouse, R.; Noda, M.; Ridaura-Sanz, V. E.; So, Y. H.; Zandarotti, A.; Worth, B. R. Dihydropyridines in synthesis and biosynthesis. II. Stable tricarbonylchromium(0) complexes. *Can. J. Chem.* **1979**, *57*, 300–303.
- (47) (a) Davies, S. G.; Edwards, A. J.; Shipton, M. R. Tricarbonylpyridinechromium complexes: stereoselective alkylations and aldol-type reactions involving α -carbanions derived from η -tricarbonyl(2-alkylpyridine)chromium complexes. *J. Chem. Soc., Perkin Trans. 1* **1991**, 1009–1017. (b) Davies, S. G.; Shipton, M. R. Tricarbonyl(pyridine)chromium complexes: conversion into tricarbonyl(dihydropyridine)chromium complexes *via* regio- and stereo-selective nucleophilic addition reactions. *J. Chem. Soc. Perkin Trans. 1* **1991**, 757–764.

- (48) (a) Donohoe, T. J.; McRiner, A. J.; Sheldrake, P. Partial reduction of electron-deficient pyridines. *Org. Lett.* **2000**, *2*, 3861–3863. (b) Donohoe, T. J.; McRiner, A. J.; Helliwell, M.; Sheldrake, P. Use of dissolving metals in the partial reduction of pyridines: formation of 2-alkyl-1,2-dihydropyridines. *J. Chem. Soc. Perkin I* **2001**, 1435–1445.
- (49) (a) Donohoe, T. J.; Johnson, D. J.; Mace, L. H.; Bamford, M. J.; Ichihara, O. Partial reduction of pyridinium salts as a versatile route to dihydropyridones. *Org. Lett.* **2005**, *7*, 435–437. (b) Donohoe, T. J.; Johnson, D. J.; MacE, L. H.; Thomas, R. E.; Chiu, J. Y. K.; Rodrigues, J. S.; Compton, R. G.; Banks, C. E.; Tomcik, P.; Bamford, M. J.; Ichihara, O. The ammonia-free partial reduction of substituted pyridinium salts. *Org. Biomol. Chem.* **2006**, *4*, 1071–1084. (c) Donohoe, T. J.; Connolly, M. J.; Walton, L. Regioselective nucleophilic addition to pyridinium salts: a new route to substituted dihydropyridones. *Org. Lett.* **2009**, *11*, 5562–5565. (d) Donohoe, T. J.; Connolly, M. J.; Rathi, A. H.; Walton, L. Intramolecular hydride addition to pyridinium salts: new routes to enantiopure dihydropyridones. *Org. Lett.* **2011**, *13*, 2074–2077.
- (50) Schroif-Gregoire, C.; Travert, N.; Zaparucha, A.; Al-Mourabit, A. Direct access to marine pyrrole-2-aminoimidazoles, oroidin, and derivatives, *via* new acyl-1,2-dihydropyridin intermediates. *Org. Lett.* **2006**, *8*, 2961–2964.
- (51) Kita, Y.; Maekawa, H.; Yamasaki, Y.; Nishiguchi, I. Selective and facile electroreductive synthesis of dihydro- and tetrahydropyridine dicarboxylic acid derivatives. *Tetrahedron Lett.* **1999**, *40*, 8587–8590.
- (52) Bull, J. A.; Mousseau, J. J.; Pelletier, G.; Charette, A. B. Synthesis of pyridine and dihydropyridine derivatives by regio- and stereoselective addition to *N*-activated pyridines. *Chem. Rev.* **2012**, *112*, 2642–2713.
- 53) Comins, D. L.; Hong, H.; Salvador, J. M. An efficient asymmetric synthesis of 1-acyl-2-alkyl-1,2-dihydropyridines. *J. Org. Chem.* **1991**, *56*, 7197–7199.
- (54) Al-awar, R. S.; Joseph, S. P.; Comins, D. L. Conversion of *N*-acyl-2,3-dihydro-4-pyridones to 4-chloro-1,2-dihydropyridines using the Vilsmeier reagent. *Tetrahedron Lett.* **1992**, *33*, 7635–7638.

- (55) (a) Hoesl, C. E.; Maurus, M.; Pabel, J.; Polborn, K.; Wanner, K. T. Generation of chiral *N*-acylpyridinium ions by means of silyl triflates and their diastereoselective trapping reactions: formation of *N*-acyldihydropyridines and *N*-acyldihydropyridones. *Tetrahedron* **2002**, *58*, 6757–6770. (b) T. Wanner, K.; E. Hoesl, C.; Pabel, J.; Polborn, K. Synthesis of sterically demanding 3-silylpyridines and their use in asymmetric synthesis with chiral *N*-acyliminium ions. *Heterocycles* **2002**, *58*, 383.
- (56) Bennasar, M.-L.; Juan, C.; Bosch, J. Addition of organocopper reagents to *N*-alkylpyridinium salts. A flexible access to polysubstituted dihydropyridines. *Tetrahedron Lett.* **2001**, *42*, 585–588.
- (57) Lavilla, R.; Gotsens, T.; Guerrero, M.; Masdeu, C.; Santano, M. C.; Minguillón, C.; Bosch, J. Azole additions upon azinium salts. *Tetrahedron* **1997**, *53*, 13959–13968.
- (58) Crotti, S.; Berti, F.; Pineschi, M. Copper-catalyzed Perkin–acyl–Mannich reaction of acetic anhydride with pyridine: expeditious entry to unconventional piperidines. *Org. Lett.* **2011**, *13*, 5152–5155.
- (59) (a) Lee, K. Y.; Lee, M. J.; Kim, J. N. Efficient introduction of aryl acetylenes to quinolinium and pyridinium salts: synthesis of 1-acyl-1,2-dihydroquinolines and 1-acyl-1,2-dihydropyridines. *Bull. Korean Chem. Soc.* **2005**, *26*, 665–667. (b) Loh, T.-P.; Lye, P.-L.; Wang, R.-B.; Sim, K.-Y. A Highly regioselective indium-mediated allylation of pyridine derivatives: synthesis of (±)-dihydropinidine from pyridine. *Tetrahedron Lett.* **2000**, *41*, 7779–7783.
- (60) Sun, Z.; Yu, S.; Ding, Z.; Ma, D. Enantioselective addition of activated terminal alkynes to 1-acylpyridinium salts catalyzed by Cu–bis(oxazoline) complexes. *J. Am. Chem. Soc.* **2007**, *129*, 9300–9301.
- (61) Black, D. A.; Beveridge, R. E.; Arndtsen, B. A. Copper-catalyzed coupling of pyridines and quinolines with alkynes: a one-step, asymmetric route to functionalized heterocycles. *J. Org. Chem.* **2008**, *73*, 1906–1910.
- (62) Christian, N.; Aly, S.; Belyk, K. Rhodium-catalyzed enantioselective addition of boronic acids to *N*-benzylnicotinate salts. *J. Am. Chem. Soc.* **2011**, *133*, 2878–

2880.

- (63) Ichikawa, E.; Suzuki, M.; Yabu, K.; Albert, M.; Kanai, M.; Shibasaki, M. New entries in Lewis acid–Lewis base bifunctional asymmetric catalyst: catalytic enantioselective Reissert reaction of pyridine derivatives. *J. Am. Chem. Soc.* **2004**, *126*, 11808–11809.
- (64) (a) Oshima, K.; Ohmura, T.; Suginome, M. Palladium-catalyzed regioselective silaboration of pyridines leading to the synthesis of silylated dihydropyridines. *J. Am. Chem. Soc.* **2011**, *133*, 7324–7327. (b) Oshima, K.; Ohmura, T.; Suginome, M. Regioselective synthesis of 1,2-dihydropyridines by rhodium-catalyzed hydroboration of pyridines. *J. Am. Chem. Soc.* **2012**, *134*, 3699–3702.
- (65) De Lera, A. R.; Reischl, W.; Okamura, W. H. On the thermal behavior of Schiff bases of retinal and its analogs: 1,2-dihydropyridine formation via six- π -electron electrocyclic ring closure of 13-*cis* isomers. *J. Am. Chem. Soc.* **1989**, *111*, 4051–4063.
- (66) (a) Tanaka, K.; Katsumura, S. Highly stereoselective asymmetric 6π -azaelectrocyclization utilizing the novel 7-alkyl substituted *cis*-1-amino-2-indanols: formal synthesis of 20-epiuleine. *J. Am. Chem. Soc.* **2002**, *124*, 9660–9661. (b) Tanaka, K.; Kobayashi, T.; Mori, H.; Katsumura, S. Development of highly stereoselective asymmetric 6π -azaelectrocyclization of conformationally flexible linear 1-azatrienes. From determination of multifunctional chiral amines, 7-alkyl *cis*-1-amino-2-indanols, to application as a new synthetic strategy: formal synthesis of 20-epiuleine. *J. Org. Chem.* **2004**, *69*, 5906–5925.
- (67) (a) Sklenicka, H. M.; Hsung, R. P.; Wei, L. L.; McLaughlin, M. J.; Gerasyuto, A. I.; Degen, S. J. Highly stereoselective formal [3+3] cycloaddition reactions of chiral vinylogous amides with α,β -unsaturated iminiums. *Org. Lett.* **2000**, *2*, 1161–1164. (b) Sydorenko, N.; Hsung, R. P.; Vera, E. L. Torquoselective 6π -electron electrocyclic ring closure of 1-azatrienes containing acyclic chirality at the *C*-terminus. *Org. Lett.* **2006**, *8*, 2611–2614.
- (68) (a) Palacios, F.; Perez de Heredia, I.; Rubiales, G. Synthesis and reactivity of electron-poor 2-azadienes. [4+2] cycloaddition reactions with alkenes and enamines. *J. Org. Chem.* **1995**, *60* (8), 2384–2390. (b) Palacios, F.; Alonso, C.; Rubiales, G.; Ezpeleta, J. M. Cycloaddition reactions of neutral 2-azadienes with

- enamines – regiospecific synthesis of highly substituted dihydropyridines and pyridines. *Eur. J. Org. Chem.* **2001**, 2001, 2115–2122.
- (69) Colby, D. A.; Bergman, R. G.; Ellman, J. A. Synthesis of dihydropyridines and pyridines from imines and alkynes *via* C–H activation. *J. Am. Chem. Soc.* **2008**, *130*, 3645–3651.
- (70) (a) Yamakawa, T.; Yoshikai, N. Annulation of α,β -unsaturated imines and alkynes *via* cobalt-catalyzed olefinic C–H activation. *Org. Lett.* **2013**, *15*, 196–199. (b) Fallon, B. J.; Garsi, J.-B.; Derat, E.; Amatore, M.; Aubert, C.; Petit, M. Synthesis of 1,2-dihydropyridines catalyzed by well-defined low-valent cobalt complexes: C–H activation made simple. *ACS Catal.* **2015**, *5*, 7493–7497.
- (71) Liu, H.; Zhang, Q.; Wang, L.; Tong, X. PPh₃-catalyzed [2+2+2] and [4+2] annulations: synthesis of highly substituted 1,2-dihydropyridines (DHPs). *Chem. Commun.* **2010**, *46*, 312–314.
- (72) Harschneck, T.; Kirsch, S. F. One-pot synthesis of 1,2-dihydropyridines: expanding the diverse reactivity of propargyl vinyl ethers. *J. Org. Chem.* **2011**, *76*, 2145–2156.
- (73) (a) Tejedor, D.; Méndez-Abt, G.; García-Tellado, F. A convenient domino access to substituted alkyl 1,2-dihydropyridine-3-carboxylates from propargyl enol ethers and primary amines. *Chem. Eur. J.* **2010**, *16*, 428–431. (b) Wei, H.; Wang, Y.; Yue, B.; Xu, P.-F. Synthesis of substituted 1,2-dihydropyridines from propargyl vinyl ethers and allenic vinyl ethers by gold-catalyzed Claisen rearrangement and 6π -aza-electrocyclization. *Adv. Synth. Catal.* **2010**, *352*, 2450–2454. (c) Tejedor, D.; Cotos, L.; Méndez-Abt, G.; García-Tellado, F. General synthesis of substituted 1,2-dihydropyridines. *J. Org. Chem.* **2014**, *79*, 10655–10661.
- (74) Xin, X.; Wang, D.; Wu, F.; Li, X.; Wan, B. Cyclization and *N*-iodosuccinimide-induced electrophilic iodocyclization of 3-aza-1,5-enynes to synthesize 1,2-dihydropyridines and 3-iodo-1,2-dihydropyridines. *J. Org. Chem.* **2013**, *78*, 4065–4074.
- (75) Trost, B. M.; Biannic, B. redox cycloisomerization approach to 1,2-dihydropyridines. *Org. Lett.* **2015**, *17*, 1433–1436.

- (76) Dai, H.; Yu, S.; Cheng, W.; Xu, Z.-F.; Li, C.-Y. Rhodium-catalyzed synthesis of 1,2-dihydropyridine by a tandem reaction of 4-(1-acetoxyallyl)-1-sulfonyl-1,2,3-triazole. *Chem. Commun.* **2017**, *53*, 6417–6420.
- (77) Matsumura, Y.; Nakamura, Y.; Maki, T.; Onomura, O. New enantiomerically pure 1,2-dihydropyridine and its use for construction of optically active 2-azabicyclo[2.2.2]octane. *Tetrahedron Lett.* **2000**, *41*, 7685–7689.
- (78) Motamed, M.; Bunnelle, E. M.; Singaram, S. W.; Sarpong, R. Pt(II)-catalyzed synthesis of 1,2-dihydropyridines from aziridiny propargylic esters. *Org. Lett.* **2007**, *9*, 2167–2170.
- (79) Ogoshi, S.; Ikeda, H.; Kurosawa, H. Formation of an aza-nickelacycle by reaction of an imine and an alkyne with nickel(0): oxidative cyclization, insertion, and reductive elimination. *Angew. Chemie Int. Ed.* **2007**, *46*, 4930–4932.
- (80) Wender, P. A.; Pedersen, T. M.; Scanio, M. J. C. Transition metal-catalyzed hetero-[5+2] cycloadditions of cyclopropyl imines and alkynes: dihydroazepines from simple, readily available starting materials. *J. Am. Chem. Soc.* **2002**, *124*, 15154–15155.
- (81) Adak, L.; Chan, W. C.; Yoshikai, N. Nickel-catalyzed, directing-group-assisted [2+2+2] cycloaddition of imine and alkynes. *Chem. Asian J.* **2011**, *6*, 359–362.
- (82) Amatore, M.; Leboeuf, D.; Malacria, M.; Gandon, V.; Aubert, C. Highly enantioselective rhodium-catalyzed [2+2+2] cycloaddition of diynes to sulfonimines. *J. Am. Chem. Soc.* **2013**, *135*, 4576–4579.
- (83) Frutos, M. R.; Álvarez, E.; Díaz-Requejo, M. M.; Pérez, P. J. Selective synthesis of *N*-substituted 1,2-dihydropyridines from furans by copper-induced concurrent tandem catalysis. *J. Am. Chem. Soc.* **2010**, *132*, 4600–4607.
- (84) Brunner, B.; Stogaitis, N.; Lautens, M. Synthesis of 1,2-dihydropyridines using vinyloxiranes as masked dienolates in imino-aldol reactions. *Org. Lett.* **2006**, *8*, 3473–3476.
- (85) Yavari, I.; Bayat, M. J.; Sirouspour, M.; Souri, S. One-pot synthesis of highly functionalized 1,2-dihydropyridines from primary alkylamines, alkyl isocyanides,

- and acetylenic esters. *Tetrahedron* **2010**, *66*, 7995–7999.
- (86) Ramaraju, P.; Mir, N. A.; Singh, D.; Gupta, V. K.; Kant, R.; Kumar, I. Enantioselective synthesis of *N*-PMP-1,2-dihydropyridines *via* formal [4+2] cycloaddition between aqueous glutaraldehyde and imines. *Org. Lett.* **2015**, *17*, 5582–5585.
- (87) Shao, Y.; Zhu, K.; Qin, Z.; Li, E.; Li, Y. Lewis acid-catalyzed cyclization of enamines with propargylic alcohols: regioselective synthesis of multisubstituted 1,2-dihydropyridines. *J. Org. Chem.* **2013**, *78*, 5731–5736.
- (88) Liu, Y.-W.; Xie, Y.-B.; Li, D.-J.; Wang, L. Efficient iron-catalyzed synthesis of polysubstituted 1,2-dihydropyridine derivatives. *Russ. J. Gen. Chem.* **2015**, *85*, 2163–2166.
- (89) Koley, S.; Chowdhury, S.; Chanda, T.; Janaki Ramulu, B.; Samai, S.; Motisa, L.; Singh, M. S. Lewis acid mediated three-component one-flask regioselective synthesis of densely functionalized 4-amino-1,2-dihydropyridines *via* cascade Knoevenagel/Michael/cyclization sequence. *Tetrahedron* **2015**, *71*, 301–307.
- (90) Cao, S.; Xin, L.; Liu, Y.; Wan, J.-P.; Wen, C. Regioselective three-component reactions of enamines, 2-aminopyridines and enals for the synthesis of 1,2-dihydropyridines. *RSC Adv.* **2015**, *5*, 27372–27374.
- (91) Xie, Y.-B.; Ye, S.-P.; Chen, W.-F.; Hu, Y.-L.; Li, D.-J.; Wang, L. Brønsted-acid-catalyzed multicomponent one-pot reaction: efficient synthesis of polysubstituted 1,2-dihydropyridines. *Asian J. Org. Chem.* **2017**, *6*, 746–750.
- (92) Wan, J. P.; Lin, Y.; Jing, Y.; Xu, M.; Liu, Y. Selectivity tunable divergent synthesis of 1,4- and 1,2-dihydropyridines *via* three-component reactions. *Tetrahedron* **2014**, *70*, 7874–7880.
- (93) Challa, C.; John, M.; Lankalapalli, R. S. Cascade synthesis of 1,2-dihydropyridine from dienaminodioxide and an imine: a three-component approach. *Tetrahedron Lett.* **2013**, *54*, 3810–3812.
- (94) Choudhary, S.; Pawar, A. P.; Yadav, J.; Sharma, D. K.; Kant, R.; Kumar, I. One-pot synthesis of chiral tetracyclic dibenzo[*b,f*][1,4]oxazepine-fused 1,2-

- dihydropyridines (DHPs) under metal-free conditions. *J. Org. Chem.* **2018**, *83*, 9231–9239.
- (95) Evans, B. E.; Rittle, K. E.; Bock, M. G.; DiPardo, R. M.; Freidinger, R. M.; Whitter, W. L.; Lundell, G. F.; Veber, D. F.; Anderson, P. S.; Chang, R. S. L.; Lotti, V. J.; Cerino, D. J.; Chen, T. B.; Kling, P. J.; Kunkel, K. A.; Springer, J. P.; Hirshfield, J. Methods for drug discovery: development of potent, selective, orally effective cholecystokinin antagonists. *J. Med. Chem.* **1988**, *31*, 2235–2246.
- (96) (a) Popovic, D.; Nuss, P.; Vieta, E. Revisiting loxapine: a systematic review. *Ann. Gen. Psychiatry* **2015**, *14*, 15. (b) Heel, R. C.; Brogden, R. N.; Speight, T. M.; Avery, G. S. Loxapine: a review of its pharmacological properties and therapeutic efficacy as an antipsychotic agent. *Drugs* **1978**, *15*, 198–217. (c) Currier, G.; Walsh, P. Safety and efficacy review of inhaled loxapine for treatment of agitation. *Clin. Schizophr. Relat. Psychoses* **2013**, *7*, 25–32. (d) Jue, S. G.; Dawson, G. W.; Brogden, R. N. Amoxapine: a review of its pharmacology and efficacy in depressed states. *Drugs* **1982**, *24*, 1–23.
- (97) Gijssen, H. J. M.; Berthelot, D.; Zaja, M.; Brône, B.; Geuens, I.; Mercken, M. Analogues of morphanthridine and the tear gas dibenz[*b,f*][1,4]oxazepine (CR) as extremely potent activators of the human transient receptor potential ankyrin 1 (TRPA1) channel. *J. Med. Chem.* **2010**, *53*, 7011–7020.
- (98) (a) Hallinan, E. A.; Hagen, T. J.; Husa, R. K.; Tsymbalov, S.; Rao, S. N.; VanHoeck, J. P.; Rafferty, M. F.; Stapelfeld, A.; Savage, M. A.; Reichman, M. *N*-substituted dibenzoxazepines as analgesic PGE₂ antagonists. *J. Med. Chem.* **1993**, *36*, 3293–3299. (b) Hallinan, E. A.; Hagen, T. J.; Tsymbalov, S.; Husa, R. K.; Lee, A. C.; Stapelfeld, A.; Savage, M. A. Aminoacetyl moiety as a potential surrogate for diacylhydrazine group of SC-51089, a potent PGE₂ antagonist, and its analogs. *J. Med. Chem.* **1996**, *39*, 609–613. (c) Hallinan, E. A.; Hagen, T. J.; Tsymbalov, S.; Stapelfeld, A.; Savage, M. A. 2,4-Disubstituted oxazoles and thiazoles as latent pharmacophores for diacylhydrazine of SC-51089, a potent PGE₂ antagonist. *Bioorg. Med. Chem.* **2001**, *9*, 1–6.
- (99) Smits, R. A.; Lim, H. D.; Stegink, B.; Bakker, R. A.; de Esch, I. J. P.; Leurs, R. Characterization of the histamine H₄ receptor binding site. Part 1. Synthesis and

- pharmacological evaluation of dibenzodiazepine derivatives. *J. Med. Chem.* **2006**, *49*, 4512–4516.
- (100) Dols, P. P. M. A.; Folmer, B. J. B.; Hamersma, H.; Kuil, C. W.; Lucas, H.; Ollero, L.; Rewinkel, J. B. M.; Hermkens, P. H. H. SAR study of 2,3,4,14b-tetrahydro-1H-dibenzo[*b,f*]pyrido[1,2-*d*][1,4]oxazepines as progesterone receptor agonists. *Bioorg. Med. Chem. Lett.* **2008**, *18*, 1461–1467.
- (101) (a) Jain, M. S.; Surana, S. J. Synthesis and evaluation of antipsychotic activity of 11-(4'-(*N*-aryl carboxamido/*N*-aryl- α -phenyl-acetamido)-piperazinyl)-dibenz[*b,f*][1,4]-oxazepine derivatives. *Arab. J. Chem.* **2017**, *10*, S2032–S2039. (b) Lotesta, S. D.; Marcus, A. P.; Zheng, Y.; Leftheris, K.; Noto, P. B.; Meng, S.; Kandpal, G.; Chen, G.; Zhou, J.; McKeever, B.; Bukhtiyarov, Y.; Zhao, Y.; Lala, D. S.; Singh, S. B.; McGeehan, G. M. Identification of spirooxindole and dibenzoxazepine motifs as potent mineralocorticoid receptor antagonists. *Bioorg. Med. Chem.* **2016**, *24*, 1384–1391. (c) Lynch, S. M.; Tafesse, L.; Carlin, K.; Ghatak, P.; Kyle, D. J. Dibenzazepines and dibenzoxazepines as sodium channel blockers. *Bioorg. Med. Chem. Lett.* **2015**, *25*, 43–47.
- (102) (a) Khlebnikov, A. F.; Novikov, M. S.; Petrovskii, P. P.; Konev, A. S.; Yufit, D. S.; Selivanov, S. I.; Frauendorf, H. Stereoselective cycloaddition of dibenzoxazepinium ylides to acetylenes and fullerene C₆₀. Conformational behavior of 3-aryldibenzo[*b,f*]pyrrolo[1,2-*d*][1,4]oxazepine systems. *J. Org. Chem.* **2010**, *75*, 5211–5215. (b) Zhang, J.-Q.; Qi, Z.-H.; Yin, S.-J.; Li, H.-Y.; Wang, Y.; Wang, X.-W. Brønsted or Lewis acid initiated multicomponent cascade reaction: diastereoselective synthesis of imidazolidinyl spirooxindole derivatives. *ChemCatChem* **2016**, *8*, 2797–2807. (c) Khlebnikov, A. F.; Novikov, M. S.; Petrovskii, P. P.; Magull, J.; Ringe, A. Dibenzoxazepinium ylides: facile access and 1,3-dipolar cycloaddition reactions. *Org. Lett.* **2009**, *11*, 979–982.
- (103) Nagarajan, K.; David, J.; Kaul, C. L.; Maller, R. K.; Rao, R. R.; Grewal, R. S. Sintamil -a new dibenzoxazepine antidepressant. *Indian J. Physiol. Pharmacol.* **1975**, *19*, 39–42.
- (104) Chakrabarti, J. K.; Hicks, T. A. 2-[10,11-dihydro-11-oxodibenz[*b,f*][1,4]oxazepin-7 or 8-yl] propanoic acids as potential anti-inflammatory agents. *Eur. J. Med.*

- Chem.* **1987**, *22*, 161–163.
- (105) Klunder, J. M.; Hargrave, K. D.; West, M.; Cullen, E.; Pal, K.; Behnke, M. L.; Kapadia, S. R.; McNeil, D. W.; Wu, J. C.; Chow, G. C.; Adams, J. Novel non-nucleoside inhibitors of HIV-1 reverse transcriptase. 2. Tricyclic pyridobenzoxazepinones and dibenzoxazepinones. *J. Med. Chem.* **1992**, *35*, 1887–1897.
- (106) Binaschi, M.; Boldetti, A.; Gianni, M.; Maggi, C. A.; Gensini, M.; Bigioni, M.; Parlani, M.; Giolitti, A.; Fratelli, M.; Valli, C.; Terao, M.; Garattini, E. Antiproliferative and differentiating activities of a novel series of histone deacetylase inhibitors. *ACS Med. Chem. Lett.* **2010**, *1*, 411–415.
- (107) Liu, Y.; Chu, C.; Huang, A.; Zhan, C.; Ma, Y.; Ma, C. Regioselective synthesis of fused oxazepinone scaffolds through one-pot Smiles rearrangement tandem reaction. *ACS Comb. Sci.* **2011**, *13*, 547–553.
- (108) Hu, F.; Liu, H.; Jia, J.; Ma, C. Transition-metal-free synthesis of indole-fused dibenzo[*b,f*][1,4]oxazepines *via* Smiles rearrangement. *Org. Biomol. Chem.* **2016**, *14*, 11076–11079.
- (109) Sapegin, A.; Kalinin, S.; Smirnov, A.; Dorogov, M.; Krasavin, M. Dibenzobenzopyrazolo[1,5-*d*][1,4]oxazepines: facile construction of a rare heterocyclic system *via* tandem aromatic nucleophilic substitution-Smiles rearrangement-denitrocyclization. *Synthesis* **2012**, *44*, 2401–2407.
- (110) Feng, J.-B.; Wu, X.-F. Base-promoted synthesis of dibenzoxazepinamines and quinazolinimines under metal-free conditions. *Green Chem.* **2015**, *17*, 4522–4526.
- (111) (a) Hone, N. D.; Salter, J. I.; Reader, J. C. Solid-phase synthesis of dibenzoxazepinones. *Tetrahedron Lett.* **2003**, *44*, 8169–8172. (b) Samet, A. V.; Marshalkin, V. N.; Kislyi, K. A.; Chernysheva, N. B.; Strelenko, Y. A.; Semenov, V. V. Synthetic utilization of polynitroaromatic compounds. 3. Preparation of substituted dibenz[*b,f*][1,4]oxazepine-11(10*H*)-ones from 2,4,6-trinitrobenzoic acid *via* nucleophilic displacement of nitro groups. *J. Org. Chem.* **2005**, *70*, 9371–9376.
- (112) Tselikhovsky, D.; Buchwald, S. L. Concise palladium-catalyzed synthesis of dibenzodiazepines and structural analogues. *J. Am. Chem. Soc.* **2011**, *133*, 14228–

14231.

- (113) Shen, C.; Neumann, H.; Wu, X.-F. A highly-efficient palladium-catalyzed aminocarbonylation/S_NAr approach to dibenzoxazepinones. *Green Chem.* **2015**, *17*, 2994–2999.
- (114) Kitching, M. O.; Hurst, T. E.; Snieckus, V. Copper-catalyzed cross-coupling interrupted by an opportunistic Smiles rearrangement: an efficient domino approach to dibenzoxazepinones. *Angew. Chemie Int. Ed.* **2012**, *51*, 2925–2929.
- (115) (a) Zhang, Z.; Dai, Z.; Ma, X.; Liu, Y.; Ma, X.; Li, W.; Ma, C. Cu-catalyzed one-pot synthesis of fused oxazepinone derivatives *via* sp² C–H and O–H cross-dehydrogenative coupling. *Org. Chem. Front.* **2016**, *3*, 799–803. (b) Zhou, Y.; Zhu, J.; Li, B.; Zhang, Y.; Feng, J.; Hall, A.; Shi, J.; Zhu, W. Access to different isomeric dibenzoxazepinones through copper-catalyzed C–H etherification and C–N bond construction with controllable Smiles rearrangement. *Org. Lett.* **2016**, *18*, 380–383.
- (116) Sang, P.; Yu, M.; Tu, H.; Zou, J.; Zhang, Y. Highly regioselective synthesis of fused seven-membered rings through copper-catalyzed cross-coupling. *Chem. Commun.* **2013**, *49*, 701–703.
- (117) Ganguly, N. C.; Mondal, P.; Roy, S.; Mitra, P. Ligand-free copper-catalyzed efficient one-pot access of benzo[*b*]pyrido[3,2-*f*][1,4]oxazepinones through *O*-heteroarylation-Smiles rearrangement-cyclization cascade. *RSC Adv.* **2014**, *4*, 55640–55648.
- (118) Zaware, N.; Ohlmeyer, M. A novel synthetic approach to 11-substituted dibenzo[*b,f*][1,4]oxazepines. *Heterocycl. Commun.* **2014**, *20*, 189–191.
- (119) (a) Lu, S.-M.; Alper, H. Intramolecular carbonylation reactions with recyclable palladium-complexed dendrimers on silica: synthesis of oxygen, nitrogen, or sulfur-containing medium ring fused heterocycles. *J. Am. Chem. Soc.* **2005**, *127*, 14776–14784. (b) Yang, Q.; Cao, H.; Robertson, A.; Alper, H. Synthesis of dibenzo[*b,f*][1,4]oxazepin-11(10*H*)-ones *via* intramolecular cyclocarbonylation reactions using PdI₂/Cytos 292 as the catalytic system. *J. Org. Chem.* **2010**, *75*, 6297–6299.

- (120) (a) Fakhraian, H.; Nafary, Y.; Yarahmadi, A.; Hadj-Ghanbary, H. Improved etherification procedure for the preparation of dibenz[*b,f*][1,4]oxazepine. *J. Heterocycl. Chem.* **2008**, *45*, 1469–1471. (b) Bunce, R. A.; Schammerhorn, J. E. Dibenzo-fused seven-membered nitrogen heterocycles by a tandem reduction-lactamization reaction. *J. Heterocycl. Chem.* **2006**, *43*, 1031–1035.
- (121) (a) Ghafarzadeh, M.; Moghadam, E. S.; Faraji, F. Microwave assisted synthesis of dibenzoxazepines. *J. Heterocycl. Chem.* **2013**, *50*, 754–757. (b) Lin, Y.-C.; Li, N.-C.; Cherng, Y.-J. Microwave-assisted synthesis of substituted dibenzo[*b,f*][1,4]thiazepines, dibenzo[*b,f*][1,4]oxazepines, benzothiazoles, and benzimidazoles. *J. Heterocycl. Chem.* **2014**, *51*, 808–814.
- (122) Guo, X.; Zhang-Negrerie, D.; Du, Y. Iodine(III)-mediated construction of the dibenzoxazepinone skeleton from 2-(aryloxy)benzamides through oxidative C–N formation. *RSC Adv.* **2015**, *5*, 94732–94736.
- (123) (a) Ghandi, M.; Zarezadeh, N.; Abbasi, A. One-pot tandem Ugi-4CR/S_NAr approach to highly functionalized quino[2,3-*b*][1,5]benzoxazepines. *Mol. Divers.* **2016**, *20*, 483–495. (b) Xing, X.; Wu, J.; Luo, J.; Dai, W.-M. C-N bond-linked conjugates of dibenz[*b,f*][1,4]oxazepines with 2-oxindole. *Synlett* **2006**, *2006*, 2099–2103. (c) Shi, J.; Wu, J.; Cui, C.; Dai, W.-M. Microwave-assisted intramolecular Ullmann diaryl etherification as the post-Ugi annulation for generation of dibenz[*b,f*][1,4]oxazepine scaffold. *J. Org. Chem.* **2016**, *81*, 10392–10403.
- (124) (a) Roy, S.; Gajbhiye, R.; Mandal, M.; Pal, C.; Meyyapan, A.; Mukherjee, J.; Jaisankar, P. Synthesis and antibacterial evaluation of 3,3'-diindolylmethane derivatives. *Med. Chem. Res.* **2014**, *23*, 1371–1377. (b) Sung, W. S.; Lee, D. G. *In vitro* antimicrobial activity and the mode of action of indole-3-carbinol against human pathogenic microorganisms. *Biol. Pharm. Bull.* **2007**, *30*, 1865–1869. (c) Ko, M.-O.; Kim, M.-B.; Lim, S.-B. Relationship between chemical structure and antimicrobial activities of isothiocyanates from cruciferous vegetables against oral pathogens. *J. Microbiol. Biotechnol.* **2016**, *26*, 2036–2042. (d) Kumar, G. S. S.; Kumaresan, S.; Prabhu, A. A. M.; Bhuvanesh, N.; Seethalakshmi, P. G. An efficient one pot syntheses of aryl-3,3'-bis(indolyl)methanes and studies on their spectral characteristics, DPPH radical scavenging-, antimicrobial-, cytotoxicity-,

- and antituberculosis activity. *Spectrochim. Acta - Part A Mol. Biomol. Spectrosc.* **2013**, *101*, 254–263. (e) Kamal, A.; Khan, M. N. A.; Srinivasa Reddy, K.; Srikanth, Y. V. V.; Kaleem Ahmed, S.; Pranay Kumar, K.; Murthy, U. S. N. An efficient synthesis of bis(indolyl)methanes and evaluation of their antimicrobial activities. *J. Enzyme Inhib. Med. Chem.* **2009**, *24*, 559–565. (f) Damodiran, M.; Muralidharan, D.; Perumal, P. T. Regioselective synthesis and biological evaluation of bis(indolyl)methane derivatized 1,4-disubstituted 1,2,3-bis-triazoles as anti-infective agents. *Bioorg. Med. Chem. Lett.* **2009**, *19*, 3611–3614. (g) Kunimasa, K.; Kobayashi, T.; Kaji, K.; Ohta, T. Antiangiogenic effects of indole-3-carbinol and 3,3'-diindolylmethane are associated with their differential regulation of ERK1/2 and Akt in tube-forming HUVEC. *J. Nutr.* **2010**, *140*, 1–6. (h) Cho, H. J.; Seon, M. R.; Lee, Y. M.; Kim, J.; Kim, J.-K.; Kim, S. G.; Park, J. H. Y. 3,3'-Diindolylmethane suppresses the inflammatory response to lipopolysaccharide in murine macrophages. *J. Nutr.* **2008**, *138*, 17–23. (i) Li, Y.; Kong, D.; Ahmad, A.; Bao, B.; Sarkar, F. H. Antioxidant function of isoflavone and 3,3'-diindolylmethane: are they important for cancer prevention and therapy? *Antioxid. Redox Signal.* **2013**, *19*, 139–150. (j) Benabadji, S. H.; Wen, R.; Zheng, J.; Dong, X.; Yuan, S. Anticarcinogenic and antioxidant activity. *Acta Pharmacol. Sin.* **2004**, *25*, 666–671. (k) Pillaiyar, T.; Köse, M.; Sylvester, K.; Weighardt, H.; Thimm, D.; Borges, G.; Förster, I.; von Kügelgen, I.; Müller, C. E. Diindolylmethane derivatives: potent agonists of the immunostimulatory orphan G protein-coupled receptor GPR84. *J. Med. Chem.* **2017**, *60*, 3636–3655.
- (125) (a) Clark, R.; Lee, J.; Lee, S.-H. Synergistic anticancer activity of capsaicin and 3,3'-diindolylmethane in human colorectal cancer. *J. Agric. Food Chem.* **2015**, *63*, 4297–4304. (b) Xu, Y.; Zhang, J.; Shi, W.; Liu, Y. Anticancer effects of 3,3'-diindolylmethane are associated with G1 arrest and mitochondria-dependent apoptosis in human nasopharyngeal carcinoma cells. *Oncol. Lett.* **2013**, *5*, 655–662. (c) Ahmad, A.; A Sakr, W.; Wahidur Rahman, K. Anticancer properties of indole compounds: mechanism of apoptosis induction and role in chemotherapy. *Curr. Drug Targets* **2010**, *11*, 652–666. (d) Aronchik, I.; Bjeldanes, L. F.; Firestone, G. L. Direct inhibition of elastase activity by indole-3-carbinol triggers a CD40-TRAF regulatory cascade that disrupts NF- κ B transcriptional activity in human breast cancer cells. *Cancer Res.* **2010**, *70*, 4961–4971. (e) Aggarwal, B. B.;

Ichikawa, H. Molecular targets and anticancer potential of indole-3-carbinol and its derivatives. *Cell Cycle* **2005**, *4*, 1201–1215. (f) Safe, S.; Papineni, S.; Chintharlapalli, S. Cancer chemotherapy with indole-3-carbinol, bis(3'-indolyl)methane and synthetic analogs. *Cancer Lett.* **2008**, *269*, 326–338. (g) Bhargava, S. The role of diindolylmethane in the prevention and treatment of cancer. *World J. Pharm. Pharm. Sci.* **2014**, *3*, 359–369. (h) Pan, J. H.; Abernathy, B.; Kim, Y. J.; Lee, J. H.; Kim, J. H.; Shin, E. C.; Kim, J. K. Cruciferous vegetables and colorectal cancer prevention through microRNA regulation: a review. *Crit. Rev. Food Sci. Nutr.* **2018**, *58*, 2026–2038. (i) Weng, J.-R.; Tsai, C.-H.; Kulp, S. K.; Chen, C.-S. Indole-3-carbinol as a chemopreventive and anti-cancer agent. *Cancer Lett.* **2008**, *262*, 153–163. (j) Kim, S. Cellular and molecular mechanisms of 3,3'-diindolylmethane in gastrointestinal cancer. *Int. J. Mol. Sci.* **2016**, *17*, 1155–1167. (k) Sreevalsan, S.; Jutooru, I.; Chadalapaka, G.; Walker, M.; Safe, S. 1,1-Bis(3'-indolyl)-1-(*p*-bromophenyl)methane and related compounds repress survivin and decrease γ -radiation-induced survivin in colon and pancreatic cancer cells. *Int. J. Oncol.* **2009**, *35*, 1191–1199. (l) Lei, P.; Abdelrahim, M.; Cho, S. D.; Liu, X.; Safe, S. Structure-dependent activation of endoplasmic reticulum stress-mediated apoptosis in pancreatic cancer by 1,1-bis(3'-indolyl)-1-(*p*-substituted phenyl)methanes. *Mol. Cancer Ther.* **2008**, *7*, 3363–3372. (m) Li, X.; Lee, S.-O.; Safe, S. Structure-dependent activation of NR4A2 (Nurr1) by 1,1-bis(3'-indolyl)-1-(aromatic)methane analogs in pancreatic cancer cells. *Biochem. Pharmacol.* **2012**, *83*, 1445–1455. (n) Lei, P.; Abdelrahim, M.; Cho, S. D.; Liu, S.; Chintharlapalli, S.; Safe, S. 1,1-Bis(3'-indolyl)-1-(*p*-substituted phenyl)methanes inhibit colon cancer cell and tumor growth through activation of c-jun N-terminal kinase. *Carcinogenesis* **2008**, *29*, 1139–1147. (o) Abdelrahim, M.; Newman, K.; Vanderlaag, K.; Samudio, I.; Safe, S. 3,3'-Diindolylmethane (DIM) and its derivatives induce apoptosis in pancreatic cancer cells through endoplasmic reticulum stress-dependent upregulation of DR5. *Carcinogenesis* **2006**, *27*, 717–728. (p) Abdelbaqi, K.; Lack, N.; Guns, E. T.; Kotha, L.; Safe, S.; Sanderson, J. T. Antiandrogenic and growth inhibitory effects of ring-substituted analogs of 3,3'-diindolylmethane (ring-DIMs) in hormone-responsive LNCaP human prostate cancer cells. *Prostate* **2011**, *71*, 1401–1412.

(126) Del Priore, G.; Gudipudi, D. K.; Montemarano, N.; Restivo, A. M.; Malanowska-

- Stega, J.; Arslan, A. A. Oral diindolylmethane (DIM): pilot evaluation of a nonsurgical treatment for cervical dysplasia. *Gynecol. Oncol.* **2010**, *116* (3), 464–467.
- (127) <https://clinicaltrials.gov/ct2/show/study/NCT00888654?term=diindolylmethane&cond=Prostate+Cancer&rank=1> (accessed on December 18, 2017)
- (128) McGuire, K. P.; Ngoubilly, N.; Neavyn, M.; Lanza-Jacoby, S. 3,3'-Diindolylmethane and paclitaxel act synergistically to promote apoptosis in HER2/Neu human breast cancer cells. *J. Surg. Res.* **2006**, *132*, 208–213.
- (129) (a) Qin, C.; Morrow, D.; Stewart, J.; Spencer, K.; Porter, W.; Smith, R.; Phillips, T.; Abdelrahim, M.; Samudio, I.; Safe, S. A new class of peroxisome proliferator-activated receptor γ (PPAR γ) agonists that inhibit growth of breast cancer cells: 1,1-bis (3'-indolyl)-1-(*p*-substituted phenyl) methanes. *Mol. Cancer Ther.* **2004**, *3*, 247–260. (b) York, M.; Abdelrahim, M.; Chintharlapalli, S.; Lucero, S. D.; Safe, S. 1,1-Bis(3'-indolyl)-1-(*p*-substituted phenyl)methanes induce apoptosis and inhibit renal cell carcinoma growth. *Clin. Cancer Res.* **2007**, *13*, 6743–6752. (c) Lei, P.; Abdelrahim, M.; Safe, S. 1,1-Bis(3'-Indolyl)-1-(*p*-substituted phenyl)methanes inhibit ovarian cancer cell growth through peroxisome proliferator-activated receptor-dependent and independent pathways. *Mol. Cancer Ther.* **2006**, *5*, 2324–2336. (d) Dae Cho, S.; Lee, S.-O.; Chintharlapalli, S.; Abdelrahim, M.; Khan, S.; Yoon, K.; Kamat, A. M.; Safe, S. Activation of nerve growth factor-induced B α by methylene-substituted diindolylmethanes in bladder cancer cells induces apoptosis and inhibits tumor growth. *Mol. Pharmacol.* **2010**, *77*, 396–404. (e) Vanderlaag, K.; Su, Y.; Frankel, A. E.; Grage, H.; Smith, R.; Khan, S.; Safe, S. 1,1-Bis(3'-indolyl)-1-(*p*-substituted phenyl)methanes inhibit proliferation of estrogen receptor-negative breast cancer cells by activation of multiple pathways. *Breast Cancer Res. Treat.* **2008**, *109*, 273–283. (f) Hong, J.; Samudio, I.; Chintharlapalli, S.; Safe, S. 1,1-Bis(3'-indolyl)-1-(*p*-substituted phenyl)methanes decrease mitochondrial membrane potential and induce apoptosis in endometrial and other cancer cell lines. *Mol. Carcinog.* **2008**, *47*, 492–507.
- (130) (a) Jia, X.; Zhong, L.; Song, Y.; Hu, Y.; Wang, G.; Sun, S. Consumption of citrus and cruciferous vegetables with incident type 2 diabetes mellitus based on a meta-

- analysis of prospective study. *Prim. Care Diabetes* **2016**, *10*, 272–280. (b) Deng, W.; Zong, J.; Bian, Z.; Zhou, H.; Yuan, Y.; Zhang, R.; Guo, H.; Zhang, Y.; Shen, D.; Li, H.; Tang, Q. Indole-3-carbinol protects against pressure overload induced cardiac remodeling *via* activating AMPK- α . *Mol. Nutr. Food Res.* **2013**, *57*, 1680–1687. (c) Choi, Y.; Kim, Y.; Park, S.; Lee, K. W.; Park, T. indole-3-carbinol prevents diet-induced obesity through modulation of multiple genes related to adipogenesis, thermogenesis or inflammation in the visceral adipose tissue of mice. *J. Nutr. Biochem.* **2012**, *23*, 1732–1739. (d) Choi, H.-S.; Jeon, H.-J.; Lee, O.-H.; Lee, B.-Y. Indole-3-carbinol, a vegetable phytochemical, inhibits adipogenesis by regulating cell cycle and AMPK α Signaling. *Biochimie* **2014**, *104*, 127–136.
- (131) Lee, J.; Yue, Y.; Park, Y.; Lee, S.-H. 3,3'-Diindolylmethane suppresses adipogenesis using AMPK α -dependent mechanism in 3T3-L1 adipocytes and *Caenorhabditis elegans*. *J. Med. Food* **2017**, *20*, 646–652.
- (132) Choi, K.-M.; Yoo, H.-S. 3,3'-Diindolylmethane enhances glucose uptake through activation of insulin signaling in 3T3-L1 adipocytes. *Obesity* **2018**, *26*, 1153–1160.
- (133) Pal, C.; Dey, S.; Mahato, S. K.; Vinayagam, J.; Pradhan, P. K.; Giri, V. S.; Jaisankar, P.; Hossain, T.; Baruri, S.; Ray, D.; Biswas, S. M. Eco-friendly synthesis and study of new plant growth promoters: 3,3'-diindolylmethane and its derivatives. *Bioorganic Med. Chem. Lett.* **2007**, *17*, 4924–4928.
- (134) Roy, A.; Chowdhury, S.; Sengupta, S.; Mandal, M.; Jaisankar, P.; D'Annessa, I.; Desideri, A.; Majumder, H. K. Development of derivatives of 3,3'-diindolylmethane as potent *Leishmania donovani* bi-subunit topoisomerase IB poisons. *PLoS One* **2011**, *6*, e28493.
- (135) (a) Praveen, P.; Parameswaran, P.; Majik, M. Bis(indolyl)methane alkaloids: isolation, bioactivity, and syntheses. *Synthesis* **2015**, *47*, 1827–1837. (b) Bell, R.; Carmeli, S.; Sar, N. Vibrindole A, a metabolite of the marine bacterium, *Vibrio parahaemolyticus*, isolated from the toxic mucus of the boxfish *Ostracion cubicus*. *J. Nat. Prod.* **1994**, *57*, 1587–1590. (c) Kobayashi, M.; Aoki, S.; Gato, K.; Matsunami, K.; Kurosu, M.; Kitagawa, I. Marine natural products. XXXIV. Trisindoline, a new antibiotic indole trimer, produced by a bacterium of *Vibrio* sp. Separated from the marine sponge *Hyrtios altum*. *Chem. Pharm. Bull.* **1994**, *42*,

- 2449–2451. (d) Khuzhaev, B. U.; Aripova, S. F.; Shakirov, R. S. Arundine - a new dimeric alkaloid from the roots of *Arundo donax*. *Chem. Nat. Compd.* **1994**, *30*, 635–636. (e) Veluri, R.; Oka, I.; Wagner-Döbler, I.; Laatsch, H. New indole alkaloids from the north sea bacterium *Vibrio parahaemolyticus* Bio249. *J. Nat. Prod.* **2003**, *66*, 1520–1523. (f) Cai, S. X.; Li, D. H.; Zhu, T. J.; Wang, F. P.; Xiao, X.; Gu, Q. Q. Two new indole alkaloids from the marine-derived bacterium *Aeromonas* sp. CB101. *Helv. Chim. Acta* **2010**, *93*, 791–795. (g) Osawa, T.; Namiki, M. Structure elucidation of streptindole, a novel genotoxic metabolite isolated from intestinal bacteria. *Tetrahedron Lett.* **1983**, *24*, 4719–4722.
- (136) Kirkus, M.; Tsai, M.-H.; Grazulevicius, J. V.; Wu, C.-C.; Chi, L.-C.; Wong, K.-T. New indole–carbazole hybrids as glass-forming high-triplet-energy materials. *Synth. Met.* **2009**, *159*, 729–734.
- (137) (a) He, X.; Hu, S.; Liu, K.; Guo, Y.; Xu, J.; Shao, S. Oxidized bis(indolyl)methane: a simple and efficient chromogenic-sensing molecule based on the proton transfer signaling mode. *Org. Lett.* **2006**, *8*, 333–336. (b) Martínez, R.; Espinosa, A.; Tárraga, A.; Molina, P. Bis(indolyl)methane derivatives as highly selective colourimetric and ratiometric fluorescent molecular chemosensors for Cu²⁺ cations. *Tetrahedron* **2008**, *64*, 2184–2191.
- (138) Lafzi, F.; Kilic, H.; Ertugrul, B.; Arik, M.; Saracoglu, N. Bis(indolyl)methane substituted tetraphenylethylene derivatives as AIE active materials. *J. Lumin.* **2019**, *208*, 174–182.
- (139) (a) J Ji, S.-J.; Zhou, M.-F.; Gu, D.-G.; Jiang, Z.-Q.; Loh, T.-P. Efficient Fe^{III}-catalyzed synthesis of bis(indolyl)methanes in ionic liquids. *Eur. J. Org. Chem.* **2004**, *2004*, 1584–1587. (b) Chen, D.; Yu, L.; Wang, P. G. Lewis acid-catalyzed reactions in protic media. Lanthanide-catalyzed reactions of indoles with aldehydes or ketones. *Tetrahedron Lett.* **1996**, *37*, 4467–4470. (c) Kundu, P.; Maiti, G. A mild and versatile synthesis of bis(indolyl)methanes and tris(indolyl)alkanes catalyzed by antimony trichloride. *Indian J. Chem. - Sect. B Org. Med. Chem.* **2008**, *47*, 1402–1406. (d) Qu, H. E.; Xiao, C.; Wang, N.; Yu, K. H.; Hu, Q. S.; Liu, L. X. RuCl₃·3H₂O catalyzed reactions: facile synthesis of bis(indolyl)methanes under mild conditions. *Molecules* **2011**, *16*, 3855–3868. (e) Beltrá, J.; Gimeno, M. C.; Herrera, R. P. A new approach for the synthesis of bisindoles through AgOTf

- as catalyst. *Beilstein J. Org. Chem.* **2014**, *10*, 2206–2214. (f) Nagarajan, R.; Perumal, P. T. Electrophilic substitution of indoles catalyzed by triphenyl phosphonium perchlorate: synthesis of 3-acetyl indoles and bis-indolylmethane derivatives. *Synth. Commun.* **2002**, No. 32, 105–109. (g) Bandgar, B. P.; Shaikh, K. A. Molecular iodine-catalyzed efficient and highly rapid synthesis of bis(indolyl)methanes under mild conditions. *Tetrahedron Lett.* **2003**, *44*, 1959–1961. (h) Firouzabadi, H.; Iranpoor, N.; Jafari, A. A. Aluminumdodecatungstophosphate (AlPW₁₂O₄₀), a versatile and a highly water tolerant green lewis acid catalyzes efficient preparation of indole derivatives. *J. Mol. Catal. A Chem.* **2006**, *244*, 168–172. (i) Lin, H.; Zang, Y.; Sun, X.; Lin, G. Highly efficient synthesis of unsymmetrical 3,3'-bis(1*H*-indol-3-yl)methanes in water. *Chinese J. Chem.* **2012**, *30*, 2309–2314. (j) Kumar, G. S.; Kumar, A. S.; Swetha, A.; Babu, B. M.; Meshram, H. M. An unexpected C-C bond cleavage of acetophenones: synthesis of bis(heteroaryl)arylmethanes and triarylmethanes via SeO₂/lanthanide chloride catalyzed Friedel-Crafts arylation. *Synlett* **2016**, *27*, 631–639. (k) Zahran, M.; Abdin, Y.; Salama, H. Eco-friendly and efficient synthesis of bis(indolyl)methanes under microwave irradiation. *Arkivoc* **2008**, *2008*, 256–265. (l) Ramesh, C.; Banerjee, J.; Pal, R.; Das, B. Silica supported sodium hydrogen sulfate and amberlyst-15: two efficient heterogeneous catalysts for facile synthesis of bis- and tris(1*H*-indol-3-yl)methanes from indoles and carbonyl compounds. *Adv. Synth. Catal.* **2003**, *345*, 557–559. (m) Mahadevan, A.; Sard, H.; Gonzalez, M.; McKew, J. C. A general method for C₃ reductive alkylation of indoles. *Tetrahedron Lett.* **2003**, *44*, 4589–4591. (n) Reddy, A. V.; Ravinder, K.; Reddy, V. L. N.; Goud, T. V.; Ravikanth, V.; Venkateswarlu, Y. Zeolite catalyzed synthesis of bis(indolyl)methanes. *Synth. Commun.* **2003**, *33*, 3687–3694.
- (140) Shiri, M.; Zolfigol, M. A.; Kruger, H. G.; Tanbakouchian, Z. Bis- and trisindolylmethanes (BIMs and TIMs). *Chem. Rev.* **2010**, *110*, 2250–2293.
- (141) (a) Khazaei, A.; Zolfigol, M. A.; Faal-rastegar, T. Ionic liquid tributyl (carboxymethyl) phosphonium bromide as an efficient catalyst for the synthesis of bis(indolyl)methanes under solvent-free conditions. *J. Chem. Res.* **2013**, *37*, 617–619. (b) Veisi, H.; Hemmati, S.; Veisi, H. highly efficient method for synthesis of bis(indolyl)methanes catalyzed by FeCl₃-based ionic liquid. *J. Chinese Chem. Soc.* **2009**, *56*, 240–245. (c) Siadatifard, S. H.; Abdoli-senejani, M.; Bodaghifard, M. A.

- An efficient method for synthesis of bis(indolyl)methane and di-bis(indolyl)methane derivatives in environmentally benign conditions using TBAHS. *Cogent Chem.* **2016**, *2*, 1188435. (d) Khatab, T. K.; Shaker, A. M. A. N.; Osama, Y. Evaluation of the optical and structural properties of constructed bis-indole derivatives using (Sm₂O₃/SiO₂) catalyst. *Silicon* **2018**, *10*, 2173–2179. (e) Srivastava, A.; Agarwal, A.; Gupta, S. K.; Jain, N. Graphene oxide decorated with Cu(I)Br nanoparticles: A reusable catalyst for the synthesis of potent bis(indolyl)methane based anti HIV drugs. *RSC Adv.* **2016**, *6*, 23008–23011. (f) García, J. P.; López, H.; López, Y.; Rojas, S. Synthesis of bis(indolyl)methanes catalyzed by triethylborane. *Lett. Org. Chem.* **2015**, *12*, 332. (g) Nguyen, H. T. D.; Nguyen, T. T.; Nguyen, P. T. K.; Tran, P. H. A highly active copper-based metal-organic framework catalyst for a Friedel–Crafts alkylation in the synthesis of bis(indolyl)methanes under ultrasound irradiation. *Arab. J. Chem.* **2017**. (h) Sharma, D. K.; Hussain, A.; Lambu, M. R.; Yousuf, S. K.; Maiety, S.; Singh, B.; Mukherjee, D. Fe/Al pillared clay catalyzed solvent-free synthesis of bisindolylmethanes using diversly substituted indoles and carbonyl compounds. *RSC Adv.* **2013**, *3* (2211–2215).
- (142) Mendes, S. R.; Thurow, S.; Penteado, F.; Silva, M. S.; Gariani, R. A.; Perin, G.; Lenardão, E. J. Synthesis of bis(indolyl)methanes using ammonium niobium oxalate (ANO) as an efficient and recyclable catalyst. *Green Chem.* **2015**, *17*, 4334–4339.
- (143) (a) Palmieri, A.; Petrini, M. Recent advances in the synthesis of unsymmetrical bisindolylmethane derivatives. *Synthesis* **2018**, *50*. (b) Chalaye-Mauger, H.; Denis, J. N.; Averbuch-Pouchot, M. T.; Vallée, Y. The reactions of nitrones with indoles. *Tetrahedron* **2000**, *56*, 791–804. (c) de la Herrán, G.; Segura, A.; Csáky, A. G. Benzylic substitution of gramines with boronic acids and rhodium or iridium catalysts. *Org. Lett.* **2007**, *9*, 961–964. (d) Pathak, T. P.; Osiak, J. G.; Vaden, R. M.; Welm, B. E.; Sigman, M. S. Synthesis and preliminary biological study of bisindolylmethanes accessed by an acid-catalyzed hydroarylation of vinyl indoles. *Tetrahedron* **2012**, *68*, 5203–5208. (e) Abe, T.; Ikeda, T.; Itoh, T.; Hatae, N.; Toyota, E.; Ishikura, M. One-pot access to 3,3'-bisindolylmethanes through the intermolecular Pummerer reaction. *Heterocycles* **2014**, *88*, 187–191. (f) Abe, T.; Nakamura, S.; Yanada, R.; Choshi, T.; Hibino, S.; Ishikura, M. One-pot

- construction of 3,3'-bisindolylmethanes through Bartoli indole synthesis. *Org. Lett.* **2013**, *15*, 3622–3625. (g) Zhao, D.; Wang, Y.; Zhu, M. X.; Shen, Q.; Zhang, L.; Du, Y.; Li, J. X. Copper(II)-catalyzed C-H(sp³) oxidation and C-N cleavage: synthesis of methylene-bridged compounds using TMEDA as a carbon source in water. *RSC Adv.* **2013**, *3*, 10272–10276.
- (144) (a) Wen, H.; Wang, L.; Xu, L.; Hao, Z.; Shao, C.-L.; Wang, C.-Y.; Xiao, J. Fluorinated alcohol-mediated S_N1-type reaction of indolyl alcohols with diverse nucleophiles. *Adv. Synth. Catal.* **2015**, *357*, 4023–4030. (b) Xiao, J.; Wen, H.; Wang, L.; Xu, L.; Hao, Z.; Shao, C.-L.; Wang, C.-Y. Catalyst-free dehydrative S_N1-type reaction of indolyl alcohols with diverse nucleophiles “on water.” *Green Chem.* **2016**, *18*, 1032–1037.
- (145) Zhuo, M.-H.; Jiang, Y.-J.; Fan, Y.-S.; Gao, Y.; Liu, S.; Zhang, S. Enantioselective synthesis of triarylmethanes by chiral imidodiphosphoric acids catalyzed Friedel–Crafts reactions. *Org. Lett.* **2014**, *16*, 1096–1099.
- (146) (a) Pu, F.; Li, Y.; Song, Y.-H.; Xiao, J.; Liu, Z.-W.; Wang, C.; Liu, Z.-T.; Chen, J.-G.; Lu, J. Copper-catalyzed coupling of indoles with dimethylformamide as a methylenating reagent. *Adv. Synth. Catal.* **2016**, *358*, 539–542. (b) Kaswan, P.; Nandwana, N. K.; DeBoef, B.; Kumar, A. Vanadyl acetylacetonate catalyzed methylenation of imidazo[1,2-*a*]pyridines by using dimethylacetamide as a methylene source: direct access to bis(imidazo[1,2-*a*]pyridin-3-yl)methanes. *Adv. Synth. Catal.* **2016**, *358*, 2108–2115.
- (147) Deb, M. L.; Borpatra, P. J.; Saikia, P. J.; Baruah, P. K. Introducing tetramethylurea as a new methylene precursor: a microwave-assisted RuCl₃-catalyzed cross dehydrogenative coupling approach to bis(indolyl)methanes. *Org. Biomol. Chem.* **2017**, *15*, 1435–1443.
- (148) (a) Badigenchala, S.; Ganapathy, D.; Das, A.; Singh, R.; Sekar, G. Iron(II) chloride–1,1'-binaphthyl-2,2'-diamine (FeCl₂–BINAM) complex catalyzed domino synthesis of bisindolylmethanes from indoles and primary alcohols. *Synthesis* **2013**, *46*, 101–109. (b) Hikawa, H.; Yokoyama, Y. Pd-catalyzed C–H activation in water: synthesis of bis(indolyl)methanes from indoles and benzyl alcohols. *RSC Adv.* **2013**, *3*, 1061–1064. (c) Putra, A. E.; Takigawa, K.; Tanaka, H.; Ito, Y.; Oe,

- Y.; Ohta, T. Transition-metal-catalyzed regioselective alkylation of indoles with alcohols. *Eur. J. Org. Chem.* **2013**, *2013*, 6344–6354.
- (149) Gopalaiah, K.; Chandrudu, S.; Devi, A. Iron-catalyzed oxidative coupling of benzylamines and indoles: novel approach for synthesis of bis(indolyl)methanes. *Synthesis* **2015**, *47*, 1766–1774.
- (150) Liao, M.; Zhang, X.; Yue, P. TEMPO/CuI synergetic catalyzed oxidative cross-coupling of indoles with benzylamines: synthesis of bis(indolyl)phenylmethanes. *Synth. Commun.* **2018**, *48*, 1694–1700.
- (151) Xiang, J.; Wang, J.; Wang, M.; Meng, X.; Wu, A. One-pot total synthesis of streptindole, arsindoline B and their congeners through tandem decarboxylative deaminative dual-coupling reaction of amino acids with indoles. *Org. Biomol. Chem.* **2015**, *13*, 4240–4247.
- (152) Chen, C.-C.; Hong, B.-C.; Li, W.-S.; Chang, T.-T.; Lee, G.-H. Synthesis of biologically active bis(indolyl)methane derivatives by bisindole alkylation of tetrahydroisoquinolines with visible-light induced ring-opening fragmentation. *Asian J. Org. Chem.* **2017**, *6*, 426–431.
- (153) Pillaiyar, T.; Gorska, E.; Schnakenburg, G.; Müller, C. E. General synthesis of unsymmetrical 3,3'-(aza)diindolylmethane derivatives. *J. Org. Chem.* **2018**, *83*, 9902–9913

Chapter-2

New 1,2-Dihydropyridine Based Fluorophores and Their Applications as Fluorescent Probes

2.1. Abstract

New 1,2-dihydropyridine (1,2-DHP) based fluorophores **5a-5h** were designed and synthesized by a one-pot four-component condensation reaction using dienaminodioxide (**1**), aldehyde (**2**), and an *in situ* generated hydrazone (**3'**) mediated by trifluoroacetic acid (Figure 2.1). The photophysical properties of 1,2-DHPs were studied in detail and a few of them exhibited selective mitochondrial staining ability in HeLa cell lines (cervical cancer cells). A detailed photophysical investigation led to the design of 1,2-DHP **5h** as an optimal fluorophore suitable for its potential application as a small molecule probe in the aqueous medium. Also, 1,2-DHP **4h** exhibited six fold enhanced emission intensity than its phosphorylated analogue **5h'** in long wavelength region ($\lambda_{em} \sim 600$ nm) which makes 1,2-DHP **5h'** meet the requirement as a bio-probe for protein tyrosine phosphatases, shown in L6 muscle cell lysate.

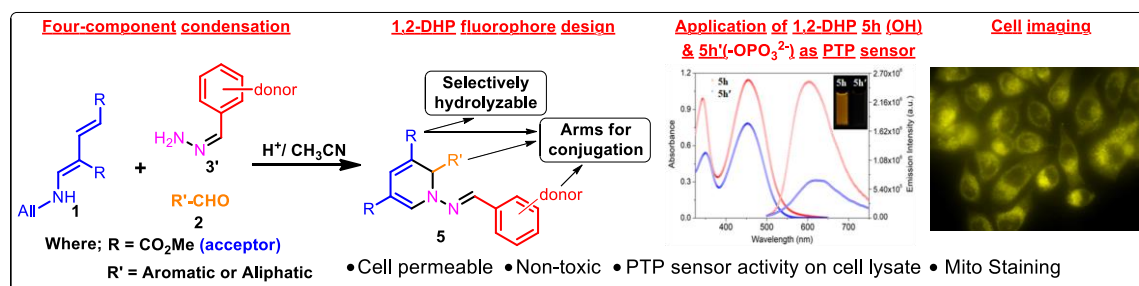


Figure 2.1. The design of 1,2-dihydropyridine based fluorophore

2.2. Introduction

Small molecule based organic fluorophores are essential for sensing and imaging of biological specimen with high sensitivity and fast response.¹ Even though a large variety of fluorophores are known, only a few have optimal performance since a majority of them often suffer from photobleaching, autofluorescence and cytotoxic behavior that limit their further applications in biology.² A number of heterocyclic fluorophores were reported for fluorescent labeling of biomolecules, sensing and bio-imaging applications, however, for most of these molecules, the emission maxima were observed in the green window of less than 500 nm.³ Consequently, the discovery of new heterocyclic fluorophore scaffolds

with improved photophysical properties is highly warranted. Fluorescent properties exhibited by 1,4-dihydropyridines (1,4-DHPs)⁴ and our recent interest in 1,2-DHPs,⁵ have inspired us to develop new 1,2-DHP based fluorophores with improved photophysical features.

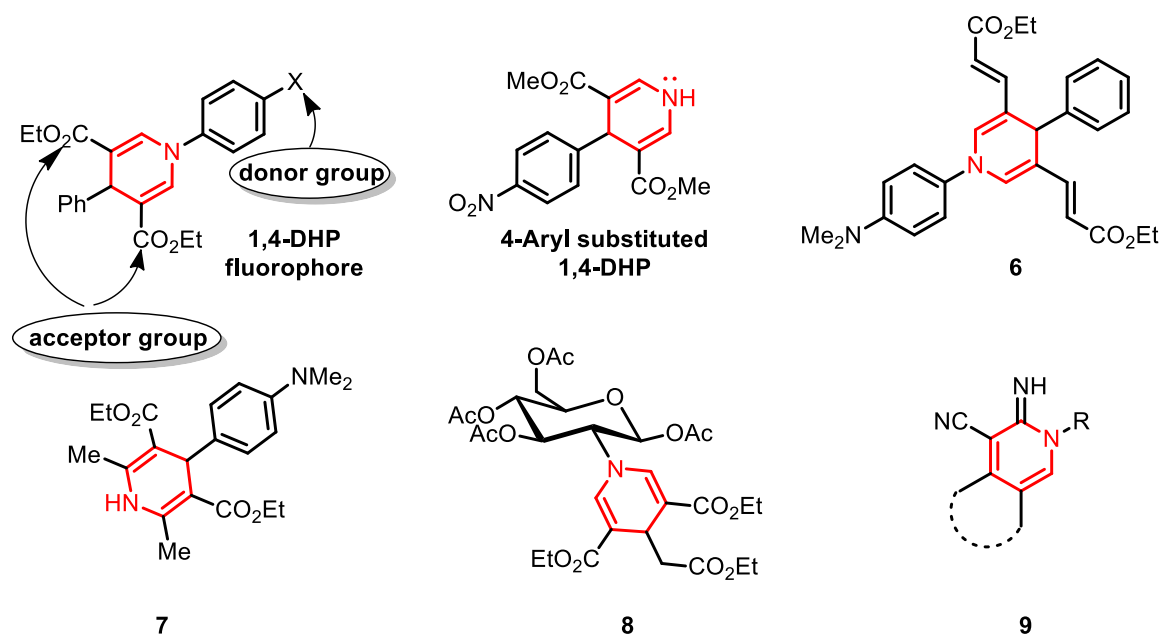


Figure 2.2A. Examples of 1,2- and 1,4-DHP fluorescent molecules

1,4-DHPs are known to exhibit blue fluorescence with appropriately substituted electron-donating groups at the 1-position and electron-withdrawing groups at 3- and 5-positions (Figure 2.2A). Sueki *et al.* studied the effect of substituents at 3- and 5-position of the 1,4-DHP on the fluorescence property, which led to the discovery of a 3,4,5-trisubstituted 1,4-DHP **6**, having a fluorescence emission in the range 403–596 nm (Figure 2.2A).⁶ Furthermore, a higher Stokes shift was observed by the presence of an electron-donating aryl system in the 4-position of 1,4-DHP, which is attributed to an internal charge transfer in the excited state between the two π -systems. For example, the fluorescence property and the observation of higher Stokes shift of *N,N*-Dimethylamino substituted dihydropyridine **7** was reported by Affeldt *et al.* in 2011 (Figure 2.2A).⁷ The 4-Aryl substituted 1,4-DHP comprising two different chromophores separated by a sp^3 carbon served as a tunable photoactivated dyad involving energy and electron transfer process between them (Figure 2.2A).⁸ The fluorophore ability of 1,4-DHP was further extended as a chemosensor where a water-soluble glucopyranosyl 1,4-DHP **8** is used in the detection of 2,4,6-trinitrophenol (Figure 2.2A).⁹ 1,2-DHPs, however, were not

explored in detail for their photophysical properties to an extent as that of 1,4-DHPs but 2-pyridones which are structural analogues of 1,2-DHPs were recently reported as fluorescent probes.¹⁰ Recently, ylidene malononitrile enamines were reported as fluorescent “turn-on” indicators for their ability to undergo cyclization with 1° amines to produce fluorescent 1,2-DHP products **9** (Figure 2.2A).¹¹

In the quest for developing new fluorophores with improved photophysical properties, herein we have explored 1,2-DHPs with extended π -conjugation as novel fluorophores. As *N*-phenyl-1,2-DHPs absorb in the near UV region (Table 2.3.3), the corresponding derivatives with absorption in the visible region would be preferred for biological applications. Hence, the present 1,2-DHP design (Figure 2.2B) involves a push-pull system with different electron-rich *N*-benzylideneamine substitutions that offer tuning of their photophysical behaviour.¹² This new *N*-benzylideneamine appended 1,2-DHP offered a remarkable bathochromic shift in the absorption and emission profile with large Stokes shifts (Table 2.3.4). The application of these fluorophores was demonstrated as selective mitochondrial staining agents in HeLa cells. Furthermore, the design offers different sites for appendage to bioactives or functionalities required for conjugation and such applicability has been demonstrated here as a probe for protein tyrosine phosphatase enzymes in L6 muscle cell lysate.

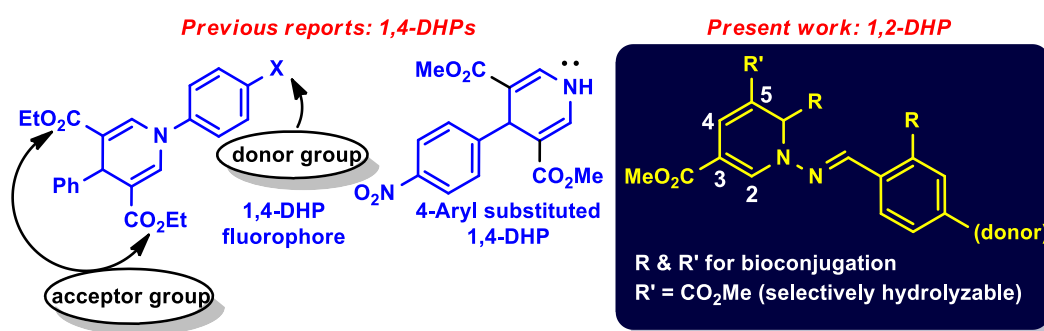


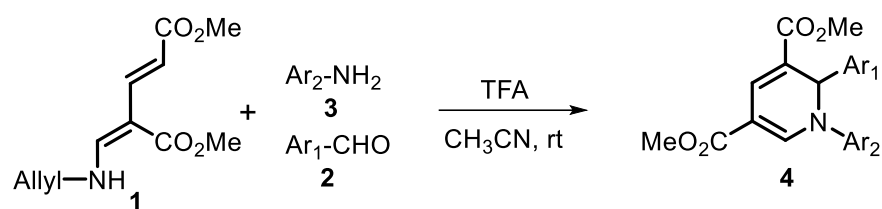
Figure 2.2B. Design strategy of the *N*-benzylideneamine appended 1,2-DHP based fluorophore.

2.3. Results and discussions

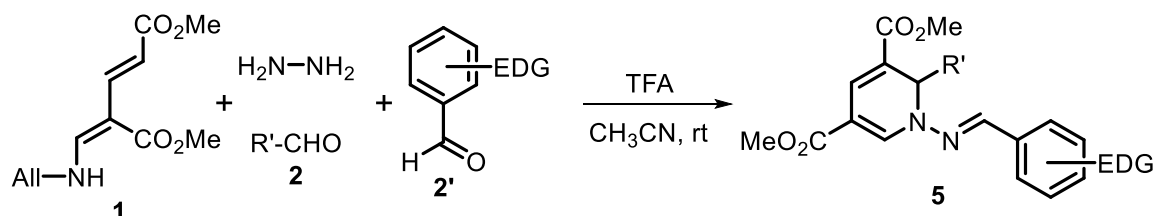
2.3.1. Synthesis

From our lab, we reported a one-pot multicomponent synthesis of 1,2-DHPs **4** from dienaminodioxide **1** and imines, generated from aromatic aldehydes **2** and amines **3**, mediated by trifluoroacetic acid at room temperature.⁵ As an extension of this methodology, the aromatic amine is replaced with an *in situ* generated hydrazone **3'** and by condensation with other components, the expected *N*-benzylideneamine appended 1,2-DHP **5** was observed under mild conditions, thus serving as a facile one-pot four-component reaction (Scheme 2.3.1). A series of 1,2-DHPs **5a-5g** were synthesized in moderate to good yields (20-60%) by utilizing hydrazones of differing electronic properties to decipher their photophysical properties (Table 2.3.1). 1,2-DHPs **5a-5b** were prepared to assess the role of phenyl substitution in the 6-position. The remaining 1,2-DHPs **5c-5g** were synthesized with acetaldehyde to evaluate the effect of the phenyl group as a contributing factor behind the 1,2-DHP's fluorophore ability. This methodology offers a choice of appending any aliphatic or aromatic group at the 6-position, thus, a suitable place for conjugation with bioactives or biomolecules. In addition, these 1,2-DHPs can undergo regioselective hydrolysis of 5-CO₂Me which was supported by its single crystal X-ray structure of the analogue 1,2-DHP **5j**, synthesized by partial hydrolysis of 1,2-DHP **5g** followed by esterification with 4-nitrophenol (Scheme 2.3.2). This selectivity can be realized by difference in nitrogen lone pair delocalization with 3- and 5-CO₂Me, thus offering another site for conjugation *via* an amide linkage. Furthermore, we have designed and synthesized a water soluble fluorophore 1,2-DHP **5h** by utilizing aldehyde **2h** generated from triethylene glycol monomethyl ether, and *N,N*-diethyl salicylaldehyde **2'h** which further offers an appropriate hydroxyl group substituent for appending any cleavable targeting group such as phosphate for *in vitro* phosphatase sensing application (Scheme 2.3.3). We have also synthesized an array *N*-phenyl 1,2-DHP **4a-4h**, to compare their photophysical properties with *N*-benzylideneamine appended 1,2-DHP (Table 2.3.2). *N*-phenyl substituted tetracyclic 1,2-DHP **4j** and its phosphorylated analogue **4j'** also was synthesized (Scheme 2.3.3).

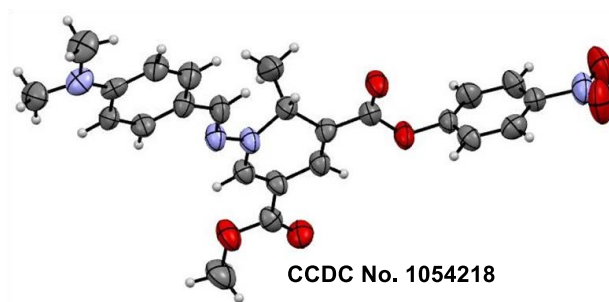
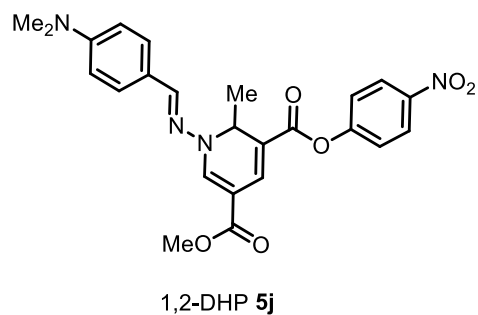
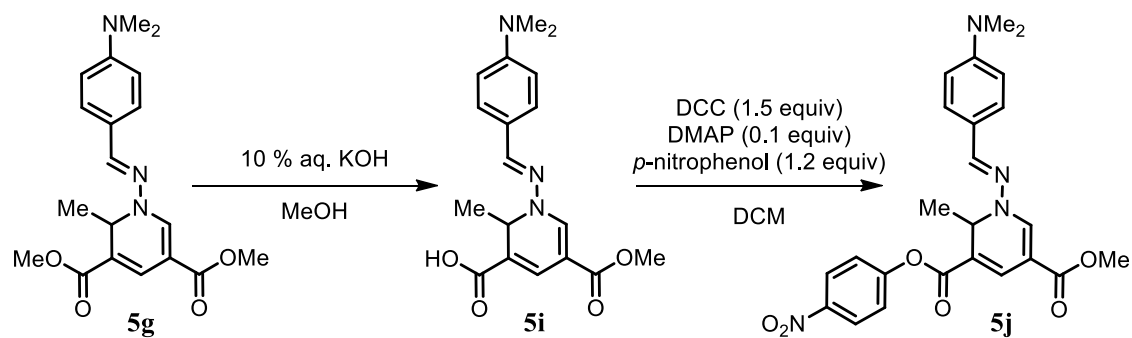
Our previous work



Our present work

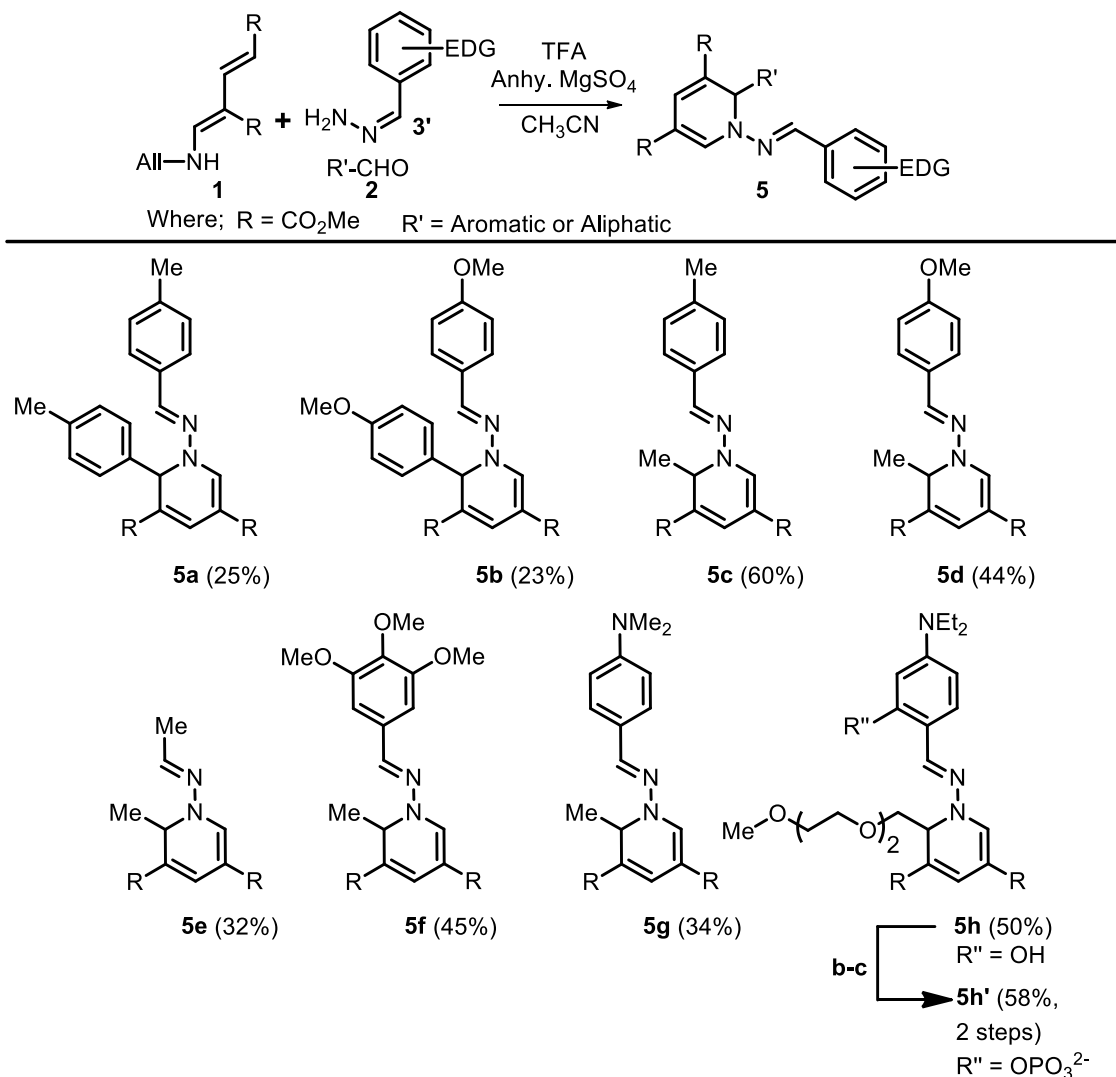


Scheme 2.3.1. Synthesis of *N*-phenyl (**4**) and *N*-benzylideneamine (**5**) appended 1,2-DHP



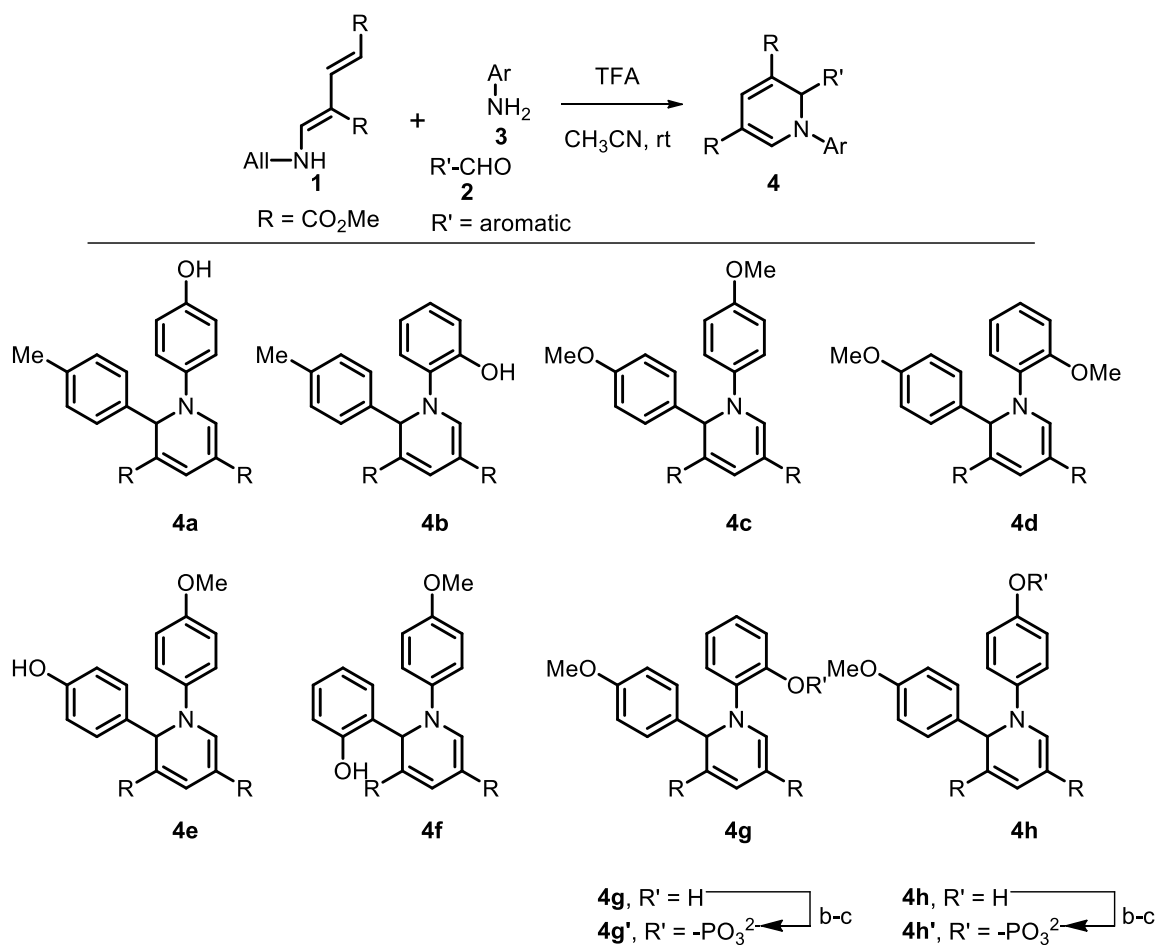
Scheme 2.3.2. Synthesis and ORTEP diagram of 4-nitrophenyl ester of 1,2-DHP **5j**

Table 2.3.1. *N*-benzylideneamine appended 1,2-DHP fluorophores **5a-5h'** by four-component condensation reaction^a

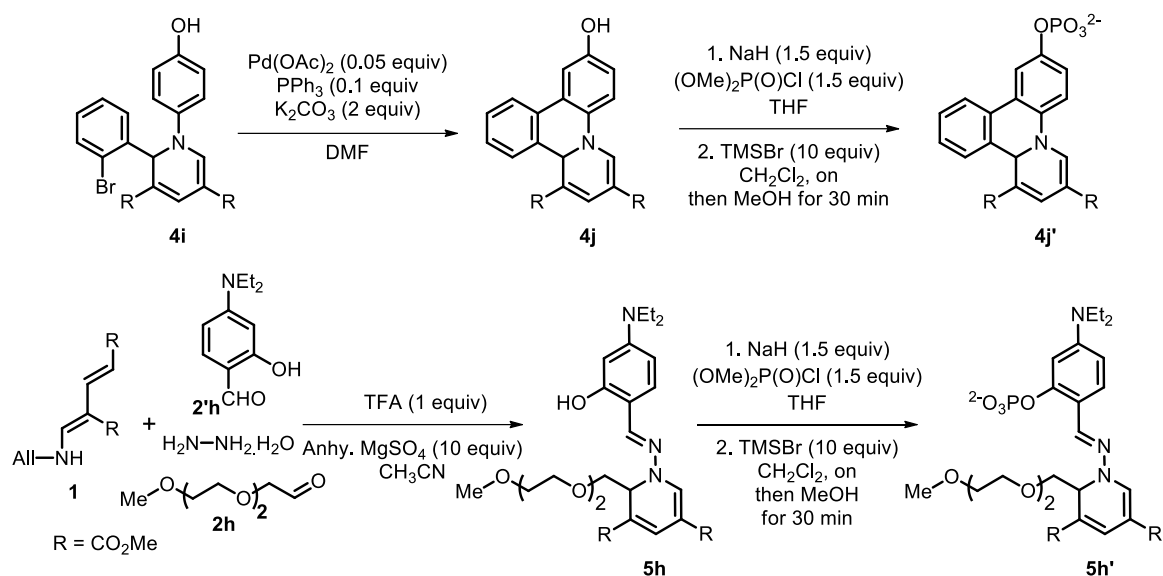


^aReagents and conditions: a) TFA (1 equiv), CH₃CN, rt, overnight; b) (OMe)₂P(O)Cl (1.5 equiv), NaH (1.5 equiv), THF, rt, 3 h; c) (i) TMSBr (10 equiv), CH₂Cl₂ (ii) MeOH.

Table 2.3.2. *N*-phenyl 1,2-DHP fluorophores **4a-4h'** by three-component condensation reaction^a



^aReagents and conditions: a) TFA (1 equiv), CH_3CN , rt, overnight; b) $(\text{OMe})_2\text{P}(\text{O})\text{Cl}$ (1.5 equiv), NaH (1.5 equiv), THF, rt, 3 h; c) (i) TMSBr (10 equiv), CH_2Cl_2 (ii) MeOH.



Scheme 2.3.3. Synthesis of tetracyclic 1,2-DHP **4j'** and synthesis of 1,2-DHP **5h'**

2.3.2. Photophysical properties

Table 2.3.3. Photophysical characterization of *N*-phenyl 1,2-DHPs **4a-4j'**

Entry	$\lambda_{\max}(\text{nm})^{[a]}$	$\epsilon (\text{M}^{-1} \text{cm}^{-1})^{[b]}$	$\lambda_{\text{em}} (\text{nm})$	$\Delta^{[c]}$	$\Phi^{[d]}$
4a	403	8179	528	5874	0.05
4b	400	8461	513	5507	0.05
4c	403	8642	524	5730	0.08
4d	397	6401	506	5426	0.02
4e	403	6972	521	5620	0.07
4f	408	4932	522	5353	0.05
4g	399	7893	508	5378	0.05
4h	404	9886	532	5955	0.04
4g'	397	5909	506	5426	0.03
4h'	400	7907	524	5916	0.06
4j	425	8668	537	4907	0.04
4j'	420	6568	530	4941	0.03

^[a] Measured in methanol at room temperature. ^[b] Molar extinction coefficient. ^[c] Stokes shift (cm^{-1}). ^[d] Quantum yield, determined at room temperature relative to coumarin 153 in MeOH ($\Phi = 0.46$).

The photophysical properties of *N*-phenyl 1,2-DHPs **4a-4j'** in methanol were characterized by absorption and emission spectroscopy. The details of absorption and emission maxima and quantum yield are provided in Table 2.3.3. The quantum yields for 1,2-DHP **4a-4j'** were determined by a relative comparison method using coumarin 153 as a standard and were found to be in the range of 0.02-0.08.¹³ As expected *N*-phenyl

substituted 1,2-DHP shows absorption maxima in the near UV region with $\lambda_{\max} \sim 400$ nm and have a low quantum yield.

Table 2.3.4. Photophysical characterization of 1,2-DHP **5a-5h'**

Entry	$\lambda_{\max}(\text{nm})^{[a]}$	$\epsilon (\text{M}^{-1} \text{cm}^{-1})^{[b]}$	$\lambda_{\text{em}} (\text{nm})$	$\Delta^{[c]}$	$\Phi^{[d]}$	$\tau^{[e]} (\text{ns})$
5a	419	10454	522	4709	0.059	1.41
5b	422	15461	524	4613	0.084	1.41
5c	419	16293	534	5140	0.067	1.06
5d	422	12261	527	4721	0.098	1.28
5e	396	5388	507	5529	0.032	0.43
5f	420	13741	530	4942	0.077	0.99
5g	436	23292	582	5753	0.125	1.12
5h	448	27300	586	5256	0.122	1.20
	†455	27400	583	4825	0.127	1.95
	‡454	25000	609	5606	0.012	1.94
5h'	448	15500	594	5486	0.094	1.07
	†458	16723	611	5467	0.025	n.d. ^[f]

^[a] Measured in methanol at room temperature. ^[b] Molar extinction coefficient. ^[c] Stokes shift (cm^{-1}). ^[d] Quantum yield, determined at room temperature relative to coumarin 153 in MeOH ($\Phi = 0.46$). ^[e] Fluorescence lifetime ($\lambda_{\text{ex}} = 418$ nm) was measured using time-correlated single photon counting (TCSPC) and monitoring at the respective emission maximum. ^[f] n.d. = Not determined due to weak fluorescence. † Measured in Tris buffer (25 mM, pH 7.4, 0.3% DMSO). ‡ Measured in Hepes buffer (25 mM, pH 7.4, 0.3% DMSO).

The photophysical properties of 1,2-DHPs **5a-5h** viz. absorption, emission, quantum yields and emission lifetime measurements are provided in Table 2.3.4 and figure 2.3A and B. The present design involves D- π -A or push-pull type system, thus the nature and position of the substituents on the 1,2-DHP moiety are crucial to tune their intramolecular charge transfer (ICT) properties which leads to different photophysical properties. 1,2-DHPs **5a-5h** exhibited maximum absorption wavelengths (λ_{\max}) between 396–448 nm in methanol with strong molar extinction coefficients (5388 to 27300 $\text{M}^{-1} \text{cm}^{-1}$) and emit in long wavelength region of 500–600 nm. 1,2-DHPs **5a** and **5b** exhibited similar photophysical properties, however, replacement of phenyl group at the sixth position with a methyl group did not offer any change in the properties of 1,2-DHPs **5c**, **5d** and **5f** when compared to the former. These results indicate that the tuning of fluorophoric properties of these 1,2-DHPs can be made by variations in the *N*-benzylideneamine moiety. Thus, the sixth position of 1,2-DHP is an ideal position for conjugation with other biomolecules for fluorophore tagging. To assess the role of *N*-benzylideneamine in 1,2-DHP, the *N*-

ethanimine appended 1,2-DHP **5e** was also synthesized and indeed it was found poorly emissive when compared to all other 1,2-DHPs because of reduced ICT character with lowest molar extinction coefficients ($\epsilon = 5388 \text{ M}^{-1} \text{ cm}^{-1}$). As expected, 1,2 DHP **5g** with strong donating group led to a significant bathochromic shift of λ_{max} (ca. 20 nm) and λ_{em} (ca. 50 nm) with higher molar extinction coefficient ($\epsilon = 23292 \text{ M}^{-1} \text{ cm}^{-1}$).

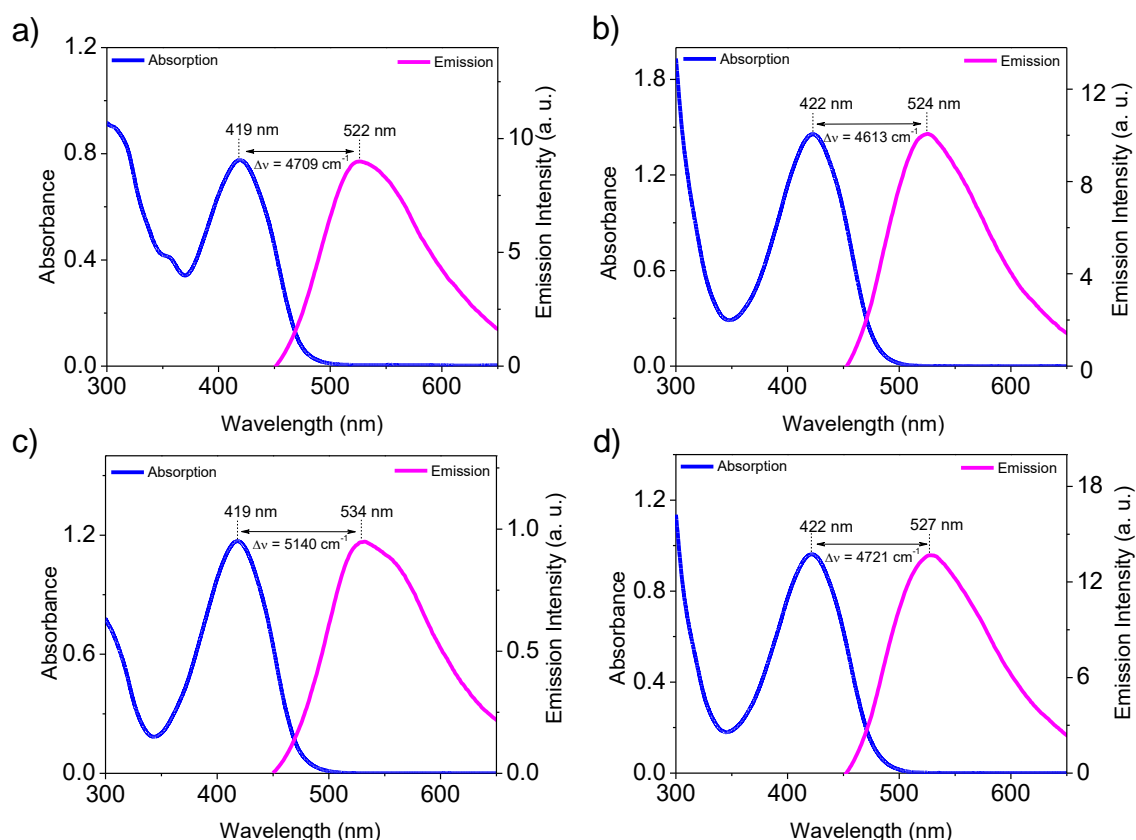


Figure 2.3A. Absorption and emission ($\lambda_{\text{ex}} = 430 \text{ nm}$) spectra of 1,2-DHPs in MeOH at room temperature. a) **5a**, b) **5b**, c) **5c**, and d) **5d**.

The fluorescence quantum yields for 1,2-DHPs **5a-5g** were determined by a relative comparison method using coumarin 153¹³ as a standard and were found to be in the range of 0.032-0.125 with 1,2-DHP **5g** being the highest. These compounds exhibited a remarkable Stokes shift values which can help in obtaining better fluorescence imaging with minimum self-absorption of the fluorophore. It is already established that for better cellular imaging, compounds should have absorption in the visible region and high fluorescence quantum yield. In this regard, based on the observed photophysical properties, the present design of 1,2-DHPs possess the potential for their application as bio-probes.

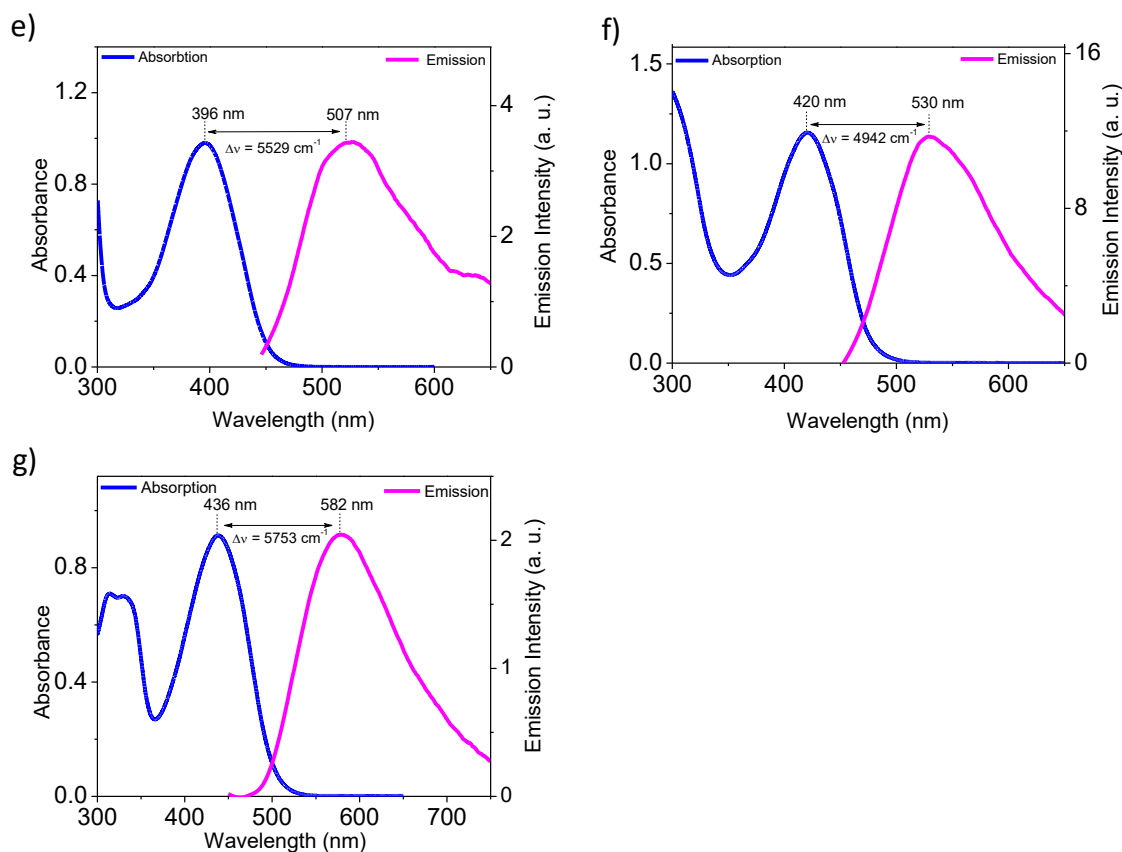


Figure 2.3B. Absorption and emission ($\lambda_{\text{ex}} = 430 \text{ nm}$) spectra of 1,2-DHPs in MeOH at room temperature. e) **5e**, f) **5f**, and g) **5g**.

2.3.3. Applications

The mitochondrial membrane has a negative potential of -180 mV , therefore, it is typical to use cationic dyes for imaging these organelles.¹⁴ The push-pull system in 1,2-DHPs (Figure 2.2B) renders the ring nitrogen of 1,2-DHP to attain a sufficient positive charge, thus, 1,2-DHPs may have an ability to serve as mitochondrial staining agents. Further, to assess the potential of 1,2-DHPs for specific mitochondrial staining, 1,2-DHPs **5a-5g** were studied in HeLa cells. Initially, cytotoxicity of 1,2-DHPs were evaluated using MTT assay and it was found that 1,2-DHPs exhibit greater than 80% cell viability at $30 \mu\text{M}$ (Figure 2.3C).

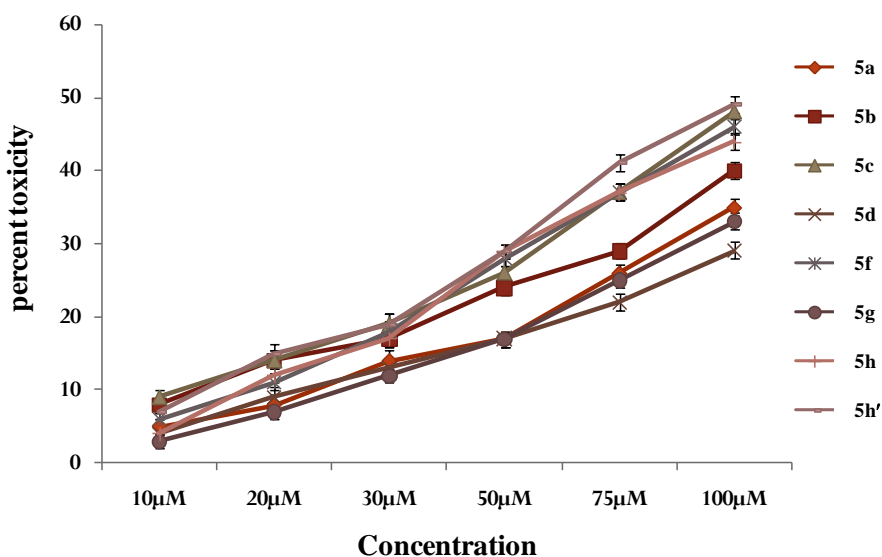


Figure 2.3C. Cytotoxicity assessed by MTT assay in HeLa cells. Different concentrations of **5a**, **5b**, **5c**, **5d**, **5f**, **5g**, **5h** and **5h'** were evaluated. Values are the mean \pm SD of three different experiments.

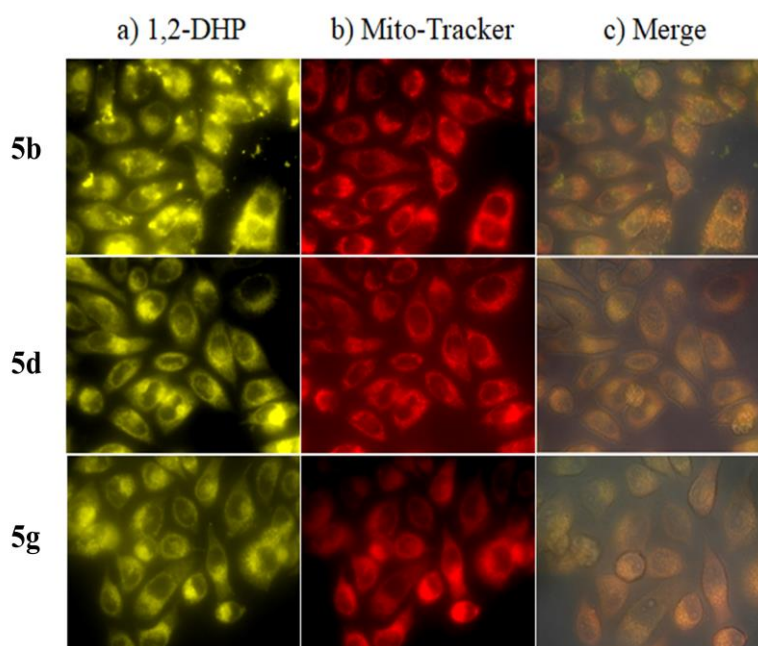


Figure 2.3D. Fluorescent images of HeLa cells a) treated with 1,2-DHPs **5b**, **5d** and **5g** (30 μ M) for 10 min, b) MitoTracker red CMXRos (CMXRos, 50 nM) for 30 min, c) merged image of (a) and (b) with bright field image (60 X magnification). Excitation wavelength: 440 nm (for 1,2-DHP) and 540 nm (for CMXRos) and Emission wavelength: 515 nm (for 1,2-DHP) and 645 nm (for CMXRos). Pearson's correlation coefficients were obtained as 0.79, 0.86 and 0.75 for 1,2-DHPs **5b**, **5d** and **5g**, respectively.

HeLa cells were incubated with 30 μ M of 1,2-DHPs for 10 minutes, and excess compound was washed with HBSS buffer solution. As shown in Figure 2.3D, 1,2-DHPs were localised mostly in the cytoplasm and specifically stained mitochondria in HeLa cells, and no nuclear uptake was observed. Additionally, the co-staining experiment with MitoTracker red CMXRos (CMXRos), a commercially available mitochondria imaging dye, confirmed the localisation of 1,2-DHPs in the mitochondria supported by Pearson's correlation coefficient in the range of 0.75-0.89. Among all the 1,2-DHPs under study, 1,2-DHP **5b**, **5d** and **5g** were found to exhibit high fluorescence intensity compared to others.

As a proof of concept, to justify the importance of the new 1,2-DHP as a fluorescent probe, we have synthesized a phosphorylated analogue **5h'** from 1,2-DHP **5h** (Scheme 2.3.3). It is well known that direct and rapid analysis of the crude lysate for endogenous phosphatase enzyme such as protein tyrosine phosphatases (PTPs) are of prime interest owing to their significant role in insulin signaling pathways¹⁵ and a variety of disease states¹⁶ including hepatocellular carcinoma¹⁷ as well as metabolic disorders.¹⁸ PTPs are significant targets in many diseases, and there is a growing need for direct determination of endogenous protein phosphatase activity.¹⁹ The UV-vis absorption spectrum of the 1,2-DHP **5h'** in methanol exhibited absorption maximum at 448 nm, and the corresponding emission spectrum shows a peak at 594 nm, while in aqueous buffer medium (25 mM HEPES buffer, pH 7.4) a small bathochromic shift was observed both in absorption and emission spectra (Figure 2.3E). The quantum yield of 1,2-DHP **5h'** in HEPES buffer medium is reduced to 0.007 which can be rationalized by differences in the electron density involved in conjugation with phosphate and phenoxide groups. This difference of electronic distribution reflected in fluorescence lifetime profile also. 1,2-DHP **5h** in HEPES buffer exhibited a fluorescence lifetime of 1.94 ns which is good enough for imaging experiments,²⁰ while its phosphorylated analogue 1,2-DHP **5h'** did not show any decay profile due to its weak fluorescence property (Table 2.3.4).

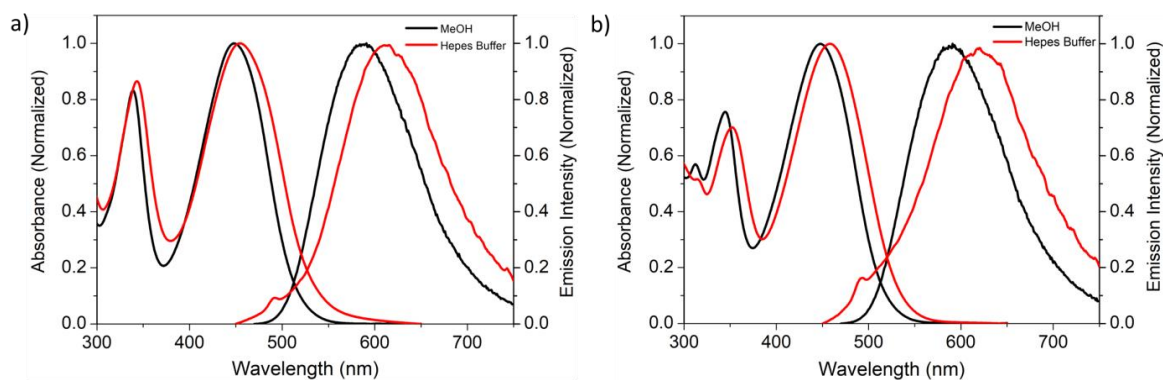


Figure 2.3E. Absorption and emission spectral profile (normalized) of a) 1,2-DHP **5h** and b) 1,2-DHP **5h'** in methanol and Hepes buffer (25 mM, pH 7.4, 0.3% DMSO) at room temperature.

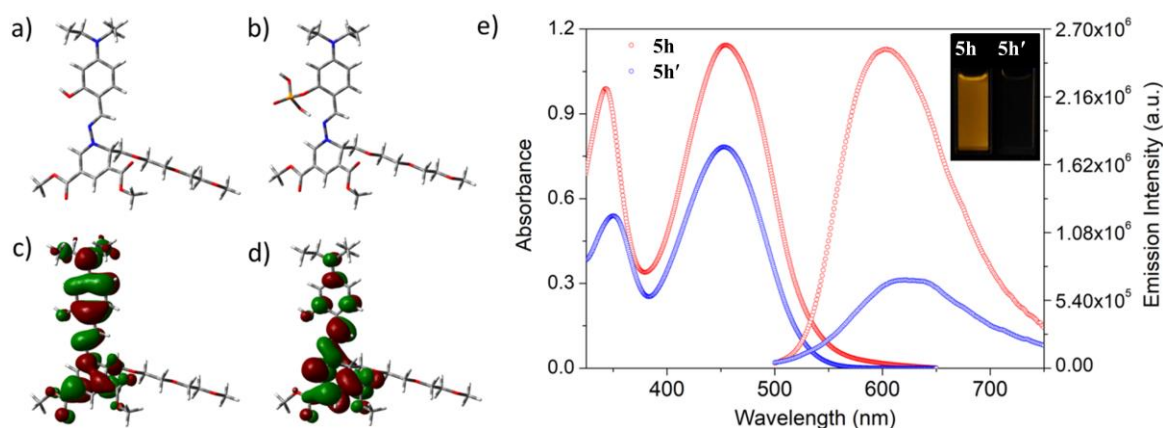


Figure 2.3F. Energy minimized structure of a) 1,2-DHP **5h** and b) 1,2-DHP **5h'** at DFT level and corresponding c) HOMO and d) LUMO of 1,2-DHP **5h**. e) Absorption, emission ($\lambda_{\text{ex}} = 450$ nm) spectra of 1,2-DHPs **5h** and **5h'** at room temperature (25 mM Hepes buffer, pH 7.4, 0.3% DMSO) and corresponding visual fluorescence change (inset).

To get the structural details of 1,2-DHPs **5h** and **5h'**, both the structures in its ground state were optimized using DFT with the B3LYP²¹ exchange correlation functional and the 6-31G** basis set²² with Gaussian G09 package²³ and the corresponding structures have been given in Figure 2.3Fa-b. The HOMO-LUMO of 1,2-DHP **5h** have been given in Figure 2.3Fc and 2.3Fd respectively, which show that the HOMO of 1,2-DHP **5h** is largely localized on the diethylaniline group whereas the LUMO is predominantly confined on 1,2-DHP core, thus supporting our concept of push-

pull system. In aqueous medium, at physiological pH (Hepes buffer, pH 7.4), the fluorescence emission properties of 1,2-DHPs **5h** and **5h'** showed distinct change. 1,2-DHP **5h** with free hydroxyl group exhibited a six-fold higher orange fluorescence to that of 1,2-DHP **5h'** appended with a phosphate group (Figure 2.3Fe). The corresponding fluorescence changes were also reflected in visual appearance of both the solutions (Figure 2.3Fe, inset).

This significant difference in emission intensity inspired us to explore 1,2-DHP **5h'** as a phosphatase sensor. As it is well known that, blinking and photobleaching of the fluorophores may cause problems for the imaging experiments,²⁴ thus the photostability of 1,2-DHP **5h'** was first tested by monitoring the fluorescence intensity as a function of time upon continuous irradiation ($\lambda = 445$ nm) in Hepes buffer solution (25 mM, pH 7.4, 0.3% DMSO) over a period of 20 minutes under aerobic conditions and was found to be quite stable (Figure 2.3G).

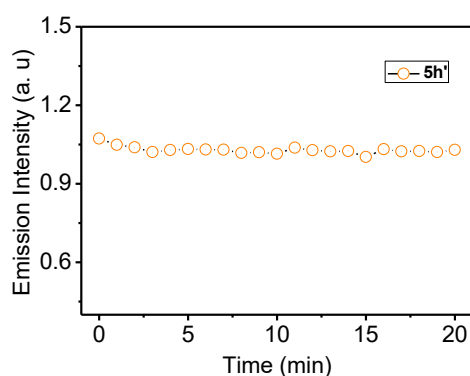


Figure 2.3G. Photostability of 1,2-DHP **5h'**.

Encouraged by the fluorescence features of 1,2-DHPs **5h** and **5h'**, we further investigated its suitability as a probe for biological systems. The cytotoxicity of 1,2-DHPs **5h** and **5h'** was determined by MTT assay in L6 cell lines. Cells were treated with different concentration of 1,2-DHPs **5h** and **5h'** ranging from 1 μ M to 30 μ M and after 2 hour treatment we found that both 1,2-DHPs **5h** and **5h'** were less than 20% toxic upto 30 μ M (Figure 2.3Ha).

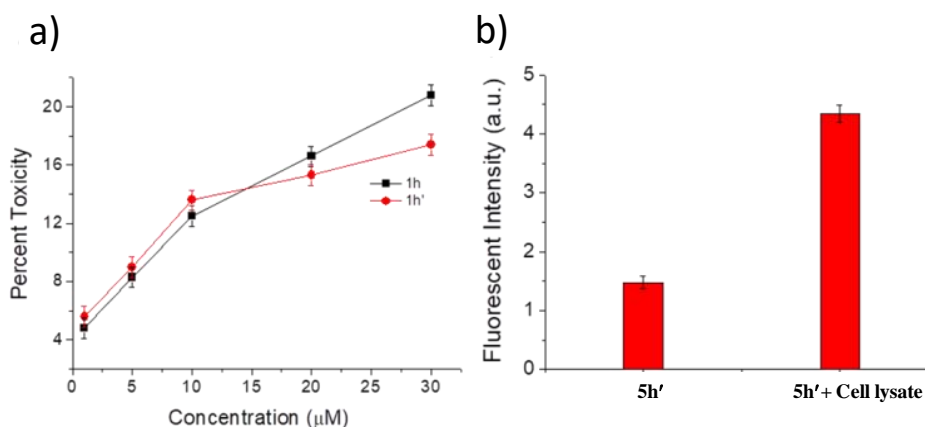


Figure 2.3H. a) Cytotoxicity of 1,2-DHPs **5h** and **5h'** in L6 myoblast by MTT assay at different concentrations. Values are the means \pm SD of three different experiments. b) Comparative emission intensity for the direct assessment of protein tyrosine phosphatase activity of 1,2-DHP **5h'** from cell lysate.

In our next attempt, we investigated the applicability of 1,2-DHP **5h'** as a chemosensor in presence of PTPs from L6 muscle cell lysate as a preliminary study. This enzymatic reaction was performed in a 96 micro-well plate by the addition of cell lysate (5 μ L, 0.8 μ g/ μ L) to a 100 μ L aqueous solution of 1,2-DHP **5h'** (30 μ M) in Hepes buffer (25 mM, pH 7.4, 0.3% DMSO). After incubation at room temperature for 15 min, the fluorescence intensities were measured at an excitation wavelength of 450 nm and emission at 590 nm. The increase in fluorescence intensity with time clearly indicated cleavage of phosphate group which is a result of conversion of 1,2-DHP **5h'** to 1,2-DHP **5h** (Figure 2.3Hb), thus, indicating the suitability of 1,2-DHP **5h'** as a fluorescent bio-probe useful for monitoring the activity of PTPs. Further to demonstrate the interference of 1,2-DHP **5h'** with other biologically relevant analytes, we measured the change in fluorescence intensity of **5h'** in presence of various metal ions, reactive oxygen species and under different pH conditions. Interestingly, there was no influence of these analytes in varying the fluorescence intensity 1,2-DHP **5h'** (Figure 2.3I and Figure 2.3J).

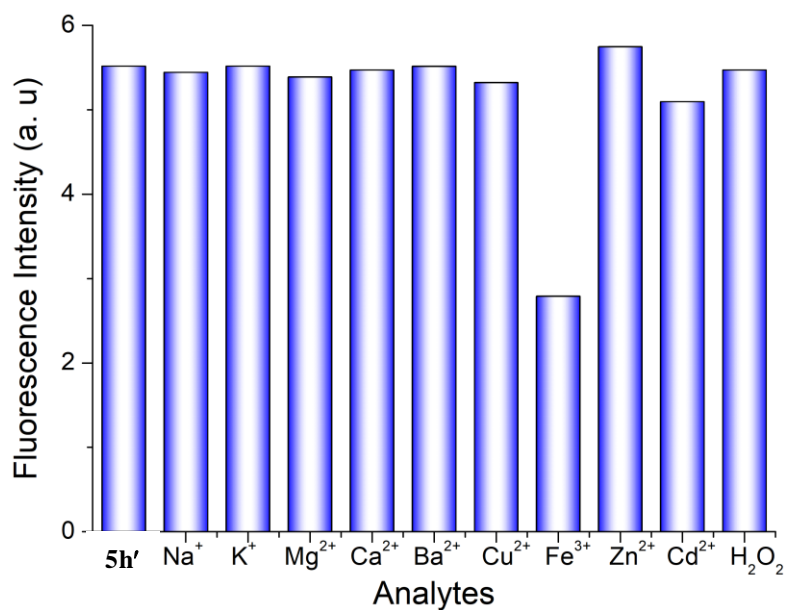


Figure 2.3I. Changes in the fluorescence intensity of 1,2-DHP **5h'** (10 μ M in aqueous solution at pH 7.4) in presence various biologically important metal ions (100 μ M) and reactive oxygen species H₂O₂ (10 μ M).

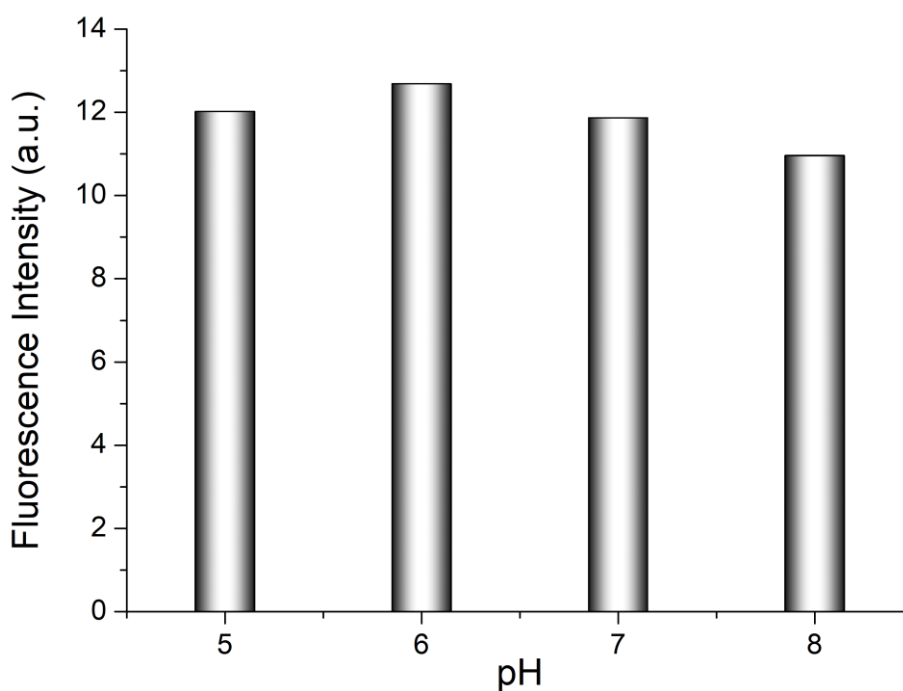


Figure 2.3J. Changes in the fluorescence intensity of 1,2-DHP **5h'**(10 μ M) at different pH (5 to 8).

2.4. Conclusion

In summary, we have designed and synthesized a new class of 1,2-DHP based fluorophores by a facile one-step multicomponent protocol, and their photophysical properties were studied in detail. The results indicate that 1,2-DHPs with an extended *N*-benzylideneamine appendage have an absorption and emission maxima around 420 and 600 nm, respectively, having prominent Stokes shift. In particular, 1,2-DHPs **5g** and **5h** showed remarkable photophysical properties with high fluorescence. Furthermore, 1,2-DHPs **5b**, **5d** and **5g** are recognised as well-suited mitochondrial staining agents in HeLa cells. The potential of fluorophore 1,2-DHP **5h'** as a fluorescent probe in tyrosine phosphatase activity on the cell lysate was also explored. Synthetic accessibility and scope for conjugation warrants the utility of 1,2-DHP as a potential fluorescent probe for biological applications.

2.5. Experimental section

2.5.1. General experimental methods

All the reactions were conducted using undistilled solvents, whereas CH₂Cl₂ was distilled over CaH₂ which was used for the demethylation of the phosphate ester of 1,2-DHP **5h**. Silica gel 60 F₂₅₄ aluminium TLC plates were used to monitor the reactions with short and long wavelength UV and visible lights to visualize the spots. Column chromatography was performed on silica gel 100-200 and 230-400 mesh. Shimadzu HPLC instrument with C18-phenomenex reversed phase column (250 × 21.2 mm, 5 μm) was used for the purification of 1,2-DHP **5h'** using methanol and water. ¹H, ¹³C and ³¹P NMR spectra were recorded on a Bruker Avance II spectrometer at 500, 125 and 202 MHz, respectively. Chemical shifts are given in ppm using solvent residual peak of chloroform δ 7.26, methanol δ 3.31 ppm as reference, and coupling constants in Hz. HR-ESI-MS analysis was recorded on a Thermo Scientific Exactive-LCMS instrument with ions given in *m/z*. Absorption spectra were recorded using a Shimadzu UV-2450, UV-Visible spectrophotometer using quartz cuvette with a 1 cm path length. Fluorescence spectrum of the 1,2-DHPs were recorded on a FluoroLog-322 (Horiba), which was equipped with a 450 W Xe arc lamp as the excitation source. The fluorescence quantum yields were determined with the relative method employing an optically matched solution

of coumarin 153 in MeOH as the reference ($\Phi_R = 0.46$). The following equation was used for calculating quantum yield,

$$\Phi_S = \frac{\text{Abs}_R}{\text{Abs}_S} \times \frac{\text{Area}_S}{\text{Area}_R} \times \frac{n_S^2}{n_R^2} \times \Phi_R$$

Where, the subscript R and S refers to the reference and samples respectively. Abs, Area and n are the absorbance at the excitation wavelength, area under the fluorescence spectrum and refractive index of the solvent, respectively. Fluorescence lifetimes were measured using an IBH (FluoroCube) time correlated single photon counting (TCSPC) system. L6 myoblast and HeLa cells were obtained from National Centre for Cell Sciences, Pune, India. Tris buffer (25 mM, pH 7.4, 0.3% DMSO), Hepes buffer (25 mM, pH 7.4, 0.3% DMSO) and Hanks balanced salt solution (HBSS, pH 7.4) buffers were used for the cell culture studies. The cells were visualized using a fluorescent microscope (Pathway 855, BD Bioscience, USA). Pearson's correlation coefficients were calculated using ImageJ software with JACoP plugin.

2.5.2. General procedure for the synthesis of 1,2-DHP 4a-4i

To a solution of compound **1** in CH₃CN was added pertinent aldehyde (1.2 equiv), amine (1.2 equiv), and TFA (1.0 equiv) in a sequence at room temperature. The reaction mixture usually develops a bright yellow color within 15 min which is an indication of the formation of 1,2-DHP. After complete consumption of **1**, as observed on TLC, the reaction mixture was quenched with saturated NaHCO₃, extracted with ethyl acetate, dried (Na₂SO₄) and concentrated. The resulting residue was purified by flash column chromatography to afford 1,2-DHP derivative.

2.5.3. General procedure for the synthesis of hydrazone

To a solution of hydrazine hydrate (10 equiv) in ethanol (10 mL) was added pertinent aldehyde (1 equiv) and the resulting mixture was stirred under reflux overnight. After complete consumption of the aldehyde, as indicated by ¹H NMR, the reaction mixture was diluted with water and extracted with CH₂Cl₂. The organic layer was dried over anhydrous Na₂SO₄, concentrated, and the resulting residue was used directly for the next step without further purification.

2.5.4. General procedure for the synthesis of 1,2-DHPs 5a-5g

To a solution of dieneaminodioate (0.77 mmol, 1 equiv) in CH₃CN (3 mL) was added aldehyde (1.15 mmol, 1.5 equiv), hydrazone (1.15 mmol, 1.5 equiv) and trifluoroacetic

acid (0.77 mmol, 1 equiv) at room temperature. The reaction mixture usually develops a yellow to dark red coloration immediately, which is an indication of the formation of 1,2-DHP. After complete consumption of dieneaminodioate, as observed on TLC, the reaction mixture was quenched with saturated aqueous NaHCO₃ and extracted with EtOAc. The organic layer was dried over anhydrous Na₂SO₄, concentrated and the resulting residue was purified by column chromatography to afford the desired 1,2-DHP.

2.5.5. Procedure for the synthesis of 1,2-DHP 5h

To a solution of triethylene glycol monomethyl ether (7.92 mmol, 1 equiv) in CH₂Cl₂ at room temperature was added Dess-Martin periodinane (19.8 mmol, 2.5 equiv) in one portion. After one hour of stirring, the reaction mixture was filtered through a celite pad and washed with EtOAc. The resulting filtrate was concentrated under reduced pressure, and the ¹H NMR of the crude mixture confirmed the formation of the aldehyde. The crude aldehyde without further purification was treated with hydrazine hydrate (6.66 mmol, 3 equiv) in presence of trifluoroacetic acid (1.11 mmol, 0.5 equiv) and anhydrous MgSO₄ (22.2 mmol, 10 equiv) in CH₃CN (10 mL) solvent. After 15 min, dieneaminodioate (2.22 mmol, 1 equiv) and trifluoroacetic acid (1.11 mmol, 0.5 equiv) were added. The mixture was then allowed to stir for 8h at room temperature. After complete consumption of dieneaminodioate, as observed on TLC, the reaction mixture was quenched with saturated aqueous NaHCO₃ and extracted with EtOAc. The organic layer was dried over anhydrous Na₂SO₄, concentrated and the resulting residue was purified by column chromatography to afford the desired 1,2-DHP **5h**.

2.5.6. Procedure for the synthesis of 1,2-DHP 5h'

To a stirred solution of 1,2-DHP **5h** (0.53 mmol, 1 equiv) and NaH (60% dispersion in oil, 0.79 mmol, 1.5 equiv) in THF (4 mL) at room temperature under nitrogen atmosphere was added dimethyl chlorophosphate (0.79 mmol, 1.5 equiv). After 3h of stirring at room temperature, the reaction mixture was quenched with water and extracted with EtOAc. The organic layer was dried over anhydrous Na₂SO₄, filtered and the solvent was evaporated under reduced pressure. The crude product was purified by column chromatography on silica gel to afford the diethyl phosphate ester of 1,2-DHP **1h**. To a solution of this diethyl phosphate ester of 1,2-DHP **5h** (0.11 mmol, 1 equiv) in dry CH₂Cl₂ (3 mL) was added bromotrimethylsilane (1.08 mmol, 10 equiv) dropwise at room temperature. The reaction mixture was stirred overnight at room temperature under nitrogen atmosphere and quenched with MeOH (5 mL), stirring was continued for further

30 mins. The reaction mixture was then concentrated and purified by reversed-phase HPLC using H₂O/methanol to afford 1,2-DHP **5h'**. Phosphorylated analogues **4g'**, **4h'** and **4j'** were synthesised using this procedure.

2.5.7. Procedure for the synthesis of 1,2-DHP 5j'

To a solution of 1,2-DHP **5g** (0.08 mmol, 1 equiv) in MeOH (4 mL) was added 10% aqueous KOH (2.5 mL) and stirred at room temperature overnight. The reaction mixture was then evaporated, diluted with 20% aqueous KHSO₄ (4 mL), and extracted with CHCl₃/MeOH (7:1, 2 x 30 mL). The organic layer was dried over anhydrous Na₂SO₄, concentrated and the resulting residue was purified by column chromatography using CHCl₃/MeOH 98:2 to afford the mono-carboxylic acid product of 1,2-DHP **5g** (92%).

To a solution of mono-carboxylic acid (0.03 mmol, 1 equiv) in CH₂Cl₂ (1.5 mL) were added *p*-nitrophenol (0.03 mmol, 1.2 equiv), *N,N'*-dicyclohexylcarbodiimide (0.04 mmol, 1.5 equiv), and 4-dimethylaminopyridine (0.003 mmol, 0.1 equiv) at room temperature. After complete consumption of the starting material, the reaction mixture was quenched with saturated aqueous NaHCO₃ (5 mL) and extracted with CH₂Cl₂ (2 x 10 mL). The organic layer was washed thrice with saturated NaHCO₃. The combined organic layers were dried over anhydrous Na₂SO₄, concentrated and the resulting residue was purified by column chromatography using hexane/EtOAc 95:5 to afford 1,2-DHP **5j** as an orange red needle like crystalline product.

2.5.8. Cellular studies:

2.5.8A. Cell culture and treatment:

Rat skeletal muscle cell lines (L6 myoblasts) and Cervical cancer cell line (HeLa) were maintained in DMEM supplemented with 10% FBS, 1% antibiotic–antimycotic mix at 37 °C under 5% CO₂ atmosphere.

2.5.8B. Cell viability study of 1,2 DHPs 5h and 5h' on L6 myoblast:

MTT assay was performed to check the cytotoxicity of the compounds. The viability of L6 myoblast was measured by means of MTT assay. Cytotoxicities of 1,2 DHPs **5h** and **5h'** (1 μM, 5 μM, 10 μM, 20 μM and 30 μM) were standardized based on concentration. Briefly, cells after incubation with the compound were washed and MTT (0.5 g/L), dissolved in DMEM, was added to each well for the estimation of mitochondrial dehydrogenase activity as described previously by Mosmann.²⁵ After an additional 2 h of incubation at 37 °C in a CO₂ incubator, 10% SDS in DMSO was added to each well, and the absorbance at 570 nm of solubilized MTT formazan products were measured after 45

min using a micro-plate reader (BIOTEK-USA). Results were expressed as percentage of cytotoxicity.

$$\text{Percentage of Toxicity} = \frac{\text{Absorbance of Control} - \text{Absorbance of Sample}}{\text{Absorbance of Control}} \times 100$$

2.5.8C. Preparation of cell lysate:

Cells were grown in T25 flasks, after attaining 60% confluency, cells were differentiated in DMEM containing 2% horse serum for 5 days. Differentiated cells were then washed three times with HEPES buffer (25 mM, pH 7.4). Cells were scraped off from the plates using a cell scraper, centrifuged and the proteins were extracted from the cell pellet using 0.15 M KCl (4 °C for 30 min). The protein content of the lysate was then measured using BCA protein assay kit.

2.5.8D. Cell viability on HeLa Cell:

Viability of HeLa cell was measured by means of MTT assay as explained before for the L6 myoblast. Cytotoxicities of **5a**, **5b**, **5c**, **5d**, **5f**, **5g**, **5h** and **5h'** (10 μM, 20 μM, 30 μM, 50 μM, 75 μM and 100 μM) were carried out based on the concentrations.

2.5.8E. Co-Localization study of 1,2-DHPs with MitoTracker CMXRos:

Cells were grown in 96 well black clear bottom plates (BD Biosciences, Franklin Lakes, NJ) and after attaining 90% confluency the cells were taken for the experiments. HeLa cells were incubated with Mito-Tracker CMXRos (50 nM) for 20 minutes at 37°C followed by addition of corresponding 1,2-DHPs (30 μM) and incubated for 10 minutes. This was followed by washing the cells twice with HBSS to remove unbound dye. The cells were visualized under a fluorescent microscope (Pathway 855, BD Bioscience, USA)

2.5.9. Spectral details of products

Dimethyl 1-(4-hydroxyphenyl)-2-(p-tolyl)-1,2-dihydropyridine-3,5-dicarboxylate (4a)

¹H NMR (CDCl₃, 500 MHz): δ = 7.94 (s, 1H), 7.73 (d, *J* = 1 Hz, 1H), 7.24 (d, *J* = 8 Hz, 2H), 7.08 (d, *J* = 8 Hz, 2H), 6.94 (d, *J* = 8 Hz, 2H), 6.78 (d, *J* = 8 Hz, 2H), 5.98 (s, 1H), 3.80 (s, 3H), 3.74 (s, 3H), 2.31 ppm (s, 3H); ¹³C NMR (CDCl₃, 125 MHz): δ = 166.7, 166.3, 158.3, 156.1, 146.7, 137.8, 133.7, 130.9, 127.9, 123.8, 115.5, 114.6, 113.6, 100.6, 62.0, 51.6, 51.3, 21.3 ppm; HR-ESI-MS: *m/z* calcd for C₂₂H₂₁NNaO₅: 402.1317 [M + Na]⁺; found: 402.1313.

Dimethyl 1-(2-hydroxyphenyl)-2-(p-tolyl)-1,2-dihydropyridine-3,5-dicarboxylate (4b)

¹H NMR (CDCl₃, 500 MHz): δ = 7.87 (s, 1H), 7.44 (s, 1H), 7.17 (d, J = 7.5 Hz, 2H), 7.13 (d, J = 8 Hz, 1H), 7.04 (d, J = 7.5 Hz, 2H), 6.92 (d, J = 8 Hz, 1H), 6.85 (d, J = 8 Hz, 1H), 6.79 (t, J = 7.5 Hz, 1H) 5.94 (s, 1H), 3.79 (s, 3H), 3.70 (s, 3H), 2.30 ppm (s, 3H); ¹³C NMR (CDCl₃, 125 MHz): δ = 166.6, 166.4, 150.6, 150.0, 138.5, 137.9, 132.1, 131.3, 129.3, 129.2, 128.1, 127.1, 120.9, 117.3, 113.7, 99.2, 62.2, 51.6, 51.2, 21.1 ppm; HR-ESI-MS: m/z calcd for C₂₂H₂₁NNaO₅: 402.1317 [M + Na]⁺; found: 402.1311.

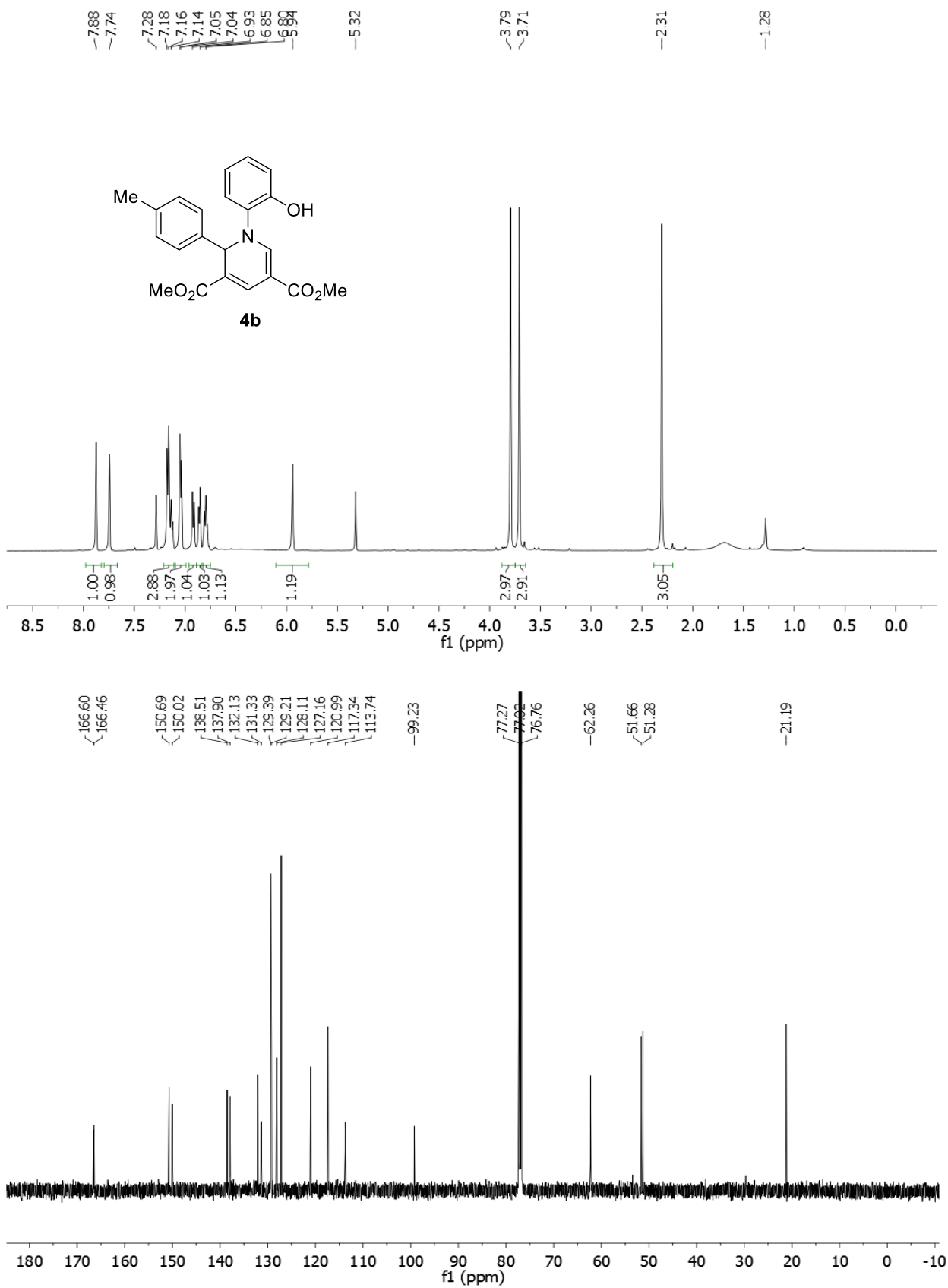
Dimethyl 1,2-bis(4-methoxyphenyl)-1,2-dihydropyridine-3,5-dicarboxylate (4c)

¹H NMR (CDCl₃, 500 MHz): δ = 7.96 (s, 1H), 7.74 (s, 1H), 7.32 (d, J = 8 Hz, 2H), 7.06 (d, J = 8 Hz, 2H), 6.84 (d, J = 8.5 Hz, 2H), 6.82 (d, J = 8 Hz, 2H), 5.97 (s, 1H), 3.79 (s, 3H), 3.78 (s, 3H), 3.73 ppm (s, 3H); ¹³C NMR (CDCl₃, 125 MHz): δ = 166.3, 166.2, 159.5, 158.2, 146.5, 137.9, 134.1, 130.8, 127.6, 123.5, 114.6, 114.0, 113.5, 101.1, 61.8, 55.5, 55.2, 55.0, 51.5, 51.1 ppm; HR-ESI-MS: m/z calcd for C₂₃H₂₃NNaO₆: 432.1423 [M + Na]⁺; found: 432.1420.

Dimethyl 1-(2-methoxyphenyl)-2-(4-methoxyphenyl)-1,2-dihydropyridine-3,5-dicarboxylate (4d)

¹H NMR (CDCl₃, 500 MHz): δ = 7.82 (d, J = 1 Hz, 1H), 7.66 (s, 1H), 7.24 (m, 1H), 7.14 (m, 3H), 6.93 (dd, J = 7.5, 0.5, Hz, 1H), 6.83 (m, 2H), 6.73 (d, J = 8 Hz, 2H), 5.84 (s, 1H), 3.77 (s, 3H), 3.75 (s, 3H), 3.73 (s, 3H) 3.67 ppm (s, 3H); ¹³C NMR (CDCl₃, 125 MHz): δ = 166.4, 166.2, 159.5, 153.7, 150.0, 133.6, 132.8, 131.7, 129.0, 128.6, 128.2, 128.1, 127.6, 125.6, 120.9, 113.6, 113.5, 112.2, 98.3, 62.0, 55.8, 55.1, 51.4, 51.0 ppm; HR-ESI-MS: m/z calcd for C₂₃H₂₃NNaO₆: 432.1423 [M + Na]⁺; found: 432.1429.

Figure 2.5A. ¹H and ¹³C NMR Spectra of 4b



Dimethyl 2-(4-hydroxyphenyl)-1-(4-methoxyphenyl)-1,2-dihydropyridine-3,5-dicarboxylate (**4e**)

¹H NMR (CDCl₃, 500 MHz): δ = 7.84 (s, 1H), 7.66 (s, 1H), 7.12 (d, J = 7.5 Hz, 2H), 6.91 (d, J = 8 Hz, 2H), 6.71 (d, J = 8 Hz, 2H), 6.61 (d, J = 8 Hz, 2H), 5.84 (s, 1H), 3.72 (s, 3H), 3.70 (s, 3H), 3.63 ppm (s, 3H); ¹³C NMR (CDCl₃, 125 MHz): δ = 166.7, 166.3, 158.3, 156.1, 146.7, 137.8, 133.7, 130.9, 127.9, 123.8, 115.5, 114.6, 113.6, 100.6, 62.0, 55.5, 51.6, 51.3 ppm; HR-ESI-MS: m/z calcd for C₂₂H₂₁NNaO₆: 418.1266 [M + Na]⁺; found: 418.1260.

Dimethyl 2-(2-hydroxyphenyl)-1-(4-methoxyphenyl)-1,2-dihydropyridine-3,5-dicarboxylate (**4f**)

¹H NMR (CDCl₃, 500 MHz): δ = 8.13 (s, 1H), 7.71 (d, J = 1 Hz, 1H), 7.37 (dd, J = 8, 1.5 Hz, 1H), 7.14 (td, J = 8.5, 1.5 Hz, 1H), 6.92 (m, 3H), 6.79 (td, J = 7.5, 1 Hz, 1H), 6.73 (d, J = 9 Hz, 2H), 6.07 (s, 1H), 3.75 (s, 3H), 3.72 (s, 3H), 3.68 ppm (s, 3H); ¹³C NMR (CDCl₃, 125 MHz): δ = 168.9, 166.0, 158.2, 150.6, 146.4, 137.5, 132.5, 130.5, 130.0, 126.8, 121.9, 121.8, 119.3, 114.7, 111.4, 101.5, 56.1, 55.5, 52.5, 51.4 ppm; HR-ESI-MS: m/z calcd for C₂₂H₂₁NNaO₆: 418.1266 [M + Na]⁺; found: 418.1276.

Dimethyl 1-(2-hydroxyphenyl)-2-(4-methoxyphenyl)-1,2-dihydropyridine-3,5-dicarboxylate (**4g**)

¹H NMR (CDCl₃, 500 MHz): δ = 7.86 (d, J = 1.5 Hz, 1H), 7.76 (s, 2H), 7.16 (d, J = 6.5 Hz, 1H), 7.08 (td, J = 8.5, 2 Hz, 1H), 6.89 (dd, J = 8, 1 Hz, 1H), 6.77 (dd, J = 8, 1.5 Hz, 1H), 6.74 (d, J = 8 Hz, 1H), 6.70 (d, J = 9 Hz, 1H), 5.99 (s, 1H), 3.77 (s, 3H), 3.73 (s, 3H), 3.68 ppm (s, 3H); ¹³C NMR (CDCl₃, 125 MHz): δ = 166.8, 166.7, 159.6, 150.7, 150.3, 133.2, 132.2, 131.0, 129.0, 128.6, 128.0, 120.6, 117.2, 113.8, 113.5, 98.4, 61.6, 55.1, 51.7, 51.3 ppm; HR-ESI-MS: m/z calcd for C₂₂H₂₁NNaO₆: 418.1266 [M + Na]⁺; found: 418.1261.

Dimethyl 1-(4-hydroxyphenyl)-2-(4-methoxyphenyl)-1,2-dihydropyridine-3,5-dicarboxylate (**4h**)

¹H NMR (CDCl₃, 500 MHz): δ = 7.91 (s, 1H), 7.74 (d, J = 1 Hz, 1H), 7.27 (d, J = 6.5 Hz, 2H), 6.92 (d, J = 7 Hz, 2H), 6.79 (d, J = 8.5 Hz, 2H), 6.77 (d, J = 8.5 Hz, 2H), 5.93 (s,

1H), 3.80 (s, 3H), 3.76 (s, 3H), 3.73 ppm (s, 3H); ¹³C NMR (CDCl₃, 125 MHz): δ = 166.9, 166.6, 159.5, 155.4, 146.7, 137.3, 133.8, 131.0, 127.6, 123.7, 116.1, 114.0, 113.1, 100.5, 61.9, 60.5, 55.2, 51.4 ppm; HR-ESI-MS: *m/z* calcd for C₂₂H₂₁NNaO₆: 418.1266 [M + Na]⁺; found: 418.1269.

Dimethyl-2-(4-methoxyphenyl)-1-(2-(phosphonooxy)phenyl)-1,2-dihydropyridine-3,5-dicarboxylate (4g)

¹H NMR (CDCl₃, 500 MHz): δ = 7.74 (s, 1H), 7.72 (s, 1H), 7.53 (d, *J* = 8 Hz, 1H), 7.29 (t, *J* = 7.5 Hz, 1H), 7.14 (d, *J* = 7 Hz, 2H), 7.00 (t, *J* = 6 Hz, 1H), 6.81 (d, *J* = 7 Hz, 1H), 6.77 (d, *J* = 9 Hz, 2H), 5.96 (s, 1H), 3.74 (s, 3H), 3.73 (s, 3H), 3.64 ppm (s, 3H); ¹³C NMR (CDCl₃, 125 MHz): δ = 165.3, 165.1, 158.9, 150.0, 149.9, 133.8, 133.6, 133.4, 130.6, 128.3, 128.2, 127.7, 121.8, 121.4, 121.2, 113.7, 113.6, 99.5, 96.7, 60.9, 60.8, 54.9, 51.3, 51.2, 50.7 ppm; HR-ESI-MS: *m/z* calcd for C₂₂H₂₁NO₉P: 474.0954 [M - 1]⁻; found: 474.0959.

Dimethyl-2-(4-methoxyphenyl)-1-(4-(phosphonooxy)phenyl)-1,2-dihydropyridine-3,5-dicarboxylate (4h)

¹H NMR (CDCl₃, 500 MHz): δ = 7.99 (s, 1H), 7.64 (s, 1H), 7.21 (m, 6H), 7.80 (m, 2H), 6.02 (s, 1H), 3.77 (s, 3H), 3.73 (s, 3H), 3.70 ppm (s, 3H); ¹³C NMR (CDCl₃, 125 MHz): δ = 165.5, 165.3, 159.7, 149.9, 145.3, 140.6, 133.8, 129.8, 127.4, 122.4, 121.4, 114.5, 113.9, 101.8, 60.9, 54.6, 51.0, 50.5, ppm; HR-ESI-MS: *m/z* calcd for C₂₂H₂₂NNaO₉P: 498.0930 [M + Na]⁺; found: 498.0932.

Dimethyl 2-hydroxy-9aH-pyrido[1,2-f]phenanthridine-7,9-dicarboxylate (4j)

¹H NMR (CDCl₃, 500 MHz): δ = 9.91 (s, 1H), 7.75 (d, *J* = 7.5 Hz, 1H), 7.69 (s, 1H), 7.58 (s, 1H), 7.38 (m, 4H), 6.96 (d, *J* = 7.5 Hz, 1H), 6.88 (d, *J* = 8.5 Hz, 1H), 5.68 (s, 1H), 3.74 (s, 3H), 3.62 ppm (s, 3H); ¹³C NMR (CDCl₃, 125 MHz): δ = 171.0, 170.4, 160.5, 150.8, 139.0, 138.5, 136.1, 134.6, 134.0, 132.0, 131.6, 127.6, 127.5, 124.3, 119.9, 114.4, 114.0, 102.2, 60.1, 55.6, 55.0 ppm; HR-ESI-MS: *m/z* calcd for C₂₁H₁₇NNaO₅: 386.1004 [M + Na]⁺; found: 386.1009.

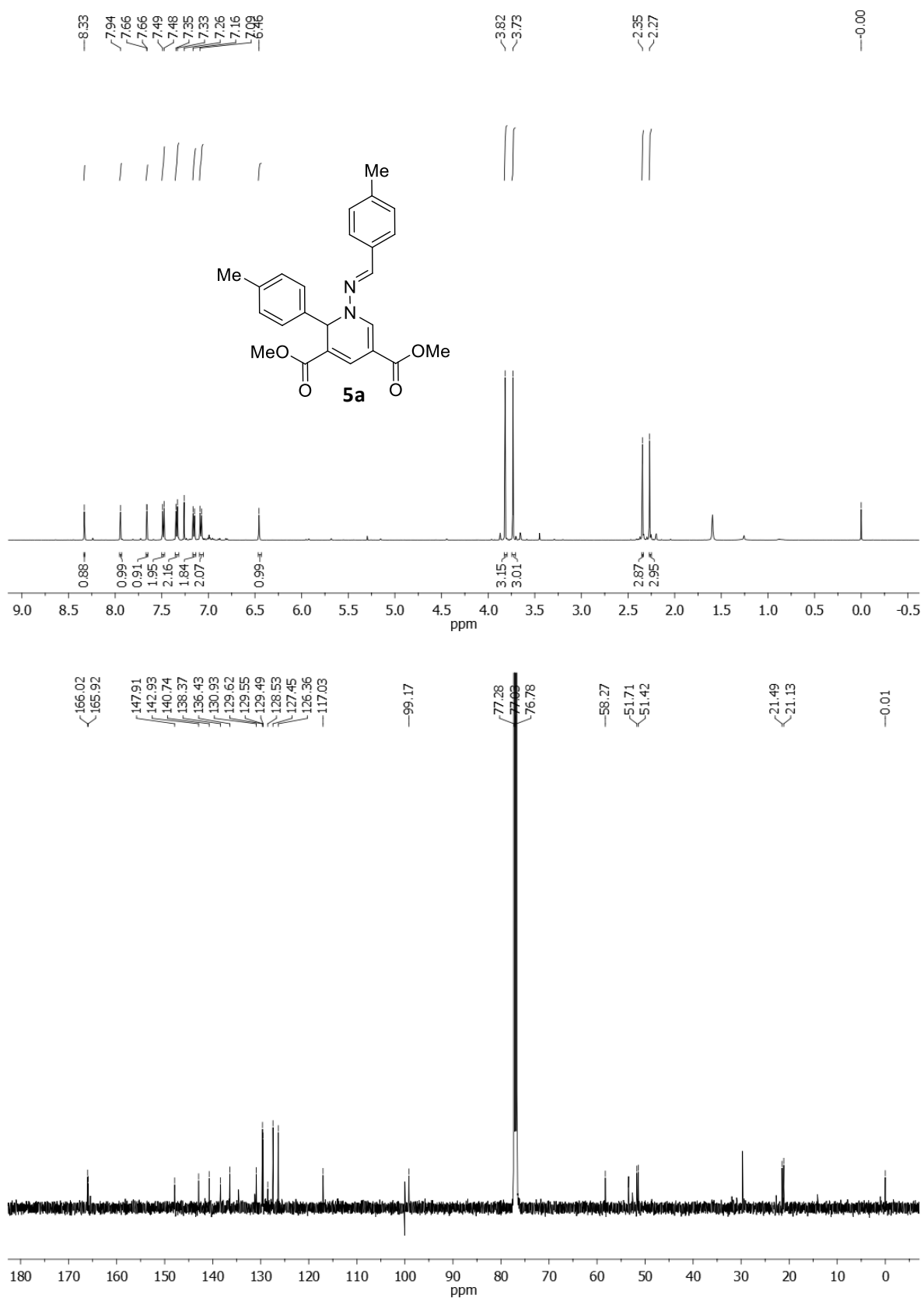
Dimethyl 2-(phosphonoxy)-9aH-pyrido[1,2-f]phenanthridine-7,9-dicarboxylate (4j')

¹H NMR (CDCl₃, 500 MHz): δ = 7.86 (m, 3H), 7.67 (s, 1H), 7.41 (t, J = 7.5 Hz, 1H), 7.35 (m, 3H), 7.01 (d, J = 7.5 Hz, 1H), 5.79 (s, 1H), 3.81 (s, 3H), 3.72 ppm (s, 3H); ¹³C NMR (CDCl₃, 125 MHz): δ = 166.8, 166.3, 146.5, 134.8, 134.7, 133.7, 130.6, 129.5, 128.0, 127.4, 123.7, 123.1, 121.0, 124.3, 119.9, 114.4, 114.0, 102.2, 60.1, 55.6, 55.0 ppm; HR-ESI-MS: m/z calcd for C₂₁H₁₇NO₈P: 442.0692 [M + 1]⁺; found: 442.0702.

(E)-Dimethyl-1-(4-methylbenzylideneamino)-2-para-tolyl-1,2-dihydropyridine-3,5-dicarboxylate (5a)

R_f 0.66 (CH₂Cl₂/hexane/EtOAc 2:7.8:0.2, developed four times); Yield 25%. ¹H NMR (500 MHz, CDCl₃): δ 8.33 (d, J = 1 Hz, 1H), 7.94 (s, 1H), 7.66 (d, J = 1.5 Hz, 1H), 7.48 (d, J = 8 Hz, 2H), 7.34 (d, J = 8 Hz, 2H), 7.15 (d, J = 8 Hz, 2H), 7.08 (d, J = 8 Hz, 2H), 6.45 (s, 1H), 3.82 (s, 3H), 3.73 (s, 3H), 2.34 (s, 3H), 2.27 (s, 3H); ¹³C NMR (125 MHz, CDCl₃): δ 166.0, 165.9, 147.9, 142.9, 140.7, 138.3, 136.4, 130.9, 129.6, 129.5, 129.4, 127.4, 126.3, 117.0, 99.2, 58.3, 51.7, 51.4, 21.4, 21.1; HR-ESI-MS: m/z calcd for C₂₄H₂₅N₂O₄: 405.1814 [M + H]⁺; found: 405.1821.

Figure 2.5B. ^1H and ^{13}C NMR Spectra of **5a**



(E)-Dimethyl-1-(4-methoxybenzylideneamino)-2-(4-methoxyphenyl)-1,2-dihydropyridine-3,5-dicarboxylate (**5b**)

R_f 0.37 (CH₂Cl₂/hexane/EtOAc 2:7.8:0.2, developed four times); Yield 23%. ¹H NMR (500 MHz, CDCl₃): δ 8.30 (s, 1H), 7.94 (s, 1H), 7.66 (d, J = 1 Hz, 1H), 7.54 (d, J = 8.5 Hz, 2H), 7.37 (d, J = 8 Hz, 2H), 6.88 (d, J = 9 Hz, 2H), 6.80 (d, J = 8.5 Hz, 2H), 6.43 (s, 1H), 3.81 (s, 6H), 3.74 (s, 3H), 3.73 (s, 3H); ¹³C NMR (125 MHz, CDCl₃): δ 165.0, 164.9, 160.4, 158.5, 146.6, 141.7, 130.7, 129.8, 128.0, 126.7, 125.3, 115.7, 113.2, 113.1, 97.8, 56.9, 54.4, 54.2, 50.7, 50.4; HR-ESI-MS: m/z calcd for C₂₄H₂₄N₂O₆Na: 459.1532 [M + Na]⁺; found: 459.1531.

(E)-Dimethyl-1-(4-methylbenzylideneamino)-2-methyl-1,2-dihydropyridine-3,5-dicarboxylate (**5c**)

R_f 0.63 (EtOAc/hexane 1:9); Yield 60%. ¹H NMR (500 MHz, CDCl₃): δ 8.03 (s, 2H), 7.64 (s, 1H), 7.60 (d, J = 8 Hz, 2H), 7.23 (d, J = 8 Hz, 2H), 5.58 (q, J = 6 Hz, 1H), 3.80 (s, 6H), 2.39 (s, 3H), 1.25 (d, J = 6 Hz, 3H); ¹³C NMR (125 MHz, CDCl₃): δ 165.9, 146.8, 141.3, 140.7, 132.2, 130.9, 129.6, 127.4, 116.1, 99.6, 51.7, 51.3, 49.4, 21.5, 16.6; HR-ESI-MS: m/z calcd for C₁₈H₂₁N₂O₄: 329.1501 [M + H]⁺; found: 329.1499.

(E)-Dimethyl-1-(4-methoxybenzylideneamino)-2-methyl-1,2-dihydropyridine-3,5-dicarboxylate (**5d**)

R_f 0.36 (CH₂Cl₂/hexane/EtOAc 2:7:1, developed four times); Yield 44%. ¹H NMR (500 MHz, CDCl₃): δ 8.02, (s, 2H), 7.66 (d, J = 9 Hz, 2H), 7.65 (s, 1H), 6.95 (d, J = 8.5 Hz, 2H), 5.56 (q, J = 6 Hz, 1H), 3.86 (s, 3H), 3.80 (s, 3H), 3.79 (s, 3H), 1.25 (d, J = 6.5 Hz, 3H); ¹³C NMR (125 MHz, CDCl₃): δ 165.9, 161.5, 146.8, 141.2, 132.3, 129.0, 126.4, 115.8, 114.4, 99.4, 55.4, 51.7, 51.3, 49.5, 16.7; HR-ESI-MS: m/z calcd for C₁₈H₂₁N₂O₅: 345.1450 [M + H]⁺; found: 345.1454.

(E)-Dimethyl-1-(ethylideneamino)-2-methyl-1,2-dihydropyridine-3,5-dicarboxylate (**5e**)

R_f 0.53 (EtOAc/Hexane 2:8, developed twice); Yield 32%. ¹H NMR (500 MHz, CDCl₃): δ 7.89 (s, 1H), 7.60 (d, J = 1 Hz, 1H), 7.48 (q, J = 5 Hz, 1H), 5.35 (q, J = 6 Hz, 1H), 3.77 (s, 3H), 3.76 (s, 3H), 2.07 (d, J = 5.5 Hz, 3H), 1.15 (d, J = 6 Hz, 3H); ¹³C NMR (125 MHz, CDCl₃): δ 166.3, 166.2, 147.2, 142.3, 132.7, 115.7, 98.9, 52.0, 51.6, 49.4, 16.8, 14.4; HR-ESI-MS: m/z calcd for C₁₂H₁₆N₂O₄Na: 275.1008 [M + Na]⁺; found: 275.1010.

(E)-Dimethyl-1-(3,4,5-trimethoxybenzylideneamino)-2-methyl-1,2-dihydropyridine-3,5-dicarboxylate (**5f**)

R_f =0.45 (EtOAc/hexane 2:8, developed four times); Yield 45%. ^1H NMR (500 MHz, CDCl_3): δ 8.05 (s, 1H), 7.97 (s, 1H), 7.64 (d, $J = 1.5$ Hz, 1H), 6.96 (s, 2H), 5.58 (q, $J = 6.5$ Hz, 1H), 3.93 (s, 6H), 3.90 (s, 3H), 3.81 (s, 6H), 1.25 (d, $J = 6$ Hz, 3H); ^{13}C NMR (125 MHz, CDCl_3): δ 165.9, 153.6, 146.8, 140.7, 140.0, 132.1, 129.1, 116.3, 104.4, 99.9, 60.9, 56.2, 51.8, 51.4, 49.5, 16.5; HR-ESI-MS: m/z calcd for $\text{C}_{20}\text{H}_{25}\text{N}_2\text{O}_7$: 405.1662 [$\text{M} + \text{H}$] $^+$; found: 405.1669.

(E)-Dimethyl-1-(4-(dimethylamino)benzylideneamino)-2-methyl-1,2-dihydropyridine-3,5-dicarboxylate (**5g**)

R_f 0.32 (EtOAc/hexane 1:9, developed thrice); Yield 34%. ^1H NMR (500 MHz, CDCl_3): δ 8.03 (s, 1H), 8.01 (s, 1H), 7.65 (s, 1H), 7.59 (d, $J = 9$ Hz, 2H), 6.71 (d, $J = 9$ Hz, 2H), 5.55 (q, $J = 6.5$ Hz, 1H), 3.79 (s, 3H), 3.78 (s, 3H), 3.04 (s, 6H), 1.25 (d, $J = 6.5$ Hz, 3H); ^{13}C NMR (125 MHz, CDCl_3): δ 166.1, 166.0, 151.9, 146.5, 142.8, 132.5, 129.0, 121.2, 114.9, 111.9, 98.5, 51.7, 51.2, 49.7, 40.2, 17.0; HR-ESI-MS: m/z calcd for $\text{C}_{19}\text{H}_{24}\text{N}_3\text{O}_4$: 358.1767 [$\text{M} + \text{H}$] $^+$; found: 358.1772.

(E)-dimethyl-1-((4-(diethylamino)-2-hydroxybenzylidene)amino)-2-((2-(2-methoxyethoxy)ethoxy)methyl)-1,2-dihydropyridine-3,5-dicarboxylate (**5h**)

R_f 0.40 (EtOAc/hexane 5:5); Yield 50%. ^1H NMR (500 MHz, MeOD): δ 8.51 (s, 1H), 8.06 (s, 1H), 7.70 (s, 1H), 7.27 (d, $J = 8.5$ Hz, 1H), 6.34 (d, $J = 8.5$ Hz, 1H), 6.18 (s, 1H), 5.68 (d, $J = 6$ Hz, 1H), 3.81 (s, 3H), 3.79 (s, 3H), 3.66-3.52 (m, 7H), 3.46-3.37 (m, 7H), 3.30 (s, 3H), 1.20 (d, $J = 7$ Hz, 6H); ^{13}C NMR (125 MHz, CDCl_3): δ 165.8, 165.7, 160.3, 151.0, 149.6, 144.4, 134.1, 133.4, 109.4, 105.9, 104.1, 99.4, 98.0, 71.8, 71.3, 71.0, 70.6, 70.5, 58.9, 54.5, 51.7, 51.3, 44.5, 12.6; HR-ESI-MS: m/z calcd for $\text{C}_{26}\text{H}_{37}\text{N}_3\text{O}_8\text{Na}$: 542.2478 [$\text{M} + \text{Na}$] $^+$; found: 542.2483.

Figure 2.5C. ^1H and ^{13}C NMR spectrum of 1,2-DHP **5h**

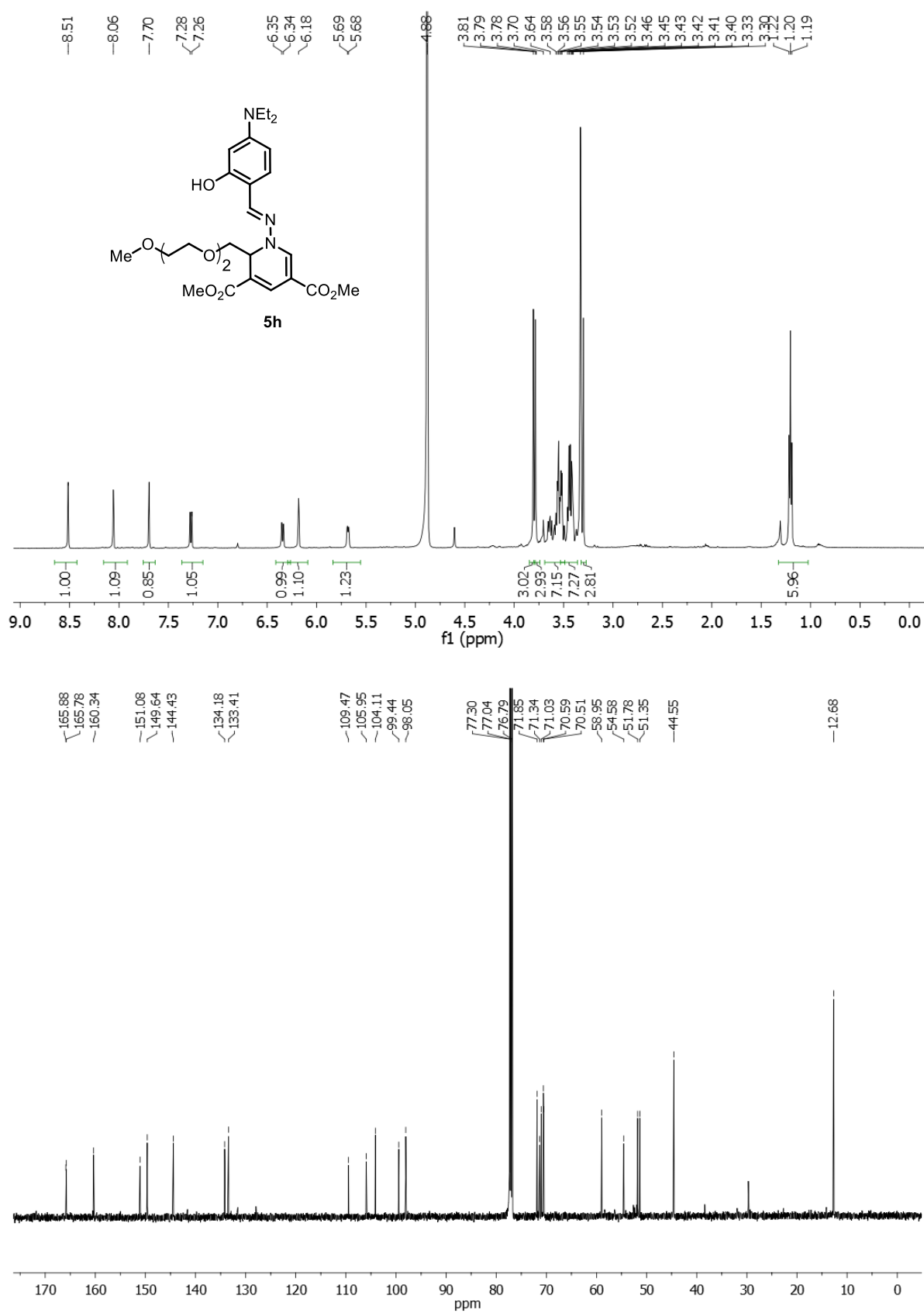


Figure 2.5D. ^1H and ^{13}C NMR spectrum of 1,2-DHP **5h'**

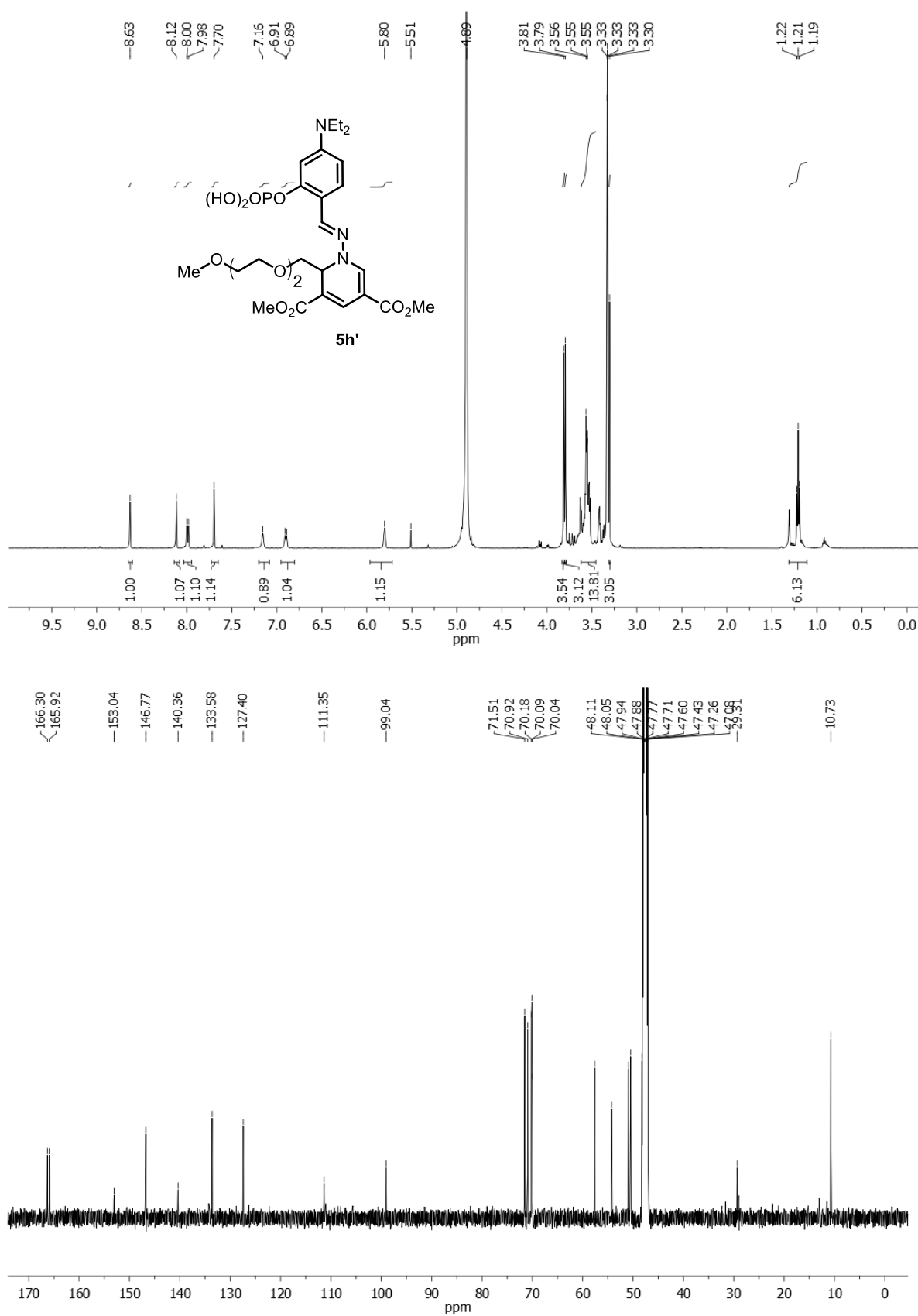
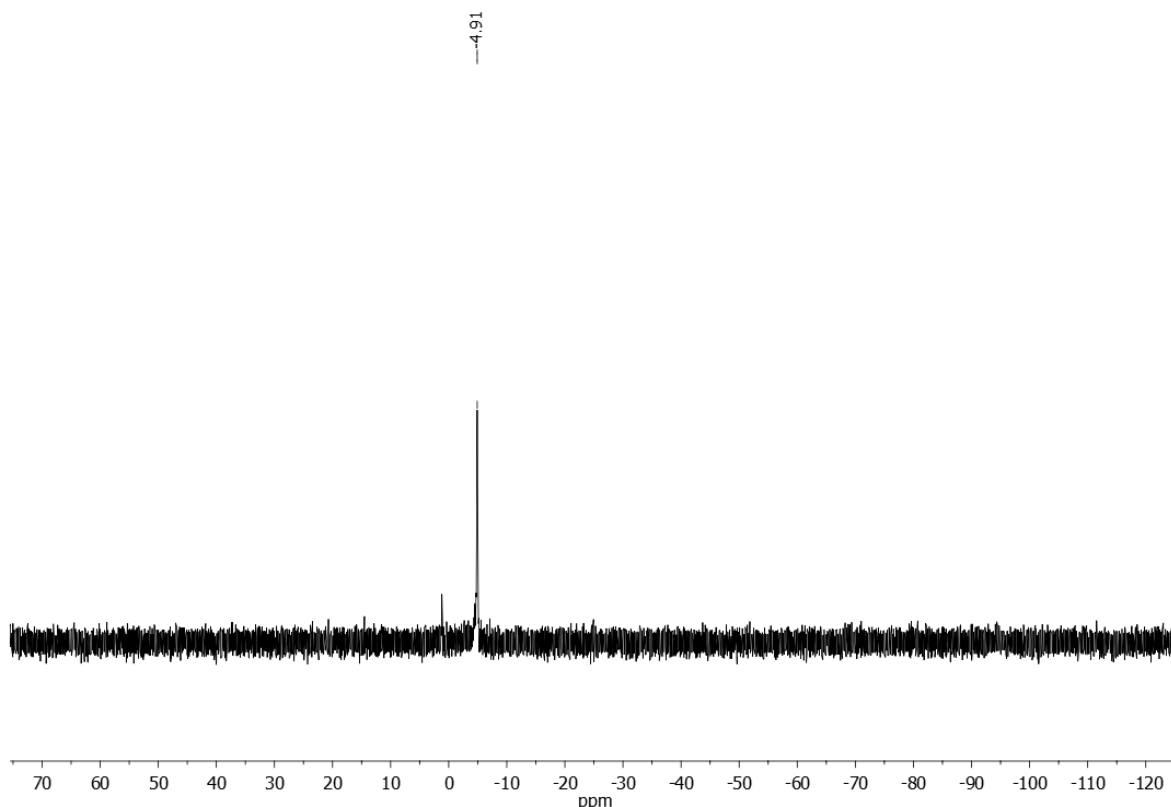


Figure 2.5E. ^{31}P NMR spectrum of 1,2-DHP **5h'**



(E)-2-(((3,5-bis(methoxycarbonyl)-2-((2-(2-methoxyethoxy)ethoxy)methyl)pyridin-1(2H)-yl)imino)methyl)-5-(diethylamino)phenyl phosphate (**5h'**)

R_f 0.42 (MeOH/EtOAc 3:7); Yield 58% (over two steps). ^1H NMR (500 MHz, MeOD): δ 8.62 (s, 1H), 8.11 (s, 1H), 7.97 (d, $J = 8.5$ Hz, 1H), 7.69 (s, 1H), 7.13 (s, 1H), 6.87 (d, $J = 8.5$ Hz, 1H), 5.79 (t, $J = 4$ Hz, 1H), 3.81 (s, 3H), 3.79 (s, 3H), 3.63-3.52 (m, 14H), 3.30 (s, 3H), 1.20 (d, $J = 7$ Hz, 6H); ^{13}C NMR (125 MHz, MeOD): δ 166.3, 165.9, 153.0, 146.7, 140.3, 133.5, 127.4, 111.3, 99.0, 71.5, 70.9, 70.2, 70.1, 70.0, 57.6, 54.2, 50.8, 50.4, 48.2, 10.7; ^{31}P NMR (202 MHz, MeOD): δ -4.91; HR-ESI-MS: m/z calcd for $\text{C}_{26}\text{H}_{38}\text{N}_3\text{O}_{11}\text{PNa}$: 622.2142 $[\text{M} + \text{Na}]^+$; found: 622.2147.

(E)-5-Methyl-3-(4-nitrophenyl)-1-(4-(dimethylamino)benzylideneamino)-2-methyl-1,2-dihydropyridine-3,5-dicarboxylate (**5j**)

R_f 0.57 (EtOAc/hexane 2:8, developed thrice); Yield 30%. ^1H NMR (500 MHz, CDCl_3): δ 8.30 (d, $J = 9$ Hz, 2H), 8.14 (s, 1H), 8.06 (s, 1H), 7.97 (s, 1H), 7.62 (d, $J = 9$ Hz, 2H), 7.36 (d, $J = 9$ Hz, 2H), 6.73 (d, $J = 9$ Hz, 2H), 5.62 (q, $J = 6.5$ Hz, 1H), 3.83 (s, 3H), 3.06

(s, 6H), 1.35 (d, $J = 6$ Hz, 3H); ^{13}C NMR (125 MHz, CDCl_3): δ 165.8, 162.9, 155.9, 152.1, 147.2, 145.0, 144.2, 135.8, 129.2, 125.1, 122.4, 120.6, 112.1, 111.8, 98.7, 51.4, 49.9, 40.1, 14.1; HR-ESI-MS: m/z calcd for $\text{C}_{24}\text{H}_{25}\text{N}_4\text{O}_6$: 465.1774 $[\text{M} + \text{H}]^+$; found: 465.1780.

2.6. References

- (1) (a) Ueno, T.; Nagano, T. Fluorescent probes for sensing and imaging. *Nat. Methods* **2011**, *8*, 642–645. (b) Kobayashi, H.; Ogawa, M.; Alford, R.; Choyke, P. L.; Urano, Y. New strategies for fluorescent probe design in medical diagnostic imaging. *Chem. Rev.* **2010**, *110*, 2620–2640. (c) Zhu, H.; Fan, J.; Du, J.; Peng, X. Fluorescent probes for sensing and imaging within specific cellular organelles. *Acc. Chem. Res.* **2016**, *49*, 2115–2126.
- (2) Arrowsmith, C. H.; Audia, J. E.; Austin, C.; Baell, J.; Bennett, J.; Blagg, J.; Bountra, C.; Brennan, P. E.; Brown, P. J.; Bunnage, M. E.; Buser-Doepner, C.; Campbell, R. M.; Carter, A. J.; Cohen, P.; Copeland, R. A.; Cravatt, B.; Dahlin, J. L.; Dhanak, D.; Edwards, A. M.; Frye, S. V.; Gray, N.; Grimshaw, C. E.; Hepworth, D.; Howe, T.; Huber, K. V. M.; Jin, J.; Knapp, S.; Kotz, J. D.; Kruger, R. G.; Lowe, D.; Mader, M. M.; Marsden, B.; Mueller-Fahrnow, A.; Müller, S.; O'Hagan, R. C.; Overington, J. P.; Owen, D. R.; Rosenberg, S. H.; Roth, B.; Ross, R.; Schapira, M.; Schreiber, S. L.; Shoichet, B.; Sundström, M.; Superti-Furga, G.; Taunton, J.; Toledo-Sherman, L.; Walpole, C.; Walters, M. A.; Willson, T. M.; Workman, P.; Young, R. N.; Zuercher, W. J. The promise and peril of chemical probes. *Nat. Chem. Biol.* **2015**, *11*, 536–541.
- (3) Gonçalves, M. S. T. Fluorescent labeling of biomolecules with organic probes. *Chem. Rev.* **2009**, *109*, 190–212.
- (4) (a) Nair, V.; Offerman, R. J.; Turner, G. A. Novel fluorescent 1,4-dihydropyridines. *J. Am. Chem. Soc.* **1986**, *108*, 8283–8285. (b) Pávez, P.; Encinas, M. V. Photophysics and photochemical studies of 1,4-dihydropyridine derivatives. *Photochem. Photobiol.* **2007**, *83*, 722–729.
- (5) Challa, C.; John, M.; Lankalapalli, R. S. Cascade synthesis of 1,2-dihydropyridine from dienaminodioxide and an imine: a three-component approach. *Tetrahedron*

- Lett.* **2013**, *54*, 3810–3812.
- (6) Sueki, S.; Takei, R.; Zaitso, Y.; Abe, J.; Fukuda, A.; Seto, K.; Furukawa, Y.; Shimizu, I. Synthesis of 1,4-dihydropyridines and their fluorescence properties. *Eur. J. Org. Chem.* **2014**, *2014*, 5281–5301, and references cited therein.
- (7) Affeldt, R. F.; Iglesias, R. S.; Rodembusch, F. S.; Russowsky, D. Photophysical properties of a series of 4-aryl substituted 1,4-dihydropyridines. *J. Phys. Org. Chem.* **2012**, *25*, 769–777.
- (8) Jimenez, A. J.; Fagnoni, M.; Mella, M.; Albin, A. Photoinduced electron and energy transfer in aryldihydropyridines. *J. Org. Chem.* **2009**, *74*, 6615–6622.
- (9) Pinrat, O.; Boonkitpatarakul, K.; Paisuwan, W.; Sukwattanasinitt, M.; Ajavakom, A. Glucopyranosyl-1,4-dihydropyridine as a new fluorescent chemosensor for selective detection of 2,4,6-trinitrophenol. *Analyst* **2015**, *140*, 1886–1893.
- (10) (a) Ershov, O. V.; Fedoseev, S. V.; Belikov, M. Y.; Ievlev, M. Y. Domino-synthesis and fluorescence properties of 4-cyano-2-oxo-1,2-dihydropyridine-3-carboxamides and 2-oxo-1,2-dihydropyridine-3,4-dicarbonitriles. *RSC Adv.* **2015**, *5*, 34191–34198. (b) Singh, R.; Rai, S. K.; Tiwari, M. K.; Mishra, A.; Tewari, A. K.; Mishra, P. C.; Singh, R. K. An excellent stable fluorescent probe: selective and sensitive detection of trace amounts of Hg⁺² ions in natural source of water. *Chem. Phys. Lett.* **2017**, *676*, 39–45. (c) Sellstedt, M.; Nyberg, A.; Rosenbaum, E.; Engström, P.; Wickström, M.; Gullbo, J.; Bergström, S.; Johansson, L. B. Å.; Almqvist, F. Synthesis and characterization of a multi ring-fused 2-pyridone-based fluorescent scaffold. *Eur. J. Org. Chem.* **2010**, *2010*, 6171–6178.
- (11) Longstreet, A. R.; Jo, M.; Chandler, R. R.; Hanson, K.; Zhan, N.; Hrudka, J. J.; Mattoussi, H.; Shatruk, M.; McQuade, D. T. Ylidenemalonitrile enamines as fluorescent “turn-on” indicators for primary amines. *J. Am. Chem. Soc.* **2014**, *136*, 15493–15496.
- (12) Bureš, F. Fundamental aspects of property tuning in push–pull molecules. *RSC Adv.* **2014**, *4*, 58826–58851.
- (13) Królicki, R.; Jarzęba, W.; Mostafavi, M.; Lampre, I. Preferential solvation of coumarin 153—the role of hydrogen bonding. *J. Phys. Chem. A* **2002**, *106*, 1708–

- 1713.
- (14) Xu, Z.; Xu, L. Fluorescent probes for the selective detection of chemical species inside mitochondria. *Chem. Commun.* **2016**, *52*, 1094–1119.
- (15) Elchebly, M.; Payette, P.; Michaliszyn, E.; Cromlish, W.; Collins, S.; Loy, A. L.; Normandin, D.; Cheng, A.; Himms-Hagen, J.; Chan, C. C.; Ramachandran, C.; Gresser, M. J.; Tremblay, M. L.; Kennedy, B. P. Increased insulin sensitivity and obesity resistance in mice lacking the protein tyrosine phosphatase-1B gene. *Science* **1999**, *283*, 1544–1548.
- (16) Stebbing, J.; Lit, L. C.; Zhang, H.; Darrington, R. S.; Melaiu, O.; Rudraraju, B.; Giamas, G. The regulatory roles of phosphatases in cancer. *Oncogene* **2014**, *33*, 939–953.
- (17) (a) Tai, W. T.; Chen, Y. L.; Chu, P. Y.; Chen, L. J.; Hung, M. H.; Shiau, C. W.; Huang, J. W.; Tsai, M. H.; Chen, K. F. Protein tyrosine phosphatase 1B dephosphorylates PITX1 and regulates p120RasGAP in hepatocellular carcinoma. *Hepatology* **2016**, *63*, 1528–1543. (b) Zheng, L. Y.; Zhou, D. X.; Lu, J.; Zhang, W. J.; Zou, D. J. Down-regulated expression of the protein-tyrosine phosphatase 1B (PTP1B) is associated with aggressive clinicopathologic features and poor prognosis in hepatocellular carcinoma. *Biochem. Biophys. Res. Commun.* **2012**, *420*, 680–684.
- (18) Masarone, M.; Federico, A.; Abenavoli, L.; Loguercio, C.; Persico, M. Non alcoholic fatty liver: epidemiology and natural history. *Rev. Recent Clin. Trials* **2014**, *9*, 126-133.
- (19) (a) He, R.-J.; Yu, Z.-H.; Zhang, R.-Y.; Zhang, Z.-Y. Protein tyrosine phosphatases as potential therapeutic targets. *Acta Pharmacol. Sin.* **2014**, *35*, 1227–1246. (b) Zhang, S.; Zhang, Z. Y. PTP1B as a drug target: recent developments in PTP1B inhibitor discovery. *Drug Discov. Today* **2007**, *12*, 373–381.
- (20) Berezin, M. Y.; Achilefu, S. Fluorescence lifetime measurements and biological imaging. *Chem. Rev.* **2010**, *110*, 2641–2684.
- (21) Becke, A. D. Density-functional thermochemistry.III. The role of exact exchange. *J. Chem. Phys.* **1993**, *98*, 5648–5652.

- (22) Lee, C.; Yang, W.; Parr, R. G. Development of the Colle-Salvetti correlation-energy formula into a functional of the electron density. *Phys. Rev. B* **1988**, *37*, 785–789.
- (23) Gaussian 09, revision A.02: Frisch, M. J.; Trucks, G. W.; Schlegel, H. B.; Scuseria, G. E.; Robb, M. A.; Cheeseman, J. R.; Scalmani, G.; Barone, V.; Petersson, G. A.; Nakatsuji, H.; Li, X.; Caricato, M.; Marenich, A.; Bloino, J.; Janesko, B. G.; Gomperts, R.; Mennucci, B.; Hratchian, H. P.; Ortiz, J. V.; Izmaylov, A. F.; Sonnenberg, J. L.; Williams-Young, D.; Ding, F.; Lipparini, F.; Egidi, F.; Goings, J.; Peng, B.; Petrone, A.; Henderson, T.; Ranasinghe, D.; Zakrzewski, V. G.; Gao, J.; Rega, N.; Zheng, G.; Liang, W.; Hada, M.; Ehara, M.; Toyota, K.; Fukuda, R.; Hasegawa, J.; Ishida, M.; Nakajima, T.; Honda, Y.; Kitao, O.; Nakai, H.; Vreven, T.; Throssell, K.; Montgomery, J. A., Jr.; Peralta, J. E.; Ogliaro, F.; Bearpark, M.; Heyd, J. J.; Brothers, E.; Kudin, K. N.; Staroverov, V. N.; Keith, T.; Kobayashi, R.; Normand, J.; Raghavachari, K.; Rendell, A.; Burant, J. C.; Iyengar, S. S.; Tomasi, J.; Cossi, M.; Millam, J. M.; Rega, N.; Millam, J. M.; Klene, M.; Adamo, C.; Cammi, R.; Ochterski, J. W.; Martin, R. L.; Morokuma, K.; Farkas, O.; Foresman, J. B.; Fox, D. J. Gaussian, Inc., Wallingford, CT, **2016**.
- (24) Marx, V. Probes: paths to photostability. *Nat. Methods* **2015**, *12*, 187–190.
- (25) Mosmann, T. Rapid colorimetric assay for cellular growth and survival: application to proliferation and cytotoxicity assays. *J. Immunol. Methods* **1983**, *65*, 55–63.

Chapter-3

Metal-Free Diaryl Etherification of Tertiary Amines by *Ortho*-C(sp²)-H Functionalization for Synthesis of Dibenzoxazepines and –ones

3.1. Abstract

This chapter describes a phenyliodine(III) diacetate (PIDA) [PhI(OAc)₂] mediated umpolung reactivity of tertiary amines (**1**) with suitably substituted *ortho*-hydroxybenzyl and phenyl groups. The reaction is exploited to facilitate *ortho*-C(sp²)-H functionalization to afford diaryl ethers **2** (Figure 3.1A). The presence of an *ortho*-CHO and secondary amine functionalities in the resulting diaryl ether, generated *in situ*, were utilized for the synthesis of dibenzoxazepines (**3**) and dibenzoxazepinones (**4**). Mild conditions and relatively broad substrate scope, and potential for further diversification of the diaryl ethers are highlights of this methodology.

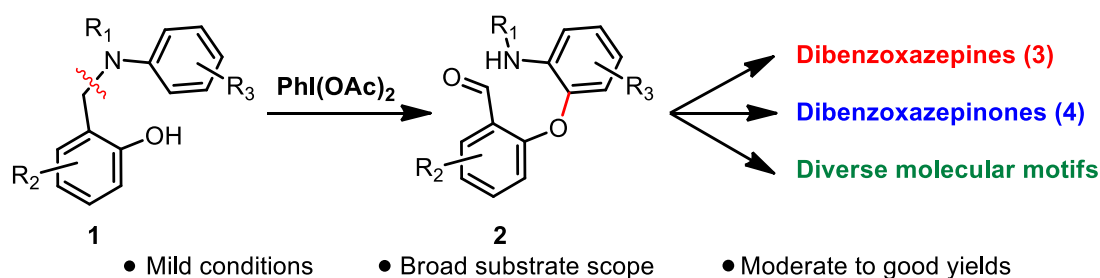


Figure 3.1A. Synthesis of diaryl ether from tertiary amine.

3.2. Introduction

As discussed in the introductory chapter, dibenzoxazepines and dibenzoxazepinones are pharmaceutically relevant molecules present in antidepressants and antipsychotics. These privileged structural motifs possess a broad range of biological activities such as anti-HIV, antitumor, antioxidant, oral contraceptive, TRPA1 agonist, sodium channel blocker, CNS depressant, anti-inflammatory, and antinociceptive properties.¹ As natural products, dibenzoxazepinones were isolated from the leaves of *Carex distachya* and from the ethanolic extracts of streptomycetes.^{1c,d} Figure 3.2A highlights some of the representatives of pharmacologically active molecules possessing dibenzoxazepine skeleton.

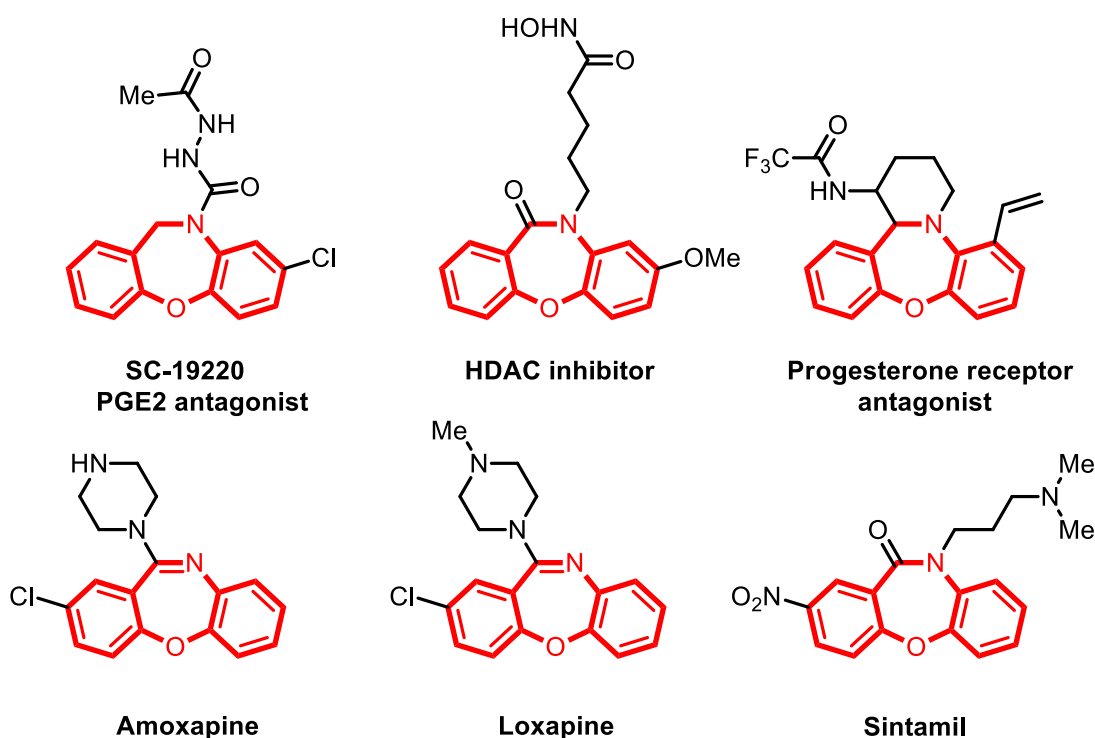
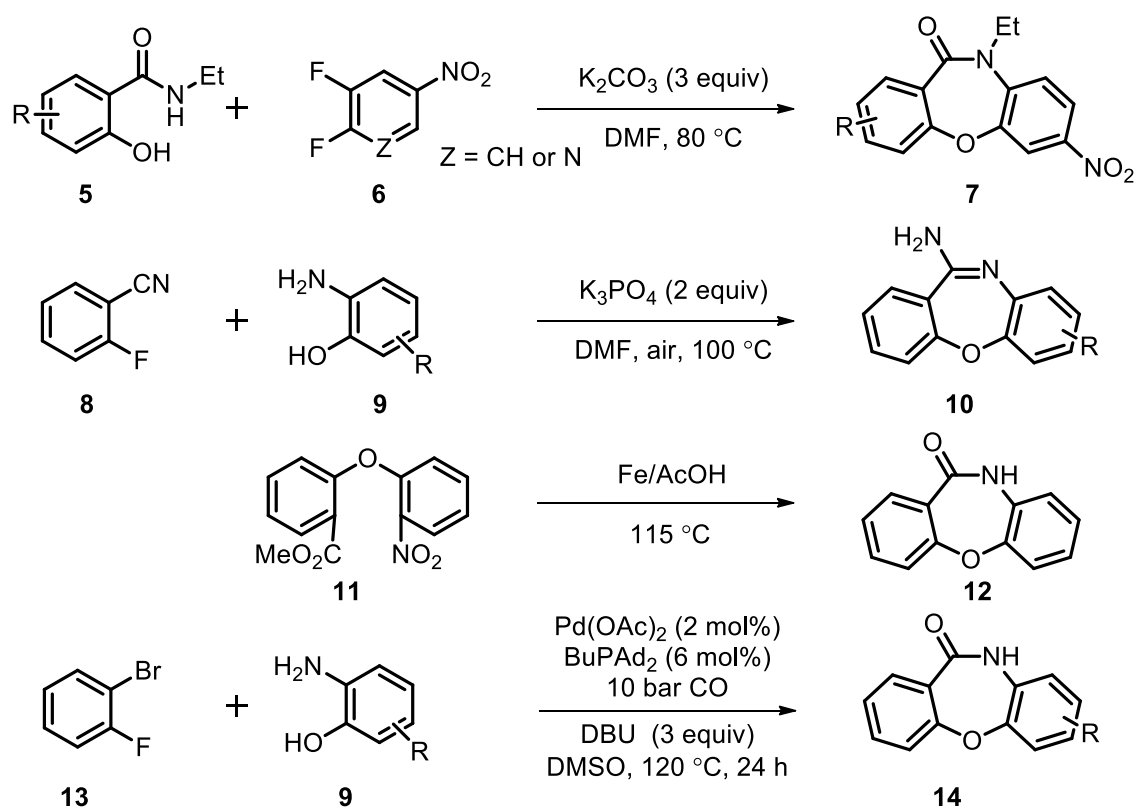


Figure 3.2A. Pharmacologically active dibenzoxazepines.

Owing to its wide occurrence in biological compounds, numerous approaches have been developed for the synthesis of dibenzoxazepine core skeleton. Traditionally, base-promoted nucleophilic aromatic substitution (S_NAr) reaction was employed to construct the seven-membered ring of dibenzoxazepinones *via* Smiles rearrangement of suitable electrophilic substrates by a domino C–O and C–N bond coupling reactions.² For instance, Liu *et al.* reported a convenient and facile methodology for the regioselective synthesis of fused oxazepinone scaffolds **7** in 2011. This process involved an efficient construction of the oxazepinone scaffold **7** by a one-pot coupling/Smiles rearrangement/cyclization approach from commercially available *N*-substituted salicylamides **5** and substituted benzenes/pyridines **6** (Scheme 3.2.1).^{2d} A base-promoted green protocol has been developed for the synthesis of dibenz[*b,f*][1,4]oxazepin-11-amines **10** by S_NAr with concomitant addition reaction by Feng *et al.*³ The reaction consists of the formation of dibenz[*b,f*][1,4]oxazepin-11-amines **10** *via* K_3PO_4 mediated coupling of 2-fluorobenzonitriles **8** and 2-aminophenols **9** (Scheme 3.2.1). Post-Ugi reaction, an intramolecular microwave-assisted diaryl etherification was used as an attractive strategy to synthesize highly substituted dibenz[*b,f*][1,4]oxazepine scaffold.⁴ Key precursors generated from diaryl etherification methodology served as suitable substrates for various intramolecular seven-membered ring formation strategies such as

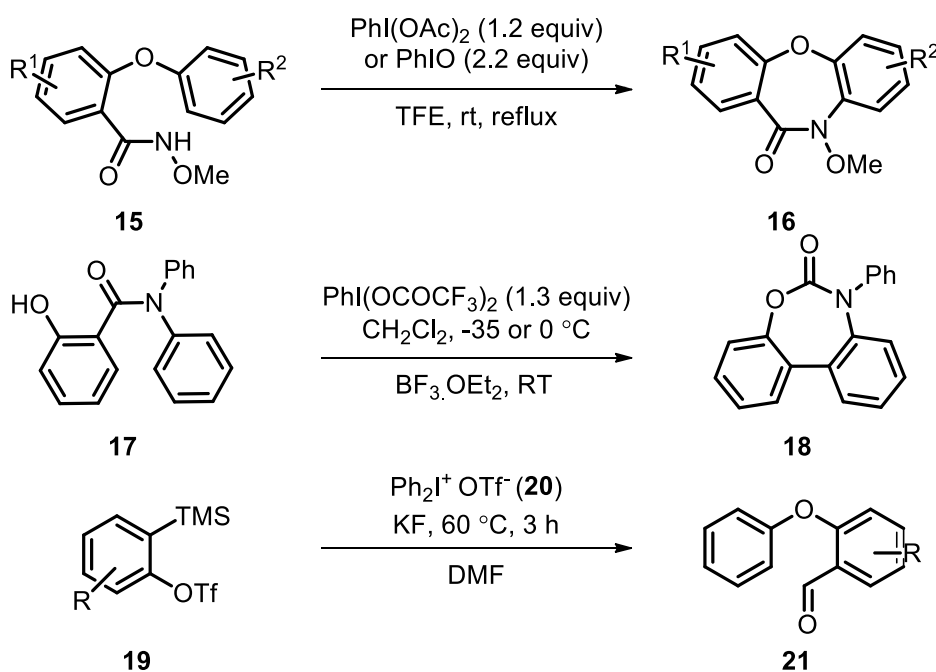
reductive lactamization, Pd-catalyzed condensation, cyclocarbonylation, Smiles rearrangement, copper-catalyzed Goldberg reaction to afford dibenzoxazepinones.⁵ For example, Bunce *et al.* used a tandem reduction-lactamization sequence as the strategy for the synthesis of dibenz[*b,f*][1,4]oxazepin-11(10*H*)-one **12** from methyl 2-(2-nitrophenoxy)benzoate **11**.^{5a} The reaction involves the reduction followed by lactamization of **11** using 6 equivalents of iron powder in acetic acid at 115 °C for 30-60 minutes (Scheme 3.2.1). Alternatively, intramolecular diaryl etherification as the later annulation event under metal-catalyzed and base-promoted conditions from substrates with suitably tethered phenol and halo-substituted phenyl units was also developed.⁶ For instance, Shen *et al.* reported a one-pot palladium-catalyzed aminocarbonylation/S_NAr sequence for the synthesis of dibenzo[*b,e*][1,4]oxazepin-11(5*H*)-ones **15** from 2-bromofluorobenzenes **13** and 2-aminophenols **9** (Scheme 3.2.1).^{6c} Dibenzoxazepines have also been used as valuable synthetic intermediates in the development of more complex heterocyclic structures.⁷



Scheme 3.2.1. Strategies for dibenzoxazepinone

On the other hand, hypervalent iodine (III) reagents have been considered as mild alternative oxidants against the toxic metals for the construction of several C–C and C–heteroatom bonds.⁸ HIR-mediated oxidative dearomatizing transformations of *ortho*-

substituted phenols were utilized in the synthesis of complex natural products.⁹ Similar to phenolic substrates, tertiary amines were also efficient substrates in HIR-mediated transformations involving functionalization of C(sp³)-H bond adjacent to nitrogen.¹⁰ Recently, Guo *et al.* reported dibenzoxazepinone **16** synthesis by hypervalent iodine (III) reagent (HIR) mediated intramolecular C-N bond formation from 2-(aryloxy)benzamides **15** synthesized by Cu-mediated diaryl etherification (Scheme 3.2.2), but failed with substrates containing strong electron-withdrawing and donating groups.¹¹ Another example involving usage of HIR reagent involved intramolecular cyclization of two aryl groups from 2-hydroxy-*N*-phenylbenzamides **17** affording dibenz[*d,f*] [1,3]oxazepin-6(*7H*)-ones **18** (Scheme 3.2.2).¹²



Scheme 3.2.2. HIR mediated intramolecular cyclisation and diaryl etherification

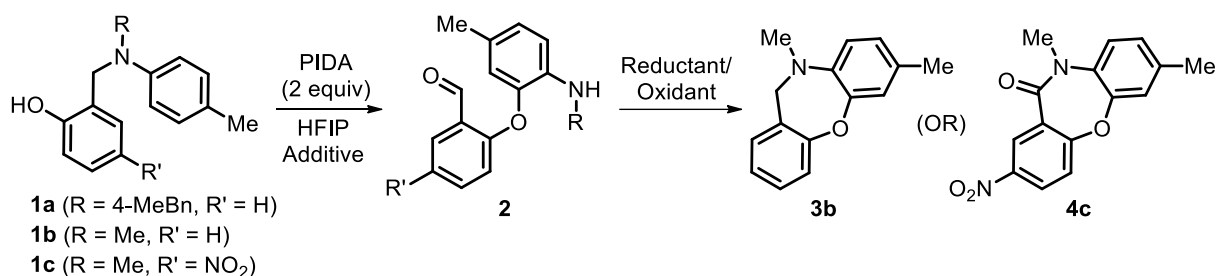
Diaryl ethers have often been seen in subunits of many synthetically challenging and medicinally important natural products, and considerable effort has been expended on its synthesis.¹³ Classically, the most reliable methods for the synthesis of diaryl ethers are base promoted nucleophilic aromatic substitution and copper-catalyzed Ullmann type coupling reaction.¹⁴ However, over the past few decades, palladium catalysed Buchwald-Hartwig coupling, copper catalysed Chan-Lam coupling and nickel or palladium catalysed decarbonylative coupling reactions were well established.¹⁵ Although in recent years, good progress has been made in the metal catalyzed and metal free diaryl etherification, further improvements are still desirable. On the other hand, *ortho* C-H

functionalization has attracted a lot of attention due to its ability to enable the direct introduction of functionality to organic molecules, in an efficient and economical manner.¹⁶ Transition metals have been shown to play an increasingly important role in this field.¹⁷ HIRs also play a crucial role in the *ortho* C-H functionalization.⁸ The metal-free alternative for diaryl etherification with HIR involving diaryliodonium salts is an attractive strategy,¹⁸ applied towards synthesis of *ortho*-CHO diaryl ethers.¹⁹ Liu *et al.* reported a three-component coupling of arynes, *N,N*-dimethylformamide (DMF), and diaryliodonium salts. In this reaction they used 2-(trimethylsilyl)aryl triflate **19** as readily accessible aryne precursor, that react with diphenyliodonium triflate Ph₂I⁺OTf⁻ **20** and potassium fluoride in DMF at 60 °C for 3 h to facilitate the formation 2-phenoxybenzaldehyde **21** (Scheme 3.2.2).

In the present study, PIDA induced umpolung reactivity of tertiary amines **1** affords diaryl ether **2** with an *ortho*-CHO and secondary amine substituents that upon subsequent treatment with NaBH(OAc)₃ and PCC provided dibenzoxazepines **3** and dibenzoxazepinones **4**, respectively. The present method serves as a metal-free alternative to the existing methods *vide supra* with a broad substrate scope. Further synthetic applications of this methodology from diaryl ether were demonstrated with an array of transformations to access other bioactive skeletons.

3.3. Results and discussions

A novel intramolecular diaryl etherification strategy for the key seven-membered ring formation to afford dibenzoxazepines was envisaged using tertiary amines with suitably substituted *ortho*-hydroxybenzyl, phenyl units under metal-free conditions by using HIRs. In an initial attempt (Table 3.3.1), tertiary amine **1a** treated with one equivalent of PIDA at room temperature using conventional HFIP as the solvent did not lead to complete consumption of the starting material. However, tertiary amine **1a** underwent a complete transformation within 10 min with two equivalents of PIDA forming a new C-O bond with concomitant C-N bond cleavage affording compound **2a** in 34% yield (entry 1). The structure of compound **2a** was unambiguously confirmed by single crystal X-ray analysis (Figure 3.3A).

Table 3.3.1. Optimization of reaction conditions^a

Entry	Additive	Reductant/ Oxidant	Yield ^h		
			2a	3b (2 steps)	4c (2 steps)
1	-	-	34	-	-
2	K ₂ CO ₃	-	46	-	-
3 ^b	-	NaBH ₄	-	67	-
4 ^b	K ₂ CO ₃	NaBH ₄	-	50	-
5 ^b	BF ₃ .Et ₂ O	NaBH ₄	-	70	-
6 ^b	-	NaBH(OAc) ₃	-	71	-
7 ^b	-	NaCNBH ₃	-	65	-
8^c	-	NaBH(OAc)₃	-	77	-
9 ^c	BF ₃ .Et ₂ O	NaBH(OAc) ₃	-	69	-
10 ^d	-	PCC	-	-	70
11^e	-	PCC	-	-	73
12 ^d	-	DMP	-	-	n.d.
13 ^d	NaHCO ₃	DMP	-	-	n.d.
14 ^d	-	NBS	-	-	n.d.
15 ^d	-	NIS	-	-	n.d.
16 ^d	-	<i>m</i> -CPBA	-	-	n.d.
17 ^d	-	DDQ	-	-	n.d.
18 ^f	-	NaClO	-	-	57
19 ^g	-	NaClO	-	-	n.d.

^aReaction conditions: All reactions were conducted at room temperature without using distilled solvents. Compound **1a/1b/1c** (0.18 mmol) in HFIP (1 mL) was the scale of the reactions for the first step. ^bTo the crude mixture of compound **2**, after quenching, reductant (3 equiv) in MeOH (1 mL) was added. ^cNaBH(OAc)₃ (3 equiv) was added to the same pot. ^dTo the isolated compound **2c** by column chromatography, oxidant (1 equiv) in DCM (1 mL) was added. ^ePCC (2 equiv) was used. ^fSolvent used in second step was AcOH. ^gSolvent used in second step was CH₃CN. ^hIsolated yields. n.d. = not detected.

Further variation of the solvents, other HIRs, oxidants and mode of additions examined were not effective for the formation of **2a** which led to the choice of PIDA and HFIP as the optimal combination. The reaction conducted in the presence of K₂CO₃, to scavenge the generated acetic acid by-product from PIDA, did not significantly improve the yield of compound **2a** (entry 2). Compound **2** with appropriately substituted aldehyde and secondary amine is prone to undergo reductive amination to afford the desired dibenzoxazepine. Accordingly, a simple tertiary amine **1b** substrate was initially

subjected to PIDA mediated oxidation to afford compound **2b** which without purification was treated with excess NaBH₄ in methanol for reductive amination. This reaction in an overall two steps produced the desired dibenzoxazepine **3b** in 67% yield (entry 3). Conducting the reductive amination step on the crude aldehyde in presence of additives (entries 4-5) and other reductants (entries 6-7) could not improve the yield of dibenzoxazepine formation considerably. Interestingly, the addition of three equivalents of NaBH(OAc)₃ in the same pot after complete consumption of tertiary amine afforded dibenzoxazepine **3b** with an enhanced yield of 77% (entry 8), and the presence of an additive could not further improve the yield (entry 9). Changing the reductant to an oxidant in the second step should produce dibenzoxazepinone **4**. An initial attempt with tertiary amine **1a** with an addition of one equivalent of PCC in dichloromethane in the same pot led to a sluggish outcome. However, treatment of one equivalent of PCC on the isolated intermediate **2c** in an overnight reaction afforded dibenzoxazepinone **4c** in 70% yield (entry 10) and an increase of PCC to two equivalents led to reaction completion within one hour with 73% yield (entry 11). Even though other oxidants (entries 12-17) failed to afford the desired product, sodium hypochlorite in acetic acid produced dibenzoxazepinone **4c** in 57% yield (entry 18) but failed while using acetonitrile as solvent (entry 19).

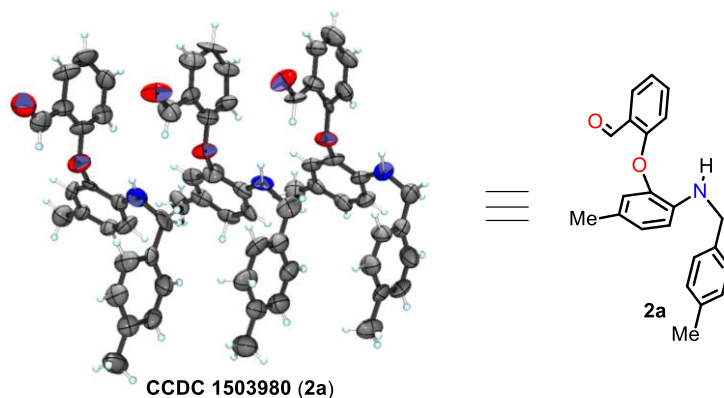
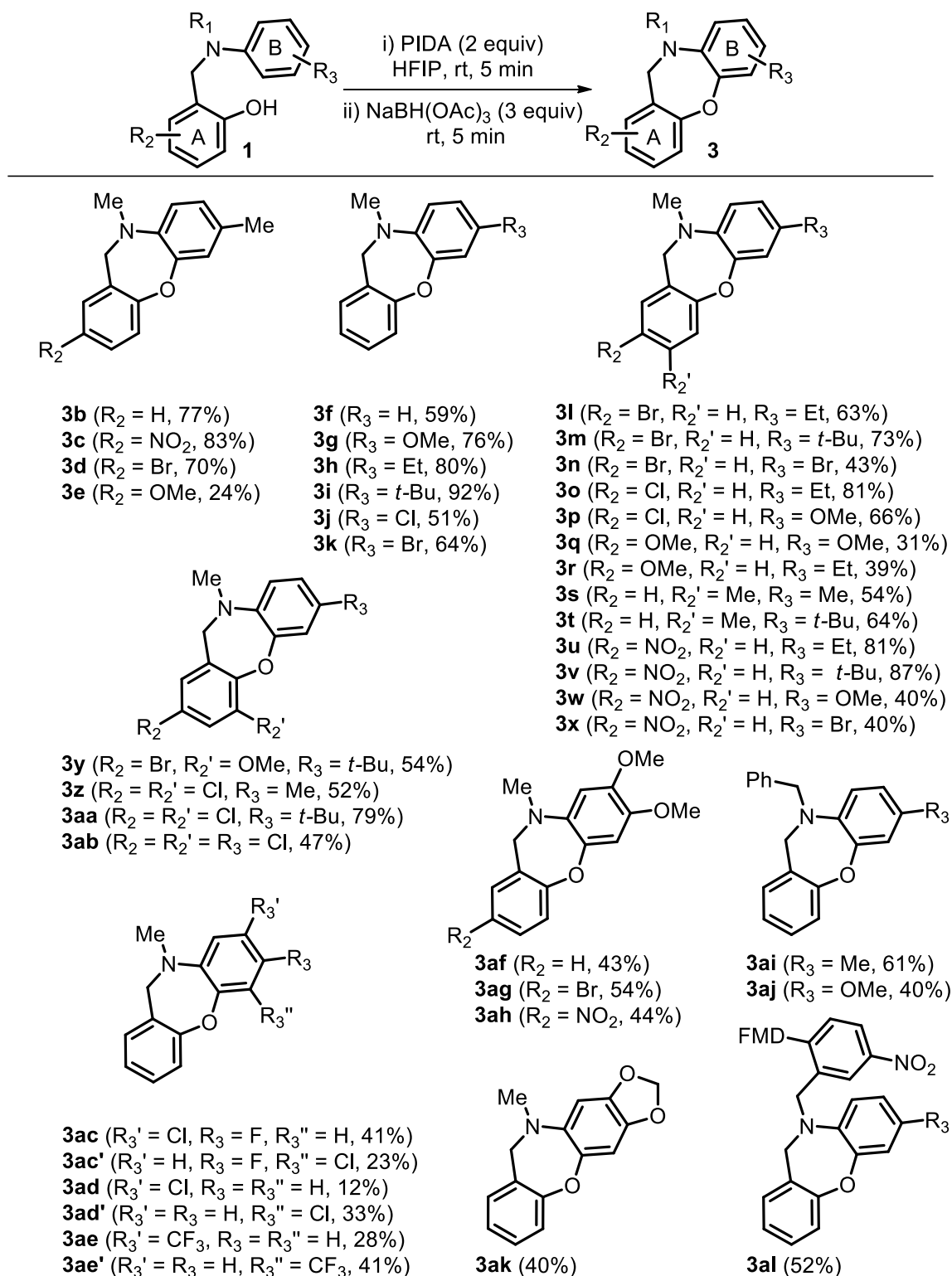
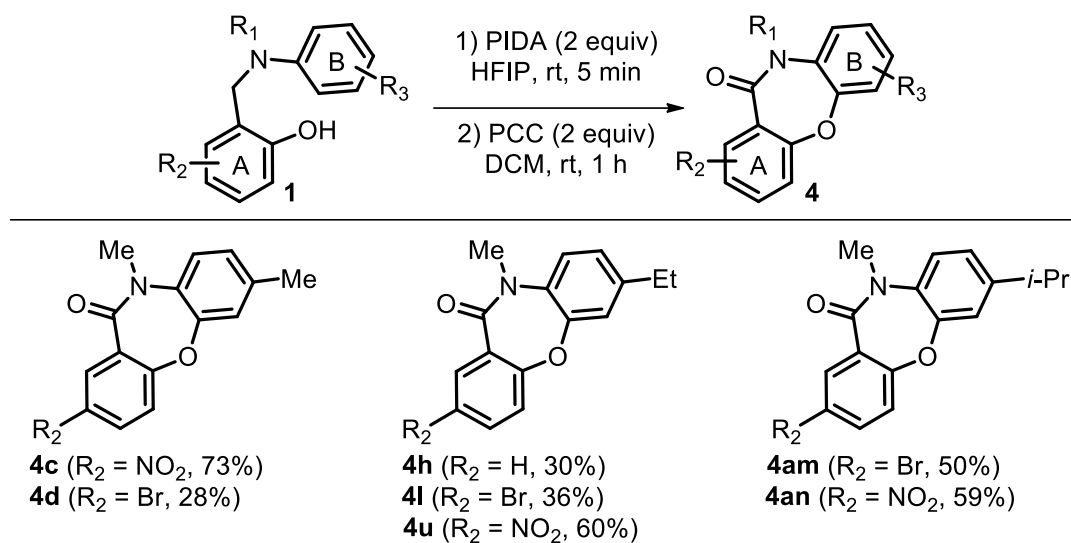


Figure 3.3A. ORTEP diagram of diaryl ether **2a**

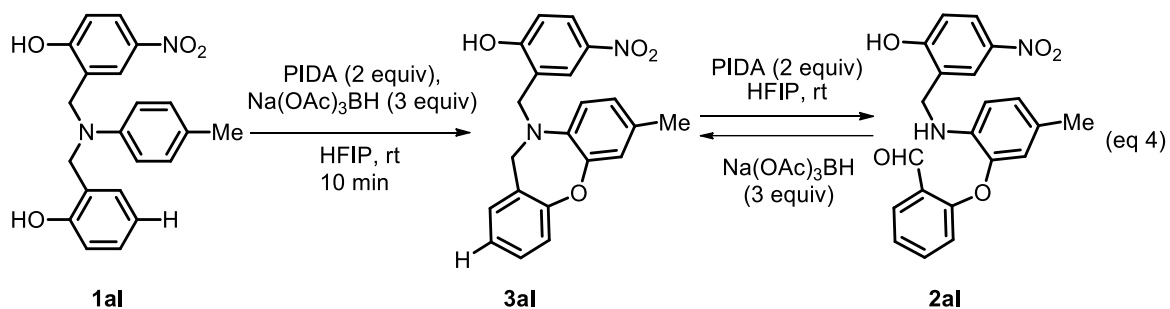
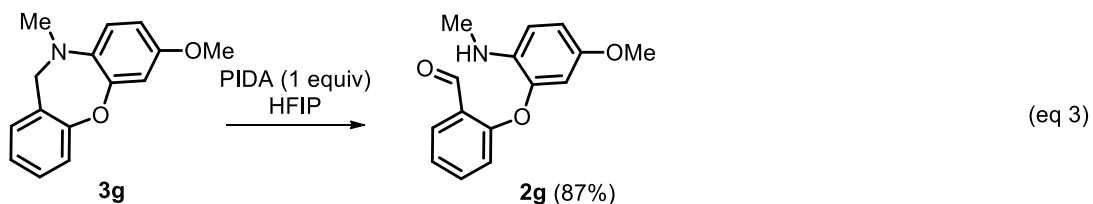
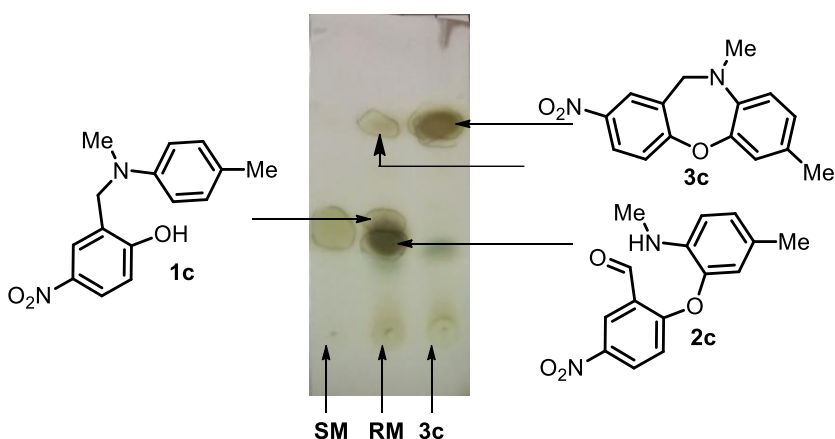
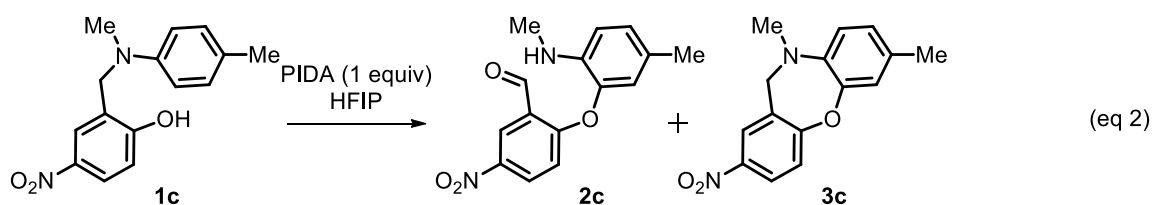
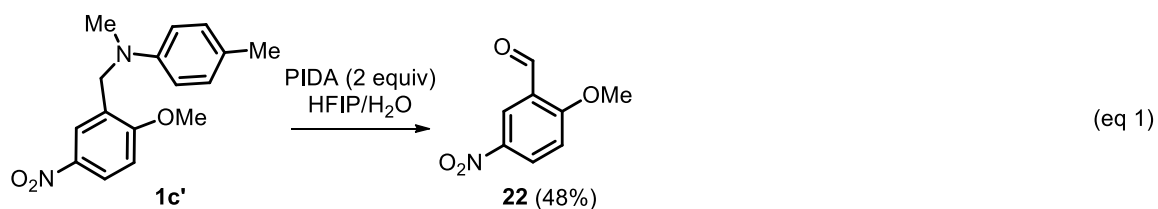
Table 3.3.2. Substrate scope for dibenzoxazepine



The optimization studies revealed the broad scope of this methodology involving varied substitutions in benzyl (A ring), phenyl (B ring) and *N*-alkyl groups of the tertiary amines as shown in table 3.3.2. Under the optimized conditions (entry 8, Table 3.3.1), tertiary amines bearing activating as well as deactivating groups in either of the mono- or di-substituted A ring and para-substituted B ring conveniently converted to dibenzoxazepines **3b–3ab** in 24–92% yields. In general, tertiary amines with deactivating groups (halo, nitro) in A ring and ones with activating groups (alkyl, methoxy) in B ring afforded dibenzoxazepines in good yields. For instance, substrate **1c** with nitro substitution in A ring and **1i** with *tert*-butyl substitution in B ring afforded dibenzoxazepines **3c** and **3i** in 83 and 92% yields, respectively. Accordingly, substrate **1v** with both nitro and *tert*-butyl substitutions in A and B rings, respectively, afforded dibenzoxazepine **3v** in 87% yield. Meta-substituted B rings afforded a mixture of separable regioisomers **3ac**, **3ac'–3ae**, **3ae'** since the nucleophilic attack by OH group is feasible in either of the *ortho*-positions of the B ring. Dimethoxy substituted B ring offered a single regioisomer **3af–3ah**, arising due to electronic reasons. Substrates with *N*-benzyl substitution afforded dibenzoxazepines **3ai** and **3aj** which serves as a third variable group in the tertiary amine for diversification. However, when the substrate bears an *ortho*-substitution in the B ring, the cyclization did not occur. Presence of a 3,4-(methylenedioxy) group in the B ring produced the desired dibenzoxazepine **3ak** in 40% yield similar to substrates, *vide supra*, with dimethoxy substituted B ring. Compound **3ak** with a tetracyclic framework could be a novel entry in the class of tetracyclic antidepressants. A successful dibenzoxazepinone **4c** formation by successive PIDA and PCC oxidations from the optimization studies prompted us to further demonstrate the substrate scope of this reaction (Table 3.3.3). Accordingly, tertiary amines with different substitutions in the A and B rings afforded dibenzoxazepinones **4** in 28–73% yields.

Table 3.3.3. Substrate scope for dibenzoxazepinone

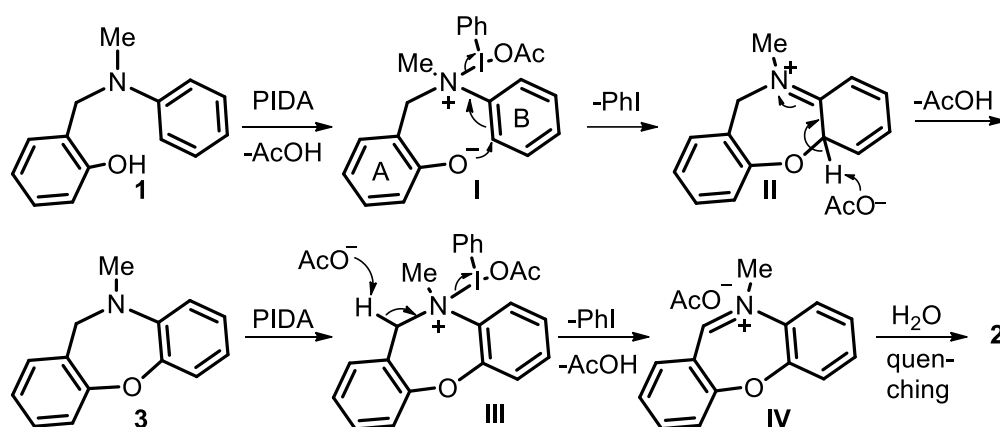
In order to understand the mechanism of the transformation, we have carried out certain control experiments (Scheme 3.3.1). The role of nucleophilic free hydroxyl group has governed by the reaction of methyl protected tertiary amine **1c** under the optimized reaction condition. In the absence of nucleophilic hydroxyl group, the competing benzylic proton abstraction takes place which upon hydrolysis produces benzaldehyde (**22**) (Scheme 3.3.1, eq. 1). While, the usage of one equivalent of PIDA produced a mixture of dibenzoxazepine **3** and diaryl ether **2** along with unreacted tertiary amine **1** as observed over TLC (Scheme 3.3.1, eq. 2). This indicates that the dibenzoxazepine is forming during the reaction, but it gets converted to diaryl ether in presence of PIDA. Moreover 1 equivalent of PIDA is not sufficient for a clean transformation. This was again confirmed by the reaction of compound **3g** with 1 equiv of PIDA which led to the formation of diaryl ether **2g** in 87% yield (Scheme 3.3.1, eq. 3) When tertiary amine with two benzylic alcohol (**1al**) is considered, the more nucleophilic phenoxide ion participated in dibenzoxazepine **3al** formation with 52% yield, confirmed by HMBC analysis of its methylated analog (Scheme 3.3.1, eq. 4). An attempt involving further cyclization using dibenzoxazepine **3al** under the optimized conditions led to seven-membered ring opening to afford the corresponding aldehyde **2al** which upon subsequent reduction reformed dibenzoxazepine **3al**.



Scheme 3.3.1. Control experiments

A plausible mechanism has been proposed similar to activation of tertiary amines in presence of PIDA.¹⁰ Oxidative dearomatization of phenols in presence of PIDA are well documented,²⁰ however, tertiary amine will be more reactive for the initial ligand exchange with PIDA. Accordingly, reaction of tertiary amine **1** with PIDA affords intermediate **I** (Scheme 3.3.2). The key nucleophilic attack of the phenoxide on the

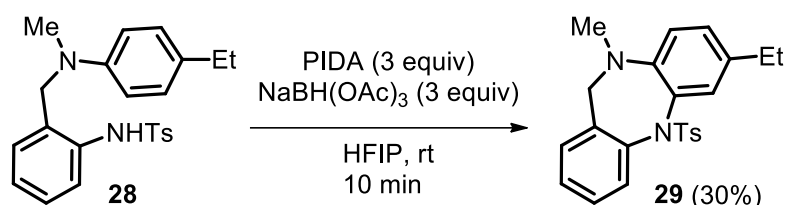
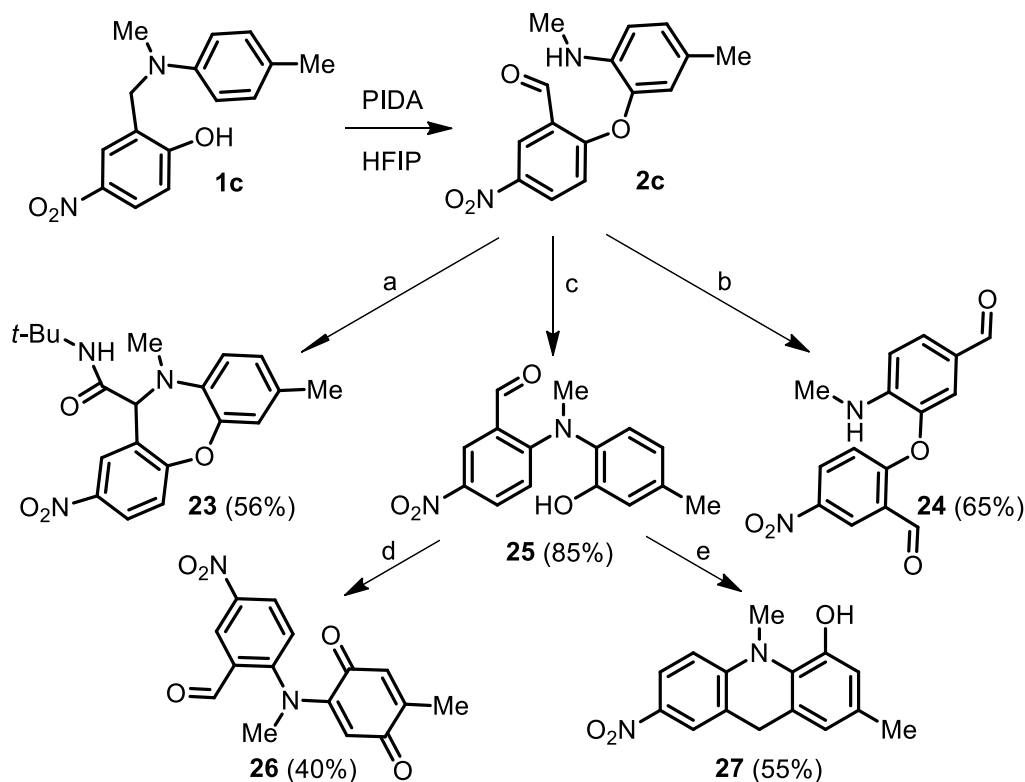
electron-deficient *ortho*-carbon of the aniline ring of **1** is proposed analogous to a reported PIDA activation.¹² This key seven-membered ring formation accompanied by elimination of phenyl iodide affords intermediate **II** that rearomatizes to provide dibenzoxazepine **3**. It is worth mentioning that stabilization of intermediate **I** by the presence of deactivating groups in A ring and activating groups in B ring promotes formation of dibenzoxazepines in good yields, observed in substrate scope. A reactive compound **3** in presence of a second equivalent of PIDA affords intermediate iminium ion **IV**, formed by abstraction of benzylic proton from the activated tertiary amine **III**. The reaction mixture was quenched upon complete consumption of compound **3** which ensure ring opening of iminium intermediate **IV** to afford diaryl ether **2**.



Scheme 3.3.2. Plausible mechanistic pathway

In order to further demonstrate the broad applicability of this methodology, an array of synthetic transformations were carried out on diaryl ether **2c** (Scheme 3.3.3). Treatment of compound **2c** with *tert*-butylisocyanide afforded a pharmaceutically relevant dibenzoxazepine-11-carboxamide **23**. A facile DDQ mediated oxidation of benzylic carbon afforded diaryl ether **24** flanked by three reactive functionalities. Presence of *para*-nitro substitution in ether facilitates an intramolecular *ipso*-substitution with secondary amine by Smiles rearrangement, interestingly, undertaken in presence of bleach to afford tertiary amine **25** in 85% yield. During this rearrangement, events that take place such as hopping of the hydroxyl group of tertiary amine **1c** from A ring to B ring and benzylic amine transformation to diphenyl amine are otherwise conceived by multi-step synthesis. Furthermore, tertiary amine **25** in presence of Dess-Martin

periodinane and *p*-TsOH afforded *para*-benzoquinone **26** and dihydroacridine **27** in 40 and 55% yields, respectively.



Reaction conditions: (a) **2c** (1 equiv), *t*-BuNC (1 equiv), InCl₃ (cat.), MeOH, 60 °C; (b) **2c** (1 equiv), NaClO (2 equiv), 1 M NaOH (cat), Bu₄NI (1.5 equiv), DCM, rt; (c) **2c** (1 equiv), AcOH (cat.), DDQ (3 equiv), DCM, rt; (d) **7** (1 equiv), DMP (1.5 equiv), DCM, rt; (e) **7** (1 equiv), *p*-TsOH (cat.), EtOH, 60 °C.

Scheme 3.3.3. Demonstration of applicability of methodology

Structural confirmation of all the products was carried out by extensive 2D NMR analysis. A further extension of this methodology to afford dibenzodiazepine **29**, categorized as privileged structure by Evans *et al.*,²¹ was obtained from tertiary amine **28** with an appropriate NHTs substitution

3.4. Conclusion

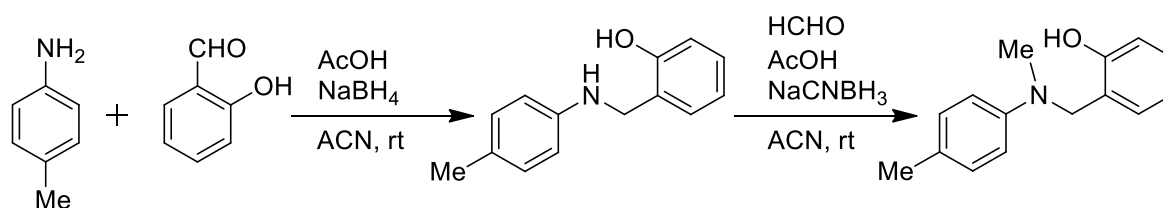
In conclusion, tertiary amines with suitably substituted *ortho*-hydroxybenzyl, phenyl groups with varied substituents underwent diaryl ether formation endowed with *ortho*-CHO and secondary amine functionalities in presence of PIDA by *ortho*-C(sp²)-H functionalization under mild conditions. An intramolecular seven-membered ring formation facilitated by NaBH(OAc)₃ and PCC provided dibenzoxazepines and dibenzoxazepinones, respectively. A broad substrate scope for dibenzoxazepine has been demonstrated, in particular, substrates with deactivating groups in A ring and activating groups in B ring offered good yields in a one-pot reaction. Furthermore, an array of synthetic transformations carried out to further demonstrate the broad applicability of this methodology afforded diverse molecular motifs

3.5. Experimental section

3.5.1. General information

Reagents and solvents were purchased as reagent grade and were used without further purification. Reactions were monitored by silica gel G-60 F₂₅₄ aluminum TLC and compounds were visualized by short/long wavelength lamps and iodine staining. Column chromatography was performed using silica gel 100-200 mesh. ¹H and ¹³C NMR were recorded on a Bruker Avance II spectrometer at 500 and 125 MHz, respectively using CDCl₃ as solvent. Data are reported as follows: chemical shift in ppm (δ), multiplicity (s = singlet, d = doublet, t = triplet, q = quartet, sept = septet, bs = broad singlet, m = multiplet), coupling constant (Hz) and integration. HRMS analysis was recorded on a Thermo Scientific Exactive-LCMS instrument by electrospray ionization method with ions given in *m/z* using Orbitrap analyzer.

3.5.2. General procedure for the synthesis of tertiary amine **1b**



Scheme 3.5.1. Synthesis of tertiary amines via double reductive amination

To a stirred solution of *p*-toluidine (3 g, 27.99 mmol, 1 equiv) and salicylaldehyde (3.4 g, 27.99 mmol, 1 equiv) in ACN (30 mL) was added 0.5 equiv of acetic acid (0.88 mL, 13.99 mmol, 0.5 equiv) and allowed to stir at room temperature for 30 min. To the cooled reaction mixture, NaBH₄ (2.1 g, 55.98 mmol, 2 equiv) was added, and stirring was continued at room temperature. After two hours, saturated NH₄Cl (25 mL) was added and extracted with DCM (2 x 30 mL), dried over anhydrous Na₂SO₄, concentrated and purified over column chromatography to afford the secondary amine. To a solution of this isolated secondary amine, formaldehyde (6.8 mL, 83.97 mmol, 3 equiv) and 0.5 equiv acetic acid (0.88 mL, 13.99 mmol, 0.5 equiv) in ACN (30 mL) was added and stirred for 30 min. NaCNBH₃ (5.3 g, 83.97 mmol, 3 equiv) was added to the reaction mixture and stirring was continued until the TLC indicated total consumption of the starting material. Subsequent quenching, extraction and purification were performed as explained for the first step to derive the desired tertiary amine. A similar procedure was followed for the synthesis of other tertiary amines.

3.5.3. General procedure for the synthesis of dibenzoxazepine **3b**

To a solution of tertiary amine **1b** (300 mg, 1.32 mmol, 1 equiv) in HFIP solvent (6 mL) was added PIDA (851 mg, 2.64 mmol, 2 equiv) at room temperature and within 5 minutes the starting material consumption took place with the formation of the diaryl ether-*ortho*-formaldehyde **2b**, as observed over TLC. NaBH(OAc)₃ (839 mg, 3.96 mmol, 3 equiv) was added to the reaction mixture and stirring was continued at room temperature. After complete consumption of diaryl ether **2b** in less than 5 minutes, as indicated by TLC, the reaction mixture was quenched with saturated NaHCO₃ (10 mL), extracted with DCM (20 mL) and dried over anhydrous Na₂SO₄. The organic layer was concentrated under reduced pressure, and the residue was purified by column chromatography

(EtOAc/hexane 1:9) to afford dibenzoxazepine **3b** in 77% yield. A similar procedure was followed for the synthesis of other dibenzoxazepines **3c-3al**.

3.5.4. General procedure for the synthesis of dibenzoxazepinone 4c

To a solution of tertiary amine **1c** (300 mg, 1.10 mmol, 1 equiv) in HFIP solvent (6 mL) was added PIDA (708 mg, 2.20 mmol, 2 equiv) at room temperature and within five minutes the starting material consumption took place with the formation of the diary ether-*ortho*-formaldehyde **2c**, as observed over TLC. The reaction mixture was quenched with saturated NaHCO₃ (10 mL) solution and extracted with DCM (20 mL). The organic layer was dried over anhydrous Na₂SO₄, concentrated and purified by column chromatography to afford the diaryl ether-*ortho*-formaldehyde **2c** (228 mg, 76%). To a solution of diaryl ether **2c** (228 mg, 0.8 mmol, 1 equiv) in DCM (5 mL) was added PCC (342 mg, 1.6 mmol, 2 equiv) at room temperature in open air and stirred for 1 hour. After completion of the starting material, as indicated by TLC, the reaction mixture was quenched with isopropanol (0.5 mL) and then with saturated aqueous NaHCO₃ (10 mL) and extracted with DCM (20 mL). The combined DCM extracts were dried over anhydrous Na₂SO₄, concentrated and purified by column chromatography (EtOAc/hexane 1.5:8.5) to afford dibenzoxazepinone **4c** in 73% yield (over two steps). A similar procedure was followed for the synthesis of other dibenzoxazepinones **4d-4an**.

3.5.5. 10-(2-methoxy-5-nitrobenzyl)-7-methyl-10,11-dihydrodibenzo[b,f][1,4]oxazepine (3al')

To a solution of **3al** (21 mg, 0.058 mmol, 1 equiv) in anhydrous DMF (1.5 mL) were added NaH (60% dispersion in oil, 2.7 mg, 0.069 mmol, 1.2 equiv) and MeI (7.2 μ L, 0.12 mmol, 2 equiv) and stirred at room temperature. After 3 hours, the reaction mixture was quenched with water (10 mL), extracted with EtOAc (3 x 10 mL), dried over anhydrous Na₂SO₄, concentrated and purified by column chromatography (EtOAc/hexane 1.5:8.5) to afford compound **3al'** in 57% yield.

3.5.6. N-(tert-butyl)-7,10-dimethyl-2-nitro-10,11-dihydrodibenzo[b,f][1,4]oxazepine-11-carboxamide (23)

To a solution of diaryl ether-*ortho*-formaldehyde **2c** (25 mg, 0.09 mmol, 1 equiv) in methanol (1 mL) were added *tert*-butyl isocyanide (7.2 mg, 0.09 mmol, 1 equiv) and a catalytic amount of InCl₃ in a sequential order at room temperature. The reaction mixture

was stirred at 60 °C for overnight. After completion of the starting material as indicated on TLC, the solvent was evaporated off and residue was purified by column chromatography (EtOAc/hexane 2:8) to afford dibenzoxazepine carboxamide (**23**) in 56% yield.

3.5.7. 2-(5-formyl-2-(methylamino)phenoxy)-5-nitrobenzaldehyde (**24**)

To a stirred solution of diaryl ether-*ortho*-formaldehyde **2c** (25 mg, 0.09 mmol, 1 equiv) in DCM (1 mL) at room temperature was added 3 drops of acetic acid. After 15 minutes of stirring, DDQ (59 mg, 0.27 mmol, 3 equiv) was added and stirring was continued for further 30 min. The reaction mixture was quenched with saturated NaHCO₃ and extracted with DCM (2 x 10 mL). The combined DCM extracts were dried over anhydrous Na₂SO₄, concentration and purification by column chromatography (EtOAc/hexane 2.5:7.5) afforded compound **24** in 65% yield.

3.5.8. 2-((2-hydroxy-4-methylphenyl)(methyl)amino)-5-nitrobenzaldehyde (**25**)

To a solution of diaryl ether-*ortho*-formaldehyde **2c** (25 mg, 0.09 mmol, 1 equiv) in DCM (1 mL) were added NaOCl (14 mg, 0.18 mmol, 2 equiv) and 0.1 mL of 1M NaOH at room temperature. Tetrabutylammonium iodide (48 mg, 0.14 mmol, 1.5 equiv) was added and stirring was continued until the completion of the starting material, as indicated on TLC. The reaction mixture was quenched with aqueous sodium bisulfite and extracted with DCM (2 x 10 mL). The combined organic layers were dried, concentrated and purified by column chromatography (EtOAc/hexane 2:8) to yield compound **25** in 85% yield.

3.5.9. 2-(methyl(4-methyl-3,6-dioxocyclohexa-1,4-dien-1-yl)amino)-5-nitrobenzaldehyde (**26**)

To a solution of 2-((2-hydroxy-4-methylphenyl)(methyl)amino)-5-nitrobenzaldehyde **7** (25 mg, 0.09 mmol, 1 equiv) in DCM (1 mL) was added Dess-Martin periodinane (58 mg, 0.14 mmol, 1.5 equiv) at room temperature. After complete consumption of compound **25** as indicated on TLC, the reaction mixture was quenched with saturated aqueous Na₂S₂O₃ and saturated NaHCO₃ and extracted with DCM (2 x 10 mL). The organic layer was dried over anhydrous Na₂SO₄, concentrated and purified by column chromatography (EtOAc/hexane 5:5) to afford compound **26** in 40% yield

3.5.10. 2,10-dimethyl-7-nitro-9,10-dihydroacridin-4-ol (**27**)

Catalytic amount of *p*-TsOH was added to a stirred solution of 2-((2-hydroxy-4-methylphenyl)(methyl)amino)-5-nitrobenzaldehyde **25** (25 mg, 0.09 mmol, 1 equiv) in ethanol (1 mL). The reaction mixture was stirred at 60 °C for overnight and then quenched with saturated aqueous NaHCO₃ (10 mL) and extracted with DCM (2 x 10 mL). The organic layer was dried over anhydrous Na₂SO₄, concentrated, and the crude mixture was subjected to column chromatography (EtOAc/hexane 1.5:8.5) to afford compound **27** in 55% yield.

3.5.11. 7-ethyl-10-methyl-5-tosyl-10,11-dihydro-5H-dibenzo[*b,e*][1,4]diazepine (**29**)

To a solution of tertiary amine **28** (51 mg, 0.13 mmol, 1 equiv) in HFIP solvent (1mL) was added PIDA (124.6 mg, 0.38 mmol, 3 equiv) at room temperature and within five minutes the starting material was consumed. NaBH(OAc)₃ (82 mg, 0.38 mmol, 3 equiv) was added to the reaction mixture and stirred at room temperature. After complete consumption of the intermediate in less than 5 minutes, the reaction mixture was quenched with saturated NaHCO₃ (2 mL) and extracted with DCM (6 mL). The organic layer was dried over anhydrous Na₂SO₄, concentrated, and the residue was purified by column chromatography (EtOAc/hexane 1:9) to afford dibenzodiazepine **29** in 30% yield.

3.5.12. Spectral details of products

2-(5-methyl-2-((4-methylbenzyl)amino)phenoxy)benzaldehyde (**2a**)

Pale yellow solid, yield: 14 mg, 46%; ¹H NMR (CDCl₃, 500 MHz): δ 10.58 (s, 1H), 7.93 (dd, *J* = 7.5, 1.5 Hz, 1H), 7.50 (td, *J* = 8.5, 1.5 Hz, 1H), 7.22 (d, *J* = 8 Hz, 2H), 7.17 (t, *J* = 7.5 Hz, 1H), 7.14 (d, *J* = 8 Hz, 2H), 6.88 (dd, *J* = 8.5, 1.5 Hz, 1H), 6.86 (d, *J* = 8.5 Hz, 1H), 6.71 (d, *J* = 1.5 Hz, 1H), 6.69 (d, *J* = 8.5 Hz, 1H), 4.42 (bs, 1H), 4.34 (s, 2H), 2.34 (s, 3H), 2.22 (s, 3H); ¹³C NMR (CDCl₃, 125 MHz): δ 189.3, 160.2, 142.3, 138.0, 136.8, 136.1, 135.8, 129.3, 128.4, 127.2, 126.8, 126.1, 122.8, 120.3, 117.2, 112.3, 47.8, 21.0, 20.4; HR-ESI-MS: *m/z* calcd for C₂₂H₂₂NO₂: 332.1651 [M + H]⁺; found: 332.1658 minor peak, and *m/z* calcd for C₂₂H₂₀NO: 314.1539 [M - OH]⁺; found: 314.1553 base peak.

Figure 3.5A. ^1H and ^{13}C -NMR of diaryl ether **2a**

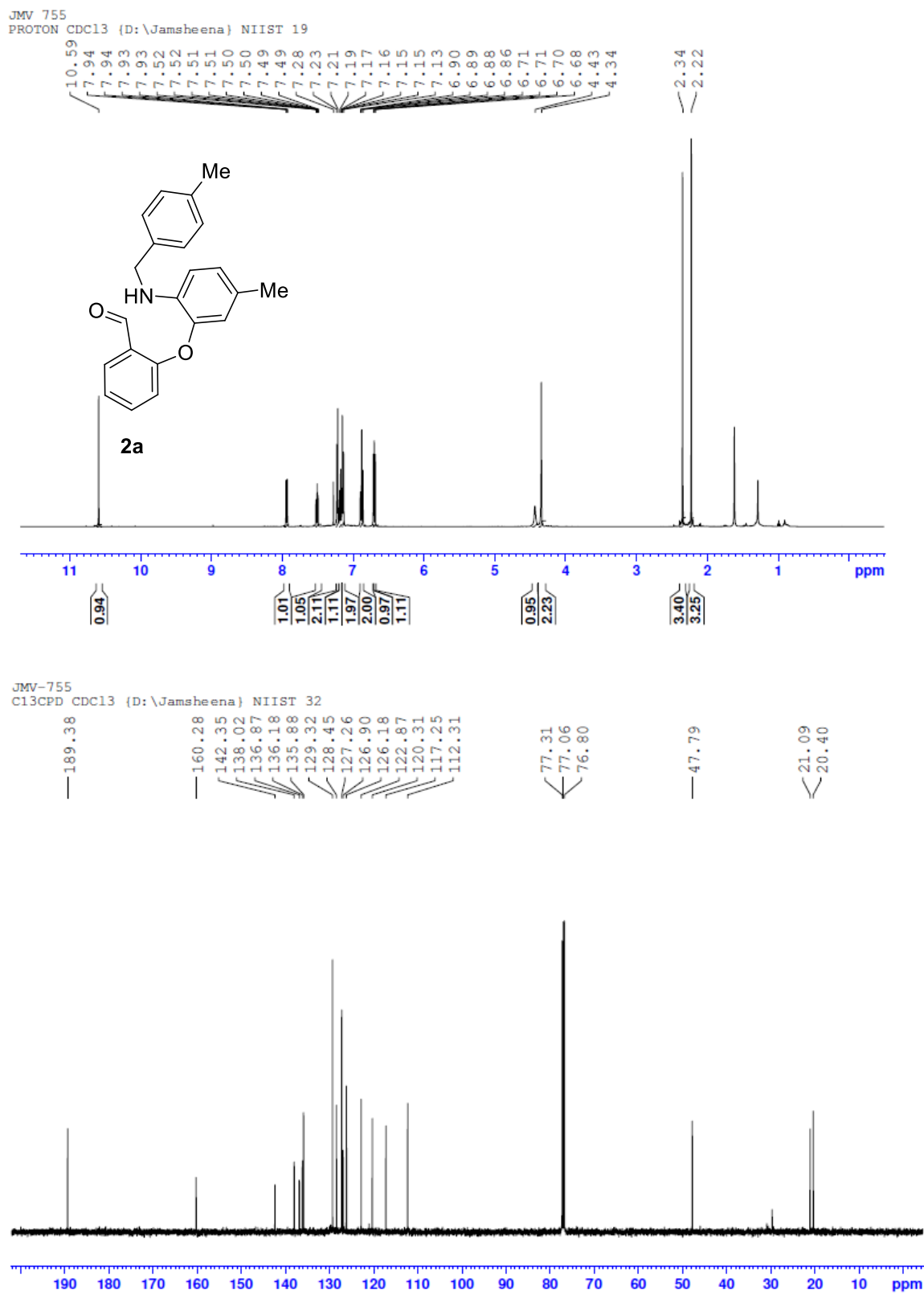
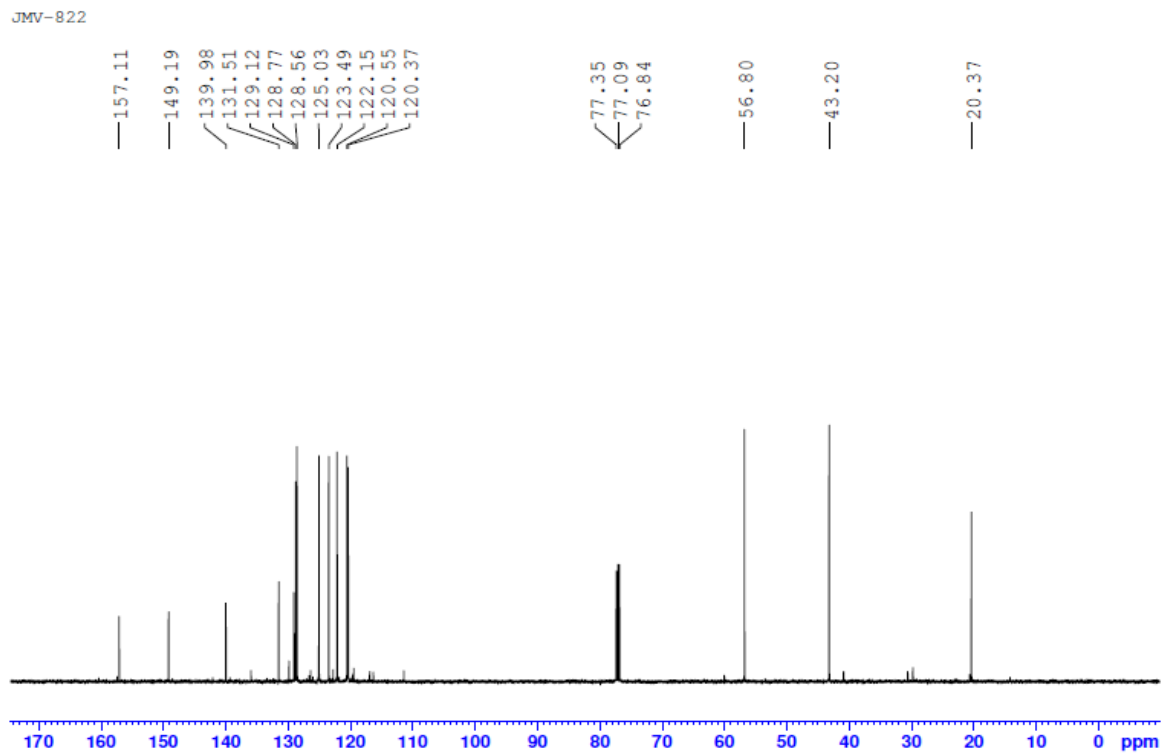
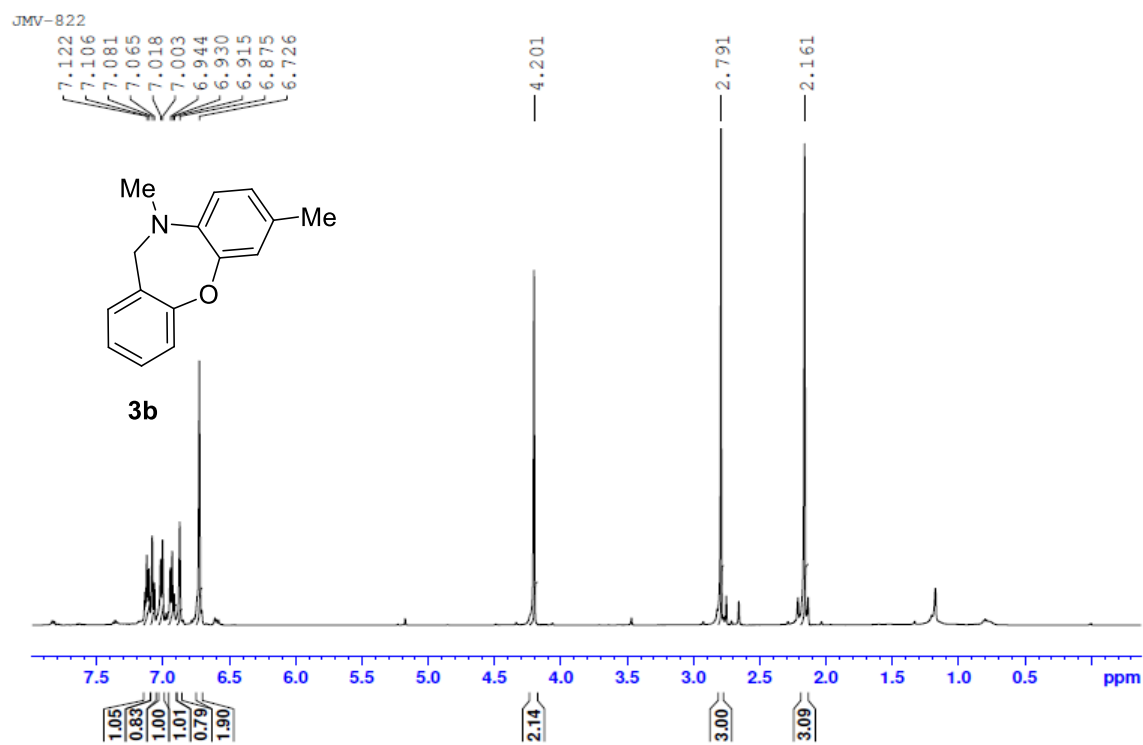


Figure 3.5B. ^1H and ^{13}C -NMR of **3b**



2-(5-methyl-2-(methylamino)phenoxy)-5-nitrobenzaldehyde (**2c**)

Yellow solid, yield: 23 mg, 76%; ¹H NMR (CDCl₃, 500 MHz): δ 10.64 (s, 1H), 8.76 (d, *J* = 3 Hz, 1H), 8.29 (dd, *J* = 9.5, 3 Hz, 1H), 7.06 (d, *J* = 8.5 Hz, 1H), 6.89 (d, *J* = 9.5 Hz, 1H), 6.81 (d, *J* = 1 Hz, 1H), 6.75 (d, *J* = 8 Hz, 1H), 3.90 (bs, 1H), 2.86 (s, 3H), 2.29 (s, 3H); ¹³C NMR (CDCl₃, 125 MHz): δ 187.2, 164.4, 142.6, 140.1, 139.2, 130.4, 128.0, 127.1, 125.0, 124.7, 121.3, 116.4, 112.0, 30.4, 20.3; HR-ESI-MS: *m/z* calcd for C₁₅H₁₄N₂NaO₄: 309.0851 [M + Na]⁺; found: 309.0855 minor peak, and *m/z* calcd for C₁₅H₁₃N₂O₃: 269.0921 [M - OH]⁺; found: 269.0929 base peak.

7,10-dimethyl-10,11-dihydrodibenzo[*b,f*][1,4]oxazepine (**3b**)

Pale yellow liquid, yield: 23 mg, 77%; ¹H NMR (CDCl₃, 500 MHz): δ 7.12 (t, *J* = 7.5 Hz, 1H), 7.07 (d, *J* = 8 Hz, 1H), 7.01 (d, *J* = 7.5 Hz, 1H), 6.93 (t, *J* = 7 Hz, 1H), 6.87 (s, 1H), 6.72 (s, 2H), 4.20 (s, 2H), 2.79 (s, 3H), 2.16 (s, 3H); ¹³C NMR (CDCl₃, 125 MHz): δ 157.1, 149.1, 139.9, 131.5, 129.1, 128.7, 128.5, 125.0, 123.4, 122.1, 120.5, 120.3, 56.8, 43.2, 20.3; HR-ESI-MS: *m/z* calcd for C₁₅H₁₄NO: 224.1075 [M - H]⁺; found: 224.1073.

7,10-dimethyl-2-nitro-10,11-dihydrodibenzo[*b,f*][1,4]oxazepine (**3c**)

Yellow solid, yield: 42 mg, 83%; ¹H NMR (CDCl₃, 500 MHz): δ 8.11 (dd, *J* = 9, 3 Hz, 1H), 8.02 (d, *J* = 3 Hz, 1H), 7.25 (d, *J* = 9 Hz, 1H), 6.99 (s, 1H), 6.90 (m, 2H), 4.29 (s, 2H), 2.93 (s, 3H), 2.29 (s, 3H); ¹³C NMR (CDCl₃, 125 MHz): δ 161.3, 148.3, 142.7, 139.7, 132.5, 129.0, 125.7, 124.7, 124.2, 121.9, 121.2, 120.0, 57.5, 42.6, 20.3; HR-ESI-MS: *m/z* calcd for C₁₅H₁₅N₂O₃: 271.1083 [M + H]⁺; found: 271.1076.

2-bromo-7,10-dimethyl-10,11-dihydrodibenzo[*b,f*][1,4]oxazepine (**3d**)

Pale yellow liquid, yield: 31 mg, 70%; ¹H NMR (CDCl₃, 500 MHz): δ 7.35 (dd, *J* = 8.5, 2.5 Hz, 1H), 7.26 (d, *J* = 2.5 Hz, 1H), 7.07 (d, *J* = 8.5 Hz, 1H), 6.96 (s, 1H), 6.85 (s, 2H), 4.26 (s, 2H), 2.91 (s, 3H), 2.28 (s, 3H); ¹³C NMR (CDCl₃, 125 MHz): δ 156.1, 148.8, 139.6, 131.8, 131.4, 131.3, 131.2, 125.2, 122.2, 122.0, 120.6, 115.8, 56.3, 43.1, 20.3; HR-ESI-MS: *m/z* calcd for C₁₅H₁₅BrNO: 304.0337 [M + H]⁺; found: 304.0326.

2-methoxy-7,10-dimethyl-10,11-dihydrodibenzo[*b,f*][1,4]oxazepine (**3e**)

Pale brown liquid, yield: 20 mg, 24%; ¹H NMR (CDCl₃, 500 MHz): δ 7.01 (d, *J* = 8.5 Hz, 1H), 6.85 (s, 1H), 6.72 (m, 2H), 6.66 (dd, *J* = 9, 3 Hz, 1H), 6.58 (d, *J* = 3 Hz, 1H), 4.20 (s, 2H), 3.69 (s, 3H), 2.80 (s, 3H), 2.17 (s, 3H); ¹³C NMR (CDCl₃, 125 MHz): δ 155.4, 151.1, 149.4, 139.7, 131.3, 130.2, 124.9, 122.0, 121.0, 120.8, 113.9, 113.1, 56.5, 55.6, 43.3, 20.3; HR-ESI-MS: *m/z* calcd for C₁₆H₁₈NO₂: 256.1338 [M + H]⁺; found: 256.1339.

10-methyl-10,11-dihydrodibenzo[*b,f*][1,4]oxazepine (**3f**)

Pale yellow liquid, yield: 29 mg, 59%; ¹H NMR (CDCl₃, 500 MHz): δ 7.26 (d, *J* = 7.5 Hz, 1H), 7.20 (d, *J* = 8 Hz, 1H), 7.16 (m, 2H), 7.07 (t, *J* = 7.5 Hz, 1H), 7.02 (t, *J* = 7.5 Hz, 1H), 6.90 (d, *J* = 8 Hz, 1H), 6.84 (t, *J* = 7.5 Hz, 1H), 4.39 (s, 2H), 2.97 (s, 3H); ¹³C NMR (CDCl₃, 125 MHz): δ 157.2, 148.9, 142.3, 129.3, 128.7, 128.5, 124.5, 123.6, 121.6, 121.1, 120.3, 119.9, 56.5, 42.9; HR-ESI-MS: *m/z* calcd for C₁₄H₁₄NO: 212.1075 [M + H]⁺; found: 212.1078.

7-methoxy-10-methyl-10,11-dihydrodibenzo[*b,f*][1,4]oxazepine (**3g**)

Pale yellow solid, yield: 38 mg, 76%; ¹H NMR (CDCl₃, 500 MHz): δ 7.25 (t, *J* = 8 Hz, 1H), 7.20 (d, *J* = 8 Hz, 1H), 7.12 (d, *J* = 7.5 Hz, 1H), 7.06 (t, *J* = 7.5 Hz, 1H), 6.94 (d, *J* = 9 Hz, 1H), 6.76 (s, 1H), 6.64 (dd, *J* = 8.5, 1 Hz, 1H), 4.28 (s, 2H), 3.79 (s, 3H), 2.87 (s, 3H); ¹³C NMR (CDCl₃, 125 MHz): δ 156.5, 155.1, 150.7, 136.0, 129.0, 128.6, 128.4, 123.4, 122.3, 120.4, 110.2, 106.9, 57.0, 55.6, 43.5; HR-ESI-MS: *m/z* calcd for C₁₅H₁₆NO₂: 242.1181 [M + H]⁺; found: 242.1178.

7-ethyl-10-methyl-10,11-dihydrodibenzo[*b,f*][1,4]oxazepine (**3h**)

Pale brown liquid, yield: 38 mg, 80%; ¹H NMR (CDCl₃, 500 MHz): δ 7.22 (td, *J* = 7, 1.5 Hz, 1H), 7.18 (dd, *J* = 8, 1 Hz, 1H), 7.12 (dd, *J* = 7.5, 1.5 Hz, 1H), 7.03 (td, *J* = 7, 1 Hz, 1H), 6.99 (s, 1H), 6.85 (m, 2H), 4.31 (s, 2H), 2.90 (s, 3H), 2.56 (q, *J* = 7.5 Hz, 2H), 1.21 (t, *J* = 7.5 Hz, 3H); ¹³C NMR (CDCl₃, 125 MHz): δ 157.1, 149.2, 140.1, 137.9, 129.1, 128.7, 128.5, 123.7, 123.4, 120.9, 120.5, 120.3, 56.7, 43.1, 27.8, 15.5; HR-ESI-MS: *m/z* calcd for C₁₆H₁₈NO: 240.1388 [M + H]⁺; found: 240.1398.

7-(tert-butyl)-10-methyl-10,11-dihydrodibenzo[*b,f*][1,4]oxazepine (**3i**)

Pale brown liquid, yield: 46 mg, 92%; ¹H NMR (CDCl₃, 500 MHz): δ 7.26 (m, 2H), 7.21 (s, 1H), 7.16 (d, *J* = 7 Hz, 1H), 7.08 (m, 2H), 6.91 (d, *J* = 8.5 Hz, 1H), 4.36 (s, 2H), 2.95 (s, 3H), 1.34 (s, 9H); ¹³C NMR (CDCl₃, 125 MHz): δ 157.2, 148.6, 144.9, 139.7, 129.2, 128.7, 128.5, 123.4, 121.2, 120.4, 120.0, 118.6, 56.7, 43.1, 34.0, 31.3; HR-ESI-MS: *m/z* calcd for C₁₈H₂₂NO: 268.1701 [M + H]⁺; found: 268.1749.

7-chloro-10-methyl-10,11-dihydrodibenzo[*b,f*][1,4]oxazepine (**3j**)

Pale yellow liquid, yield: 26 mg, 51%; ¹H NMR (CDCl₃, 500 MHz): δ 7.17 (td, *J* = 8, 1.5 Hz, 1H), 7.08 (d, *J* = 8 Hz, 1H), 7.06 (dd, *J* = 7.5, 1.5 Hz, 1H), 7.04 (d, *J* = 2.5 Hz, 1H), 6.98 (td, *J* = 7.5, 1 Hz, 1H), 6.86 (dd, *J* = 8.5, 2.5 Hz, 1H), 6.68 (d, *J* = 8.5 Hz, 1H), 4.26 (s, 2H), 2.83 (s, 3H); ¹³C NMR (CDCl₃, 125 MHz): δ 156.9, 148.6, 141.0, 129.3, 128.9, 128.5, 124.8, 124.3, 124.0, 121.8, 120.6, 120.2, 56.0, 42.9; HR-ESI-MS: *m/z* calcd for C₁₄H₁₁ClNO: 244.0529 [M - H]⁺; found: 244.0528.

7-bromo-10-methyl-10,11-dihydrodibenzo[*b,f*][1,4]oxazepine (**3k**)

Pale yellow liquid, yield: 32 mg, 64%; ¹H NMR (CDCl₃, 500 MHz): δ 7.19 (d, *J* = 2 Hz, 1H), 7.16 (dd, *J* = 8, 1.5 Hz, 1H), 7.07 (d, *J* = 7 Hz, 1H), 7.06 (dd, *J* = 7.5, 1.5 Hz, 1H), 7.00 (d, *J* = 8.5 Hz, 1H), 6.98 (m, 1H), 6.62 (d, *J* = 8.5 Hz, 1H), 4.27 (s, 2H), 2.84 (s, 3H); ¹³C NMR (CDCl₃, 125 MHz): δ 157.0, 148.7, 141.4, 129.4, 128.9, 128.5, 127.2, 124.6, 124.0, 120.8, 120.2, 111.6, 55.9, 42.8; HR-ESI-MS: *m/z* calcd for C₁₄H₁₁BrNO: 288.0024 [M - H]⁺; found: 288.0021.

2-bromo-7-ethyl-10-methyl-10,11-dihydrodibenzo[*b,f*][1,4]oxazepine (**3l**)

Pale yellow liquid, yield: 31 mg, 63%; ¹H NMR (CDCl₃, 500 MHz): δ 7.23 (dd, *J* = 8.5, 2.5 Hz, 1H), 7.15 (d, *J* = 2.5 Hz, 1H), 6.97 (d, *J* = 8.5 Hz, 1H), 6.87 (s, 1H), 6.77 (s, 2H), 4.16 (s, 2H), 2.80 (s, 3H), 2.47 (q, *J* = 8 Hz, 2H), 1.13 (t, *J* = 7.5 Hz, 3H); ¹³C NMR (CDCl₃, 125 MHz): δ 156.1, 148.9, 139.7, 138.3, 131.4, 131.3, 131.2, 124.0, 122.2, 120.7, 120.6, 115.8, 56.3, 43.1, 27.8, 15.4; HR-ESI-MS: *m/z* calcd for C₁₆H₁₇BrNO: 318.0494 [M + H]⁺; found: 318.0466.

2-bromo-7-(tert-butyl)-10-methyl-10,11-dihydrodibenzo[*b,f*][1,4]oxazepine (**3m**)

Pale brown solid, yield: 36 mg, 73%; ¹H NMR (CDCl₃, 500 MHz): δ 7.24 (dd, *J* = 9, 2.5 Hz, 1H), 7.16 (d, *J* = 2.5 Hz, 1H), 7.04 (d, *J* = 2.5 Hz, 1H), 6.99 (d, *J* = 8.5 Hz, 1H), 6.95 (dd, *J* = 8.5, 2.5 Hz, 1H), 6.77 (d, *J* = 8.5 Hz, 1H), 4.17 (s, 2H), 2.81 (s, 3H), 1.21 (s, 9H); ¹³C NMR (CDCl₃, 125 MHz): δ 156.2, 148.3, 145.2, 139.3, 131.4, 131.3, 122.2, 121.4, 120.1, 118.5, 115.8, 56.2, 43.0, 34.0, 31.3; HR-ESI-MS: *m/z* calcd for C₁₈H₂₁BrNO: 346.0807 [M + H]⁺; found: 346.0804.

2,7-dibromo-10-methyl-10,11-dihydrodibenzo[*b,f*][1,4]oxazepine (**3n**)

Pale yellow liquid, yield: 24 mg, 43%; ¹H NMR (CDCl₃, 500 MHz): δ 7.27 (dd, *J* = 8.5, 2.5 Hz, 1H), 7.20 (d, 2.5 Hz, 1H), 7.16 (d, 2.5 Hz, 1H), 7.01 (dd, *J* = 8.5, 2.5 Hz, 1H), 6.96 (d, *J* = 8.5 Hz, 1H), 6.63 (d, *J* = 8.5 Hz, 1H), 4.21 (s, 2H), 2.83 (s, 3H); ¹³C NMR (CDCl₃, 125 MHz): δ 156.0, 148.3, 141.1, 131.8, 131.5, 131.2, 127.5, 124.5, 122.1, 121.0, 116.4, 111.9, 55.5, 42.8; HR-ESI-MS: *m/z* calcd for C₁₄H₁₀Br₂NO: 365.9129 [M - H]⁺; found: 365.9141.

2-chloro-7-ethyl-10-methyl-10,11-dihydrodibenzo[*b,f*][1,4]oxazepine (**3o**)

Pale yellow liquid, yield: 43 mg, 81%; ¹H NMR (CDCl₃, 500 MHz): δ 7.09 (dd, *J* = 8.5, 2.5 Hz, 1H), 7.02 (d, *J* = 8.5 Hz, 1H), 7.01 (d, *J* = 2.5 Hz, 1H), 6.88 (s, 1H), 6.77 (m, 2H), 4.16 (s, 2H), 2.81 (s, 3H), 2.48 (q, *J* = 8 Hz, 2H), 1.13 (t, *J* = 7.5 Hz, 3H); ¹³C NMR (CDCl₃, 125 MHz): δ 155.5, 148.9, 139.8, 138.2, 130.7, 128.4, 128.3, 128.2, 124.0, 121.8, 120.7, 120.6, 56.4, 43.1, 27.8, 15.4; HR-ESI-MS: *m/z* calcd for C₁₆H₁₇ClNO: 274.0999 [M + H]⁺; found: 274.0986.

2-chloro-7-methoxy-10-methyl-10,11-dihydrodibenzo[*b,f*][1,4]oxazepine (**3p**)

Pale yellow liquid, yield: 28 mg, 66%; ¹H NMR (CDCl₃, 500 MHz): δ 7.19 (dd, *J* = 9, 2.5 Hz, 1H), 7.13 (d, *J* = 8.5 Hz, 1H), 7.10 (d, *J* = 2.5 Hz, 1H), 6.93 (d, *J* = 9 Hz, 1H), 6.72 (d, *J* = 3 Hz, 1H), 6.64 (dd, *J* = 9, 3 Hz, 1H), 4.22 (s, 2H), 3.79 (s, 3H), 2.86 (s, 3H); ¹³C NMR (CDCl₃, 125 MHz): δ 155.2, 155.0, 150.4, 135.7, 130.4, 128.6, 128.3, 128.2, 122.4, 121.8, 110.4, 106.8, 56.7, 55.6, 43.4; HR-ESI-MS: *m/z* calcd for C₁₅H₁₅ClNO₂: 276.0791 [M + H]⁺; found: 276.0785.

2,7-dimethoxy-10-methyl-10,11-dihydrodibenzo[*b,f*][1,4]oxazepine (**3q**)

Pale brown liquid, yield: 27 mg, 31%; ¹H NMR (CDCl₃, 500 MHz): δ 7.12 (d, *J* = 9 Hz, 1H), 6.91 (d, *J* = 8.5 Hz, 1H), 6.77 (dd, *J* = 9, 3 Hz, 1H), 6.72 (d, *J* = 3 Hz, 1H), 6.67 (d, *J* = 3 Hz, 1H), 6.61 (dd, *J* = 9, 3 Hz, 1H), 4.26 (s, 2H), 3.79 (s, 3H), 3.78 (s, 3H), 2.86 (s, 3H); ¹³C NMR (CDCl₃, 125 MHz): δ 155.4, 155.0, 150.9, 150.6, 135.8, 129.9, 122.6, 121.0, 114.0, 113.1, 110.1, 106.8, 56.7, 55.6, 43.6; HR-ESI-MS: *m/z* calcd for C₁₆H₁₈NO₃: 272.1287 [M + H]⁺; found: 272.1288.

7-ethyl-2-methoxy-10-methyl-10,11-dihydrodibenzo[*b,f*][1,4]oxazepine (**3r**)

Pale brown liquid, yield: 21 mg, 39%; ¹H NMR (CDCl₃, 500 MHz): δ 7.13 (d, *J* = 9 Hz, 1H), 6.98 (s, 1H), 6.86 (m, 2H), 6.77 (dd, *J* = 8.5, 3 Hz, 1H), 6.69 (d, *J* = 3 Hz, 1H), 4.31 (s, 2H), 3.79 (s, 3H), 2.92 (s, 3H), 2.57 (q, *J* = 7.5 Hz, 2H), 1.23 (t, *J* = 7.5 Hz, 3H); ¹³C NMR (CDCl₃, 125 MHz): δ 155.4, 151.1, 149.4, 139.8, 137.8, 130.2, 123.6, 121.0, 120.8, 120.7, 113.9, 113.1, 56.4, 55.6, 43.3, 27.7, 15.4; HR-ESI-MS: *m/z* calcd for C₁₇H₂₀NO₂: 270.1494 [M + H]⁺; found: 270.1487.

3,7,10-trimethyl-10,11-dihydrodibenzo[*b,f*][1,4]oxazepine (**3s**)

Pale yellow solid, yield: 27 mg, 54%; ¹H NMR (CDCl₃, 500 MHz): δ 6.99 (m, 2H), 6.94 (s, 1H), 6.84 (d, *J* = 7.5 Hz, 1H), 6.79 (m, 2H), 4.25 (s, 2H), 2.88 (s, 3H), 2.31 (s, 3H), 2.25 (s, 3H); ¹³C NMR (CDCl₃, 125 MHz): δ 156.9, 149.2, 139.9, 138.6, 131.4, 128.5, 125.9, 124.9, 124.1, 122.1, 120.8, 120.6, 56.5, 43.1, 21.0, 20.3; HR-ESI-MS: *m/z* calcd for C₁₆H₁₈NO: 240.1388 [M + H]⁺; found: 240.1388.

7-(tert-butyl)-3,10-dimethyl-10,11-dihydrodibenzo[*b,f*][1,4]oxazepine (**3t**)

Pale yellow solid, yield: 34 mg, 64%; ¹H NMR (CDCl₃, 500 MHz): δ 7.18 (s, 1H), 7.07 (s, 1H), 7.05 (t, *J* = 8 Hz, 2H), 6.88 (d, *J* = 8 Hz, 2H), 4.32 (s, 2H), 2.93 (s, 3H), 2.36 (s, 3H), 1.33 (s, 9H); ¹³C NMR (CDCl₃, 125 MHz): δ 157.1, 148.7, 144.7, 139.7, 138.6, 128.4, 126.1, 124.1, 121.1, 120.8, 120.1, 118.6, 56.4, 43.0, 34.0, 31.3, 21.0; HR-ESI-MS: *m/z* calcd for C₁₉H₂₄NO: 282.1858 [M + H]⁺; found: 282.1852.

7-ethyl-10-methyl-2-nitro-10,11-dihydrodibenzo[*b,f*][1,4]oxazepine (**3u**)

Pale yellow liquid, yield: 40 mg, 81%; ¹H NMR (CDCl₃, 500 MHz): δ 8.02 (dd, *J* = 9, 3 Hz, 1H), 7.92 (d, *J* = 2.5 Hz, 1H), 7.16 (d, *J* = 9 Hz, 1H), 6.92 (s, 1H), 6.83 (m, 2H), 4.20 (s, 2H), 2.84 (s, 3H), 2.50 (q, *J* = 7.5 Hz, 2H), 1.14 (t, *J* = 7.5 Hz, 3H); ¹³C NMR (CDCl₃, 125 MHz): δ 161.3, 148.4, 142.7, 139.8, 139.0, 129.0, 124.6, 124.4, 124.2, 121.2, 120.7, 120.1, 57.5, 42.6, 27.8, 15.4; HR-ESI-MS: *m/z* calcd for C₁₆H₁₇N₂O₃: 285.1239 [M + H]⁺; found: 285.1229.

7-(tert-butyl)-10-methyl-2-nitro-10,11-dihydrodibenzo[*b,f*][1,4]oxazepine (**3v**)

Orange solid, yield: 44 mg, 87%; ¹H NMR (CDCl₃, 500 MHz): δ 8.14 (d, *J* = 8.5 Hz, 1H), 8.04 (s, 1H), 7.30 (d, *J* = 9 Hz, 1H), 7.19 (s, 1H), 7.12 (d, *J* = 8 Hz, 1H), 6.95 (d, *J* = 8.5 Hz, 1H), 4.32 (s, 2H), 2.96 (s, 3H), 1.33 (s, 9H); ¹³C NMR (CDCl₃, 125 MHz): δ 161.5, 147.9, 146.0, 142.7, 139.4, 129.1, 124.6, 124.3, 121.9, 121.2, 119.7, 118.4, 57.4, 42.5, 34.1, 31.3; HR-ESI-MS: *m/z* calcd for C₁₈H₂₁N₂O₃: 313.1552 [M + H]⁺; found: 313.1532.

7-methoxy-10-methyl-2-nitro-10,11-dihydrodibenzo[*b,f*][1,4]oxazepine (**3w**)

Yellow solid, yield: 16 mg, 40%; ¹H NMR (CDCl₃, 500 MHz): δ 8.03 (dd, *J* = 8.5, 2.5 Hz, 1H), 7.93 (d, *J* = 3 Hz, 1H), 7.18 (d, *J* = 9 Hz, 1H), 6.89 (d, *J* = 9 Hz, 1H), 6.66 (d, *J* = 3 Hz, 1H), 6.59 (dd, *J* = 9, 3 Hz, 1H), 4.18 (s, 2H), 3.71 (s, 3H), 2.80 (s, 3H); ¹³C NMR (CDCl₃, 125 MHz): δ 160.8, 155.7, 149.8, 142.8, 135.7, 128.7, 124.9, 124.1, 121.9, 121.3, 110.8, 106.9, 57.8, 55.6, 42.9; HR-ESI-MS: *m/z* calcd for C₁₅H₁₅N₂O₄: 287.1032 [M + H]⁺; found: 287.1023.

7-bromo-10-methyl-2-nitro-10,11-dihydrodibenzo[*b,f*][1,4]oxazepine (**3x**)

Yellow solid, yield: 17 mg, 40%; ¹H NMR (CDCl₃, 500 MHz): δ 8.17 (dd, *J* = 9, 3 Hz, 1H), 8.06 (d, *J* = 2.5 Hz, 1H), 7.32 (d, *J* = 2.5 Hz, 1H), 7.28 (d, *J* = 8.5 Hz, 1H), 7.17 (dd, *J* = 8.5, 2 Hz, 1H), 6.81 (d, *J* = 8.5 Hz, 1H), 4.36 (s, 2H), 2.97 (s, 3H); ¹³C NMR (CDCl₃, 125 MHz): δ 161.2, 148.0, 143.2, 141.2, 129.5, 127.9, 124.6, 124.5, 124.4, 121.2, 120.8, 112.9, 56.5, 42.5; HR-ESI-MS: *m/z* calcd for C₁₄H₁₂BrN₂O₃: 335.0031 [M + H]⁺; found: 335.0009.

2-bromo-7-(tert-butyl)-4-methoxy-10-methyl-10,11-dihydrodibenzo[*b,f*][1,4]oxazepine
(**3y**)

Pale brown solid, yield: 27 mg, 54%; ¹H NMR (CDCl₃, 500 MHz): δ 7.21 (d, *J* = 2 Hz, 1H), 7.03 (dd, *J* = 8.5, 2.5 Hz, 1H), 6.99 (d, *J* = 2 Hz, 1H), 6.91 (d, *J* = 2 Hz, 1H), 6.82 (d, *J* = 8.5 Hz, 1H), 4.31 (s, 2H), 3.90 (s, 3H), 2.91 (s, 3H), 1.30 (s, 9H); ¹³C NMR (CDCl₃, 125 MHz): δ 151.7, 147.6, 145.6, 144.5, 139.1, 132.7, 122.9, 121.5, 120.1, 119.0, 115.8, 115.1, 56.4, 55.5, 43.1, 34.0, 31.3; HR-ESI-MS: *m/z* calcd for C₁₉H₂₃BrNO₂: 376.0912 [M + H]⁺; found: 376.0899.

2,4-dichloro-7,10-dimethyl-10,11-dihydrodibenzo[*b,f*][1,4]oxazepine (**3z**)

Yellow solid, yield: 25 mg, 52%; ¹H NMR (CDCl₃, 500 MHz): δ 7.31 (d, *J* = 2.5 Hz, 1H), 7.06 (d, *J* = 1.5 Hz, 1H), 7.04 (d, *J* = 2.5 Hz, 1H), 6.83 (dd, *J* = 8, 1.5 Hz, 1H), 6.78 (d, *J* = 8 Hz, 1H), 4.30 (s, 2H), 2.88 (s, 3H), 2.26 (s, 3H); ¹³C NMR (CDCl₃, 125 MHz): δ 151.9, 147.5, 139.0, 132.8, 131.3, 128.8, 128.5, 126.8, 126.4, 125.6, 122.6, 120.7, 55.6, 43.2, 20.2; HR-ESI-MS: *m/z* calcd for C₁₅H₁₄Cl₂NO: 294.0452 [M + H]⁺; found: 294.0441.

7-(tert-butyl)-2,4-dichloro-10-methyl-10,11-dihydrodibenzo[*b,f*][1,4]oxazepine (**3aa**)

Pale brown liquid, yield: 37 mg, 79%; ¹H NMR (CDCl₃, 500 MHz): δ 7.34 (s, 1H), 7.27 (s, 1H), 7.07 (s, 1H), 7.06 (d, *J* = 8.5 Hz, 1H), 6.83 (d, *J* = 8.5 Hz, 1H), 4.34 (s, 2H), 2.93 (s, 3H), 1.31 (s, 9H); ¹³C NMR (CDCl₃, 125 MHz): δ 152.1, 147.0, 144.6, 138.8, 133.0, 128.8, 128.5, 126.8, 126.4, 121.9, 120.0, 119.2, 55.5, 43.0, 34.0, 31.2; HR-ESI-MS: *m/z* calcd for C₁₈H₂₀Cl₂NO: 336.0922 [M + H]⁺; found: 336.0991.

2,4,7-trichloro-10-methyl-10,11-dihydrodibenzo[*b,f*][1,4]oxazepine (**3ab**)

Pale brown liquid, yield: 23 mg, 47%; ¹H NMR (CDCl₃, 500 MHz): δ 7.33 (d, *J* = 2.5 Hz, 1H), 7.23 (d, *J* = 2.5 Hz, 1H), 7.07 (d, *J* = 2.5 Hz, 1H), 6.96 (dd, *J* = 8.5, 2.5 Hz, 1H), 6.72 (d, *J* = 9 Hz, 1H), 4.34 (s, 2H), 2.91 (s, 3H); ¹³C NMR (CDCl₃, 125 MHz): δ 151.6, 146.8, 140.1, 133.0, 129.2, 129.1, 126.6, 126.5, 125.1, 124.6, 122.3, 120.6, 55.0, 42.9; HR-ESI-MS: *m/z* calcd for C₁₄H₁₁Cl₃NO: 313.9906 [M + H]⁺; found: 313.9897.

8-chloro-7-fluoro-10-methyl-10,11-dihydrodibenzo[*b,f*][1,4]oxazepine (**3ac**)

Pale yellow liquid, yield: 20 mg, 41%; ¹H NMR (CDCl₃, 500 MHz): δ 7.28 (td, *J* = 7, 1.5 Hz, 1H), 7.17 (d, *J* = 8 Hz, 1H), 7.15 (d, *J* = 8 Hz, 1H), 7.09 (t, *J* = 7.5 Hz, 1H), 6.96 (d, *J* = 9.5 Hz, 1H), 6.89 (d, *J* = 7.5 Hz, 1H), 4.33 (s, 2H), 2.91 (s, 3H); ¹³C NMR (CDCl₃, 125 MHz): δ 156.4, 152.9, 150.9, 147.6, 139.5, 128.8, 128.7, 124.0, 120.5, 115.5, 110.0, 56.2, 43.1; HR-ESI-MS: *m/z* calcd for C₁₄H₁₂ClFNO: 264.0591 [M + H]⁺; found: 264.0582.

6-chloro-7-fluoro-10-methyl-10,11-dihydrodibenzo[*b,f*][1,4]oxazepine (**3ac'**)

Pale yellow liquid, yield: 11 mg, 23%; ¹H NMR (CDCl₃, 500 MHz): δ 7.27 (d, *J* = 8 Hz, 1H), 7.18 (td, *J* = 7.5, 2 Hz, 1H), 7.03 (m, 2H), 6.75 (t, *J* = 9 Hz, 1H), 6.69 (dd, *J* = 9, 5.5 Hz, 1H), 4.24 (s, 2H), 2.83 (s, 3H); ¹³C NMR (CDCl₃, 125 MHz): δ 155.8, 154.3, 152.4, 146.4, 140.3, 128.7, 128.6, 124.3, 121.0, 117.7, 114.6, 111.0, 56.4, 43.1; HR-ESI-MS: *m/z* calcd for C₁₄H₁₂ClFNO: 264.0591 [M + H]⁺; found: 264.0596.

8-chloro-10-methyl-10,11-dihydrodibenzo[*b,f*][1,4]oxazepine (**3ad**)

Pale yellow liquid, yield: 7 mg, 12%; ¹H NMR (CDCl₃, 500 MHz): δ 7.17 (td, *J* = 7.5, 1.5 Hz, 1H), 7.07 (m, 2H), 6.99 (td, *J* = 7.5, 1 Hz, 1H), 6.95 (d, *J* = 8.5 Hz, 1H), 6.68 (d, *J* = 2.5 Hz, 1H), 6.63 (dd, *J* = 8.5, 2.5 Hz, 1H), 4.31 (s, 2H), 2.87 (s, 3H); ¹³C NMR (CDCl₃, 125 MHz): δ 157.1, 146.6, 142.9, 129.5, 129.4, 129.0, 128.4, 124.0, 122.6, 120.1, 119.8, 118.6, 56.0, 42.6; HR-ESI-MS: *m/z* calcd for C₁₄H₁₃ClNO: 246.0686 [M + H]⁺; found: 246.0676.

6-chloro-10-methyl-10,11-dihydrodibenzo[*b,f*][1,4]oxazepine (**3ad'**)

Pale yellow liquid, yield: 17 mg, 33%; ¹H NMR (CDCl₃, 500 MHz): δ 7.37 (d, *J* = 8 Hz, 1H), 7.27 (td, *J* = 8, 2 Hz, 1H), 7.15 (dd, *J* = 7.5, 1.5 Hz, 1H), 7.10 (td, *J* = 7.5, 1 Hz, 1H), 6.92 (m, 2H), 6.77 (t, *J* = 5 Hz, 1H), 4.41 (s, 2H), 2.98 (s, 3H); ¹³C NMR (CDCl₃, 125 MHz): δ 156.6, 144.7, 144.1, 129.2, 128.8, 128.3, 126.9, 124.4, 124.2, 121.5, 121.0, 117.5, 56.3, 42.9; HR-ESI-MS: *m/z* calcd for C₁₄H₁₁ClNO: 244.0529 [M - H]⁺; found: 244.0525.

10-methyl-8-(trifluoromethyl)-10,11-dihydrodibenzo[*b,f*][1,4]oxazepine (**3ae**)

Yellowish solid, yield: 14 mg, 28%; ¹H NMR (CDCl₃, 500 MHz): δ 7.19 (td, *J* = 7.5, 1.5 Hz, 1H), 7.09 (m, 3H), 7.01 (td, *J* = 7, 1 Hz, 1H), 6.94 (s, 1H), 6.93 (d, *J* = 7 Hz, 1H), 4.34 (s, 2H), 2.91 (s, 3H); ¹³C NMR (CDCl₃, 125 MHz): δ 156.9, 150.0, 142.2, 129.6, 129.1, 128.4, 126.7, 124.1, 123.0, 122.0, 120.2, 117.0, 116.1, 55.8, 42.6; HR-ESI-MS: *m/z* calcd for C₁₅H₁₃F₃NO: 280.0949 [M + H]⁺; found: 280.0946.

10-methyl-6-(trifluoromethyl)-10,11-dihydrodibenzo[*b,f*][1,4]oxazepine (**3ae'**)

Yellowish solid, yield: 21 mg, 41%; ¹H NMR (CDCl₃, 500 MHz): δ 7.19 (m, 2H), 7.05 (dd, *J* = 7, 0.5 Hz, 1H), 7.00 (m, 2H), 6.94 (m, 2H), 4.32 (s, 2H), 2.88 (s, 3H); ¹³C NMR (CDCl₃, 125 MHz): δ 156.5, 146.2, 143.5, 129.5, 128.9, 128.1, 124.8, 124.2, 123.8, 123.2, 122.6, 120.6, 118.0, 55.8, 43.0; HR-ESI-MS: *m/z* calcd for C₁₅H₁₃F₃NO: 280.0949 [M + H]⁺; found: 280.0945.

7,8-dimethoxy-10-methyl-10,11-dihydrodibenzo[*b,f*][1,4]oxazepine (**3af**)

Pale brown solid, yield: 21 mg, 43%; ¹H NMR (CDCl₃, 500 MHz): δ 7.24 (td, *J* = 8, 2 Hz, 1H), 7.17 (dd, *J* = 8, 1 Hz, 1H), 7.13 (dd, *J* = 7.5, 1.5 Hz, 1H), 7.05 (td, *J* = 7.5, 1.5 Hz, 1H), 6.73 (s, 1H), 6.54 (s, 1H), 4.30 (s, 2H), 3.85 (s, 3H), 3.84 (s, 3H), 2.86 (s, 3H); ¹³C NMR (CDCl₃, 125 MHz): δ 157.3, 145.4, 144.1, 143.4, 134.8, 129.0, 128.8, 128.5, 123.4, 120.1, 106.2, 105.8, 56.6, 56.3, 56.2, 43.5; HR-ESI-MS: *m/z* calcd for C₁₆H₁₆NO₃: 270.1130 [M - H]⁺; found: 270.1131.

2-bromo-7,8-dimethoxy-10-methyl-10,11-dihydrodibenzo[*b,f*][1,4]oxazepine (**3ag**)

Pale brown solid, yield: 27 mg, 54%; ¹H NMR (CDCl₃, 500 MHz): δ 7.34 (d, *J* = 9 Hz, 1H), 7.26 (s, 1H), 7.06 (d, *J* = 8.5 Hz, 1H), 6.70 (s, 1H), 6.53 (s, 1H), 4.24 (s, 2H), 3.85 (s, 6H), 2.86 (s, 3H); ¹³C NMR (CDCl₃, 125 MHz): δ 156.3, 145.6, 144.4, 143.1, 134.5, 131.6, 131.3, 131.0, 122.0, 115.8, 106.2, 105.6, 56.4, 56.3, 56.2, 43.5; HR-ESI-MS: *m/z* calcd for C₁₆H₁₇BrNO₃: 350.0392 [M + H]⁺; found: 350.0370.

7,8-dimethoxy-10-methyl-2-nitro-10,11-dihydrodibenzo[*b,f*][1,4]oxazepine (**3ah**)

Yellow solid, yield: 20 mg, 44%; ¹H NMR (CDCl₃, 500 MHz): δ 8.14 (dd, *J* = 9, 3 Hz, 1H), 8.04 (d, *J* = 2.5 Hz, 1H), 7.26 (d, *J* = 9 Hz, 1H), 6.74 (s, 1H), 6.59 (s, 1H), 4.30 (s, 2H), 3.88 (s, 3H), 3.87 (s, 3H), 2.91 (s, 3H); ¹³C NMR (CDCl₃, 125 MHz): δ 161.5, 145.9, 144.8, 142.8, 138.6, 134.6, 131.5, 128.9, 125.0, 124.2, 121.1, 105.5, 103.6, 57.5, 56.3, 56.2, 43.0; HR-ESI-MS: *m/z* calcd for C₁₆H₁₇N₂O₅: 317.1137 [M + H]⁺; found: 317.1137.

10-benzyl-7-methyl-10,11-dihydrodibenzo[*b,f*][1,4]oxazepine (**3ai**)

Pale yellow liquid, yield: 31 mg, 61%; ¹H NMR (CDCl₃, 500 MHz): δ 7.34 (m, 4H), 7.29 (m, 2H), 7.22 (d, *J* = 8 Hz, 1H), 7.07 (m, 2H), 7.01 (s, 1H), 6.84 (d, *J* = 8 Hz, 1H), 6.78 (d, *J* = 8.5 Hz, 1H), 4.33 (s, 2H), 4.31 (s, 2H), 2.29 (s, 3H); ¹³C NMR (CDCl₃, 125 MHz): δ 158.0, 148.4, 139.2, 139.0, 131.0, 130.1, 128.8, 128.7, 128.6, 127.6, 127.2, 124.9, 123.5, 122.2, 121.6, 120.3, 59.4, 52.0, 20.3; HR-ESI-MS: *m/z* calcd for C₂₁H₂₀NO: 302.1545 [M + H]⁺; found: 302.1607.

10-benzyl-7-methoxy-10,11-dihydrodibenzo[*b,f*][1,4]oxazepine (**3aj**)

Pale yellow liquid, yield: 20 mg, 40%; ¹H NMR (CDCl₃, 500 MHz): δ 7.43 (d, *J* = 7.5 Hz, 2H), 7.39 (t, *J* = 7 Hz, 2H), 7.33 (d, *J* = 7 Hz, 1H), 7.28 (d, *J* = 6 Hz, 1H), 7.22 (d, *J* = 7.5 Hz, 1H), 7.06 (t, *J* = 7 Hz, 1H), 7.02 (d, *J* = 7.5 Hz, 1H), 6.95 (d, *J* = 8.5 Hz, 1H), 6.76 (s, 1H), 6.59 (d, *J* = 9 Hz, 1H), 4.25 (s, 2H), 4.20 (s, 2H), 3.80 (s, 3H); ¹³C NMR (CDCl₃, 125 MHz): δ 157.3, 155.0, 150.5, 139.0, 135.4, 129.6, 129.1, 128.6, 128.5, 128.0, 127.2, 124.3, 123.4, 120.3, 110.2, 106.7, 59.7, 55.6, 52.1; HR-ESI-MS: *m/z* calcd for C₂₁H₂₀NO₂: 318.1494 [M + H]⁺; found: 318.1478.

11-methyl-10,11-dihydro-[1,3]dioxolo[4',5':4,5]benzo[1,2-*b*]benzo[*f*][1,4]oxazepine (**3ak**)

Pale yellow solid, yield: 19 mg, 40%; ¹H NMR (CDCl₃, 500 MHz): δ 7.12 (td, *J* = 7.5, 2 Hz, 1H), 7.07 (d, *J* = 7.5 Hz, 1H), 6.98 (d, *J* = 6 Hz, 1H), 6.94 (t, *J* = 7 Hz, 1H), 6.62 (s, 1H), 6.47 (s, 1H), 5.80 (s, 2H), 4.14 (s, 2H), 2.76 (s, 3H); ¹³C NMR (CDCl₃, 125 MHz): δ 156.5, 145.0, 144.1, 142.1, 137.0, 128.8, 128.3, 128.2, 123.4, 120.4, 102.9, 101.4, 101.3, 57.3, 43.2; HR-ESI-MS: *m/z* calcd for C₁₅H₁₄NO₃: 256.0974 [M + H]⁺; found: 256.0969.

2-((7-methyldibenzo[*b,f*][1,4]oxazepin-10(11H)-yl)methyl)-4-nitrophenol (**3al**)

Yellow solid, yield: 26 mg, 52%; ¹H NMR (CDCl₃, 500 MHz): δ 11.31 (bs, 1H), 8.16 (dd, *J* = 9, 2.5 Hz, 1H), 7.95 (d, *J* = 3 Hz, 1H), 7.32 (td, *J* = 8, 1.5 Hz, 1H), 7.26 (d, *J* = 7.5 Hz, 1H), 7.12 (d, *J* = 8 Hz, 1H), 7.08 (m, 2H), 6.96 (d, *J* = 9 Hz, 1H), 6.95 (dd, *J* = 6.5, 1 Hz, 1H), 6.91 (dd, *J* = 8, 1.5 Hz, 1H), 4.39 (s, 2H), 4.30 (s, 2H), 2.33 (s, 3H); ¹³C NMR (CDCl₃, 125 MHz): δ 164.1, 156.0, 152.0, 140.6, 136.8, 136.5, 129.4, 129.2, 125.6, 125.3, 125.0, 124.0, 123.9, 122.6, 121.1, 120.8, 116.9, 58.3, 53.4, 20.6; HR-ESI-MS: *m/z* calcd for C₂₁H₁₉N₂O₄: 363.1345 [M + H]⁺; found: 363.1356.

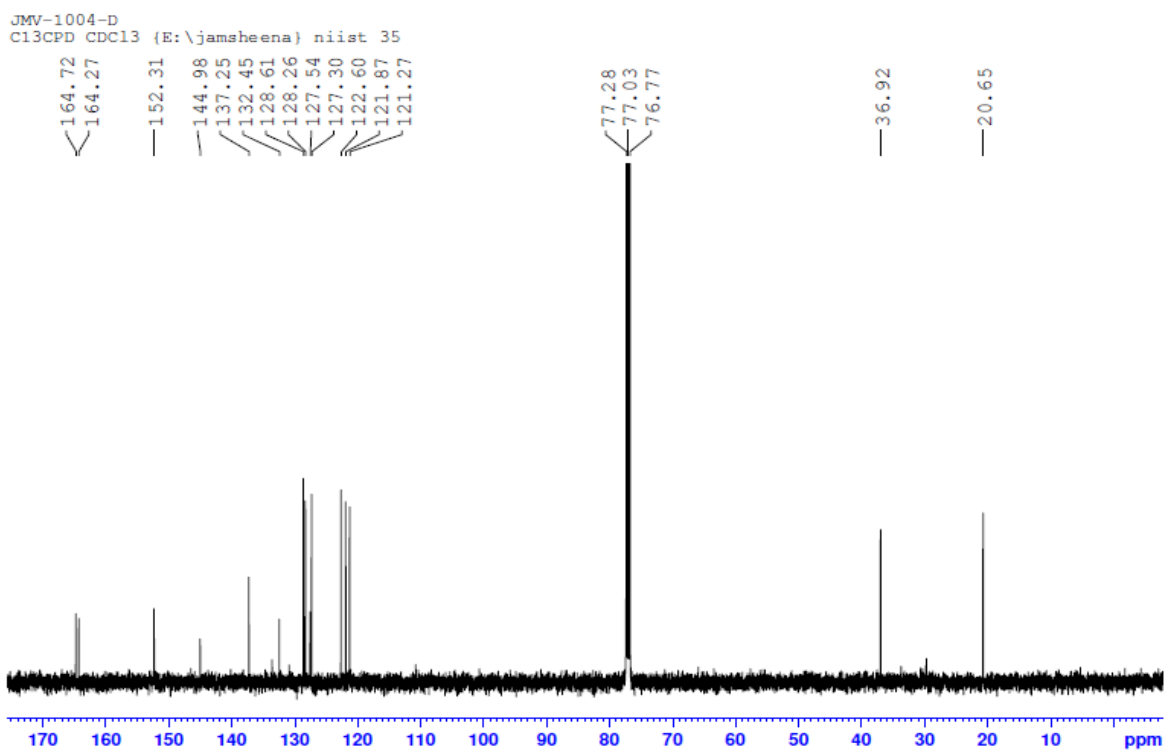
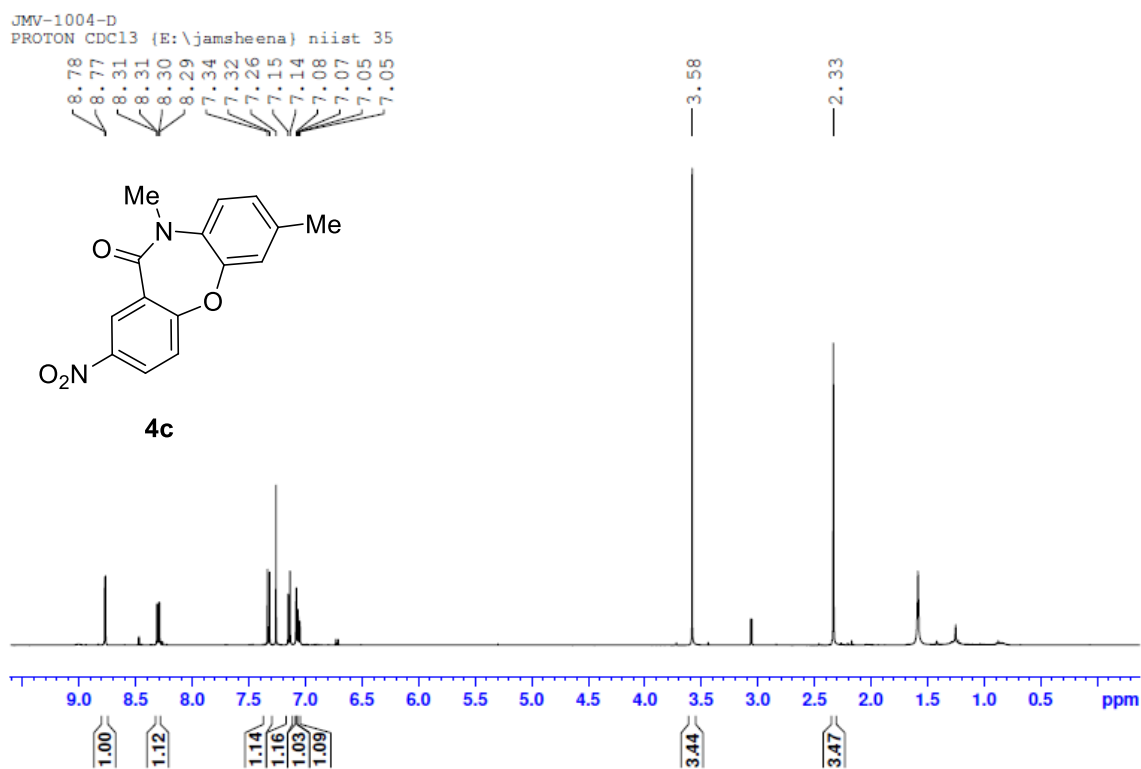
10-(2-methoxy-5-nitrobenzyl)-7-methyl-10,11-dihydrodibenzo[*b,f*][1,4]oxazepine (**3al'**)

Yellow solid, yield: 12 mg, 57%; ¹H NMR (CDCl₃, 500 MHz): δ 8.24 (d, *J* = 2.5 Hz, 1H), 8.14 (dd, *J* = 9, 3 Hz, 1H), 7.20 (td, *J* = 8, 1.5 Hz, 1H), 7.13 (d, *J* = 8 Hz, 1H), 7.01 (m, 2H), 6.90 (s, 1H), 6.87 (d, *J* = 9 Hz, 1H), 6.63 (dd, *J* = 8.5, 1 Hz, 1H), 6.57 (d, *J* = 8.5 Hz, 1H), 4.30 (s, 2H), 4.22 (s, 2H), 3.87 (s, 3H), 2.17 (s, 3H); ¹³C NMR (CDCl₃, 125 MHz): δ 162.2, 158.2, 147.9, 141.7, 138.7, 131.0, 130.3, 129.1, 128.8, 128.5, 125.0, 124.7, 123.9, 123.8, 122.2, 121.0, 120.3, 109.8, 56.1, 54.3, 52.4, 20.2; HR-ESI-MS: *m/z* calcd for C₂₂H₂₁N₂O₄: 377.1501 [M + H]⁺; found: 377.1508.

7,10-dimethyl-2-nitrodibenzo[*b,f*][1,4]oxazepin-11(10H)-one (**4c**)

Yellow solid, yield: 37 mg, 73%; ¹H NMR (CDCl₃, 500 MHz): δ 8.77 (d, *J* = 3 Hz, 1H), 8.30 (dd, *J* = 9, 3 Hz, 1H), 7.32 (d, *J* = 8.5 Hz, 1H), 7.14 (d, *J* = 8.5 Hz, 1H), 7.08 (s, 1H), 7.05 (d, *J* = 9.5 Hz, 1H), 3.58 (s, 3H), 2.33 (s, 3H); ¹³C NMR (CDCl₃, 125 MHz): δ 164.7, 164.2, 152.3, 144.9, 137.2, 132.4, 128.6, 128.2, 127.5, 127.3, 122.6, 121.8, 121.2, 36.9, 20.6; HR-ESI-MS: *m/z* calcd for C₁₅H₁₃N₂O₄: 285.0875 [M + H]⁺; found: 285.0876.

Figure 3.5C. ^1H and ^{13}C -NMR of **4c**



2-bromo-7,10-dimethyldibenzo[*b,f*][1,4]oxazepin-11(10H)-one (**4d**)

Yellow solid, yield: 23 mg, 28%; ¹H NMR (CDCl₃, 500 MHz): δ 8.00 (s, 1H), 7.55 (dd, *J* = 8.5, 1.5 Hz, 1H), 7.12 (d, *J* = 8 Hz, 1H), 7.09 (d, *J* = 8.5 Hz, 1H), 7.06 (s, 1H), 7.03 (d, *J* = 8.5 Hz, 1H), 3.57 (s, 3H), 2.34 (s, 3H); ¹³C NMR (CDCl₃, 125 MHz): δ 165.0, 159.6, 153.1, 136.8, 136.1, 134.8, 132.9, 128.1, 126.6, 122.4, 121.7, 121.6, 117.9, 36.8, 20.6; HR-ESI-MS: *m/z* calcd for C₁₅H₁₃BrNO₂: 318.0130 [M + H]⁺; found: 318.0134.

7-ethyl-10-methyldibenzo[*b,f*][1,4]oxazepin-11(10H)-one (**4h**)

Pale yellow liquid, yield: 25 mg, 30%; ¹H NMR (CDCl₃, 500 MHz): δ 7.90 (d, *J* = 8 Hz, 1H), 7.46 (t, *J* = 7.5 Hz, 1H), 7.22 (t, *J* = 8.5 Hz, 2H), 7.15 (d, *J* = 8 Hz, 1H), 7.11 (s, 1H), 7.04 (dd, *J* = 8, 1.5 Hz, 1H), 3.59 (s, 3H), 2.64 (q, *J* = 7.5 Hz, 2H), 1.24 (t, *J* = 7.5 Hz, 3H); ¹³C NMR (CDCl₃, 125 MHz): δ 166.5, 160.6, 153.5, 142.9, 133.5, 133.4, 132.2, 126.3, 125.2, 125.1, 122.3, 120.5, 119.8, 36.7, 28.0, 15.2; HR-ESI-MS: *m/z* calcd for C₁₆H₁₆NO₂: 254.1181 [M + H]⁺; found: 254.1175.

2-bromo-7-ethyl-10-methyldibenzo[*b,f*][1,4]oxazepin-11(10H)-one (**4l**)

Orange solid, yield: 22 mg, 36%; ¹H NMR (CDCl₃, 500 MHz): δ 7.98 (d, *J* = 2.5 Hz, 1H), 7.53 (dd, *J* = 8.5, 2.5 Hz, 1H), 7.13 (d, *J* = 8 Hz, 1H), 7.07 (d, *J* = 9 Hz, 1H), 7.06 (m, 1H), 7.03 (dd, *J* = 8, 1.5 Hz, 1H), 3.55 (s, 3H), 2.61 (q, *J* = 7.5 Hz, 2H), 1.22 (t, *J* = 7.5 Hz, 3H); ¹³C NMR (CDCl₃, 125 MHz): δ 165.1, 159.6, 153.2, 143.2, 136.1, 134.8, 133.0, 128.1, 125.4, 122.4, 121.7, 120.4, 117.9, 36.8, 28.0, 15.2; HR-ESI-MS: *m/z* calcd for C₁₆H₁₄BrNNaO₂: 354.0106 [M + Na]⁺; found: 354.0112.

7-ethyl-10-methyl-2-nitrodibenzo[*b,f*][1,4]oxazepin-11(10H)-one (**4u**)

Yellow solid, yield: 12 mg, 60%; ¹H NMR (CDCl₃, 500 MHz): δ 8.79 (d, *J* = 3 Hz, 1H), 8.32 (dd, *J* = 9, 3 Hz, 1H), 7.36 (d, *J* = 8.5 Hz, 1H), 7.19 (d, *J* = 8 Hz, 1H), 7.12 (d, *J* = 2 Hz, 1H), 7.11 (dd, *J* = 8, 2 Hz, 1H), 3.61 (s, 3H), 2.66 (q, *J* = 7.5 Hz, 2H), 1.25 (t, *J* = 7.5 Hz, 3H); ¹³C NMR (CDCl₃, 125 MHz): δ 164.7, 164.2, 152.4, 144.9, 143.6, 132.5, 128.6, 128.2, 127.5, 126.0, 122.6, 121.2, 120.6, 36.8, 27.9, 15.1; HR-ESI-MS: *m/z* calcd for C₁₆H₁₅N₂O₄: 299.1032 [M + H]⁺; found: 299.1036.

2-bromo-7-isopropyl-10-methyldibenzo[*b,f*][1,4]oxazepin-11(10H)-one (**4am**)

Orange solid, yield: 29 mg, 50%; ¹H NMR (CDCl₃, 500 MHz): δ 8.00 (d, *J* = 3 Hz, 1H), 7.55 (dd, *J* = 8.5, 2.5 Hz, 1H), 7.16 (d, *J* = 8.5 Hz, 1H), 7.11 (d, *J* = 7 Hz, 1H), 7.10 (s, 1H), 7.08 (dd, *J* = 8, 2.5 Hz, 1H), 3.57 (s, 3H), 2.90 (sept, *J* = 7 Hz, 1H), 1.25 (d, *J* = 7 Hz, 6H); ¹³C NMR (CDCl₃, 125 MHz): δ 165.0, 159.6, 153.2, 147.9, 136.1, 134.8, 133.0, 128.1, 124.0, 122.4, 121.7, 119.0, 117.9, 36.8, 33.4, 23.7; HR-ESI-MS: *m/z* calcd for C₁₇H₁₇BrNO₂: 346.0443 [M + H]⁺; found: 346.0447.

7-isopropyl-10-methyl-2-nitrodibenzo[*b,f*][1,4]oxazepin-11(10H)-one (**4an**)

Yellow solid, yield: 60 mg, 59%; ¹H NMR (CDCl₃, 500 MHz): δ 8.78 (d, *J* = 2.5 Hz, 1H), 8.31 (dd, *J* = 9, 3 Hz, 1H), 7.34 (d, *J* = 9 Hz, 1H), 7.18 (d, *J* = 9 Hz, 1H), 7.11 (m, 2H), 3.58 (s, 3H), 2.89 (sept, *J* = 7 Hz, 1H), 1.23 (d, *J* = 7, 6H); ¹³C NMR (CDCl₃, 125 MHz): δ 164.7, 164.2, 152.4, 148.3, 144.9, 132.5, 128.6, 128.2, 127.5, 124.7, 122.6, 121.3, 119.1, 36.9, 33.5, 23.7; HR-ESI-MS: *m/z* calcd for C₁₇H₁₇N₂O₄: 313.1188 [M + H]⁺; found: 313.1178.

Figure 3.5D. ^1H and ^{13}C -NMR of **23**

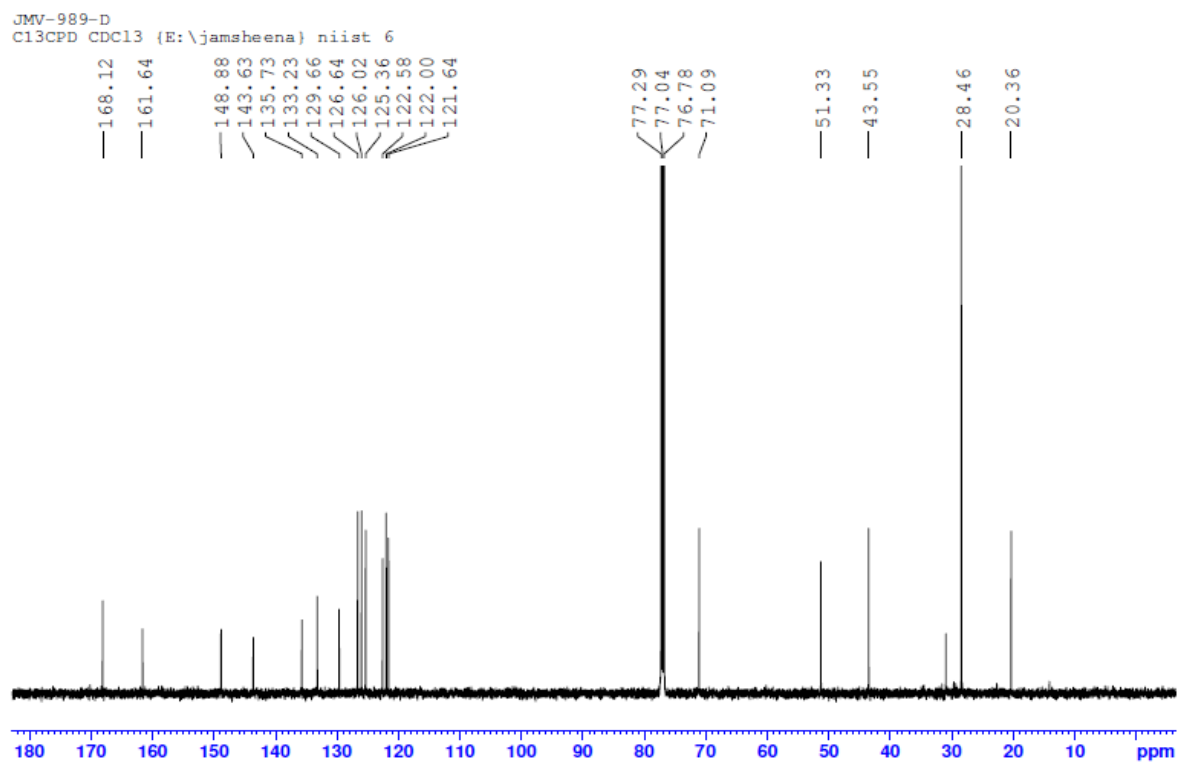
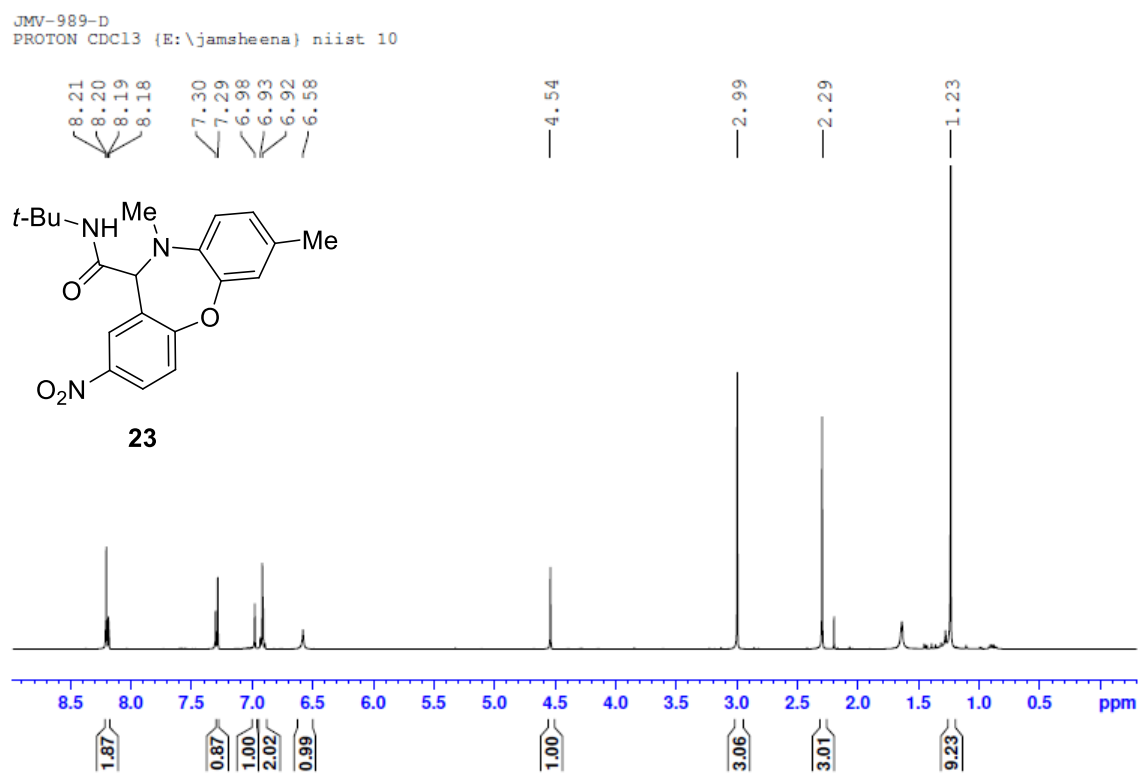


Figure 3.5E. ¹H and ¹³C-NMR of 24

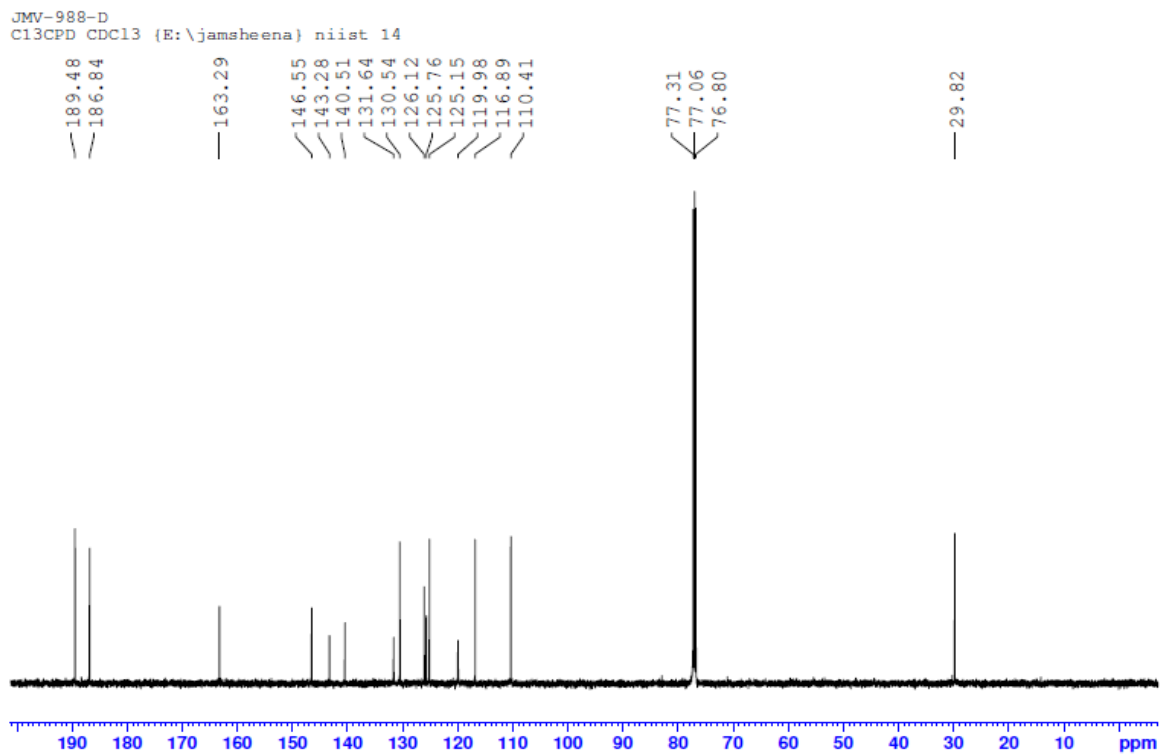
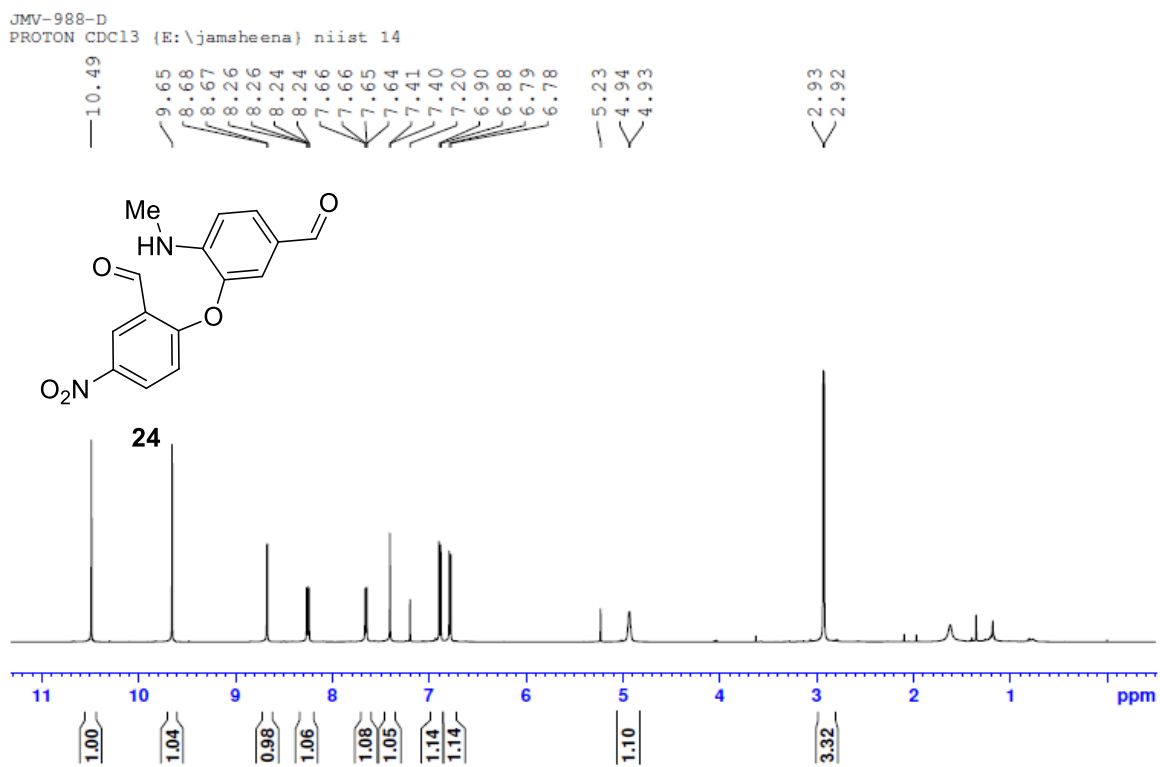
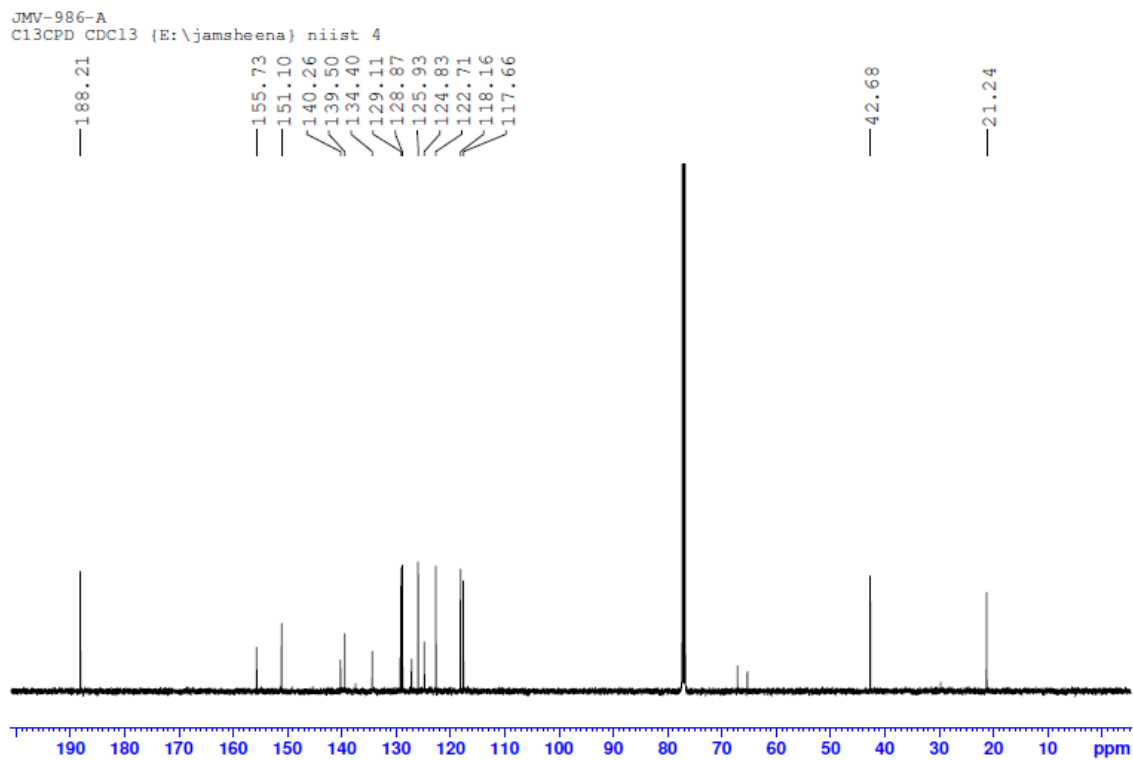
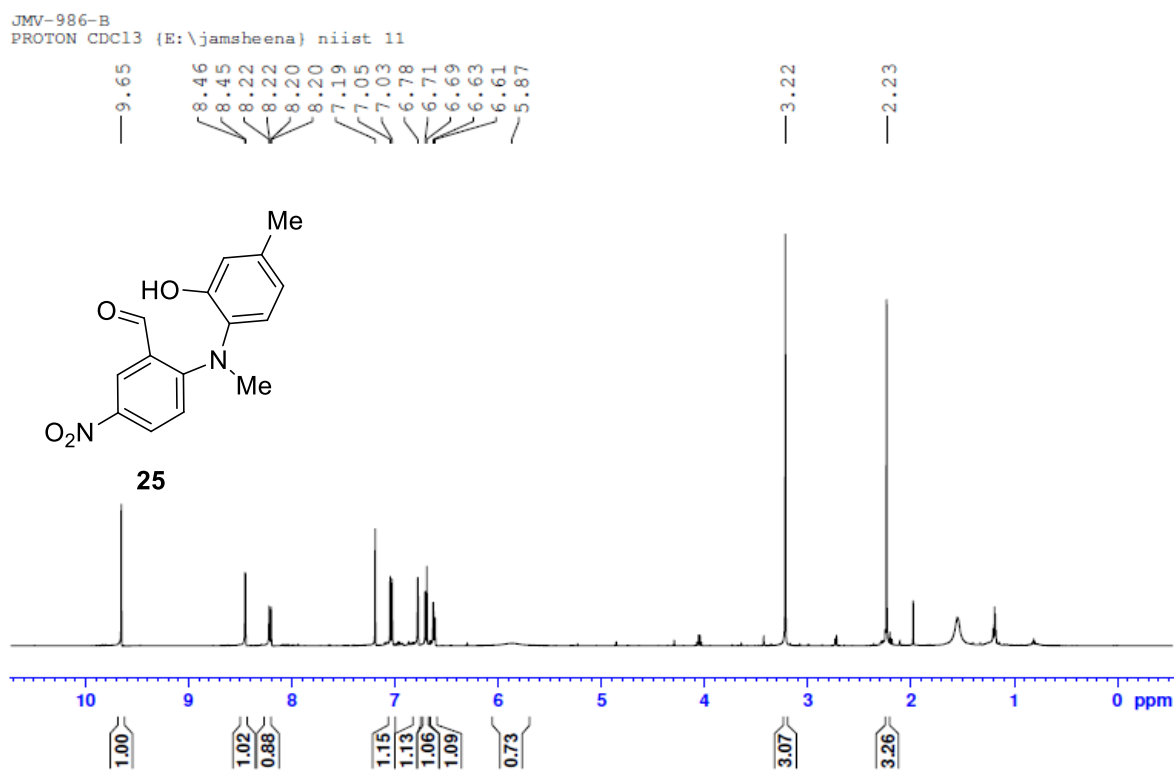


Figure 3.5F. ^1H and ^{13}C -NMR of **25**



N-(tert-butyl)-7,10-dimethyl-2-nitro-10,11-dihydrodibenzo[*b,f*][1,4]oxazepine-11-carboxamide (**23**)

Yellow solid, yield: 18 mg, 56%; ¹H NMR (CDCl₃, 500 MHz): δ 8.19 (m, 2H), 7.28 (s, 1H), 6.97 (s, 1H), 6.91 (m, 2H), 6.58 (bs, 1H), 4.53 (s, 1H), 2.99 (s, 3H), 2.29 (s, 3H), 1.23 (s, 9H); ¹³C NMR (CDCl₃, 125 MHz): δ 168.1, 161.6, 148.8, 143.6, 135.7, 133.2, 129.6, 126.6, 126.0, 125.3, 122.5, 122.0, 121.6, 71.0, 51.3, 43.5, 28.4, 20.3; HR-ESI-MS: *m/z* calcd for C₂₀H₂₃N₃NaO₄: 392.1586 [M + Na]⁺; found: 392.1571.

2-(5-formyl-2-(methylamino)phenoxy)-5-nitrobenzaldehyde (**24**)

Yellow solid, yield: 17 mg, 65%; ¹H NMR (CDCl₃, 500 MHz): δ 10.48 (s, 1H), 9.65 (s, 1H), 8.67 (d, *J* = 3 Hz, 1H), 8.25 (dd, *J* = 9, 2.5 Hz, 1H), 7.64 (dd, *J* = 8.5, 1.5 Hz, 1H), 7.40 (d, *J* = 1.5 Hz, 1H), 6.88 (d, *J* = 9 Hz, 1H), 6.78 (d, *J* = 8.5 Hz, 1H), 4.93 (q, *J* = 5 Hz, 1H), 2.93 (d, *J* = 5.5 Hz, 3H); ¹³C NMR (CDCl₃, 125 MHz): δ 189.4, 186.8, 163.2, 146.5, 143.2, 140.5, 131.6, 130.5, 126.1, 125.7, 125.1, 119.9, 116.8, 110.4, 29.8; HR-ESI-MS: *m/z* calcd for C₁₅H₁₂N₂NaO₅: 323.0644 [M + Na]⁺; found: 323.0631 minor peak, and *m/z* calcd for C₁₆H₁₆N₂NaO₆: 355.0906 [M + MeOH + Na]⁺; found: 355.0892 base peak.

2-((2-hydroxy-4-methylphenyl)(methyl)amino)-5-nitrobenzaldehyde (**25**)

Yellow solid, yield: 21 mg, 85%; ¹H NMR (CDCl₃, 500 MHz): δ 9.65 (s, 1H), 8.45 (d, *J* = 3 Hz, 1H), 8.21 (dd, *J* = 9, 2.5 Hz, 1H), 7.03 (d, *J* = 9 Hz, 1H), 6.77 (s, 1H), 6.70 (d, *J* = 8 Hz, 1H), 6.62 (d, *J* = 8 Hz, 1H), 5.87 (bs, 1H), 3.21 (s, 3H), 2.23 (s, 3H); ¹³C NMR (CDCl₃, 125 MHz): δ 188.2, 155.7, 151.1, 140.2, 139.5, 134.4, 129.1, 128.8, 125.9, 124.8, 122.7, 118.1, 117.6, 42.6, 21.2; HR-ESI-MS: *m/z* calcd for C₁₅H₁₄N₂NaO₄: 309.0851 [M + Na]⁺; found: 309.0846.

2-(methyl(4-methyl-3,6-dioxocyclohexa-1,4-dien-1-yl)amino)-5-nitrobenzaldehyde (**26**)

Red solid, yield: 11 mg, 40%; ¹H NMR (CDCl₃, 500 MHz): δ 10.15 (s, 1H), 8.75 (d, *J* = 2.5 Hz, 1H), 8.39 (dd, *J* = 8.5, 2.5 Hz, 1H), 7.21 (d, *J* = 8.5 Hz, 1H), 6.35 (d, *J* = 1.5 Hz, 1H), 6.07 (s, 1H), 3.27 (s, 3H), 2.06 (d, *J* = 1.5 Hz, 3H); ¹³C NMR (CDCl₃, 125 MHz): δ 187.7, 186.4, 183.0, 154.6, 149.0, 147.4, 145.9, 131.8, 131.3, 129.1, 128.3, 126.7, 110.9, 43.3, 15.7; HR-ESI-MS: *m/z* calcd for C₁₆H₁₆N₂NaO₆: 355.0906 [M + MeOH + Na]⁺; found: 355.0914.

2,10-dimethyl-7-nitro-9,10-dihydroacridin-4-ol (**27**)

Yellow solid, yield: 13 mg, 55%; ^1H NMR (CDCl_3 , 500 MHz): δ 8.10 (dd, $J = 9, 2.5$ Hz, 1H), 7.98 (d, $J = 2.5$ Hz, 1H), 6.92 (d, $J = 9$ Hz, 1H), 6.58 (s, 1H), 6.48 (s, 1H), 4.78 (bs, 1H), 3.85 (s, 2H), 3.66 (s, 3H), 2.24 (s, 3H); ^{13}C NMR (CDCl_3 , 125 MHz): δ 151.8, 144.9, 140.7, 133.7, 128.4, 127.2, 125.5, 123.6, 123.2, 121.1, 116.4, 112.7, 39.6, 32.8, 20.4; HR-ESI-MS: m/z calcd for $\text{C}_{15}\text{H}_{14}\text{N}_2\text{NaO}_3$: 293.0902 $[\text{M} + \text{Na}]^+$; found: 293.0908.

7-ethyl-10-methyl-5-tosyl-10,11-dihydro-5H-dibenzo[*b,e*][1,4]diazepine (**29**)

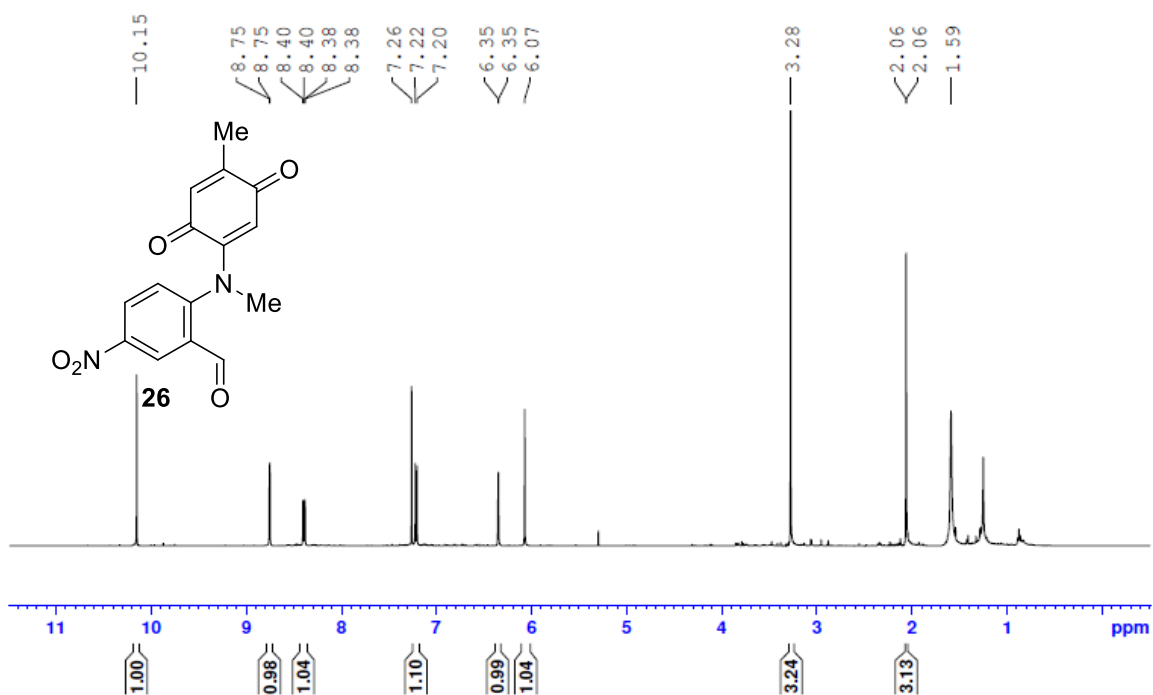
Pale yellow liquid, yield: 15 mg, 30%; ^1H NMR (CDCl_3 , 500 MHz): δ 7.64 (dd, $J = 8, 1$ Hz, 1H), 7.43 (d, $J = 8$ Hz, 2H), 7.30 (d, $J = 2$ Hz, 1H), 7.28 (td, $J = 7.5, 1.5$ Hz, 1H), 7.22 (td, $J = 7.5, 1.5$ Hz, 1H), 7.17 (d, $J = 7.5$ Hz, 2H), 7.04 (dd, $J = 8.5, 2$ Hz, 1H), 7.00 (dd, $J = 7.5, 1$ Hz, 1H), 6.71 (d, $J = 8.5$ Hz, 1H), 3.98 (d, $J = 15.5$ Hz, 1H), 3.57 (d, $J = 15.5$ Hz, 1H), 2.57 (q, $J = 7.5$ Hz, 2H), 2.44 (s, 3H), 2.38 (s, 3H), 1.20 (t, $J = 7.5$ Hz, 3H); ^{13}C NMR (CDCl_3 , 125 MHz): δ 144.5, 142.8, 138.5, 137.8, 136.8, 134.3, 131.4, 130.6, 130.5, 128.9, 128.8, 128.3, 127.9, 127.8, 127.7, 118.5, 57.1, 42.2, 27.7, 21.5, 15.3; HR-ESI-MS: m/z calcd for $\text{C}_{23}\text{H}_{25}\text{N}_2\text{O}_2\text{S}$: 393.1637 $[\text{M} + \text{H}]^+$; found: 393.1622.

2-methoxy-5-nitrobenzaldehyde (**22**)

Yellow solid, yield: 11 mg, 48%; ^1H NMR (CDCl_3 , 500 MHz): δ 10.45 (s, 1H), 8.71 (d, $J = 3$ Hz, 1H), 8.45 (dd, $J = 9, 3$ Hz, 1H), 7.12 (d, $J = 9$ Hz, 1H), 4.07 (s, 3H); ^{13}C NMR (CDCl_3 , 125 MHz): δ 187.4, 165.5, 141.7, 130.6, 124.7, 112.2, 56.7.²²

Figure 3.5G. ^1H and ^{13}C -NMR of 26

JMV-1016-A
PROTON CDC13 (E:\jamsheena) niist 5



JMV-1016-A
C13CPD CDC13 (E:\jamsheena) niist 5

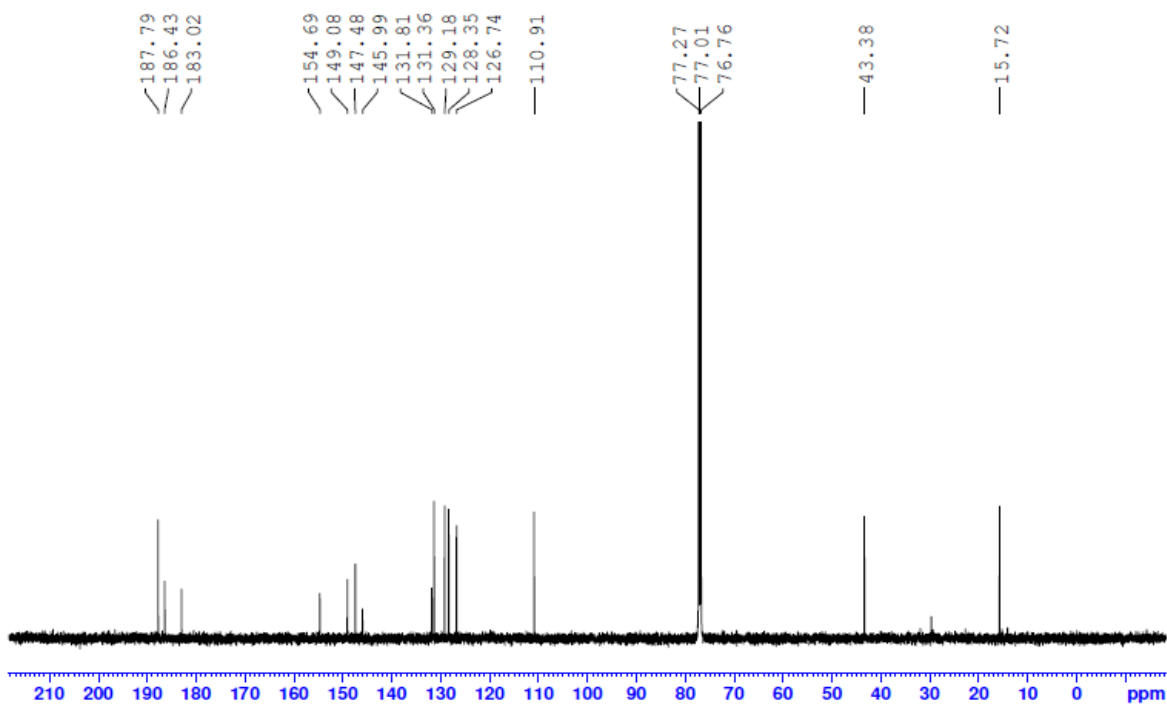


Figure 3.5H. ^1H and ^{13}C -NMR of **27**

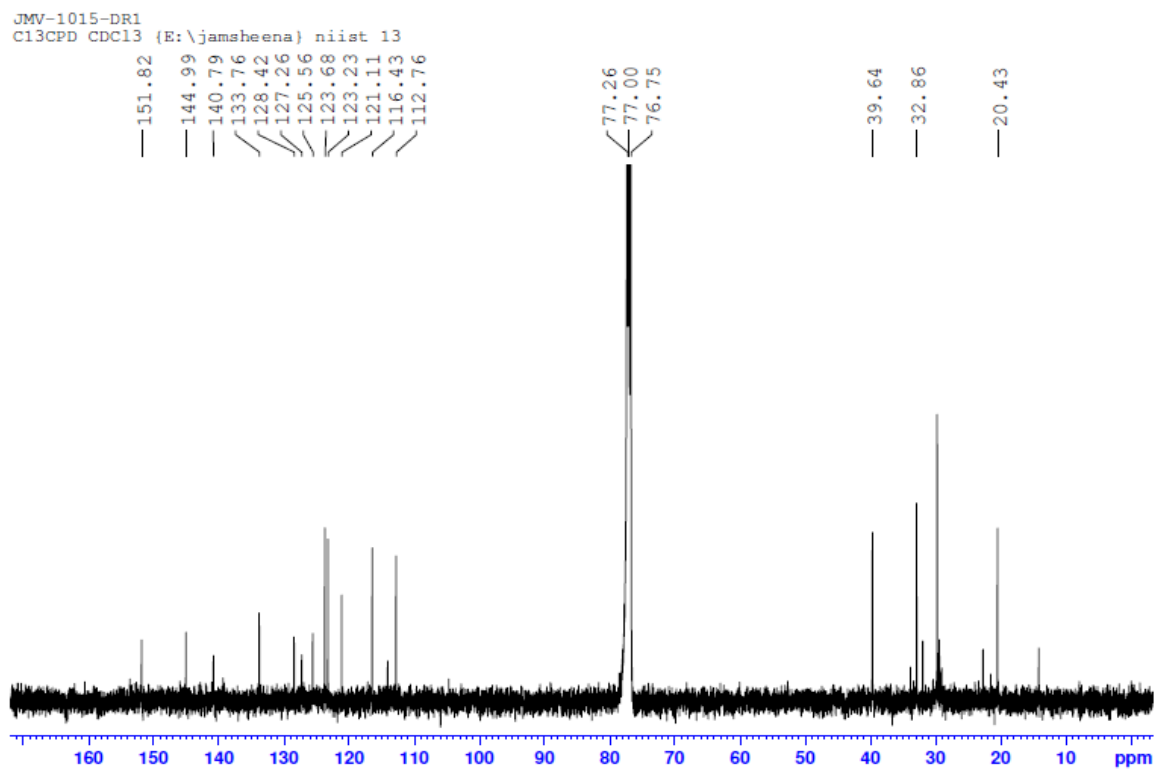
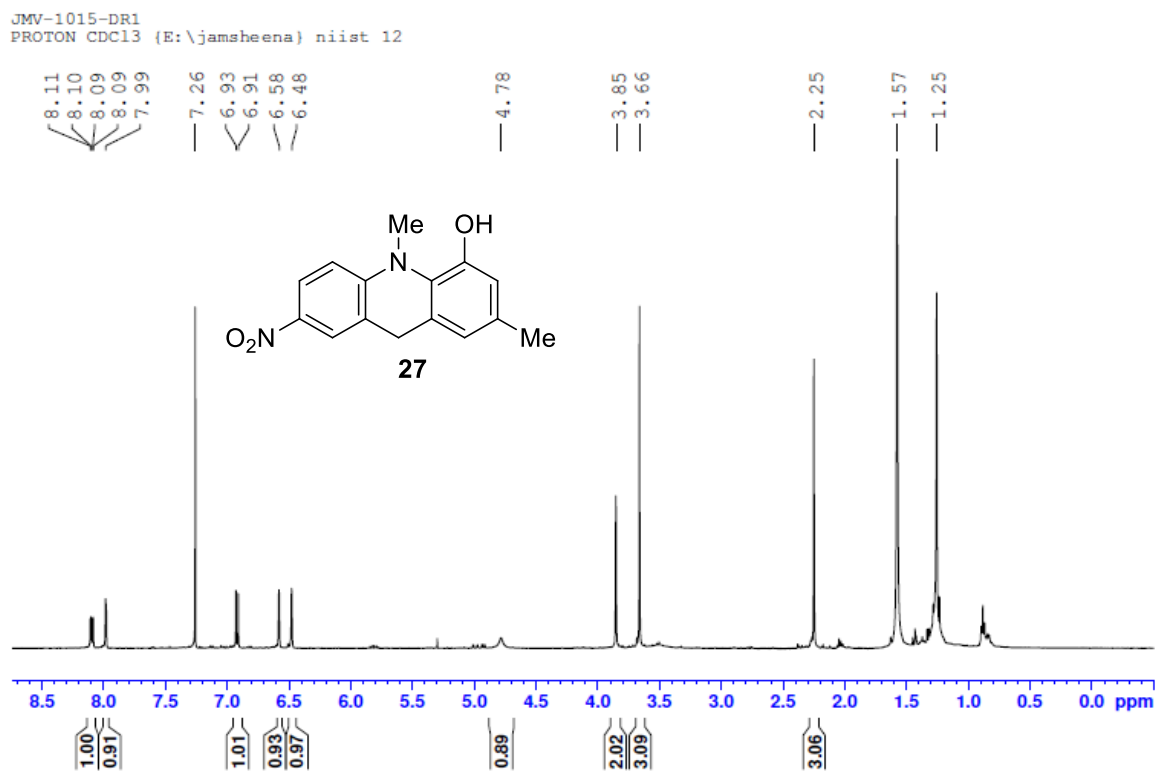
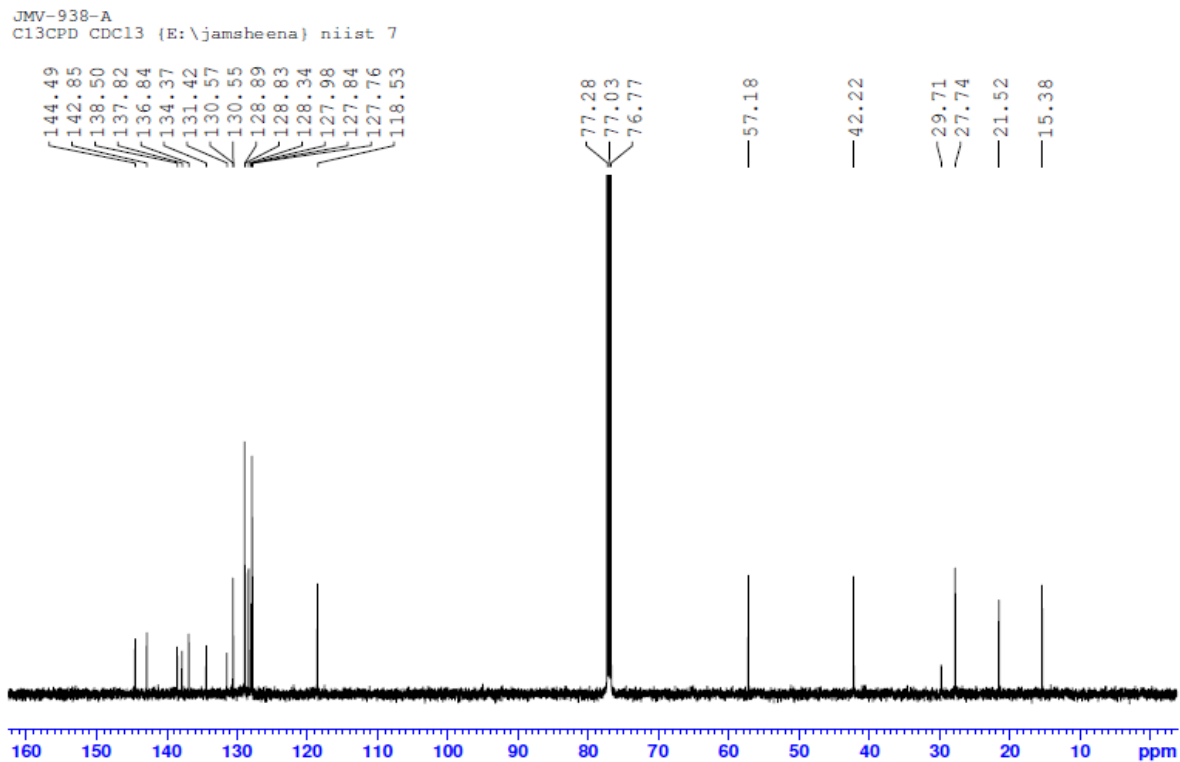
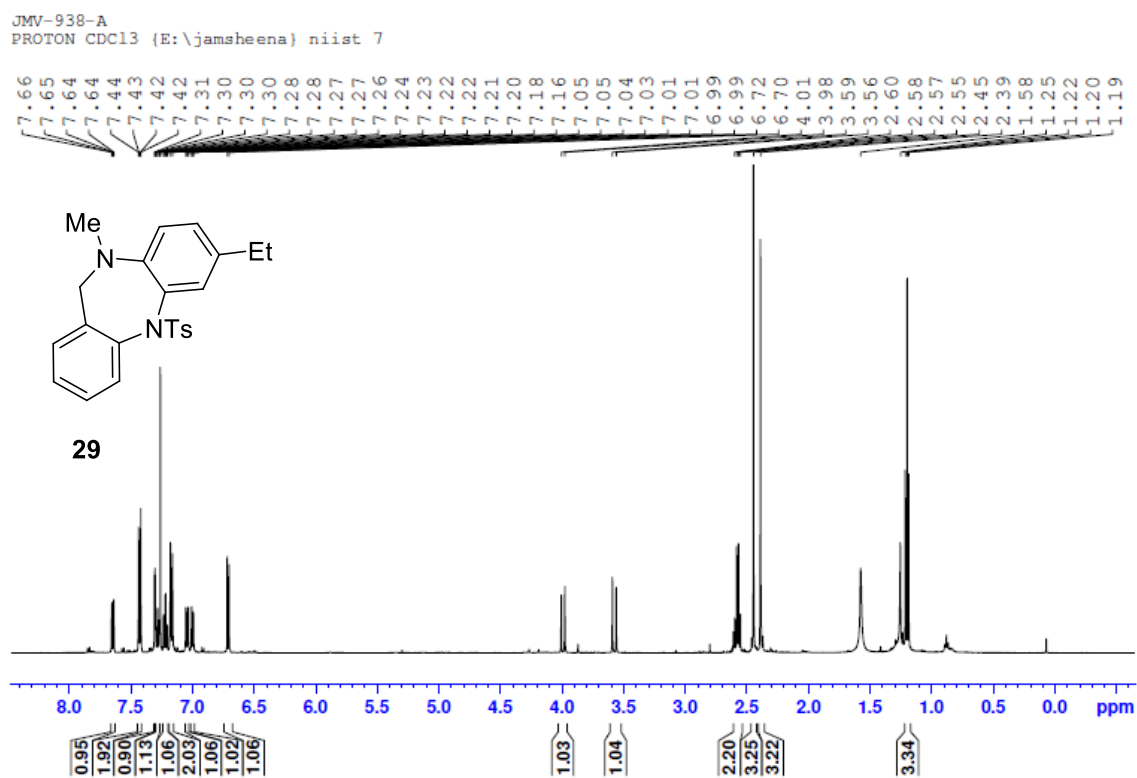


Figure 3.5I. ^1H and ^{13}C -NMR of **29**



3.6. References

- (1) (a) Klunder, J. M.; Hargrave, J. K. D.; West, M.; Cullen, E.; Mark, P.; Kapadia, S. R.; Mcneil, D. W.; Wu, J. C.; Chow, G. C.; Adamst, J. Novel non-nucleoside inhibitors of HIV-1 reverse transcriptase. 2. Tricyclic pyridobenzoxazepinones and dibenzoxazepinones. *J. Med. Chem.* **1992**, *35*, 1887–1897. (b) Binaschi, M.; Boldetti, A.; Gianni, M.; Maggi, C. A.; Gensini, M.; Bigioni, M.; Parlani, M.; Giolitti, A.; Fratelli, M.; Valli, C.; Terao, M.; Garattini, E. Antiproliferative and differentiating activities of a novel series of histone deacetylase inhibitors. *ACS Med. Chem. Lett.* **2010**, *1*, 411–415. (c) Fiorentino, A.; D’Abrosca, B.; Pacifico, S.; Cefarelli, G.; Uzzo, P.; Monaco, P. Natural dibenzoxazepinones from leaves of *Carex distachya*: structural elucidation and radical scavenging activity. *Bioorganic Med. Chem. Lett.* **2007**, *17*, 636–639. (d) Liu, N.; Song, F.; Shang, F.; Huang, Y. Mycemycins A-E, new dibenzoxazepinones isolated from two different streptomycetes. *Mar. Drugs* **2015**, *13*, 6247–6258. (e) Dols, P. P. M. A.; Folmer, B. J. B.; Hamersma, H.; Kuil, C. W.; Lucas, H.; Ollero, L.; Rewinkel, J. B. M.; Hermkens, P. H. H. SAR study of 2,3,4,14b-tetrahydro-1*H*-dibenzo[*b,f*]pyrido[1,2-*d*][1,4]oxazepines as progesterone receptor agonists. *Bioorg. Med. Chem. Lett.* **2008**, *18*, 1461–1467. (f) Gijsen, H. J. M.; Berthelot, D.; Zaja, M.; Brone, B.; Geuens, I.; Mercken, M. Analogues of morphanthridine and the tear gas dibenz[*b,f*][1,4]oxazepine (CR) as extremely potent activators of the human transient receptor potential ankyrin 1 (TRPA1) Channel. *J. Med. Chem.* **2010**, *53*, 7011–7020. (g) Lynch, S. M.; Tafesse, L.; Carlin, K.; Ghatak, P.; Kyle, D. J. Dibenzazepines and dibenzoxazepines as sodium channel blockers. *Bioorganic Med. Chem. Lett.* **2015**, *25*, 43–47. (h) Nagarajan, K.; David, J.; Kulkarni, Y. S.; Hendi, S. B.; Shenoy, S. J.; Upadhyaya, P. Piperazinylbenzonaphthoxazepines with CNS depressant properties. *Eur. J. Med. Chem.* **1986**, No. 21, 21–26. (i) Smits, R. A.; Lim, H. D.; Stegink, B.; Bakker, R. A.; de Esch, I. J. P.; Leurs, R. Characterization of the histamine H₄ receptor binding site. Part 1. Synthesis and pharmacological evaluation of dibenzodiazepine derivatives. *J. Med. Chem.* **2006**, *49*, 4512–4516. (j) Hallinan, E. A.; Hagen, T. J.; Tsymbalov, S.; Husa, R. K.; Lee, A. C.; Stapelfeld, A.; Savage, M. A. Aminoacetyl moiety as a potential surrogate for diacylhydrazine group of SC-51089, a potent PGE₂ antagonist, and its analogs. *J. Med. Chem.* **1996**, *39*, 609–613.

- (2) (a) Sapegin, A.; Reutskaya, E.; Smirnov, A.; Korsakov, M.; Krasavin, M. Facile entry into structurally diverse , privileged , (hetero) arene-fused *N*-alkoxy 3,4-dihydrobenzo[*f*][1,4]oxazepin-5(2*H*)-ones. *Tetrahedron Lett.* **2016**, *57*, 5877–5880. (b) Hurst, T.; Kitching, M.; da Frota, L.; Guimarães, K.; Dalziel, M.; Snieckus, V. Metal-free synthesis of dibenzoxazepinones *via* a one-pot *S_NAr* and Smiles rearrangement process: orthogonality with copper-catalyzed cyclizations. *Synlett* **2015**, *26*, 1455–1460. (c) Liu, S.; Hu, Y.; Qian, P.; Hu, Y.; Ao, G.; Chen, S.; Zhang, S.; Zhang, Y. An efficient cascade approach to dibenzoxazepinones *via* nucleophilic aromatic substitution and Smiles rearrangement. *Tetrahedron Lett.* **2015**, *56*, 2211–2213. (d) Liu, Y.; Chu, C.; Huang, A.; Zhan, C.; Ma, Y.; Ma, C. Regioselective synthesis of fused oxazepinone scaffolds through one-pot Smiles rearrangement tandem reaction. *ACS Comb. Sci.* **2011**, *13*, 547–553.
- (3) Feng, J.; Wu, X. Base-promoted synthesis of dibenzoxazepinamines and quinazolinimines under metal-free conditions. *Green Chem.* **2015**, *17*, 4522–4526.
- (4) (a) Shi, J.; Wu, J.; Cui, C.; Dai, W. Microwave-assisted intramolecular Ullmann diaryl etherification as the post-Ugi annulation for generation of dibenz[*b,f*][1,4]oxazepine scaffold. *J. Org. Chem.* **2016**, *81*, 10392–10403. (b) Xing, X.; Wu, J.; Luo, J.; Dai, W.-M. C-N bond-linked conjugates of dibenz[*b,f*][1,4]oxazepines with 2-oxindole. *Synlett* **2006**, *2006*, 2099–2103.
- (5) (a) Bunce, R. A.; Schammerhorn, J. E. Dibenzo-fused seven-membered nitrogen heterocycles by a tandem reduction-lactamization reaction. *J. Heterocycl. Chem.* **2006**, *43*, 1031–1035. (b) Tselikhovsky, D.; Buchwald, S. L. Concise palladium-catalyzed synthesis of dibenzodiazepines and structural analogues. *J. Am. Chem. Soc.* **2011**, *133*, 14228–14231. (c) Yang, Q.; Cao, H.; Robertson, A.; Alper, H. Synthesis of dibenzo[*b,f*][1,4]oxazepin-11(10*H*)-ones *via* intramolecular cyclocarbonylation reactions using PdI₂/Cytop 292 as the catalytic system. *J. Org. Chem.* **2010**, *75*, 6297–6299. (d) Zhou, Y.; Zhu, J.; Li, B.; Zhang, Y.; Feng, J.; Hall, A.; Shi, J.; Zhu, W. Access to different isomeric dibenzoxazepinones through copper-catalyzed C–H etherification and C–N bond construction with controllable Smiles rearrangement. *Org. Lett.* **2016**, *18*, 380–383. (e) Kitching, M. O.; Hurst, T. E.; Snieckus, V. Copper-catalyzed cross-coupling interrupted by an opportunistic Smiles Rearrangement: an efficient domino approach to dibenzoxazepinones.

Angew. Chemie Int. Ed. **2012**, *51*, 2925–2929.

- (6) Prabakaran, K.; Zeller, M.; Rajendra Prasad, K. Palladium-mediated intramolecular C-O and C-C coupling reactions: an efficient synthesis of benzannulated oxazepino- and pyranocarbazoles. *Synlett* **2011**, *2011*, 1835–1840. (b) Mestichelli, P.; Scott, M. J.; Galloway, W. R. J. D.; Selwyn, J.; Parker, J. S.; Spring, D. R. Concise copper-catalyzed synthesis of tricyclic biaryl ether-linked aza-heterocyclic ring systems. *Org. Lett.* **2013**, *15*, 5448–5451. (c) Shen, C.; Neumann, H.; Wu, X.-F. A highly-efficient palladium-catalyzed aminocarbonylation/S_NAr approach to dibenzoxazepinones. *Green Chem.* **2015**, *17*, 2994–2999.
- (7) (a) Zhang, J. Q.; Qi, Z. H.; Yin, S. J.; Li, H. Y.; Wang, Y.; Wang, X. W. Brønsted or lewis acid initiated multicomponent cascade reaction: diastereoselective synthesis of imidazolidinyl spirooxindole derivatives. *ChemCatChem* **2016**, *8*, 2797–2807. (b) Ren, Y.; Wang, Y.; Liu, S. Asymmetric alkynylation of seven-membered cyclic imines by combining chiral phosphoric acids and Ag(I) catalysts: synthesis of 11-substituted-10,11-dihydrodibenzo[*b,f*][1,4]oxazepine derivatives. *J. Org. Chem.* **2014**, *79*, 11759–11767. (c) Khlebnikov, A. F.; Novikov, M. S.; Petrovskii, P. P.; Konev, A. S.; Yufit, D. S.; Selivanov, S. I.; Frauendorf, H. Stereoselective cycloaddition of dibenzoxazepinium ylides to acetylenes and fullerene C₆₀. Conformational behavior of 3-aryldibenzo[*b,f*]pyrrolo[1,2-*d*][1,4]oxazepine systems. *J. Org. Chem.* **2010**, *75*, 5211–5215. (d) Khlebnikov, A. F.; Novikov, M. S.; Petrovskii, P. P.; Magull, J.; Ringe, A. Dibenzoxazepinium ylides: facile access and 1,3-dipolar cycloaddition reactions. *Org. Lett.* **2009**, *11*, 979–982.
- (8) Yoshimura, A.; Zhdankin, V. V. Advances in synthetic applications of hypervalent iodine compounds. *Chem. Rev.* **2016**, *116*, 3328–3435.
- (9) (a) Companys, S.; Pouységu, L.; Peixoto, P. A.; Chassaing, S.; Quideau, S. *Ortho*-quinol acetate chemistry: reactivity toward aryl-based nucleophiles and applications to the synthesis of natural products. *J. Org. Chem.* **2017**, *82*, 3990–3995. (b) Roche, S. P.; Porco, J. A. Dearomatization strategies in the synthesis of complex natural products. *Angew. Chemie Int. Ed.* **2011**, *50*, 4068–4093.
- (10) (a) Zhang, N.; Cheng, R.; Zhang-Negrerie, D.; Du, Y.; Zhao, K. Hypervalent

- iodine-mediated oxygenation of *N,N*-diaryl tertiary amines: intramolecular functionalization of sp^3 C–H bonds adjacent to nitrogen. *J. Org. Chem.* **2014**, *79*, 10581–10587. (b) Shen, H.; Zhang, X.; Liu, Q.; Pan, J.; Hu, W.; Xiong, Y.; Zhu, X. Direct oxidative cyanation of tertiary amines promoted by *in situ* generated hypervalent iodine(III)-CN intermediate. *Tetrahedron Lett.* **2015**, *56*, 5628–5631. (c) Yang, L.; Zhang-Negrerie, D.; Zhao, K.; Du, Y. Intramolecular functionalization of benzylic methylene adjacent to the ring nitrogen atom in *N*-aryltetrahydroisoquinoline derivatives. *J. Org. Chem.* **2016**, *81*, 3372–3379. (d) Rong, H.-J.; Yao, J.-J.; Li, J.-K.; Qu, J. Molecular iodine-mediated α -C–H oxidation of pyrrolidines to N,O-acetals: synthesis of (\pm)-preussin by late-stage 2,5-difunctionalizations of pyrrolidine. *J. Org. Chem.* **2017**, *82*, 5557–5565. (e) Deb, M. L.; Pegu, C. D.; Borpatra, P. J.; Baruah, P. K. Metal-free intramolecular α - sp^3 C–H oxygenation of *tert*-amine: an efficient approach to 1,3-oxazines. *Tetrahedron Lett.* **2016**, *57*, 5479–5483. (f) Waghmode, N. A.; Kalbandhe, A. H.; Thorat, P. B.; Karade, N. N. Metal-free new synthesis of 1,3-naphthoxazines *via* intramolecular cross dehydrogenative-coupling reaction of 1-(α -aminoalkyl)-2-naphthols using hypervalent iodine(III) reagent. *Tetrahedron Lett.* **2016**, *57*, 680–683. (g) Shu, X.-Z.; Xia, X.-F.; Yang, Y.-F.; Ji, K.-G.; Liu, X.-Y.; Liang, Y.-M. Selective functionalization of sp^3 C–H bonds adjacent to nitrogen using (diacetoxyiodo)benzene (DIB). *J. Org. Chem.* **2009**, *74*, 7464–7469.
- (11) Guo, X.; Zhang-Negrerie, D.; Du, Y. Iodine(III)-mediated construction of the dibenzoxazepinone skeleton from 2-(aryloxy)benzamides through oxidative C–N formation. *RSC Adv.* **2015**, *5*, 94732–94736.
- (12) Shang, S.; Zhang-Negrerie, D.; Du, Y.; Zhao, K. Intramolecular metal-free oxidative aryl-aryl coupling: an unusual hypervalent-iodine-mediated rearrangement of 2-substituted *N*-phenylbenzamides. *Angew. Chemie Int. Ed.* **2014**, *53*, 6216–6219.
- (13) (a) Pitsinos, E. N.; Vidali, V. P.; Couladouros, E. A. Diaryl ether formation in the synthesis of natural products. *Eur. J. Org. Chem.* **2011**, *2011*, 1207–1222. (b) Bedos-Belval, F.; Rouch, A.; Vanucci-Bacqué, C.; Baltas, M. Diaryl ether derivatives as anticancer agents – a review. *Medchemcomm* **2012**, *3*, 1356.
- (14) (a) Sawyer, J. S. Recent advances in diaryl ether synthesis. *Tetrahedron* **2000**, *56*,

- 5045–5065. (b) Frlan, R.; Kikelj, D. Recent progress in diaryl ether synthesis. *Synthesis* **2006**, *2006*, 2271–2285.
- (15) (a) Mann, G.; Hartwig, J. F. Nickel- vs palladium-catalyzed synthesis of protected phenols from aryl halides. *J. Org. Chem.* **1997**, *62*, 5413–5418. (b) Marcoux, J.-F.; Doye, S.; Buchwald, S. L. A general copper-catalyzed synthesis of diaryl ethers. *J. Am. Chem. Soc.* **1997**, *119*, 10539–10540. (c) Chan, D. M. T.; Monaco, K. L.; Wang, R.-P.; Winters, M. P. New *N*- and *O*-arylations with phenylboronic acids and cupric acetate. *Tetrahedron Lett.* **1998**, *39*, 2933–2936. (d) Chan, D. M. T.; Monaco, K. L.; Li, R.; Bonne, D.; Clark, C. G.; Lam, P. Y. S. Copper promoted C-N and C-O bond cross-coupling with phenyl and pyridylboronates. *Tetrahedron Lett.* **2003**, *44*, 3863–3865. (e) Takise, R.; Isshiki, R.; Muto, K.; Itami, K.; Yamaguchi, J. Decarbonylative diaryl ether synthesis by Pd and Ni catalysis. *J. Am. Chem. Soc.* **2017**, *139*, 3340–3343.
- (16) Abrams, D. J.; Provencher, P. A.; Sorensen, E. J. Recent applications of C–H functionalization in complex natural product synthesis. *Chem. Soc. Rev.* **2018**, *47*, 8925–8967.
- (17) (a) Singh, K. S. Recent advances in C–H bond functionalization with ruthenium-based catalysts. *Catalysts* **2019**, *9*, 173–223. (b) Davies, H. M. L.; Morton, D. Collective approach to advancing C-H functionalization. *ACS Cent. Sci.* **2017**, *3*, 936–943. (c) Rao, Y.; Shan, G.; Yang, X. Some recent advances in transition-metal-catalyzed *ortho* sp² C-H functionalization using Ru, Rh, and Pd. *Sci. China Chem.* **2014**, *57*, 930–944. (d) Davies, H. M. L.; Morton, D. Recent advances in C–H functionalization. *J. Org. Chem.* **2016**, *81*, 343–350.
- (18) Jalalian, N.; Petersen, T. B.; Olofsson, B. Metal-free arylation of oxygen nucleophiles with diaryliodonium salts. *Chem. - A Eur. J.* **2012**, *18*, 14140–14149.
- (19) Liu, F.; Yang, H.; Hu, X.; Jiang, G. Metal-free synthesis of *ortho* -CHO diaryl ethers by a three-component sequential coupling. *Org. Lett.* **2014**, *16*, 6408–6411.
- (20) (a) Quideau, S.; Pouységu, L.; Deffieux, D. Oxidative dearomatization of phenols: why, how and what for? *Synlett* **2008**, *2008*, 467–495. (b) Pouységu, L.; Deffieux, D.; Quideau, S. Hypervalent iodine-mediated phenol dearomatization in natural product synthesis. *Tetrahedron* **2010**, *66*, 2235–2261. (c) Reddy, C. R.; Prajapati, S.

- K.; Warudikar, K.; Ranjan, R.; Rao, B. B. *Ips*o-cyclization: an emerging tool for multifunctional spirocyclohexadienones. *Org. Biomol. Chem.* **2017**, *15*, 3130–3151. (d) Pelter, A. & Ward, R. S. Two-electron phenolic oxidations using phenyliodonium dicarboxylates. *Tetrahedron* **57**, 273–282 (2001).
- (21) Evans, B. E.; Rittle, K. E.; Bock, M. G.; DiPardo, R. M.; Freidinger, R. M.; Whitter, W. L.; Lundell, G. F.; Veber, D. F.; Anderson, P. S.; Chang, R. S. L.; Lotti, V. J.; Cerino, D. J.; Chen, T. B.; Kling, P. J.; Kunkel, K. A.; Springer, J. P.; Hirshfield, J. Methods for drug discovery: development of potent, selective, orally effective cholecystokinin antagonists. *J. Med. Chem.* **1988**, *31*, 2235–2246.
- (22) Jyothish, K.; Zhang, W. Introducing a podand motif to alkyne metathesis catalyst design: a highly active multidentate molybdenum (VI) catalyst that resists alkyne polymerization. *Angew. Chemie - Int. Ed.* **2011**, *50*, 3435–3438.

Chapter-4

Design, Synthesis and Cytotoxicity Evaluation of Diindolylmethane Conjugates of Biaryls and Diaryl ethers

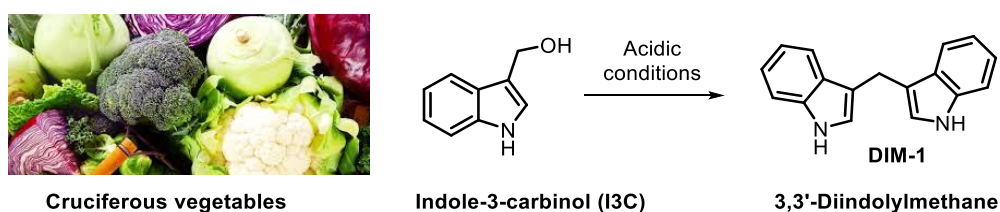
4.1. Abstract

This chapter deals with design and synthesis of diindolylmethane (DIM) derivatives conjugated with biaryls and diaryl ethers and their cytotoxicity evaluation both in human cervical (HeLa), breast (MDA-MB-231) cancer cell lines and compared against normal rat cardiac myoblasts (H9C2) cells or rat skeletal myoblast cells (L6). The first library of compounds DIM-*ortho*-biaryls **2a-2l** had variations in one of the phenyl units, prepared in a single step by condensation of biaryl-2-carbaldehydes with 1*H*-indole in the presence of *para*-toluenesulfonic acid. DIM-**2a** and DIM-**2d** exhibited GI₅₀ values of 11.00±0.707 μM and 8.33±0.416 μM, respectively in HeLa cells and were found to be nontoxic to H9C2 cells up to 20 μM. In addition, both DIM-**2a** and DIM-**2d** induced cytotoxicity in breast MDA-MB-231 cells with GI₅₀ values below 10 μM. Encouraged by the initial results, further DIM conjugates of biaryl and diaryl ethers were designed, synthesized by variation in indoles and screened their cytotoxicity in MDA-MB-231 cell line and compared against L6. Synthetic compounds with halo substitution were found to be cytotoxic against MDA-MB-231 cell lines at a micromolar range. DIM-**3aa** with a primary amine appendage possessed the highest cytotoxicity on MDA-MB-231 cell line with a GI₅₀ value of 8.27±0.233 μM. These results suggest the structure activity relationship of DIM-*ortho*-biaryls as potent therapeutic candidates for human cervical (HeLa), breast (MDA-MB-231) cancers which warrants a detailed biological studies.

4.2. Introduction

As discussed in the introductory chapter, indoles are ubiquitous heterocycles found in natural products endowed with a plethora of biological activities. ¹Bis(3'-indolyl)methane or 3, 3'- diindolylmethane **1** (DIM), a disubstituted methane with two indole units is an active metabolite of indole-3-carbinol (I3C), a glucosinolate conjugate present in various *Brassica* vegetables such as cabbage, broccoli, brussels, sprouts, *etc.* and is renowned for its potential anticancer properties. ²Many epidemiological studies have shown that a high dietary intake of cruciferous vegetables can reduce the risk of cancer attributing to the anticancer property of I3C. ³ I3C is unstable under acidic pH of the stomach and gets

converted into acid condensation products of biologically active compounds, out of which one of the most prominent by-product is the dimer **DIM-1** (Scheme 4.2.1). Hence the effects induced by I3C *in vivo* could be attributed to its condensation product **DIM-1**, which is the prime target in anticancer investigations. In 1970s, Wattenberg first described the chemo-protective abilities displayed by **DIM-1** in crucifers through many studies.⁴ The studies revealed the role of **DIM-1** in aryl hydrocarbon hydroxylase induction, carcinogen metabolism, and inhibition, and chemical neoplasia inhibition. Since then, **DIM-1** has been found to target multiple proteins and pathways for attenuation of cancer progression. The major molecular targets of **DIM-1** are shown in Figure 4.2A.⁵ **DIM-1** is a potential cancer therapeutic agent as it possesses low toxicity and cytotoxic ability to inhibit the growth of a multitude of cancer cell types *in vitro* and *in vivo*.⁶ In addition, **DIM-1** and its derivatives have myriad of activities including plant growth promotion,⁷ inhibition of *Leishmania donovani* topoisomerase I⁸ and antimicrobial activities against human pathogens.⁹



Scheme 4.2.1. Formation of **DIM-1** from I3C

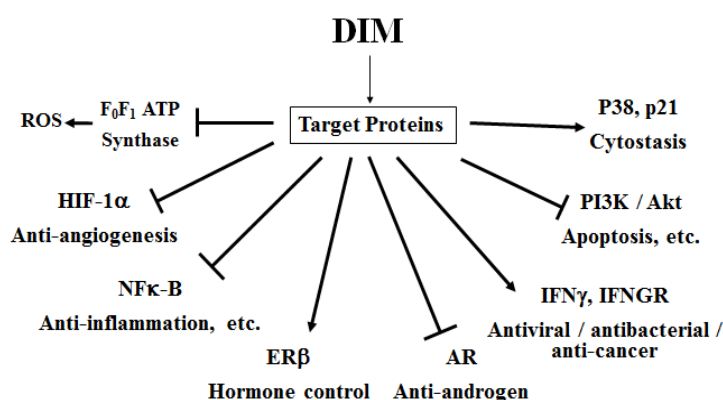


Figure 4.2A. Molecular targets of **DIM-1**

In search for more powerful anticancer agent than **DIM-1**, many derivatives of **DIM-1** have been synthesized and screened for their increased potency and pharmacological properties like specificity, bioavailability, toxicity, stability, etc.¹⁰ For instance, studies on 2,2'-diphenyl-3,3'-diindolylmethane (DPDIM) carried out by Ghosh *et al.* in 2013

revealed that it significantly induces apoptosis in carcinogen-induced Sprague-Dawley rat mammary tumour by inhibiting EGFR pathway.^{10a} Dr. Safe's lab have published many studies akin to the anticancer activity of DIM analogues. They disclose the efficiency of the 1,1-bis(3-indolyl)-1-(*p*-substitutedphenyl)methane (C-DIM) analogues as potent anticancer agents for the treatment of metastatic lung cancer. Their studies found that both DIM-C-*p*Ph-OCH₃ and DIM-C-*p*PhOH inhibit lung cancer cell and tumour growth in a metastasis model.^{10b} Another study from the same laboratory reported that 1,1-bis (3'-indolyl)-1-(*p*-biphenyl)methane (DIM-C-*p*PhC₆H₅) could be used alone or in combination with other drugs for the treatment of lung cancer.^{10c} Many novel modified analogues of **DIM-1** have been identified to exhibit improved anticancer activity than the natural counterpart.

Biaryls/biphenyls are another class of compounds prominently known for their pharmacophoric properties, present in myriad natural products of both terrestrial and marine origin. Some of the representative molecules possessing biaryl motif are highlighted in figure 4.2B.¹¹ A multi-substituted biaryl offers an opportunity to diversify its motif to various other scaffolds giving promising pharmacological properties. A study by Naik *et al.* showed that biaryl inserted noscapine analogues had a higher affinity to tubulin compared to the parent compound and that the biaryl substitution impacted their therapeutic potential towards multiple cancer types.¹² Another study by McNulty *et al.* showed that biaryl analogues of colchicine and combretastatin A4 found to exhibit anticancer activity by initiating apoptosis *via* a mechanism involving inhibition of tubulin polymerization.¹³ The immense potential displayed by biaryl pharmacophore as anticancer agents justifies the choice of using the molecule to improve the anticancer activity of **DIM-1**.

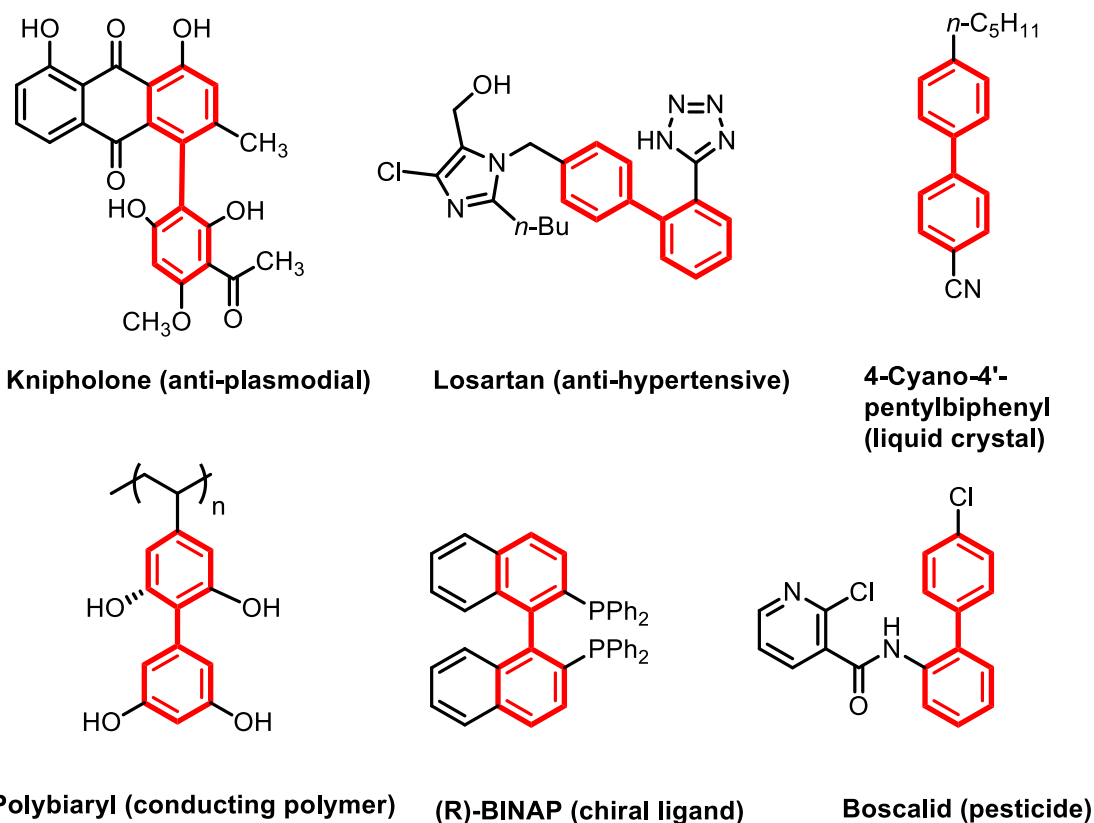


Figure 4.2B. Representative biaryl structural motifs

In this regard, we have recently reported a mild and expedient method to synthesize biaryl-2-carbaldehyde under metal-free conditions, wherein we have also demonstrated its conversion into an array of diverse molecules of which one of them was 1,1-bis(3'-indolyl)-1-(*o*-biaryl)methane (DIM-*ortho*-biaryl, Figure 4.2C).¹⁴ The biological significance of indole heterocycle and biaryl as separate entities prompted us to combine them in a single molecule to explore the bioactivity of the resulting DIM-*ortho*-biaryl motif. Studies from Dr. Safe's lab provide extensive evidence regarding the improved anticancer activity of many DIM derivatives.¹⁵ Interestingly, a considerable amount of studies were performed by Safe's group on anticancer activity of DIM-*para*-biaryl derivatives, which showed the inhibition of MCF-7 breast cancer cells, various colon cancer cells, Panc-28 pancreatic cancer cells, bladder cancer cells, renal cell carcinoma, HEC1A endometrial cancer cells and A549 lung cancer cells.^{15g,15j} Studies by Abdelrahim *et al.* 2008, Lee *et al.* 2011, and Shin *et al.* 2011, are some examples that advocate the anticancer activity of *para*-substituted derivatives of DIM.^{15g-15i} DIM-*para*-biaryl derivatives have also been shown to exhibit anti-inflammatory, antimicrobial and antioxidant effects.¹⁶ However, DIM-*meta*-biaryls and DIM-*ortho*-biaryls were not

subjected to biological screenings against *in vitro* assays. Figure 4.2C shows the basic structural skeleton of DIM-biaryl motifs. *Ortho*-substituted biaryls/biphenyls exhibit atropisomerism due to the barrier of rotation between their rings. As a result, DIM-*ortho*-biaryls with bulky substituted methane in the *ortho*-position with two 1*H*-indole units flanked on either side of the biaryl axis offer unique topological features compared to DIM-*meta*-biaryls and DIM-*para*-biaryls. The precedent set by DIM-*para*-biaryls as a new class of potential anticancer agents (*vide supra*) prompted us to explore the anticancer properties of DIM-*ortho*-biaryls for the first time owing to its interesting structural features.

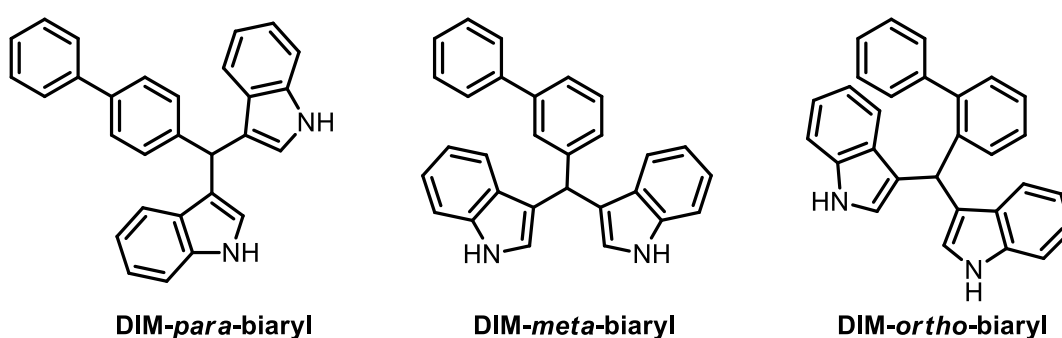


Figure 4.2C. Basic skeleton of DIM biaryl motifs

One of the main reason responsible for mortality in women across the world is cancer. But the burden of cancer is progressively articulated on the low and middle-income countries due to the increasing life expectancy and the prevalence of risk factors associated with an economic transition. According to Torre *et al.* in 2017, the three most frequently diagnosed cancers in women are breast, colorectal, and lung cancers.¹⁷ They are also responsible for the three leading causes of cancer-related death in women, globally. But in developed countries, it is breast, cervical and lung cancer that ranks the highest. As indicated by Bray *et al.* 2018 and GLOBOCAN 2018 statistics, breast cancer accounts for 25% of cancer incidence and 15% of cancer-related deaths.¹⁸ In developing countries, cervical cancer is the second most commonly diagnosed cancer and the third leading cause of cancer-associated mortality.

The current chapter deals with the study of synthetic derivatives of DIM that exhibited anticancer potential in two types of female cancers namely cervical and breast cancer.

4.3. Results and Discussion

4.3.1. Synthesis of DIM-ortho-biaryls (DIM) 2a-2l

We have synthesised a novel DIM-ortho-biaryl (DIM) **2a** owing to the unique structural feature and unprecedented structural diversity. In our previous report, we have synthesized an array of polyfunctional biaryl-2-carbaldehydes under mild conditions.¹⁴ In the present study, these carbalddehydes were utilized in the synthesis of a library of DIM-ortho-biaryls under standard conditions (Figure 4.3A).

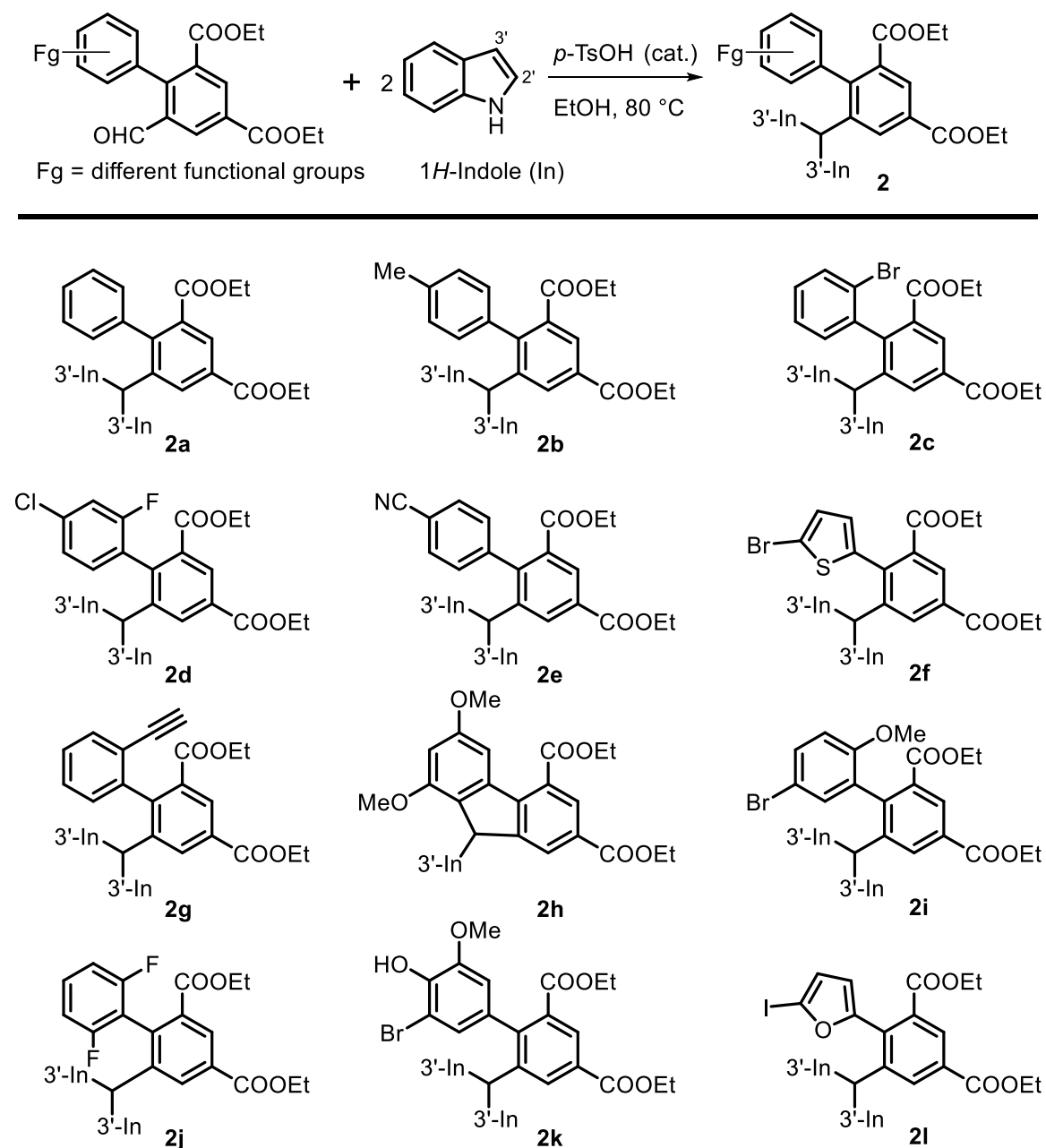


Figure 4.3A. Structures of DIM-ortho-biaryls (DIM) **2a-2l**

A series of synthetic analogues viz. DIM-**2b-2g**, **2i-2l** of compound DIM-**2a** (Figure 4.3A) were synthesized in one step by condensation of pertinent biaryl-2-carbaldehyde with two equivalents of 1*H*-indole in presence of a catalytic amount of *p*-TsOH. Variations in biaryl-2-carbaldehydes were achieved from utilizing differently substituted cinnamaldehydes in our methodology. DIM-**2h** (Figure 4.3A) with the monoindole unit was synthesised as the major product under the reaction conditions. The final products were purified by column chromatography, and structural confirmation was carried out by ¹H-, ¹³C-NMR, and HR-ESI-MS.

4.3.2. Cytotoxic effects of DIM-**2a-2l**

Initially, DIM-*ortho*-biaryls **2a-2l** were screened for cytotoxicity studies using MTT assay in HeLa (cervical), MDA-MB-231 (breast) cancer cells and H9C2 cells (Table 4.3A). Cells were exposed to varying concentrations of the DIM compounds (0, 2, 5, 10, 20 and 50 μM) for 24 h and the percentage of growth inhibition for each compound was calculated. Table 4.3A shows the GI₅₀ (concentration at which 50% of growth inhibition is achieved) values of all the 12 DIM compounds studied. The results indicated that the DIM-**2a**, **2d** and **2h** showed significant cytotoxicity towards HeLa and MDA-MB-231 cells. GI₅₀ value for DIM-**2a**, **2d** and **2h** were found to be 11.00±0.707 μM, 8.33±0.416 μM, and 1.45±0.180 μM, respectively in HeLa cells and 9.8±0.219 μM, 8.7±0.523 μM, and 8.5±0.727 μM, respectively in the MDA-MB-231 cell line. The remaining DIMs exhibited values above 20 μM. Both DIM-**2a** and **2d** were found to be non-toxic towards normal H9C2 cells, while DIM-**2h** induced toxicity at GI₅₀ value of 10.00±0.265 μM making it unfavourable for further investigations. The standard anticancer drug cisplatin, used as the positive control for HeLa cells were able to induced toxicity in both HeLa and normal cells with a GI₅₀ of 3.75±0.213 μM and 4.38±0.528 μM, respectively. Whereas, paclitaxel, the positive control was toxic towards both normal and MDA-MB-231 cells with a GI₅₀ of 24.23±0.586 nM and 34.5±0.219 nM, respectively.

Table 4.3A. Evaluation of cytotoxicity of DIM-2a-2l in HeLa, MDA-MB-231 and H9C2

Sl.No	Compounds	GI ₅₀ (μM)		
		HeLa	MDA-MB-231	H9C2
1	DIM-2a	11.00±0.707	9.8±0.219	>50
2	DIM-2b	>20	>20	>50
3	DIM-2c	>20	>20	>50
4	DIM-2d	8.33±0.416	8.7±0.523	>50
5	DIM-2e	>20	>20	>50
6	DIM-2f	>20	>20	>50
7	DIM-2g	>20	>20	>50
8	DIM-2h	1.45±0.180	8.5±0.727	10.00±0.265
9	DIM-2i	>20	>20	>50
10	DIM-2j	>20	>20	>50
11	DIM-2k	>20	>20	>50
12	DIM-2l	>20	>20	>50

Cells were treated with different concentrations of DIM-2a-2l for 24 h and the cytotoxicity was evaluated using MTT assay. Values represented are means, with standard deviations represented as ±

4.3.3. Morphological analysis by phase contrast microscopy

The cells undergoing apoptosis exhibit significant morphological changes such as cell shrinkage, membrane blebbing and formation of apoptotic bodies. Morphological changes associated with HeLa and MDA-MB-231 cell lines upon treatment with or without cisplatin/paclitaxel, DIM-2a and 2d for 24 h were observed using a phase contrast microscope attached with the camera. Control cells exhibited normal morphology with ellipsoidal (HeLa) or spindle (MDA-MB-231) and a good amount of cytoplasm within intact membrane structure while the treated cells showed significant morphological changes such as rounding up of cells and membrane breakage. Similar changes were observed with the drug cisplatin/paclitaxel also. DIM-2a and 2d treatments did not induce any noticeable morphological changes in normal H9C2 cells. The results are given in

figure 4.3B and 4.3C. The morphological alterations such as cell shrinkage, alteration in shape, membrane breakage suggested apoptosis as the cause for cytotoxicity.

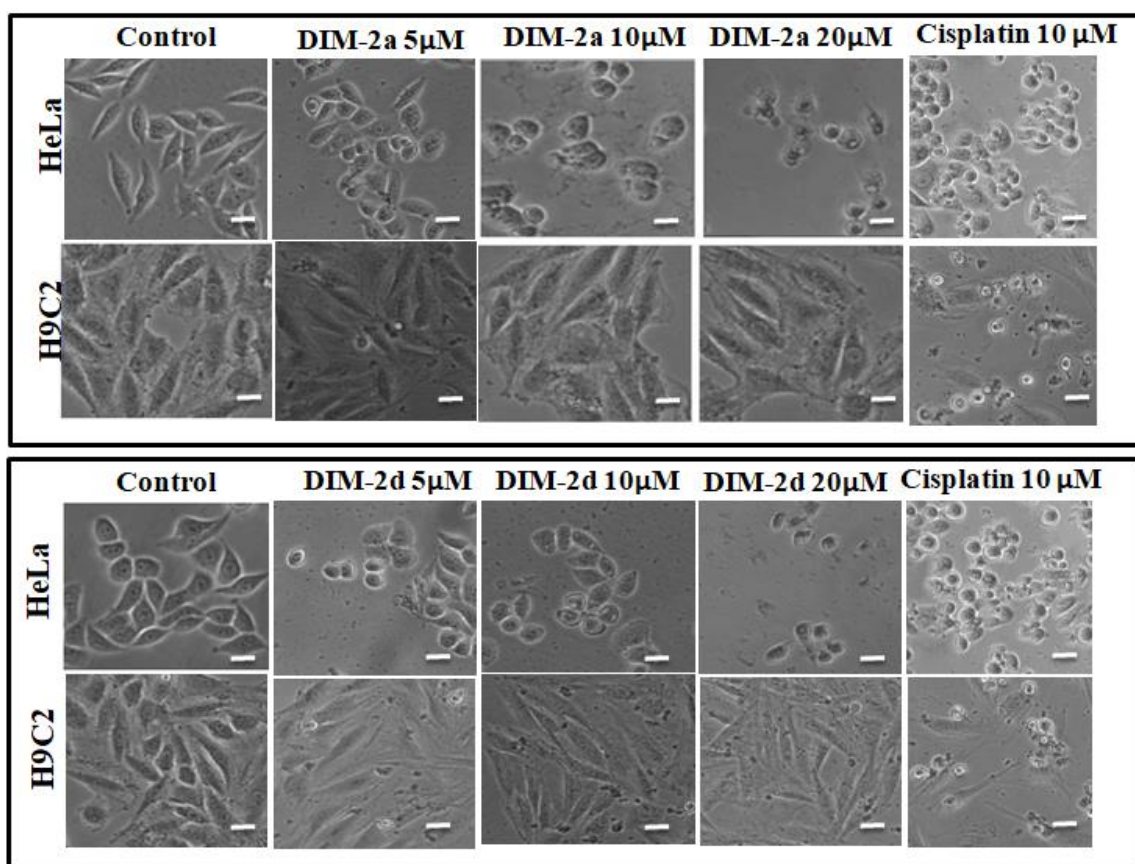


Figure 4.3B. Morphology of HeLa and H9C2 cells treated with DIM-2a and 2d

As a result, compound DIM-2a and 2d were considered as the optimal lead in the library and taken up further to check other anticancer screening parameters by Dr. Priya S. from APT division, CSIR-NIIST. Furthermore, their study on DIM-2a and 2d found that they induced caspase-dependent cellular apoptosis in a concentration-dependent manner, reduced mitochondrial membrane potential, inhibited the cell migration and downregulated the production of MMP-2 and MMP-9 in HeLa cells.

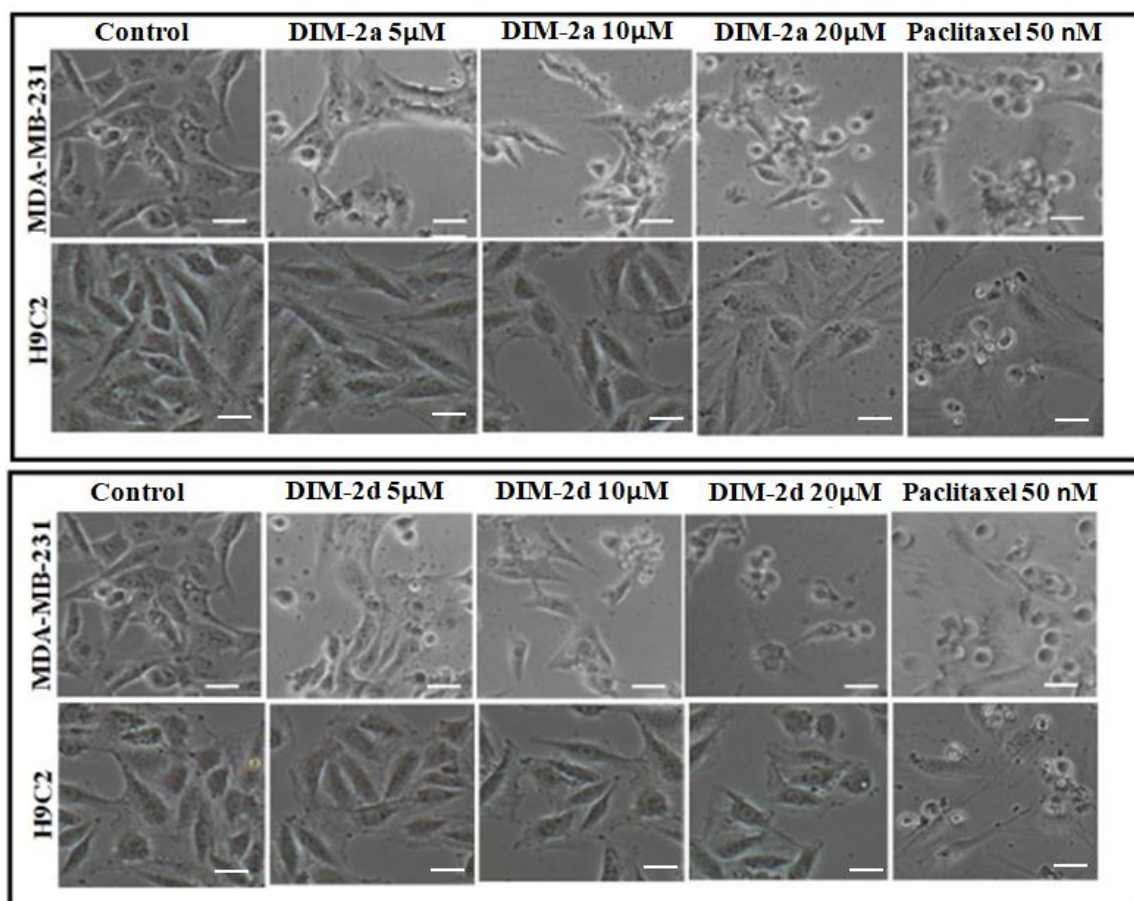


Figure 4.3C. Morphology of MDA-MB-231 and H9C2 cells treated with DIM-2a and 2d

Inspired by the attractive anticancer properties of biaryl conjugated DIMs, we have designed and synthesized a diverse series of DIMs by conjugating with biaryls **3a-3o** and diaryl ethers **4a-4p**, and explored their therapeutic effects against breast cancer cells (Figure 4.3D). Our interest was mainly focused on the identification of the substituent effect on the indole moiety and the DIM conjugates (biaryl or diary ether), to support the biological activity and whose substructure optimization would efficiently produce molecules with high antitumor activities. The incorporation of biaryl or diaryls ether, a known pharmacophore, in a single molecule may enhance the biological activity of the DIM.

Triple-negative breast cancer (TNBC) is one of the most clinically aggressive tumours that do not express the gene for estrogen, progesterone and human epidermal growth factor receptors, representing approximately 25% of breast cancers. Currently, there are no targeted therapies available for TNBC, and the available chemotherapy based treatment options exhibit poor therapeutic benefits and possess serious toxicity issues.¹⁹

The highly metastatic and poor prognosis challenges the treatment of TNBC, which necessitate the discovery of novel and safer drugs to treat this type of cancer. Recently, DIM has reported for its specific efficacy in regulating the development of breast cancer at different stages namely initiation, promotion, progression, and invasion and its derivatives display all the attributes needed for the successful attenuation of TNBC.^{2c,15d,20} Thus, we have investigated the cytotoxicity of our synthesized DIM conjugates **3a-3o** and **4a-4p** in TNBC cell line, MDA-MB-231 and compared with the activity of **DIM-1**.

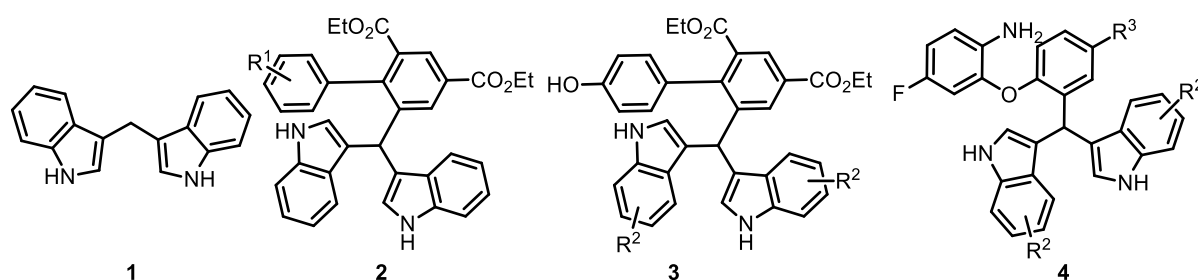
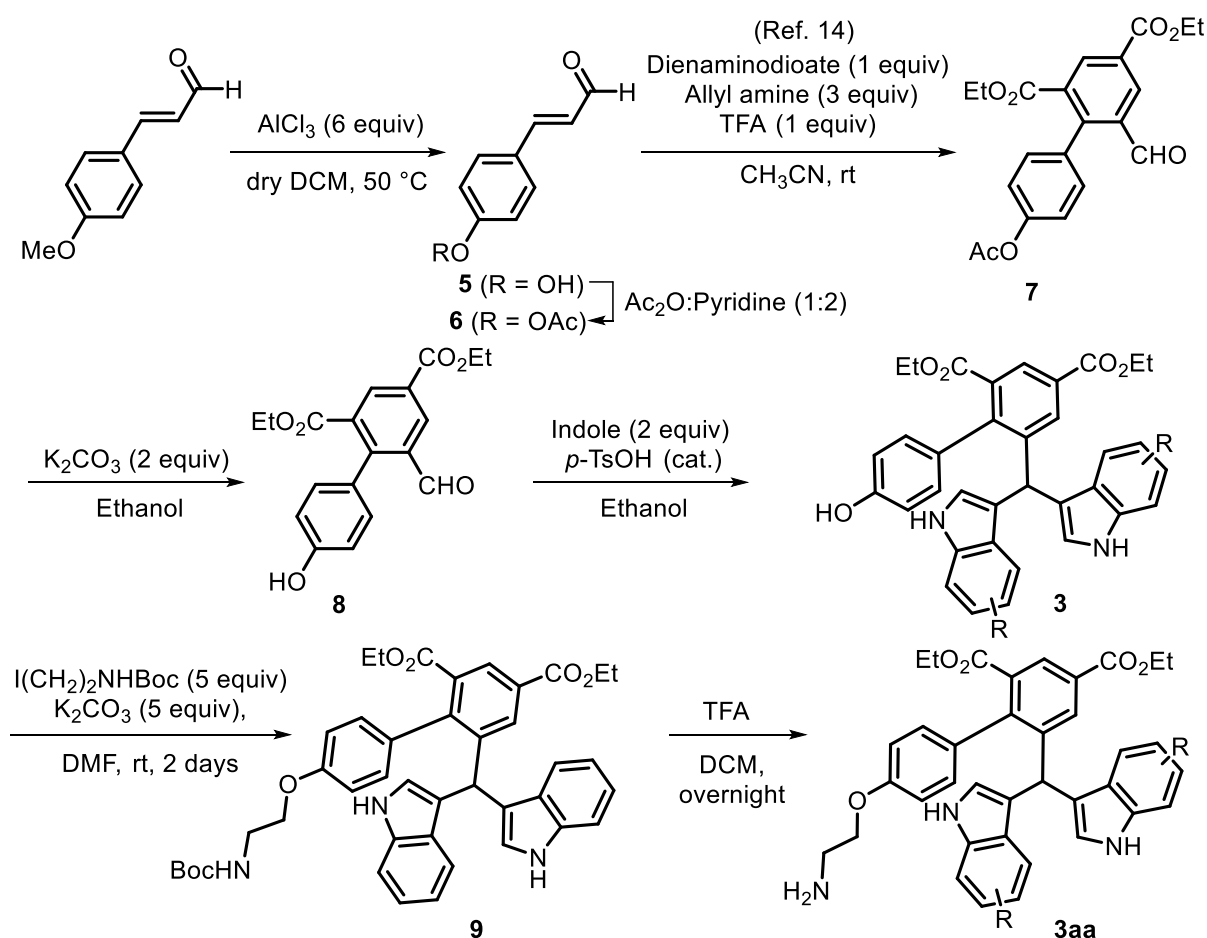


Figure 4.3D. Basic skeleton of the biaryl and diaryl ether conjugated DIMs

4.3.4. Synthesis of diindolylmethane conjugates of biaryl/diaryl ethers

The strategy for the synthesis of biaryl and diaryl ether conjugated DIM analogues **3a-3o**, **3aa** and **4a-4p** are depicted in Scheme 4.3.1 and 4.3.2. *para*-Hydroxy substitution in biaryl was sought in the design for further structural elaboration. Indoles with variable substitutions were used for the synthesis to get an insight on structure-activity relationship. Initially, 4-hydroxycinnamaldehyde **5** was synthesised from the commercially available *trans*-4-methoxycinnamaldehyde by methyl deprotection in presence of AlCl₃ (6 equiv) in DCM at 50 °C, followed by acetylation yielded cinnamaldehyde **6**. Biaryl-2-carbaldehyde **7** was synthesised from carbaldehyde **6** using our previously reported one pot four-component reaction of dienaminodioate and allylamine mediated by trifluoroacetic acid at room temperature.¹⁴ Deacetylation of biaryl **7** was performed using K₂CO₃ in ethanol, followed by condensation of biaryl **8** with pertinent indole in the presence of a catalytic amount of *p*-TsOH afforded DIM-**3**. The deacetylation attempt with K₂CO₃ in methanol yielded biaryl in which the ethyl group exchanged with methyl group. Encouraged by the previous results, additional functional group modifications for the indole ring was sought to synthesize **3b-3o** (Figure 4.3E). On the other hand, improved metabolic property and enhancement of the pharmacokinetic and physiochemical properties of fluorinated drug molecules inspired us to choose a

fluoro-tertiary amine for the synthesis of diaryl ether conjugated DIMs **4**.²¹ We used our own synthetic methodology to convert tertiary amines **10** to the corresponding diary ether-*ortho*-carbaldehyde **11**²² using phenyliodine diacetate (PIDA) followed by condensation with indole furnished DIM-**12**. As primary amines shown to display potent biological activity, benzyl deprotection was performed by classic hydrogenolysis method with 10 % Pd/C in methanol affording DIMs **4a-4p** (Figure 4.3F). All the DIMs were purified by column chromatography, and structural confirmation was carried out by ¹H-, ¹³C-NMR, and HR-ESI-MS.



Scheme 4.3.1. Synthesis of biaryl conjugated DIMs **3a-3o** and DIM-**3aa**

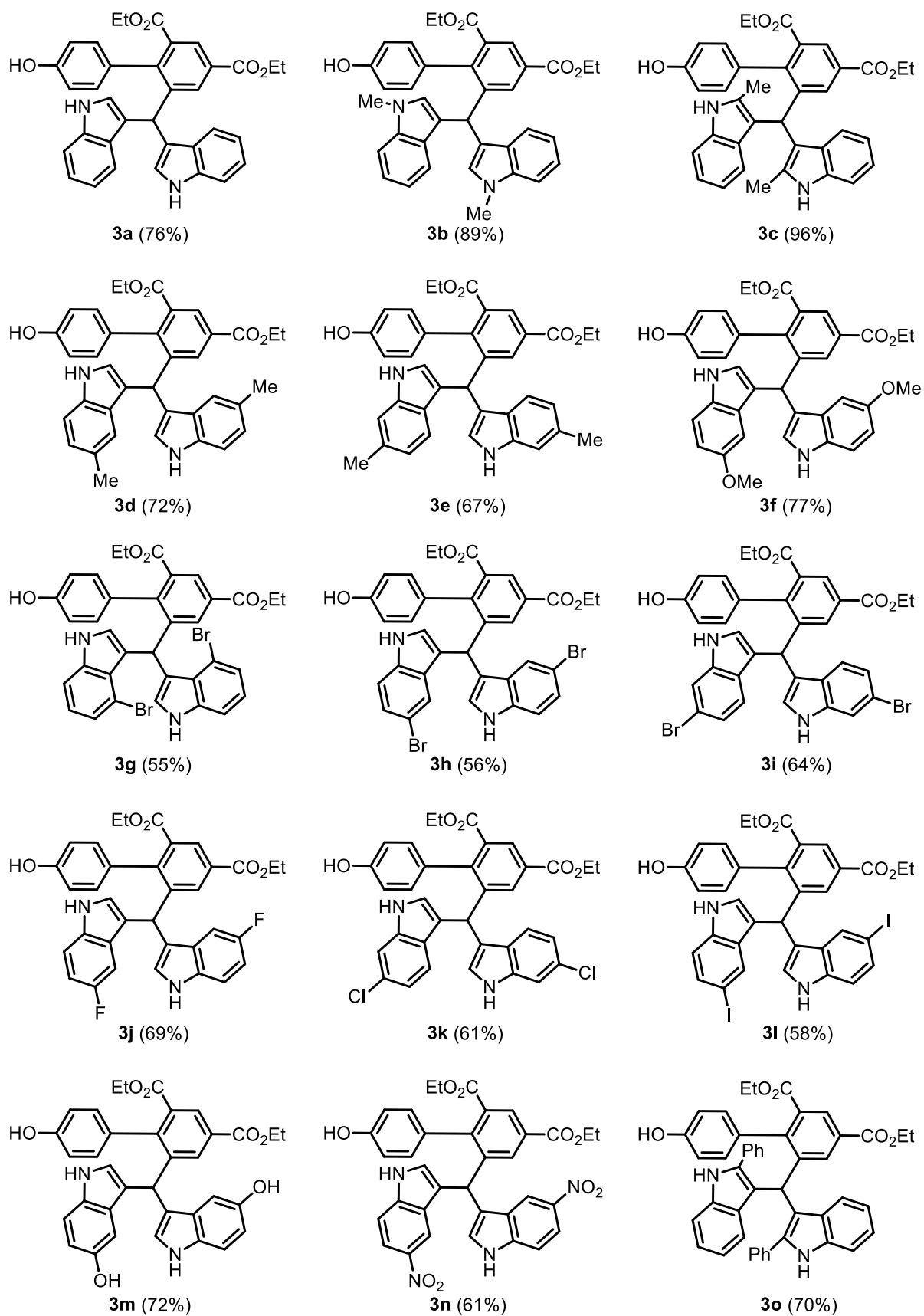
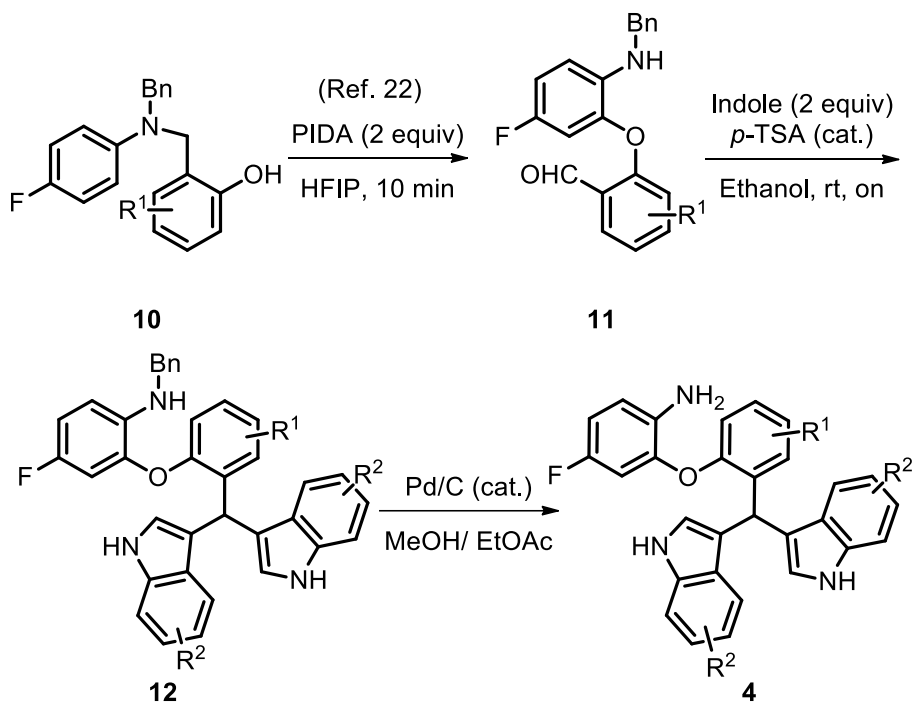


Figure 4.3E. Structures of biaryl conjugated DIMs **3a-3o**



Scheme 4.3.2. Synthesis of diaryl ether conjugated DIMs **4a-4p**

4.3.5. Antiproliferative activity of DIM conjugates of biaryl/diaryl ethers **3a-3o** and **4a-4p**

Antiproliferative activity of all the compounds in MDA-MB-231 cells was screened using MTT assay. The standard drug paclitaxel was used as the positive control. Results tabulated in table 4.3B indicated that MDA-MB-231 cells are more sensitive to the biaryl conjugated DIMs **3a-3o** than diaryl ether conjugates **4a-4p**. Biaryl conjugates **3g**, **3i**, **3j**, and **3k** reduced MDA-MB-231 cells proliferation in a concentration-dependent manner than **DIM-1** and GI_{50} value was found to be in the range of 11-15 μ M. The standard drug paclitaxel has a GI_{50} value of 34.5 ± 0.219 nM in MDA-MB-231 cells. From the library in hand, it is very clear that the halo substitutions (**3g**, **3i**, **3j**, **3k**) are found to be more active over other substituents. Unfortunately, the halo substituted derivatives **3g**, **3i**, **3j** and **3k** were toxic against normal cell line with GI_{50} values around 15 μ M (Table 4.3C). Remaining derivatives exhibited GI_{50} values greater than 30 μ M. The results from MTT assay indicated that DIM conjugation with diaryl ether did not offer any significant improvement in the activity, while the biaryl conjugated compounds shows significant cytotoxicity towards normal cell line.

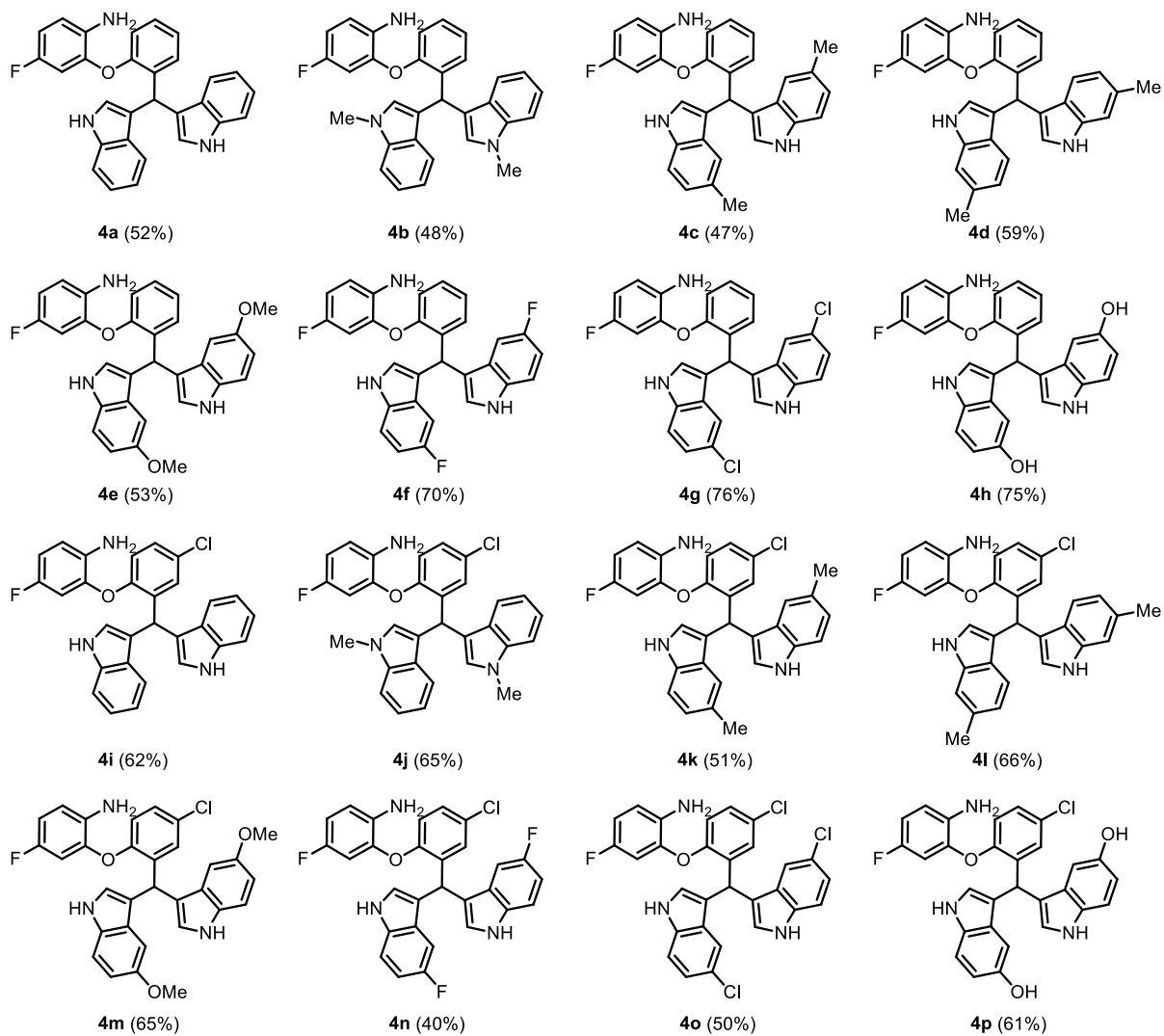


Figure 4.3F. Structures of diaryl ether conjugated DIMs **4a-4p**.

Table 4.3B. Cytotoxic activity of DIM derivatives on MDA-MB-231 cell line

Compound	GI ₅₀ (MDA-MB-231)	Compound	GI ₅₀ (MDA-MB-231)
DIM-1	>50	DIM-4a	48.81
DIM-3a	27.6±0.29	DIM-4b	>50
DIM-3b	>50	DIM-4c	>50
DIM-3c	35.9±0.022	DIM-4d	>50
DIM-3d	>50	DIM-4e	>50
DIM-3e	>50	DIM-4f	49.25
DIM-3f	>50	DIM-4g	>50
DIM-3g	11.7±0.564	DIM-4h	>50
DIM-3h	37.7±0.858	DIM-4i	>50
DIM-3i	12.12±0.345	DIM-4j	>50
DIM-3j	13.66±0.276	DIM-4k	43.8±0.02
DIM-3k	15.4±0.215	DIM-4l	48.1±0.14
DIM-3l	30.6±0.43	DIM-4m	>50
DIM-3m	42.37±0.78	DIM-4n	>50
DIM-3n	30.5±0.55	DIM-4o	42.3±0.21
DIM-3o	>50	DIM-4p	>50
DIM-3aa	8.27±0.233	Paclitaxel	34.5±0.219 nM

Cytotoxicity of cells treated with different concentrations of DIM 3a-3o, 3aa and 4a-4p for 24 h was evaluated using MTT assay. Values represented are means, with standard deviations represented as ±

It is known that the nitrogen atom can act as a good hydrogen bond acceptor or donor, properties essential to render biological activity. A free amine functionality can be appended using the free –OH of DIM 3. The free –OH of DIM-3a was subjected to alkylation with alkyl iodide to offer DIM-9, followed by the -Boc group deprotection led to the formation of the corresponding alkylated DIM biaryl 3aa (Scheme 4.3.1) with terminal primary amine. We hypothesised that the presence of amphiphilic and primary amine functionality of DIM-3aa could improve the biological activity and also improve solubility due to salt formation of the primary amine. Cytotoxicity of DIM-3aa was evaluated using MDA-MB-cell line, and the result showed better activity than the parent DIM-1 with a GI₅₀ value of 8.27±0.233. Interestingly, DIM-3aa was found to be non-toxic to normal cells up to 20 μM. Also, we have observed morphological changes associated with the cells upon treatment with DIM-3aa using phase contrast microscopy.

DIM-3aa caused significant morphological changes in the treated cell line, like rounding up of cells and membrane breakage, while untreated cells were seen spread and flattened. Similar changes were observed with the drug paclitaxel also. The results are given in figure 4.3G.

Table 4.3C. Cytotoxic activity of DIM derivatives on L6 cell line

Compound	GI ₅₀ (L6) μ M	Compound	GI ₅₀ (L6) μ M
DIM-1	>50	DIM-4a	33.7 \pm 0.11
DIM-3a	>50	DIM-4b	>50
DIM-3b	>50	DIM-4c	>50
DIM-3c	>50	DIM-4d	>50
DIM-3d	>50	DIM-4e	51.8 \pm 401
DIM-3e	>50	DIM-4f	37.0 \pm 0.407
DIM-3f	>50	DIM-4g	35.4 \pm 0.152
DIM-3g	33.3 \pm 0.363	DIM-4h	>50
DIM-3h	>50	DIM-4i	44.7 \pm 0.11
DIM-3i	23.7 \pm 0.489	DIM-4j	>50
DIM-3j	17.8 \pm 0.954	DIM-4k	>50
DIM-3k	16.3 \pm 0.375	DIM-4l	>50
DIM-3l	>50	DIM-4m	>50
DIM-3m	>50	DIM-4n	39.3 \pm 0.308
DIM-3n	>50	DIM-4o	35.9 \pm 0.484
DIM-3o	>50	DIM-4p	>50
DIM-3aa	25.9 \pm 0.364		

Cells were treated with different concentrations of DIM 3a-3o, 3aa and 4a-4p for 24 h and the cytotoxicity was evaluated using MTT assay. Values represented are means, with standard deviations represented as \pm .

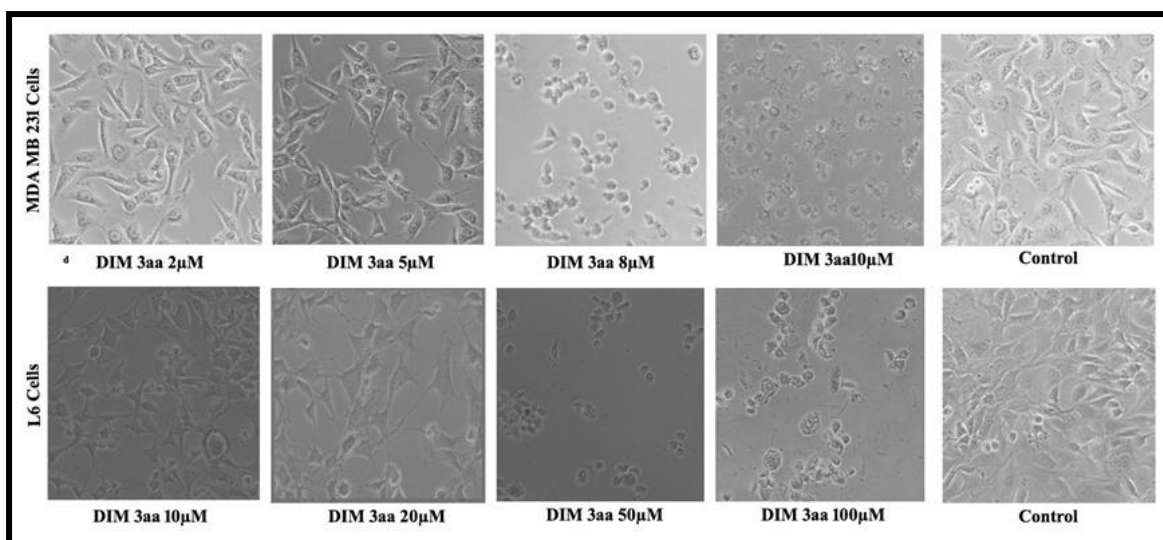


Figure 4.3G. Morphology of MDA-MB-231 and L6 cells treated with DIM-3aa

4.4. Conclusions

We have designed and synthesized a new class of DIM-*ortho*-biaryl (DIM) hybrid motif and its derivatives and evaluated the anticancer activity against HeLa and MDA-MB-231 cells. From the first library, DIM-2a and 2d induced a concentration-dependent cytotoxicity towards both HeLa and MDA-MB-231 cell lines with low GI₅₀. Lower GI₅₀ values (below 10 μM) indicate a high toxicity potential. DIM biaryl conjugates 3a-3o with halo substitutions in the indole ring 3g, 3i, 3j and 3k showed significant cytotoxicity in MDA-MB-cells but they are found to be toxic against normal L6 cells. The DIM diaryl ether conjugates 4a-p were found to be not effective against MDA-MB-231 cells. Interestingly, the primary amine appended DIM-3aa exhibited significant cytotoxicity in MDA-MB-231 cells and was found to be non-toxic to L6 normal cells up to 20 μM, warranting further detailed pharmacological studies. Interestingly, DIM-2a, 2d and 3aa are more active than the parent DIM-1 in both HeLa and MDA-MB-231 cells.

4.5. Experimental section

4.5.1. General information

Reagents and solvents were purchased as reagent grade and were used without further purification. Silica gel G-60 F₂₅₄ aluminum TLC was used to monitor the reactions while short/long wavelength lamps and iodine staining technique catered to the visualization of compounds. Column chromatography was performed using silica gel 100-200 mesh and neutral alumina. ¹H and ¹³C NMR were recorded on a Bruker Avance II spectrometer at 500 and 125 MHz, respectively using CDCl₃, CD₃OD, (CD₃)₂CO or (CD₃)₂SO as

solvents. Data are reported as follows: chemical shift in ppm (δ), multiplicity (s = singlet, d = doublet, t = triplet, q = quartet, bs = broad singlet, m = multiplet), coupling constant (Hz) and integration. HR-ESI-MS analysis was recorded on a Thermo Scientific Exactive-LCMS instrument by electrospray ionization method with ions given in m/z using Orbitrap analyzer.

4.5.2. Procedure for the synthesis of di(1H-indol-3-yl)methane (1)²³

Anhydrous InCl_3 (66 mg, 0.3 mmol, 0.1 equiv) was added to a solution of indole (350 mg, 3 mmol, 1 equiv) and hexamethylenetetramine (HMTA) (35 mg, 0.25 mmol, 0.08 equiv) in dry *i*-PrOH (5 mL). The reaction mixture turned turbid after a few minutes and stirred at room temperature for 8 h. Water (10 mL) was added to the reaction mixture followed by heating at 80 °C for 30 min, and extracted with CHCl_3 (25 mL). The organic layer was dried over anhydrous Na_2SO_4 and the solvent removed to give a solid mass. Column chromatography of the residue over silica gel using increasing concentrations of chloroform in petroleum ether yielded **1** as a white solid.

4.5.3. General procedure for the synthesis of biaryl conjugated DIM (2a-2l)

To a solution of pertinent biaryl-2-carbaldehyde (1 equiv) in ethanol (1.5 mL) were added indole (2 equiv) and *p*-TsOH (cat.), and stirred at 80 °C. After the complete conversion of the starting material, the reaction mixture was quenched with saturated aqueous NaHCO_3 (10 mL) and extracted with EtOAc (10 mL). The combined organic extracts were dried over anhydrous Na_2SO_4 , concentrated and purified by column chromatography.

4.5.4. General procedure for the synthesis of biaryl conjugated DIM (3a-3o)

4.5.4A. 4-Hydroxycinnamaldehyde (5)

Anhydrous AlCl_3 (4.9 g, 37 mmol, 6 equiv) was added to a solution of 4-methoxycinnamaldehyde (1 g, 6.16 mmol, 1 equiv) in dry DCM (8 mL) and stirred at 55 °C overnight. After completion of the starting material, as indicated by TLC, the reaction mixture was poured into ice-cold water, followed by extraction with EtOAc (50 mL x 3). The combined organic extracts were dried over anhydrous Na_2SO_4 , concentrated and purified by column chromatography.

4.5.4B. 4-Acetylcinnamaldehyde (6)

To a solution of 4-hydroxycinnamaldehyde (0.75 g, 5.06 mmol) in pyridine (7 mL), was added acetic anhydride (3.5 mL), and stirred at room temperature. After overnight stirring, the reaction mixture was quenched with saturated aqueous NaHCO_3 and

extracted with EtOAc (30 mL x 2). The combined EtOAc extracts were washed two times with water and dried over anhydrous Na₂SO₄, concentrated and purified by column chromatography.

4.5.4C. Diethyl 4'-acetoxy-6-formyl-[1,1'-biphenyl]-2,4-dicarboxylate (**7**)

To a solution of dienaminodiester (1 g, 3.95 mmol, 1 equiv) in CHCl₃/MeCN (1:1) were added cinnamaldehyde **5** (2.25 g, 11.9 mmol, 3 equiv), allyl amine (0.9 mL, 11.9 mmol, 3 equiv) and TFA (1 mL, 11.3 mmol, 3 equiv) in a sequential manner at room temperature. After immediate addition of TFA, the reaction mixture gives an intense red colour indicating the formation of trienamine. After complete consumption of the compound as visualized on TLC, the reaction mixture was quenched with saturated aqueous NaHCO₃ (20 mL) and extracted with DCM (1 x 20 mL). The organic layer was dried over anhydrous Na₂SO₄, concentrated and the crude mixture was subjected to flash column chromatography by eluting with DCM/hexane solvent system to afford the desired biaryl compound **7**.

4.5.4D. Diethyl 6-formyl-4'-hydroxy-[1,1'-biphenyl]-2,4-dicarboxylate (**8**)

To a stirred solution of biaryl **7** in EtOH (2 mL) was added K₂CO₃ (1.5-2 equiv) at room temperature and the reaction mixture was stirred for 2-5 h. After complete conversion of the starting materials, the reaction mixture was diluted with EtOH. Filtration through a pad of activated Dowex resin, followed by removal of the solvents yielded the crude deacetylated biaryl compound **8**.

4.5.4E. Diethyl 6-(di(1*H*-indol-3-yl)methyl)-4'-hydroxy-[1,1'-biphenyl]-2,4-dicarboxylate (**3a-3o**)

To a solution of biaryl **8** (40 mg, 0.12 mmol, 1 equiv) in ethanol (1.5 mL) were added pertinent indole (0.24 mmol, 2 equiv) and *p*-TsOH (cat.), and stirred at room temperature. After complete conversion of the starting material, the reaction mixture was quenched with saturated aqueous NaHCO₃ (10 mL) and extracted with EtOAc (10 mL x 1). The combined organic extracts were dried over anhydrous Na₂SO₄, concentrated and purified by column chromatography.

4.5.5. Diethyl 4'-(2-((*tert*-butoxycarbonyl)amino)ethoxy)-6-(di(1*H*-indol-3-yl)methyl)-[1,1'-biphenyl]-2,4-dicarboxylate (**9**)

To a solution of DIM **3a** (25 mg, 0.044, 1 equiv) in anhydrous DMF (1 mL), were added corresponding alkyl iodide (30 mg, 0.22 mmol, 5 equiv; synthesised from Boc-protected ethanolamine by reported procedure) and was stirred at room temperature until the conversion of the starting material was complete. The reaction mixture was quenched

with water and extracted with EtOAc (10 mL x 2). The combined organic layers was washed with water three times and dried over anhydrous Na₂SO₄. Filtration, evaporation, and purification by silica gel chromatography gave the alkylated DIM-9.

4.5.6. Diethyl 4'-(2-aminoethoxy)-6-(di(1H-indol-3-yl)methyl)-[1,1'-biphenyl]-2,4-dicarboxylate (3aa)

To a stirred solution of DIM-9 (30 mg, 0.042 mmol, 1 equiv) in dry DCM (1 mL), was added TFA (0.42 mL, 0.42 mmol, 10 equiv) and stirred at room temperature overnight. After the full exhaustion of the starting material at room temperature, the solution was concentrated in vacuum and purified by silica gel chromatography. Elution with methanol/dichloromethane furnished the desired **3aa**.

4.5.7. N-benzyl-2-(2-(di(1H-indol-3-yl)methyl)phenoxy)-4-fluoroaniline (12)

To a solution of diaryl ether **11** (35 mg, 0.11 mmol, 1 equiv; synthesised by reported procedure) in ethanol (1 mL) were added pertinent indole (0.22 equiv, 2 equiv), *p*-TsOH (cat.) and stirred at room temperature. After overnight reaction, the reaction mixture was quenched with saturated aqueous NaHCO₃ (10 mL) and extracted with EtOAc (10 mL x 1). The combined organic extracts were dried over anhydrous Na₂SO₄, concentrated and purified by column chromatography.

4.5.8. 2-(2-(di(1H-indol-3-yl)methyl)phenoxy)-4-fluoroaniline (4)

To a solution of compound **12** (45 mg, 0.04 mmol, 1 equiv) in EtOH (4 mL) was added 35 mg of 10% Pd/C. H₂ gas was purged into the reaction mixture for 2 min and was stirred overnight under an H₂ atmosphere (balloon). After consumption of the starting material, the reaction mixture was diluted with MeOH (25 mL), filtered through a Celite pad, concentrated and purified by neutral alumina column chromatography.

4.5.9. Cell Culture and Cytotoxicity Studies

The constituents required for the cell culture namely, Dulbecco's Modified Eagle Medium (DMEM), Fetal Bovine Serum (FBS), Trypsin-EDTA (10X), and Antibiotic and Antimycotic solution (100X) containing 100 µg/mL streptomycin and 100 units/L penicillin, were from HiMedia (Mumbai, India). Sterile cell culture flasks, multiwell plates, and cryo-vials were purchased from ThermoFisher Scientific (Waltham, MA, USA). Centrifuge tubes and microcentrifuge tubes were bought from Tarsons Product Pvt. Ltd. (Kolkata, India).

Human cervical cancer cell (HeLa), Human breast cancer cells (MDA-MB-231) and rat skeletal myoblast cell line (L6) were from NCCS, Pune, India and rat cardiac

myofibroblasts (H9C2) was from ATCC. Cells were cultured in DMEM (Dulbecco's modified Eagle's medium) medium supplemented with 10 % FBS (fetal bovine serum), 100 µg/mL streptomycin and 100 U/mL penicillin (Himedia, India), respectively and maintained in a humidified incubator supplied with 5% CO₂ at 37°C. Cells were subcultured at regular time intervals (doubling time ~ 28 h). Monolayers of cells in 96 well culture plates (1x10⁴ cells/well) were used for cytotoxic studies using MTT (Himedia, India) assay.²⁴ The samples were dissolved in DMSO (10 mM) and further diluted in the cell culture medium. Cells treated with different concentrations of DIMs and cisplatin/paclitaxel (positive control) for 24h were then used to compare the percentage of growth inhibition according to the following formula.

$$\% \text{ of growth inhibition} = \left[\frac{1 - \text{absorbance of treated cells}}{\text{absorbance of untreated cells}} \right] \times 100$$

4.5.10. Morphological analysis by phase contrast microscopy

Morphological changes associated with MDA-MB-231 cells upon treatment with or without cisplatin/paclitaxel and DIM derivatives for 24 h were observed using a phase contrast microscope attached to a camera (Nikon Eclipse TS-100, Nikon instruments Inc. Melville, USA).

4.5.11. Spectral details of products

Figure 4.5A. ^1H and ^{13}C -NMR of DIM-1

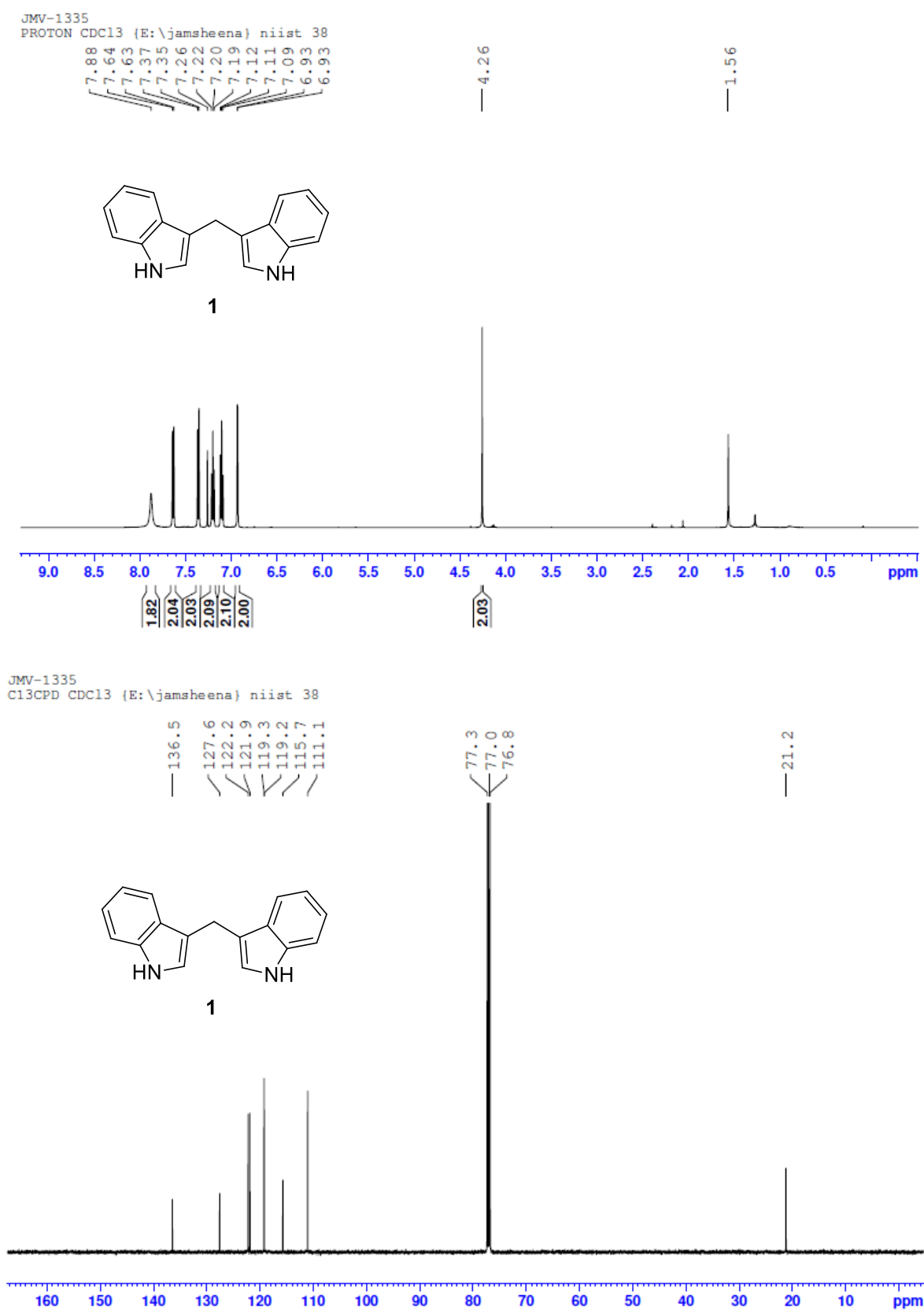
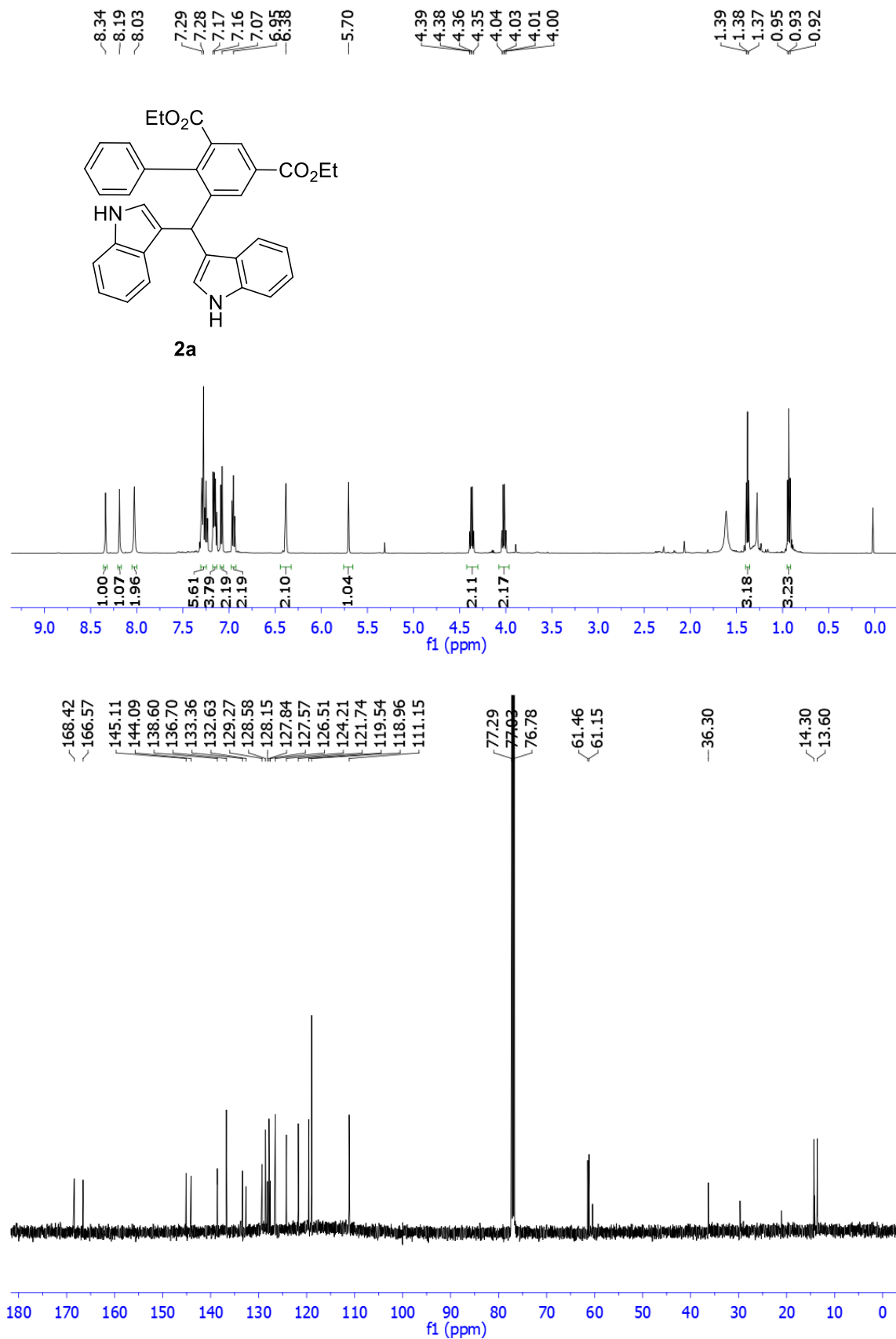


Figure 4.5B. ^1H and ^{13}C -NMR of DIM-2a



Di(1*H*-indol-3-yl)methane (1)

¹H NMR (CDCl₃, 500 MHz): δ 7.88 (bs, 2H), 7.64 (d, *J* = 8 Hz, 2H), 7.20 (t, *J* = 7.5 Hz, 2H), 7.11 (d, *J* = 7.5 Hz, 2H), 6.93 (s, 2H), 4.26 (s, 2H); ¹³C NMR(CDCl₃, 125 MHz): δ 136.5, 127.6, 122.2, 121.9, 119.3, 119.2, 115.7, 111.1, 21.2; HR-ESI-MS: *m/z* calcd for C₁₇H₁₃N₂⁺: 245.1073 [M - H]⁺; found: 245.1081.

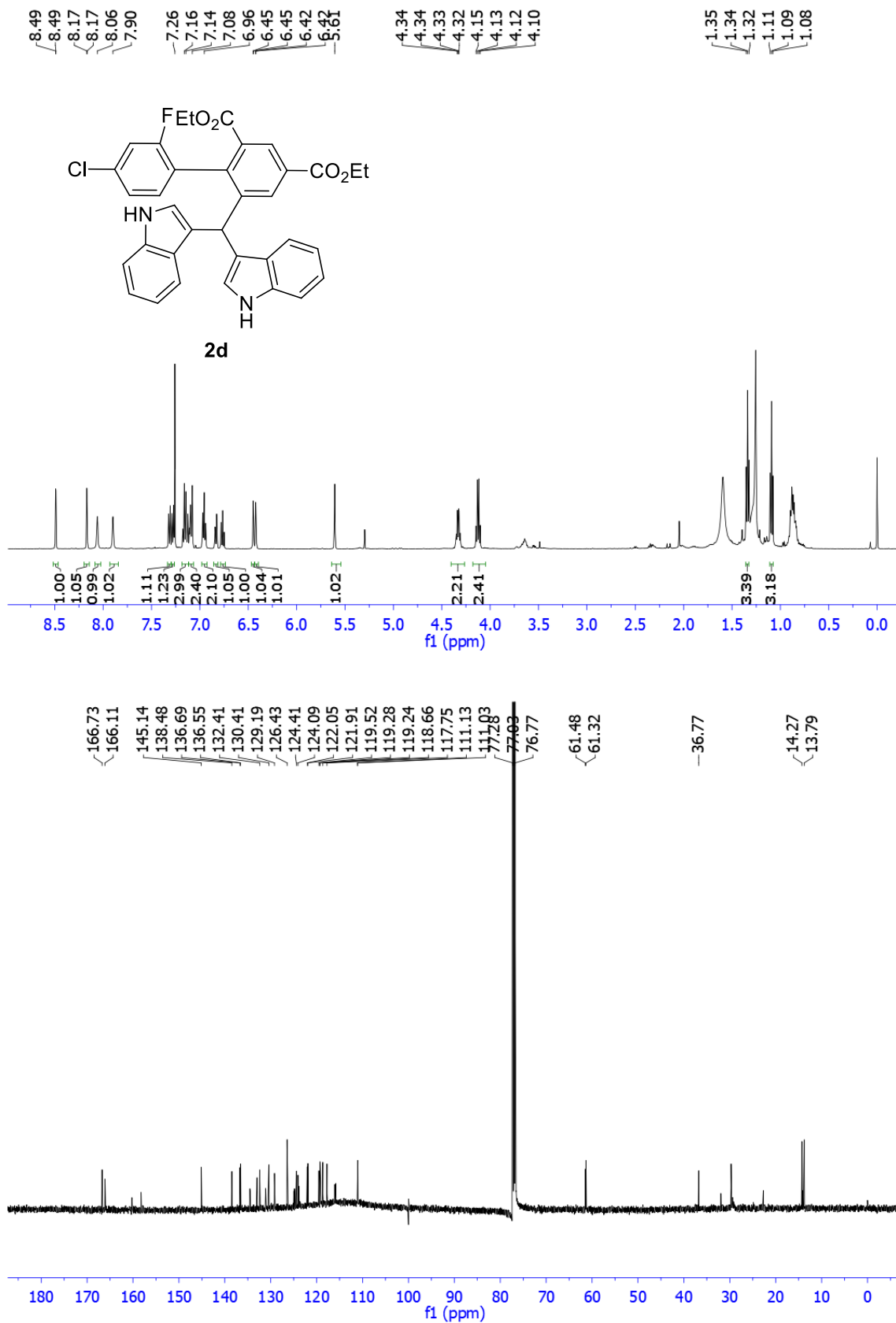
Diethyl-6-(di(1*H*-indol-3-yl)methyl)biphenyl-2,4-dicarboxylate (2a)

¹H NMR (CDCl₃, 500 MHz) δ 0.93 (t, 3H, *J* = 7 Hz), 1.38 (t, 3H, *J* = 7 Hz), 4.02 (q, 2H, *J* = 7 Hz), 4.36 (q, 2H, *J* = 7 Hz), 5.70 (s, 1H), 6.38 (s, 2H), 6.95 (t, 2H, *J* = 7 Hz), 7.07 (d, 2H, *J* = 8 Hz), 7.16 (t, 4H, *J* = 6.5 Hz), 7.26 (m, 5H), 8.03 (s, 2H), 8.19 (s, 1H), 8.34 (s, 1H); ¹³C NMR (CDCl₃, 125 MHz) δ 13.6, 14.2, 36.3, 61.1, 61.5, 111.1, 118.9, 119.5, 121.7, 124.2, 126.5, 127.5, 127.8, 128.1, 128.5, 129.2, 132.6, 133.3, 136.7, 138.6, 144.0, 145.1, 166.5, 168.4; HR-ESI-MS: *m/z* calcd for C₃₅H₃₀N₂O₄Na: 565.2103 [M + Na]⁺; found: 565.2104.

Diethyl-6-(di(1*H*-indol-3-yl)methyl)-4'-methylbiphenyl-2,4-dicarboxylate (2b)

¹H NMR (CDCl₃, 500 MHz) δ 0.97 (t, 3H, *J* = 7 Hz), 1.36 (t, 3H, *J* = 7 Hz), 2.33 (s, 3H), 4.05 (q, 2H, *J* = 7 Hz), 4.34 (q, 2H, *J* = 7 Hz), 5.75 (s, 1H), 6.45 (s, 2H), 6.94 (t, 2H, *J* = 7 Hz), 7.06 (m, 4H), 7.08 (d, 2H, *J* = 8 Hz), 7.14 (t, 2H, *J* = 7 Hz), 7.28 (d, 2H, *J* = 7.5 Hz), 8.04 (s, 2H), 8.17 (d, 1H, *J* = 2 Hz), 8.29 (d, 1H, *J* = 2 Hz); ¹³C NMR (CDCl₃, 125 MHz) δ 13.6, 14.2, 21.3, 36.2, 61.1, 61.3, 111.1, 118.8, 119.0, 119.6, 121.7, 124.1, 126.5, 127.9, 128.4, 128.5, 129.0, 132.6, 133.5, 135.5, 136.7, 137.2, 144.1, 145.2, 166.5, 168.5; HR-ESI-MS: *m/z* calcd for C₃₆H₃₂N₂O₄Na: 579.2259 [M + Na]⁺; found: 579.2269.

Figure 4.5C. ^1H and ^{13}C -NMR of DIM-2d



Diethyl-2'-bromo-6-(di(1*H*-indol-3-yl)methyl)biphenyl-2,4-dicarboxylate (2c)

¹H NMR (CDCl₃, 500 MHz) δ 1.02 (t, 3H, *J* = 7 Hz), 1.34 (t, 3H, *J* = 7 Hz), 4.08 (q, 2H, *J* = 7 Hz), 4.34 (q, 2H, *J* = 7.5 Hz), 5.58 (s, 1H), 6.47 (s, 2H), 6.82 (dd, 1H, *J* = 7, 1.5 Hz), 6.93 (m, 3H), 7.09 (m, 2H), 7.13 (m, 2H), 7.31 (t, 2H, *J* = 8 Hz), 7.39 (d, 1H, *J* = 8 Hz), 7.55 (d, 1H, *J* = 8 Hz), 7.92 (s, 1H), 8.08 (s, 1H), 8.22 (d, 1H, *J* = 2 Hz), 8.53 (d, 1H, *J* = 1.5 Hz); ¹³C NMR (CDCl₃, 125 MHz) δ 13.6, 14.2, 36.6, 61.2, 61.5, 111.0, 111.1, 117.4, 118.9, 119.0, 119.3, 119.5, 119.8, 121.7, 121.8, 123.1, 124.2, 124.9, 126.4, 126.5, 126.6, 128.9, 129.2, 129.9, 130.5, 132.2, 132.3, 133.0, 136.5, 136.7, 139.3, 144.5, 144.6, 166.5, 166.9; HR-ESI-MS: *m/z* calcd for C₃₅H₂₉BrN₂O₄Na: 643.1208 [M + Na]⁺; found: 643.1223.

Diethyl-4'-chloro-6-(di(1*H*-indol-3-yl)methyl)-2'-fluorobiphenyl-2,4-dicarboxylate (2d)

¹H NMR (CDCl₃, 500 MHz) δ 1.09 (t, 3H, *J* = 7 Hz), 1.34 (t, 3H, *J* = 7 Hz), 4.13 (q, 2H, *J* = 7 Hz), 4.34 (q, 2H, *J* = 7.5 Hz), 5.60 (s, 1H), 6.42 (s, 1H), 6.44 (s, 1H), 6.76 (t, 1H, *J* = 8 Hz), 6.83 (dd, 1H, *J* = 8, 1.5 Hz), 6.95 (t, 2H, *J* = 7 Hz), 7.09 (m, 2H), 7.16 (m, 3H), 7.30 (m, 2H), 7.89 (s, 1H), 8.06 (s, 1H), 8.16 (d, 1H, *J* = 1 Hz), 8.49 (d, 1H, *J* = 1.5 Hz); ¹³C NMR (CDCl₃, 125 MHz) δ 13.7, 14.3, 36.7, 61.3, 61.4, 111.0, 111.1, 117.7, 118.6, 119.2, 119.3, 119.5, 121.9, 122.0, 124.1, 124.4, 126.4, 129.2, 130.4, 132.4, 132.9, 136.5, 136.7, 138.4, 145.1, 166.1, 166.7; HR-ESI-MS: *m/z* calcd for C₃₅H₂₈ClFN₂O₄Na: 617.1619 [M + Na]⁺; found: 617.1629.

Diethyl-4'-cyano-6-(di(1*H*-indol-3-yl)methyl)biphenyl-2,4-dicarboxylate (2e)

¹H NMR (CDCl₃, 500 MHz) δ 1.00 (t, 3H, *J* = 7 Hz), 1.37 (t, 3H, *J* = 7 Hz), 4.05 (q, 2H, *J* = 7 Hz), 4.37 (q, 2H, *J* = 7 Hz), 5.46 (s, 1H), 6.27 (d, 2H, *J* = 1.5 Hz), 6.96 (m, 4H), 7.14 (t, 2H, *J* = 7.5 Hz), 7.21 (d, 2H, *J* = 8.5 Hz), 7.25 (d, 2H, *J* = 8 Hz), 7.48 (d, 2H, *J* = 8 Hz), 8.06 (s, 2H), 8.16 (d, 1H, *J* = 1.5 Hz), 8.43 (d, 1H, *J* = 2 Hz); ¹³C NMR (CDCl₃, 125 MHz) δ 13.7, 14.2, 36.5, 61.4, 61.7, 111.3, 111.4, 118.2, 118.7, 119.0, 119.2, 122.0, 124.2, 126.2, 128.9, 129.3, 130.2, 131.5, 132.1, 132.9, 136.6, 143.4, 144.0, 144.1, 166.2, 167.1; HR-ESI-MS: *m/z* calcd for C₃₆H₂₉N₃O₄Na: 590.2055 [M + Na]⁺; found: 590.2066.

Diethyl-4-(5-bromothiophen-2-yl)-5-(di(1*H*-indol-3-yl)methyl)isophthalate (2f)

¹H NMR (CDCl₃, 500 MHz) δ 1.12 (t, 3H, *J* = 7 Hz), 1.35 (t, 3H, *J* = 7 Hz), 4.17 (q, 2H, *J* = 7 Hz), 4.33 (q, 2H, *J* = 7 Hz), 5.90 (s, 1H), 6.31 (s, 2H), 6.50 (d, 1H, *J* = 3.5 Hz), 6.86 (d, 1H, *J* = 3.5 Hz), 6.98 (t, 2H, *J* = 7.5 Hz), 7.15 (m, 4H), 7.27 (d, 2H, *J* = 8 Hz), 8.03 (s, 2H), 8.11 (d, 1H, *J* = 1.5 Hz), 8.28 (d, 1H, *J* = 1.5 Hz); ¹³C NMR (CDCl₃, 125 MHz) δ 13.7, 14.2, 36.5, 61.6, 61.7, 111.2, 112.8, 118.7, 119.1, 119.5, 121.9, 124.2, 126.4, 128.1, 128.3, 129.6, 130.4, 132.5, 134.8, 136.7, 138.7, 139.8, 145.9, 166.1, 167.8; HR-ESI-MS: *m/z* calcd for C₃₃H₂₇BrN₂O₄SNa: 649.0772 [M + Na]⁺; found: 649.0800.

Diethyl-6-(di(1*H*-indol-3-yl)methyl)-2'-ethynylbiphenyl-2,4-dicarboxylate (2g)

¹H NMR (CDCl₃, 500 MHz) δ 0.97 (t, 3H, *J* = 7 Hz), 1.35 (t, 3H, *J* = 7 Hz), 2.96 (s, 1H), 4.05 (m, 2H), 4.34 (q, 2H, *J* = 7 Hz), 5.54 (s, 1H), 6.21 (s, 1H), 6.38 (s, 1H), 6.78 (d, 1H, *J* = 7.5 Hz), 6.91 (m, 3H), 7.07 (m, 2H), 7.14 (m, 1H), 7.20 (m, 2H), 7.27 (d, 1H, *J* = 8 Hz), 7.37 (d, 1H, *J* = 8 Hz), 7.51 (d, 1H, *J* = 8 Hz), 7.79 (s, 1H), 8.16 (s, 1H), 8.18 (d, 1H, *J* = 1.5 Hz), 8.50 (d, 1H, *J* = 1.5 Hz); ¹³C NMR (CDCl₃, 125 MHz) δ 13.6, 14.3, 36.6, 61.0, 61.4, 81.0, 82.3, 110.9, 111.1, 117.9, 118.7, 118.9, 119.4, 119.7, 119.9, 121.1, 121.6, 121.7, 124.2, 124.6, 126.4, 126.5, 127.3, 127.8, 128.9, 129.0, 129.6, 132.5, 132.6, 133.0, 136.5, 136.6, 141.7, 144.2, 144.5, 166.5, 167.2; HR-ESI-MS: *m/z* calcd for C₃₇H₃₀N₂O₄Na: 589.2103 [M + Na]⁺; found: 589.2116.

Diethyl-9-(1*H*-indol-3-yl)-6,8-dimethoxy-9*H*-fluorene-2,4-dicarboxylate (2h)

¹H NMR (CDCl₃, 500 MHz) δ 1.33 (t, 3H, *J* = 7 Hz), 1.50 (t, 3H, *J* = 7 Hz), 3.58 (s, 3H), 3.91 (s, 3H), 4.32 (m, 2H), 4.55 (q, 2H, *J* = 7 Hz), 5.36 (s, 1H), 6.46 (d, 1H, *J* = 1.5 Hz), 6.86 (m, 2H), 7.07 (t, 1H, *J* = 7.5 Hz), 7.12 (d, 1H, *J* = 1.5 Hz), 7.28 (d, 1H, *J* = 8.5 Hz), 7.68 (d, 1H, *J* = 2 Hz), 8.00 (s, 1H), 8.09 (s, 1H), 8.41 (s, 1H); ¹³C NMR (CDCl₃, 125 MHz) δ 14.3, 14.4, 43.5, 55.5, 55.6, 61.2, 61.6, 110.9, 113.8, 119.2, 119.5, 121.7, 122.7, 125.3, 126.4, 126.7, 128.5, 128.9, 129.5, 130.5, 136.4, 140.4, 149.1, 149.2, 151.2, 157.1, 160.9, 167.9; HR-ESI-MS: *m/z* calcd for C₂₉H₂₈NO₆: 486.1916 [M + H]⁺; found: 486.1925.

Diethyl-5'-bromo-6-(di(1*H*-indol-3-yl)methyl)-2'-methoxybiphenyl-2,4-dicarboxylate (2i)

¹H NMR (CDCl₃, 500 MHz) δ 1.03 (t, 3H, *J* = 7 Hz), 1.35 (t, 3H, *J* = 7 Hz), 3.56 (s, 3H), 4.08 (m, 2H), 4.33 (m, 2H), 5.59 (s, 1H), 6.48 (s, 1H), 6.55 (s, 1H), 6.71 (d, 1H, *J* = 8.5 Hz), 6.80 (d, 1H, *J* = 2.5 Hz), 6.95 (m, 2H), 7.12 (d, 1H, *J* = 8.5 Hz), 7.16 (m, 2H), 7.21 (d, 1H, *J* = 8 Hz), 7.33 (m, 2H), 7.37 (m, 1H), 7.89 (s, 1H), 8.03 (s, 1H), 8.19 (d, 1H, *J* = 1.5 Hz), 8.44 (d, 1H, *J* = 1.5 Hz); ¹³C NMR (CDCl₃, 125 MHz) δ 13.7, 14.3, 36.9, 55.2, 60.9, 61.2, 110.9, 111.0, 111.6, 112.2, 118.3, 118.7, 119.0, 119.3, 119.5, 121.7, 121.9, 124.3, 126.4, 126.7, 127.6, 127.8, 128.4, 129.6, 129.8, 131.4, 132.5, 132.6, 132.7, 136.5, 136.6, 141.1, 144.8, 155.5, 166.1, 167.2; HR-ESI-MS: *m/z* calcd for C₃₆H₃₁BrN₂O₅Na: 673.1314 [M + Na]⁺; found: 673.1314.

Diethyl-6-(di(1*H*-indol-3-yl)methyl)-2',6'-difluorobiphenyl-2,4-dicarboxylate (2j)

¹H NMR (CDCl₃, 500 MHz) δ 1.08 (t, 3H, *J* = 7 Hz), 1.35 (t, 3H, *J* = 7 Hz), 4.15 (q, 2H, *J* = 7 Hz), 4.36 (q, 2H, *J* = 7 Hz), 5.71 (s, 1H), 6.37 (s, 2H), 6.72 (t, 2H, *J* = 7.5 Hz), 6.94 (t, 2H, *J* = 7.5 Hz), 7.13 (t, 3H, *J* = 7.5 Hz), 7.21 (d, 2H, *J* = 7.5 Hz), 7.27 (d, 2H, *J* = 8 Hz), 7.96 (s, 2H), 8.16 (d, 1H, *J* = 1.5 Hz), 8.59 (d, 1H, *J* = 2 Hz); ¹³C NMR (CDCl₃, 125 MHz) δ 13.7, 14.2, 36.9, 61.2, 61.4, 110.7, 110.9, 117.6, 119.0, 119.2, 121.7, 124.4, 126.6, 129.5, 129.6, 130.7, 132.5, 132.8, 134.1, 136.5, 145.9, 158.7, 160.7, 166.1, 166.3; HR-ESI-MS: *m/z* calcd for C₃₅H₂₈F₂N₂O₄Na: 601.1914 [M + Na]⁺; found: 601.1923.

Diethyl-3'-bromo-6-(di(1*H*-indol-3-yl)methyl)-4'-hydroxy-5'-methoxybiphenyl-2,4-dicarboxylate (2k)

¹H NMR (CDCl₃, 500 MHz) δ 1.08 (t, 3H, *J* = 7 Hz), 1.36 (t, 3H, *J* = 7 Hz), 2.96 (s, 3H), 4.12 (m, 2H), 4.34 (q, 2H, *J* = 7 Hz), 5.70 (s, 1H), 5.90 (bs, 1H), 6.35 (d, 1H, *J* = 1.5 Hz), 6.50 (s, 1H), 6.59 (d, 1H, *J* = 1 Hz), 6.96 (m, 2H), 7.04 (m, 2H), 7.14 (m, 3H), 7.30 (m, 2H), 7.92 (s, 1H), 8.16 (s, 2H), 8.29 (d, 1H, *J* = 1.5 Hz); ¹³C NMR (CDCl₃, 125 MHz) δ 13.9, 14.3, 36.4, 55.2, 61.4, 107.7, 111.0, 111.1, 118.6, 119.1, 119.4, 119.6, 122.3, 124.1, 126.4, 129.6, 131.2, 132.2, 133.6, 136.6, 136.7, 142.6, 143.1, 144.4, 146.4, 166.1, 168.2; HR-ESI-MS: *m/z* calcd for C₃₆H₃₁BrN₂O₆Na: 689.1263 [M + Na]⁺; found: 689.1252.

Diethyl 5-(di(1*H*-indol-3-yl)methyl)-4-(5-iodofuran-2-yl)isophthalate (2l)

¹H NMR (CDCl₃, 500 MHz) δ 1.22 (t, 3H, $J = 7$ Hz), 1.34 (t, 3H, $J = 7$ Hz), 4.24 (q, 2H, $J = 7$ Hz), 4.33 (q, 2H, $J = 7$ Hz), 6.01 (d, 2H, $J = 3$ Hz), 6.36 (s, 2H), 6.48 (d, 1H, $J = 3.5$ Hz), 7.00 (t, 2H, $J = 7.5$ Hz), 7.16 (m, 4H), 7.29 (d, 2H, $J = 8$ Hz), 8.04 (s, 2H), 8.16 (d, 1H, $J = 1.5$ Hz), 8.31 (d, 1H, $J = 1.5$ Hz); ¹³C NMR (CDCl₃, 125 MHz) δ 14.1, 14.2, 36.4, 61.5, 61.7, 88.2, 111.2, 114.0, 118.5, 119.2, 119.5, 121.9, 122.0, 124.0, 126.4, 128.5, 130.3, 132.2, 132.9, 133.7, 136.7, 144.3, 154.5, 166.0, 168.0; HR-ESI-MS: m/z calcd for C₃₃H₂₇IN₂O₅Na: 681.0862 [M + Na]⁺; found: 681.0861.

(E)-3-(4-hydroxyphenyl)acrylaldehyde (5)

¹H NMR (CDCl₃, 500 MHz): δ 9.64 (d, $J = 8$ Hz, 1H), 7.49 (d, $J = 8.5$ Hz, 1H), 7.43 (d, $J = 15.5$ Hz, 1H), 6.90 (d, $J = 9$ Hz, 1H), 6.61 (dd, $J = 16, 8$ Hz, 1H), 5.89 (bs, 1H); ¹³C NMR (CDCl₃, 125 MHz): δ 194.1, 158.7, 153.1, 130.7, 126.9, 126.4, 116.2; HR-ESI-MS: m/z calcd for C₉H₉O₂: 149.0603 [M + H]⁺; found: 149.0604.

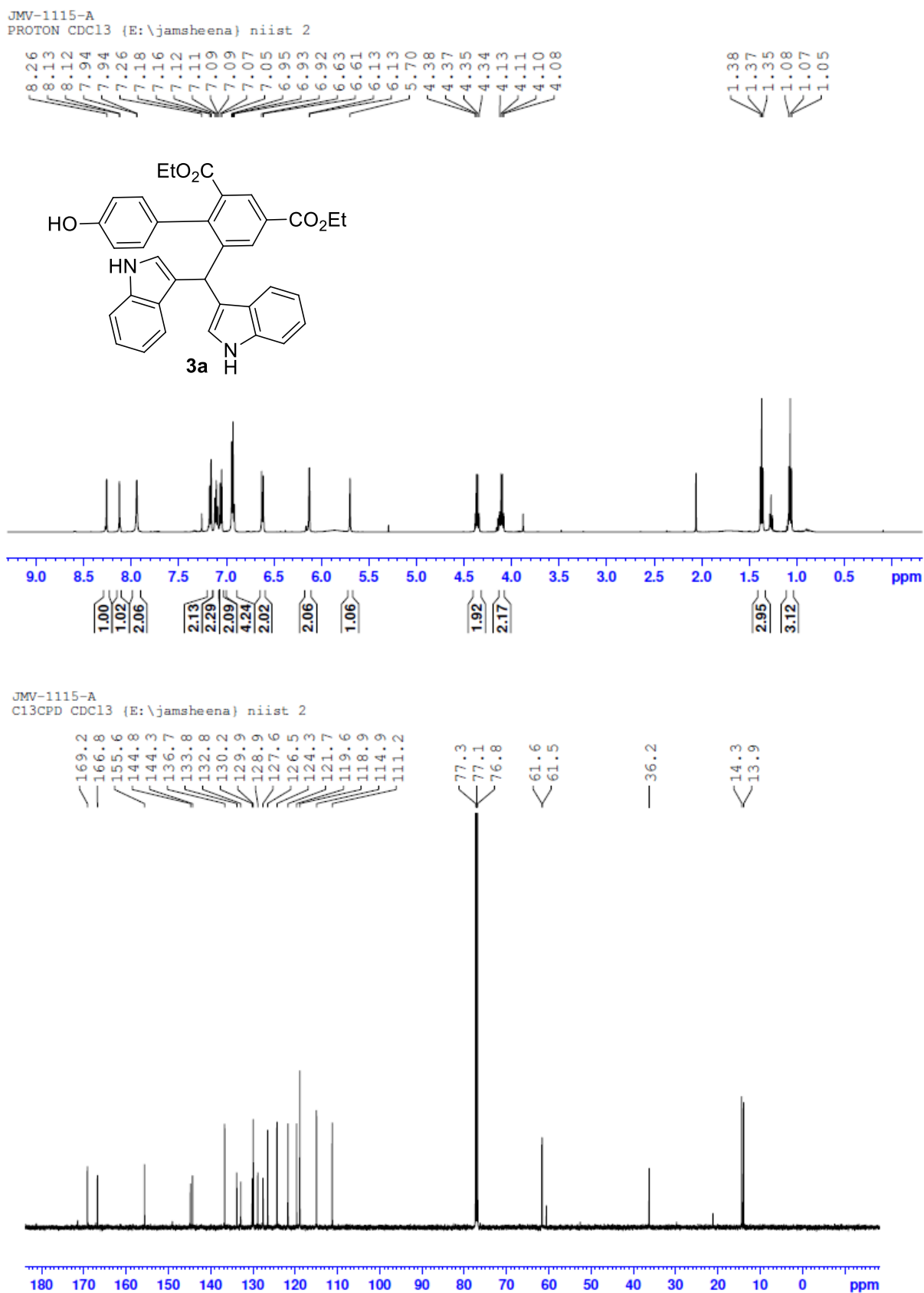
(E)-4-(3-oxoprop-1-en-1-yl)phenyl acetate (6)

¹H NMR (CDCl₃, 500 MHz): δ 9.70 (d, $J = 7.5$ Hz, 1H), 7.60 (d, $J = 8.5$ Hz, 2H), 7.47 (d, $J = 16$ Hz, 1H), 7.18 (d, $J = 8.5$ Hz, 2H), 6.68 (dd, $J = 16, 7.5$ Hz, 1H), 2.33 (s, 3H); ¹³C NMR (CDCl₃, 125 MHz): δ 193.6, 169.1, 152.8, 151.6, 131.7, 129.7, 128.7, 122.4, 21.2; HR-ESI-MS: m/z calcd for C₁₁H₉O₃⁺: 189.0546 [M - H]⁺; found: 189.0394.

Diethyl 4'-acetoxy-6-formyl-[1,1'-biphenyl]-2,4-dicarboxylate (7)

¹H NMR (CDCl₃, 500 MHz): δ 9.81 (s, 1H), 8.75 (d, $J = 2$ Hz, 1H), 8.69 (d, $J = 2$ Hz, 1H), 7.30 (d, $J = 8.5$ Hz, 2H), 7.21 (d, $J = 8.5$ Hz, 2H), 4.45 (q, $J = 7$ Hz, 2H), 4.08 (q, $J = 7$ Hz, 2H), 2.34 (s, 3H), 1.44 (t, $J = 7$ Hz, 3H), 1.02 (t, $J = 7$ Hz, 3H); ¹³C NMR (CDCl₃, 125 MHz): δ 190.6, 169.1, 166.7, 164.7, 151.0, 147.6, 135.1, 135.134.0, 132.7, 131.1, 130.7, 130.5, 121.5, 61.8, 61.8, 21.2, 14.3, 13.6; HR-ESI-MS: m/z calcd for C₂₁H₂₀NaO₇: 407.1107 [M + Na]⁺; found: 407.1105.

Figure 4.5D. ^1H and ^{13}C -NMR of DIM-3a



Diethyl 6-formyl-4'-hydroxy-[1,1'-biphenyl]-2,4-dicarboxylate (8)

¹H NMR (CDCl₃, 500 MHz): δ 9.81 (s, 1H), 8.72 (d, J = 2 Hz, 1H), 8.63 (d, J = 1.5 Hz, 1H), 7.14 (d, J = 8 Hz, 2H), 6.89 (d, J = 8.5 Hz, 2H), 4.45 (q, J = 7 Hz, 2H), 4.14 (q, J = 7 Hz, 2H), 2.34 (s, 3H), 1.43 (t, J = 7 Hz, 3H), 1.09 (t, J = 7 Hz, 3H); ¹³C NMR (CDCl₃, 125 MHz): 191.4, 167.3, 165.0, 156.6, 148.6, 135.3, 134.8, 134.1, 131.0, 130.9, 130.1, 129.4, 126.8, 115.3, 61.9, 61.8, 14.3, 13.8; HR-ESI-MS: m/z calcd for C₁₉H₁₈NaO₆: 365.1001 [M + Na]⁺; found: 365.1001.

Diethyl 6-(di(1*H*-indol-3-yl)methyl)-4'-hydroxy-[1,1'-biphenyl]-2,4-dicarboxylate (3a)

¹H NMR (CDCl₃, 500 MHz): δ 8.26 (d, J = 2 Hz, 1H), 8.13 (d, J = 2 Hz, 1H), 7.94 (d, J = 1.5 Hz, 2H), 7.17 (d, J = 8 Hz, 2H), 7.11 (d, J = 7.5 Hz, 1H), 7.06 (d, J = 8 Hz, 2H), 6.93 (m, 4H), 6.62 (d, J = 7.5 Hz, 2H), 6.13 (d, J = 1.5 Hz, 2H), 5.70 (s, 1H), 4.36 (q, J = 7 Hz, 2H), 4.11 (q, J = 7 Hz, 2H), 1.37 (t, J = 7 Hz, 3H), 1.07 (t, J = 7 Hz, 3H); ¹³C NMR (CDCl₃, 125 MHz): δ 169.2, 166.8, 155.6, 144.8, 144.3, 136.7, 133.8, 132.8, 130.2, 129.9, 128.9, 127.6, 126.5, 124.3, 121.7, 119.6, 118.9, 114.9, 111.2, 61.6, 61.5, 36.2, 14.3, 13.9; HR-ESI-MS: m/z calcd for C₃₅H₃₀N₂NaO₅: 581.2052 [M + Na]⁺; found: 581.2049.

Diethyl 6-(bis(1-methyl-1*H*-indol-3-yl)methyl)-4'-hydroxy-[1,1'-biphenyl]-2,4-dicarboxylate (3b)

¹H NMR (CDCl₃, 500 MHz): δ 8.27 (d, J = 2 Hz, 1H), 8.22 (d, J = 1.5 Hz, 1H), 7.26 (d, J = 8 Hz, 2H), 7.17 (t, J = 7 Hz, 2H), 7.08 (d, J = 8 Hz, 2H), 7.03 (d, J = 8.5 Hz, 2H), 6.93 (t, J = 7 Hz, 2H), 6.66 (d, J = 8.5 Hz, 2H), 1.89 (s, 2H), 5.79 (s, 1H), 4.33 (q, J = 7 Hz, 2H), 4.07 (q, J = 7 Hz, 2H), 3.67 (s, 6H), 1.35 (t, J = 7 Hz, 3H), 1.03 (t, J = 7 Hz, 3H); ¹³C NMR (CDCl₃, 125 MHz): δ 168.9, 166.2, 155.4, 144.7, 144.6, 137.4, 133.6, 132.7, 130.6, 130.0, 129.2, 128.7, 127.0, 121.5, 119.7, 118.6, 117.8, 114.9, 109.0, 61.3, 61.2, 36.2, 32.7, 14.3, 13.8; HR-ESI-MS: m/z calcd for C₃₇H₃₄N₂NaO₅: 609.2365 [M + Na]⁺; found: 609.2359.

Diethyl 6-(bis(2-methyl-1H-indol-3-yl)methyl)-4'-hydroxy-[1,1'-biphenyl]-2,4-dicarboxylate (3c)

¹H NMR (CDCl₃, 500 MHz): δ 8.33 (d, J = 1.5 Hz, 1H), 8.28 (d, J = 1.5 Hz, 1H), 7.74 (s, 2H), 7.10 (d, J = 8 Hz, 2H), 6.98 (t, J = 7 Hz, 2H), 6.83 (m, 4H), 6.69 (d, J = 8.5 Hz, 2H), 6.52 (d, J = 8.5 Hz, 2H), 5.72 (s, 1H), 4.29 (q, J = 7 Hz, 2H), 4.00 (q, J = 7 Hz, 2H), 1.70 (s, 6H), 1.29 (t, J = 7 Hz, 3H), 0.98 (q, J = 7 Hz, 3H); ¹³C NMR (CDCl₃, 125 MHz): δ 168.6, 166.3, 155.1, 146.0, 144.6, 135.0, 133.6, 133.3, 132.3, 130.5, 129.5, 128.9, 128.8, 128.2, 120.5, 119.1, 118.8, 114.4, 112.5, 110.2, 61.3, 61.2, 37.2, 14.2, 13.8, 12.0; HR-ESI-MS: m/z calcd for C₃₇H₃₄N₂NaO₅: 609.2365 [M + Na]⁺; found: 609.2361.

Diethyl 6-(bis(5-methyl-1H-indol-3-yl)methyl)-4'-hydroxy-[1,1'-biphenyl]-2,4-dicarboxylate (3d)

¹H NMR (CDCl₃, 500 MHz): δ 8.26 (d, J = 1.5 Hz, 1H), 8.15 (d, J = 1.5 Hz, 1H), 7.82 (s, 2H), 7.08 (d, J = 8 Hz, 2H), 6.98 (d, J = 8.5 Hz, 1H), 6.93 (d, J = 8 Hz, 2H), 6.87 (s, 2H), 6.65 (d, J = 8.5 Hz, 2H), 6.19 (s, 2H), 5.67 (s, 1H), 4.36 (q, J = 7 Hz, 2H), 4.11 (q, J = 7 Hz, 2H), 2.31 (s, 6H), 1.37 (t, J = 7 Hz, 3H), 1.07 (t, J = 7 Hz, 3H); ¹³C NMR (CDCl₃, 125 MHz): δ 169.2, 166.7, 155.7, 144.7, 144.5, 135.0, 133.7, 133.0, 130.3, 130.0, 128.9, 128.0, 127.6, 126.8, 124.4, 123.3, 119.3, 118.5, 114.9, 110.9, 61.6, 61.5, 36.2, 21.4, 14.3, 13.9; HR-ESI-MS: m/z calcd for C₃₇H₃₄N₂NaO₅: 609.2365 [M + Na]⁺; found: 609.2282.

Diethyl 6-(bis(6-methyl-1H-indol-3-yl)methyl)-4'-hydroxy-[1,1'-biphenyl]-2,4-dicarboxylate (3e)

¹H NMR ((CD₃)₂CO, 500 MHz): δ 9.89 (s, 2H), 8.51 (bs, 1H), 8.22 (d, J = 2 Hz, 1H), 8.15 (d, J = 2 Hz, 1H), 7.17 (s, 2H), 7.05 (d, J = 8.5 Hz, 2H), 6.95 (d, J = 1.5 Hz, 1H), 6.95 (d, J = 8 Hz, 2H), 6.78 (d, J = 9 Hz, 2H), 6.69 (dd, J = 8, 1 Hz, 2H), 6.64 (d, J = 2.5 Hz, 2H), 5.81 (s, 1H), 4.27 (q, J = 7 Hz, 2H), 4.00 (q, J = 7 Hz, 2H), 2.35 (s, 6H), 1.28 (t, J = 7 Hz, 3H), 0.96 (t, J = 7 Hz, 3H); ¹³C NMR (CDCl₃, 125 MHz): δ 169.2, 166.4, 156.2, 144.8, 144.5, 137.2, 137.0, 133.7, 132.6, 131.4, 129.9, 128.9, 127.6, 124.5, 124.4, 123.6, 123.4, 120.5, 119.2, 119.0, 118.9, 114.8, 111.0, 110.9, 61.2, 36.4, 21.6, 14.2, 13.7; HR-ESI-MS: m/z calcd for C₃₇H₃₄N₂NaO₅: 609.2365 [M + Na]⁺; found: 609.2284.

Diethyl 6-(bis(5-methoxy-1*H*-indol-3-yl)methyl)-4'-hydroxy-[1,1'-biphenyl]-2,4-dicarboxylate (3f)

¹H NMR (CDCl₃, 500 MHz): δ 8.27 (d, *J* = 1.5 Hz, 1H), 8.17 (d, *J* = 2 Hz, 1H), 7.97 (d, *J* = 2 Hz, 2H), 7.09 (d, *J* = 9 Hz, 2H), 6.95 (d, *J* = 8.5 Hz, 2H), 6.76 (dd, *J* = 9, 2.5 Hz, 2H), 6.64 (d, *J* = 8.5 Hz, 2H), 6.48 (d, *J* = 2.5 Hz, 2H), 6.33 (d, *J* = 1.5 Hz, 2H), 5.60 (s, 1H), 4.35 (q, *J* = 7 Hz, 2H), 4.09 (q, *J* = 7 Hz, 2H), 3.65 (s, 6H), 1.36 (t, *J* = 7 Hz, 3H), 1.05 (t, *J* = 7 Hz, 3H); ¹³C NMR (CDCl₃, 125 MHz): δ 169.0, 166.6, 155.7, 153.4, 144.7, 144.5, 133.5, 132.8, 131.9, 130.3, 129.9, 129.0, 127.8, 126.9, 125.0, 118.6, 114.9, 111.8, 111.7, 101.5, 61.5, 61.4, 55.9, 36.2, 14.3, 13.8; HR-ESI-MS: *m/z* calcd for C₃₇H₃₄N₂NaO₇: 641.2264 [M + Na]⁺; found: 641.2262.

Diethyl 6-(bis(4-bromo-1*H*-indol-3-yl)methyl)-4'-hydroxy-[1,1'-biphenyl]-2,4-dicarboxylate(3g)

¹H NMR ((CD₃)₂CO, 500 MHz): δ 10.42 (s, 1H), 10.35 (s, 1H), 8.29 (bs, 1H), 8.15 (d, *J* = 2 Hz, 1H), 7.92 (d, *J* = 2 Hz, 1H), 7.41 (s, 2H), 7.21 (s, 1H), 7.07 (m, 3H), 6.94 (m, 2H), 6.87 (m, 1H), 6.70 (s, 1H), 6.69 (s, 1H), 6.44 (s, 1H), 6.26 (s, 1H), 4.25 (q, *J* = 6.5 Hz, 2H), 3.95 (q, *J* = 7 Hz, 2H), 1.27 (t, *J* = 7 Hz, 3H), 0.90 (t, *J* = 7 Hz, 3H); ¹³C NMR ((CD₃)₂CO, 125 MHz): δ 168.5, 165.4, 156.8, 146.5, 145.0, 135.3, 131.5, 129.6, 128.5, 127.1, 122.3, 114.2, 113.7, 110.9, 60.7, 60.5, 37.0, 13.6, 13.1; HR-ESI-MS: *m/z* calcd for C₃₅H₂₈Br₂N₂NaO₅: 737.0263 [M + Na]⁺; found: 737.0162.

Diethyl 6-(bis(5-bromo-1*H*-indol-3-yl)methyl)-4'-hydroxy-[1,1'-biphenyl]-2,4-dicarboxylate (3h)

¹H NMR ((CD₃)₂CO, 500 MHz): δ 10.37 (s, 2H), 8.63 (s, 1H), 8.20 (q, *J* = 1.5 Hz, 2H), 7.40 (d, *J* = 8.5 Hz, 2H), 7.30 (d, *J* = 1.5 Hz, 2H), 7.19 (dd, *J* = 9, 1.5 Hz, 2H), 7.05 (d, *J* = 9 Hz, 2H), 6.87 (d, *J* = 1.5 Hz, 2H), 6.84 (d, *J* = 8.5 Hz, 2H), 5.82 (s, 1H), 4.30 (q, *J* = 7 Hz, 2H), 4.03 (q, *J* = 7 Hz, 2H), 1.31 (t, *J* = 7 Hz, 3H), 0.99 (t, *J* = 7.5 Hz, 3H); ¹³C NMR ((CD₃)₂CO, 125 MHz): δ 167.9, 165.1, 157.3, 144.5, 144.0, 135.9, 134.6, 131.8, 129.9, 129.3, 129.2, 128.4, 127.4, 125.9, 124.2, 117.9, 114.8, 113.4, 111.6, 60.8, 60.7, 36.2, 13.6, 13.2; HR-ESI-MS: *m/z* calcd for C₃₅H₂₇Br₂N₂O₅⁺: 713.0281 [M - H]⁺; found: 713.0305.

Diethyl 6-(bis(6-bromo-1*H*-indol-3-yl)methyl)-4'-hydroxy-[1,1'-biphenyl]-2,4-dicarboxylate (3i)

¹H NMR ((CD₃)₂CO, 500 MHz): δ 10.26 (s, 2H), 8.51 (bs, 1H), 8.18 (d, $J = 2$ Hz, 1H), 8.15 (d, $J = 2$ Hz, 1H), 7.60 (s, 2H), 7.00 (m, 6H), 6.78 (m, 4H), 5.82 (s, 1H), 4.27 (q, $J = 7$ Hz, 2H), 4.00 (q, $J = 7$ Hz, 2H), 2.35 (s, 6H), 1.28 (t, $J = 7$ Hz, 3H), 0.96 (t, $J = 7$ Hz, 3H); ¹³C NMR ((CD₃)₂CO, 125 MHz): δ 168.7, 166.0, 158.0, 145.5, 145.1, 138.9, 135.4, 132.6, 130.8, 130.3, 130.1, 128.2, 126.5, 126.2, 122.6, 121.4, 119.5, 115.6, 115.5, 115.2, 61.7, 61.5, 37.2, 14.5, 14.1; HR-ESI-MS: m/z calcd for C₃₅H₂₈Br₂N₂NaO₅: 737.0263 [M + Na]⁺; found: 737.0155.

Diethyl 6-(bis(5-fluoro-1*H*-indol-3-yl)methyl)-4'-hydroxy-[1,1'-biphenyl]-2,4-dicarboxylate (3j)

¹H NMR ((CD₃)₂CO, 500 MHz): δ 10.22 (s, 2H), 8.53 (s, 1H), 8.20 (dd, $J = 12, 2$ Hz, 2H), 7.40 (dd, $J = 9, 4.5$ Hz, 2H), 7.05 (d, $J = 8.5$ Hz, 2H), 6.86 (m, 4H), 6.81 (d, $J = 8.5$ Hz, 2H), 6.71 (dd, $J = 9.5, 2$ Hz, 2H), 5.78 (s, 1H), 4.28 (q, $J = 7$ Hz, 2H), 4.01 (q, $J = 7$ Hz, 2H), 1.29 (t, $J = 7$ Hz, 3H), 0.97 (t, $J = 7$ Hz, 3H); ¹³C NMR ((CD₃)₂CO, 125 MHz): δ 167.9, 165.1, 158.1, 157.2, 156.3, 144.6, 144.3, 134.6, 133.8, 131.8, 129.9, 129.5, 129.2, 127.3, 126.9, 126.8, 126.3, 118.4, 118.3, 114.7, 112.5, 112.9, 109.7, 109.4, 103.6, 103.4, 60.8, 60.6, 36.5, 13.6, 13.2; HR-ESI-MS: m/z calcd for C₃₅H₂₈F₂N₂NaO₅: 617.1864 [M + Na]⁺; found: 617.1779.

Diethyl 6-(bis(6-chloro-1*H*-indol-3-yl)methyl)-4'-hydroxy-[1,1'-biphenyl]-2,4-dicarboxylate (3k)

¹H NMR ((CD₃)₂CO, 500 MHz): δ 10.25 (s, 2H), 8.50 (bs, 1H), 8.17 (dd, $J = 10.5, 1.5$ Hz, 2H), 7.44 (d, $J = 1.5$ Hz, 2H), 7.03 (m, 4H), 6.88 (dd, $J = 8.5, 2$ Hz, 2H), 6.79 (m, 4H), 5.82 (s, 1H), 4.27 (q, $J = 7$ Hz, 2H), 4.01 (q, $J = 7$ Hz, 2H), 1.28 (t, $J = 7$ Hz, 3H), 0.96 (t, $J = 7$ Hz, 3H); ¹³C NMR ((CD₃)₂CO, 125 MHz): δ 167.9, 165.1, 157.1, 144.7, 144.3, 137.6, 134.5, 131.7, 129.9, 129.4, 129.2, 127.3, 126.9, 125.4, 125.3, 120.1, 119.2, 118.6, 114.7, 111.3, 60.8, 60.6, 36.3, 13.6, 13.2; HR-ESI-MS: m/z calcd for C₃₅H₂₈Cl₂N₂NaO₅: 649.1273 [M + Na]⁺; found: 649.1274.

Diethyl 6-(bis(5-iodo-1*H*-indol-3-yl)methyl)-4'-hydroxy-[1,1'-biphenyl]-2,4-dicarboxylate (3l)

¹H NMR ((CD₃)₂CO, 500 MHz): δ 10.34 (s, 2H), 8.64 (s, 1H), 8.18 (m, 2H), 7.44 (s, 2H), 7.34 (dd, *J* = 8.5, 2 Hz, 2H), 7.28 (d, *J* = 8.5 Hz, 2H), 7.04 (d, *J* = 8.5 Hz, 2H), 6.86 (d, *J* = 9 Hz, 2H), 6.82 (s, 2H), 5.80 (s, 1H), 4.28 (q, *J* = 7 Hz, 2H), 4.02 (q, *J* = 7 Hz, 2H), 1.29 (t, *J* = 7 Hz, 3H), 0.97 (t, *J* = 7 Hz, 3H); ¹³C NMR ((CD₃)₂CO, 125 MHz): δ 167.9, 165.1, 157.4, 144.4, 144.1, 136.3, 134.6, 131.9, 129.9, 129.7, 129.4, 129.3, 127.7, 127.4, 125.4, 117.7, 114.9, 113.9, 81.7, 60.9, 60.7, 36.1, 13.6, 13.2; HR-ESI-MS: *m/z* calcd for C₃₅H₂₈I₂N₂NaO₅: 832.9985 [M + Na]⁺; found: 832.9880.

Diethyl 6-(bis(5-hydroxy-1*H*-indol-3-yl)methyl)-4'-hydroxy-[1,1'-biphenyl]-2,4-dicarboxylate (3m)

¹H NMR ((CD₃)₂CO, 500 MHz): δ 9.79 (s, 2H), 8.50 (bs, 1H), 8.19 (d, *J* = 1.5 Hz, 1H), 8.16 (d, *J* = 2 Hz, 1H), 7.54 (s, 2H), 7.21 (d, *J* = 8 Hz, 2H), 7.06 (d, *J* = 8.5 Hz, 2H), 6.77 (d, *J* = 8.5 Hz, 2H), 6.66 (dd *J* = 8.7, 2 Hz, 2H), 6.62 (d, *J* = 2 Hz, 2H), 6.51 (d, *J* = 2 Hz, 2H), 5.66 (s, 1H), 4.27 (q, *J* = 7 Hz, 2H), 4.00 (q, *J* = 7 Hz, 2H), 1.29 (t, *J* = 7 Hz, 3H), 0.96 (t, *J* = 7 Hz, 3H); ¹³C NMR ((CD₃)₂CO, 125 MHz): δ 169.0, 166.1, 157.9, 151.3, 145.8, 145.5, 135.3, 132.9, 132.8, 130.8, 130.5, 129.8, 128.3, 127.9, 125.7, 118.6, 115.4, 112.6, 112.4, 104.1, 61.6, 61.4, 37.6, 14.5, 14.1; HR-ESI-MS: *m/z* calcd for C₃₅H₃₀N₂NaO₇: 613.1951 [M + Na]⁺; found: 613.1866.

Diethyl 6-(bis(5-nitro-1*H*-indol-3-yl)methyl)-4'-hydroxy-[1,1'-biphenyl]-2,4-dicarboxylate (3n)

¹H NMR ((CD₃)₂CO, 500 MHz): δ 10.90 (s, 2H), 8.59 (bs, 1H), 8.22 (dd, *J* = 10.5, 2 Hz, 2H), 8.13 (d, *J* = 2 Hz, 2H), 8.03 (dd, *J* = 9, 2.5 Hz, 2H), 7.62 (d, *J* = 9 Hz, 2H), 7.16 (s, 2H), 7.11 (d, *J* = 8.5 Hz, 2H), 6.85 (d, *J* = 8.5 Hz, 2H), 6.08 (s, 1H), 4.29 (q, *J* = 7 Hz, 2H), 4.05 (q, *J* = 7 Hz, 2H), 1.29 (t, *J* = 7 Hz, 3H), 1.00 (t, *J* = 7 Hz, 3H); ¹³C NMR ((CD₃)₂CO, 125 MHz): δ 167.7, 164.9, 157.4, 144.7143.5, 141.2, 140.2, 134.7, 131.7, 129.9, 129.5, 129.2, 128.1, 127.7, 125.8, 120.5, 117.0, 115.9, 114.9, 112.0, 60.9, 60.7, 36.1, 13.6, 13.2; HR-ESI-MS: *m/z* calcd for C₃₅H₂₈N₄NaO₉: 671.1754 [M + Na]⁺; found: 671.1661.

Figure 4.5E. ^1H and ^{13}C -NMR of DIM-3aa

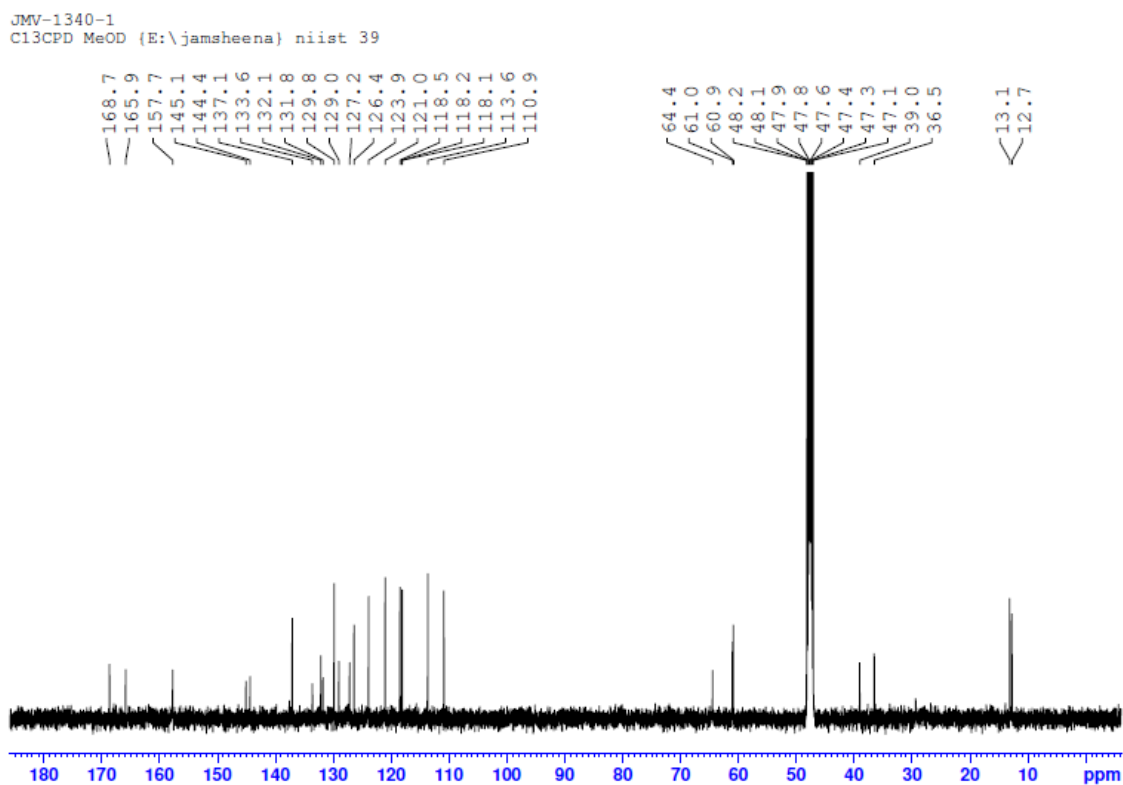
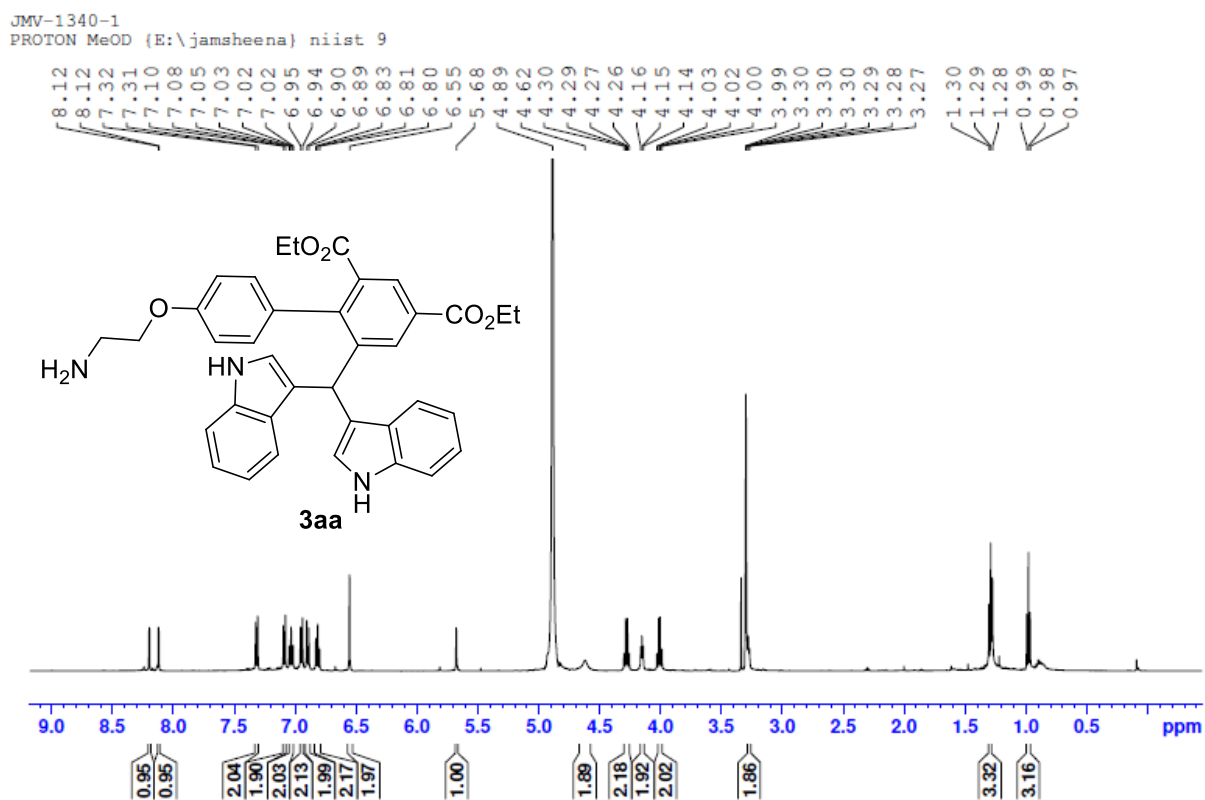
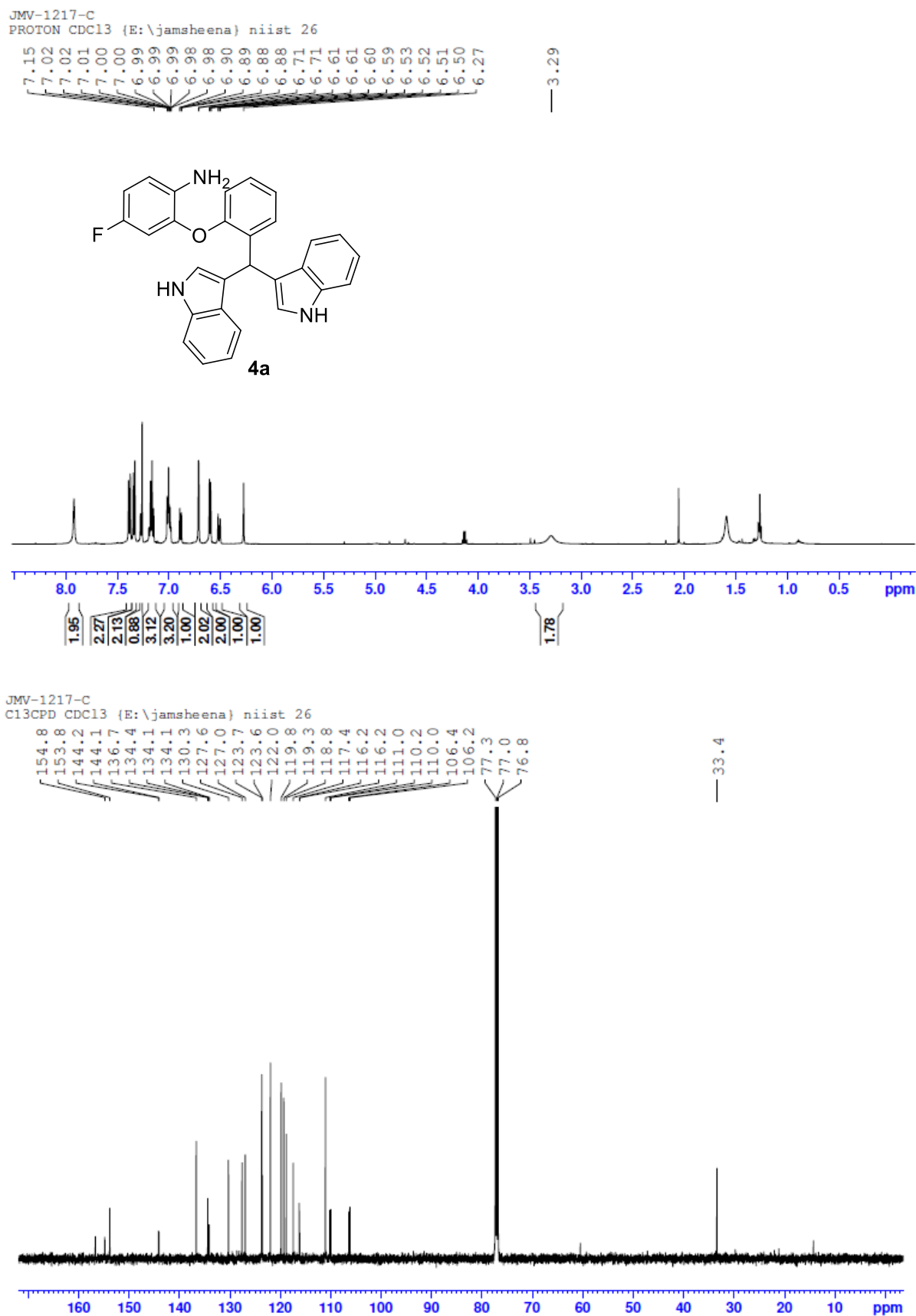


Figure 4.5F. ^1H and ^{13}C -NMR of DIM-4a



Diethyl 6-(bis(2-phenyl-1H-indol-3-yl)methyl)-4'-hydroxy-[1,1'-biphenyl]-2,4-dicarboxylate (3o)

¹H NMR ((CD₃)₂SO, 500 MHz): δ 10.85 (bs, 1H), 10.54 (bs, 1H), 8.69 (s, 1H), 7.84 (d, *J* = 2 Hz, 1H), 7.61 (d, *J* = 2 Hz, 1H), 6.90 (m, 6H), 6.75 (m, 4H), 6.56 (m, 4H), 6.39 (m, 4H), 6.18 (m, 6H), 5.73 (m, 2H), 5.46 (s, 1H), 5.09 (bs, 1H), 3.77 (m, 2H), 3.38 (q, *J* = 7 Hz, 2H), 0.74 (t, *J* = 7 Hz, 3H), 0.31 (t, *J* = 7 Hz, 3H); ¹³C NMR ((CD₃)₂CO, 125 MHz): δ 168.5, 166.0, 157.0, 146.7, 146.6, 135.7, 133.7, 129.7, 129.5, 129.1, 128.2, 119.7, 114.5, 111.9, 61.4, 61.0, 39.4, 14.2, 13.8; HR-ESI-MS: *m/z* calcd for C₄₇H₃₈N₂NaO₅: 733.2678 [M + Na]⁺; found: 733.2572.

Diethyl 4'-(2-((tert-butoxycarbonyl)amino)ethoxy)-6-(di(1H-indol-3-yl)methyl)-[1,1'-biphenyl]-2,4-dicarboxylate (9)

¹H NMR (CDCl₃, 500 MHz): δ 8.28 (d, *J* = 1.5 Hz, 1H), 8.16 (d, *J* = 1.5 Hz, 1H), 8.00 (bs, 2H), 7.30 (d, *J* = 8 Hz, 2H), 7.14 (d, *J* = 7.5 Hz, 2H), 7.07 (dd, *J* = 8, 2 Hz, 4H), 6.94 (d, *J* = 7.5 Hz, 2H), 6.76 (d, *J* = 8.5 Hz, 2H), 6.50 (s, 2H), 5.74 (s, 1H), 4.99 (bs, 1H), 4.32 (q, *J* = 7.5 Hz, 2H), 4.06 (q, *J* = 7 Hz, 2H), 3.96 (t, *J* = 4.5 Hz, 2H), 3.51 (q, *J* = 5 Hz, 2H), 1.45 (s, 9H), 1.34 (t, *J* = 7 Hz, 3H), 1.02 (t, *J* = 7 Hz, 3H); ¹³C NMR (CDCl₃, 125 MHz): δ 168.5, 166.5, 158.0, 156.0, 144.7, 144.3, 136.7, 133.6, 132.6, 131.2, 129.9, 129.1, 128.0, 126.5, 124.2, 121.8, 119.6, 119.1, 119.0, 113.9, 111.1, 79.6, 67.1, 61.4, 61.2, 40.1, 36.3, 28.4, 14.3, 13.9; HR-ESI-MS: *m/z* calcd for C₄₂H₄₃N₃NaO₇: 724.2999 [M + Na]⁺; found: 724.3009.

Diethyl 4'-(2-aminoethoxy)-6-(di(1H-indol-3-yl)methyl)-[1,1'-biphenyl]-2,4-dicarboxylate (3aa)

¹H NMR (CD₃OD, 500 MHz): δ 8.20 (d, *J* = 2 Hz, 1H), 8.12 (d, *J* = 2 Hz, 1H), 7.31 (d, *J* = 8 Hz, 2H), 7.09 (d, *J* = 9 Hz, 2H), 7.03 (t, *J* = 8 Hz, 2H), 6.95 (d, *J* = 8 Hz, 2H), 6.90 (d, *J* = 9 Hz, 2H), 6.81 (t, *J* = 7.5 Hz, 2H), 6.55 (s, 2H), 5.68 (s, 1H), 4.62 (bs, 2H), 4.28 (q, *J* = 7 Hz, 2H), 4.15 (t, *J* = 4.5 Hz, 2H), 4.01 (q, *J* = 7 Hz, 2H), 3.28 (m, 2H), 1.29 (t, *J* = 7 Hz, 3H), 0.98 (t, *J* = 7 Hz, 3H); ¹³C NMR (CD₃OD, 125 MHz): δ 168.7, 165.9, 157.7, 145.1, 144.4, 137.1, 133.6, 132.1, 131.8, 129.8, 129.0, 127.2, 126.4, 123.9, 121.0, 118.5, 118.2, 118.1, 113.6, 110.9, 64.4, 61.0, 60.9, 39.0, 36.5, 13.1, 12.7; HR-ESI-MS: *m/z* calcd for C₃₇H₃₅N₃NaO₅: 624.2474 [M + Na]⁺; found: 624.2482.

2-(2-(Di(1*H*-indol-3-yl)methyl)phenoxy)-4-fluoroaniline (4a)

¹H NMR (CDCl₃, 500 MHz): δ 7.92 (bs, 2H), 7.38 (d, $J = 8$ Hz, 2H), 7.34 (d, $J = 8.5$ Hz, 2H), 7.26 (m, 1H), 7.17 (m, 3H), 6.99 (m, 3H), 6.89 (dd, $J = 8$, 1 Hz, 1H), 6.71 (s, 1H), 6.70 (s, 1H), 6.60 (dd, $J = 7$, 1.5 Hz, 2H), 6.51 (td, $J = 9.5$, 1.5 Hz, 1H), 6.27 (s, 1H), 3.29 (bs, 2H); ¹³C NMR (CDCl₃, 125 MHz): δ 156.7, 154.8, 153.8, 144.2, 144.1, 136.7, 134.4, 134.1, 134.0, 130.3, 127.6, 127.0, 123.7, 123.6, 122.0, 119.8, 119.3, 118.8, 117.4, 116.2, 116.1, 111.0, 110.2, 110.0, 106.4, 106.2, 33.4; HR-ESI-MS: m/z calcd for C₂₉H₂₁FN₃O⁺: 446.1663 [M - H]⁺; found: 446.1681.

2-(2-(Bis(1-methyl-1*H*-indol-3-yl)methyl)-4-chlorophenoxy)-4-fluoroaniline (4b)

¹H NMR ((CD₃)₂CO, 500 MHz): δ 7.34 (m, 4H), 7.23 (m, 2H), 7.13 (t, $J = 7.5$ Hz, 2H), 6.92 (m, 3H), 6.83 (m, 2H), 6.75 (m, 2H), 6.65 (td, $J = 8.5$, 2.5 Hz, 1H), 6.43 (dd, $J = 9.5$, 2.5 Hz, 1H), 6.36 (s, 1H), 4.12 (bs, 2H), 3.75 (s, 6H); ¹³C NMR ((CD₃)₂CO, 125 MHz): δ 153.2, 152.9, 137.6, 137.2, 129.4, 128.4, 128.3, 127.6, 127.3, 121.4, 121.2, 119.4, 119.2, 119.1, 118.6, 116.3, 115.6, 110.5, 109.4, 106.6, 33.1, 31.9; HR-ESI-MS: m/z calcd for C₃₁H₂₆FN₃NaO: 498.1957 [M + Na]⁺; found: 498.1960.

2-(2-(Bis(5-methyl-1*H*-indol-3-yl)methyl)phenoxy)-4-fluoroaniline (4c)

¹H NMR ((CD₃)₂CO, 500 MHz): δ 9.89 (bs, 2H), 7.31 (d, $J = 7.5$ Hz, 1H), 7.26 (d, $J = 8.5$ Hz, 2H), 7.21 (t, $J = 7$ Hz, 1H), 7.15 (s, 2H), 7.02 (t, $J = 7.5$ Hz, 1H), 6.89 (m, 3H), 6.78 (m, 3H), 6.65 (td, $J = 8.5$, 3 Hz, 1H), 6.48 (dd, $J = 10$, 3 Hz, 1H), 6.29 (s, 1H), 4.15 (bs, 2H), 2.27 (s, 6H); ¹³C NMR ((CD₃)₂CO, 125 MHz): δ 154.1, 136.0, 135.6, 135.5, 130.3, 130.1, 127.3, 127.2, 127.1, 127.0, 124.0, 123.9, 123.2, 122.9, 122.8, 118.8, 118.0, 117.7, 117.6, 117.5, 115.6, 115.5, 111.0, 109.9, 109.8, 105.9, 105.7, 32.8, 20.7; HR-ESI-MS: m/z calcd for C₃₁H₂₆FN₃NaO: 498.1958 [M + Na]⁺; found: 498.1967.

2-(2-(Bis(6-methyl-1*H*-indol-3-yl)methyl)phenoxy)-4-fluoroaniline (4d)

¹H NMR ((CD₃)₂CO, 500 MHz): δ 9.86 (bs, 2H), 7.30 (dd, $J = 7.5$, 3 Hz, 1H), 7.22 (d, $J = 8$ Hz, 2H), 7.18 (m, 3H), 7.00 (t, $J = 7.5$ Hz, 1H), 6.84 (d, $J = 8$ Hz, 1H), 6.74 (m, 6H), 6.64 (td, $J = 8.5$, 3 Hz, 1H), 6.46 (dd, $J = 9.5$, 2.5 Hz, 1H), 6.30 (s, 1H), 4.14 (bs, 2H), 2.36 (s, 6H); ¹³C NMR ((CD₃)₂CO, 125 MHz): δ 155.6, 154.3, 153.8, 143.6, 143.5, 137.7, 136.1, 135.2, 130.5, 130.1, 128.2, 127.2, 126.9, 125.1, 123.2, 123.0, 120.2, 119.1, 118.9,

118.0, 117.0, 115.6, 111.2, 110.1, 109.9, 106.3, 106.1, 33.2, 20.9; HR-ESI-MS: m/z calcd for $C_{31}H_{26}FN_3NaO$: 498.1958 $[M + Na]^+$; found: 498.1962.

2-(2-(Bis(5-methoxy-1*H*-indol-3-yl)methyl)phenoxy)-4-fluoroaniline (4e)

1H NMR ($(CD_3)_2CO$, 500 MHz): δ 9.90 (bs, 2H), 7.34 (dd, $J = 8, 2$ Hz, 1H), 7.28 (d, $J = 9$ Hz, 2H), 7.22 (td, $J = 7.5, 1.5$ Hz, 1H), 7.04 (td, $J = 7.5, 1$ Hz, 1H), 6.90 (dd, $J = 8, 1$ Hz, 1H), 6.85 (s, 2H), 6.81 (s, 1H), 6.80 (s, 1H), 6.78 (dd, $J = 9, 6$ Hz, 1H), 6.72 (dd, $J = 8.5, 2.5$ Hz, 2H), 6.63 (td, $J = 8.5, 2.5$ Hz, 1H), 6.46 (dd, $J = 10, 3$ Hz, 1H), 6.24 (s, 1H), 4.17 (bs, 2H), 3.61 (s, 6H); ^{13}C NMR ($(CD_3)_2CO$, 125 MHz): δ 155.7, 154.1, 153.8, 153.5, 143.9, 143.8, 135.9, 135.3, 132.3, 130.2, 127.4, 127.3, 124.7, 123.3, 117.7, 117.6, 115.6, 111.9, 111.3, 109.9, 109.7, 105.7, 105.5, 101.1, 54.8, 33.2; HR-ESI-MS: m/z calcd for $C_{31}H_{26}FN_3NaO_3$: 530.1856 $[M + Na]^+$; found: 530.1871.

2-(2-(Bis(5-fluoro-1*H*-indol-3-yl)methyl)phenoxy)-4-fluoroaniline (4f)

1H NMR ($(CD_3)_2CO$, 500 MHz): δ 10.19 (bs, 2H), 7.39 (dd, $J = 8.5, 4.5$ Hz, 2H), 7.30 (dd, $J = 7.5, 1.5$ Hz, 1H), 7.04 (td, $J = 7.5, 1$ Hz, 1H), 6.99 (dd, $J = 10, 2.5$ Hz, 2H), 6.97 (s, 2H), 6.86 (m, 3H), 6.77 (dd, $J = 8.5, 5.5$ Hz, 1H), 6.63 (d, $J = 8.5, 3$ Hz, 1H), 6.40 (dd, $J = 9.5, 2.5$ Hz, 1H), 6.28 (s, 1H), 4.23 (bs, 2H); ^{13}C NMR ($(CD_3)_2CO$, 125 MHz): δ 158.9, 157.1, 156.4, 155.2, 154.6, 144.3, 144.2, 136.9, 135.3, 134.6, 130.8, 130.7, 128.5, 128.2, 128.1, 126.9, 126.8, 124.0, 118.7, 118.1, 116.5, 116.4, 113.2, 113.1, 113.0, 111.0, 119.8, 110.3, 110.1, 107.0, 106.8, 104.8, 104.5, 34.0; HR-ESI-MS: m/z calcd for $C_{29}H_{19}F_3N_3O^+$: 482.1475 $[M - H]^+$; found: 482.1492.

2-(2-(Bis(6-chloro-1*H*-indol-3-yl)methyl)phenoxy)-4-fluoroaniline (4g)

1H NMR ($(CD_3)_2CO$, 500 MHz): δ 10.23 (bs, 2H), 7.43 (s, 2H), 7.31 (d, $J = 8.5$ Hz, 2H), 7.27 (d, $J = 8$ Hz, 1H), 7.22 (t, $J = 8$ Hz, 1H), 7.03 (d, $J = 7.5$ Hz, 1H), 6.88 (m, 5H), 6.76 (dd, $J = 8.5, 5.5$ Hz, 1H), 6.63 (td, $J = 3, 8.5$ Hz, 1H), 6.40 (dd, $J = 9.5, 2.5$ Hz, 1H), 6.34 (s, 1H), 4.19 (bs, 2H); ^{13}C NMR ($(CD_3)_2CO$, 125 MHz): δ 154.3, 137.5, 136.1, 134.4, 129.9, 127.6, 126.7, 125.8, 125.1, 123.2, 120.4, 119.0, 118.1, 117.2, 115.7, 115.6, 111.2, 110.2, 110.0, 106.2, 106.0, 32.9; HR-ESI-MS: m/z calcd for $C_{29}H_{20}Cl_2FN_3NaO$: 538.0865 $[M + Na]^+$; found: 538.2076.

3,3'-((2-(2-Amino-5-fluorophenoxy)phenyl)methylene)bis(1H-indol-5-ol) (4h)

¹H NMR ((CD₃)₂CO, 500 MHz): δ 9.62 (bs, 2H), 7.40 (bs, 2H), 7.16 (dd, *J* = 7.5, 1.5 Hz, 2H), 7.07 (d, *J* = 8.5 Hz, 2H), 7.04 (dd, *J* = 8.5, 2 Hz, 1H), 6.86 (td, *J* = 8, 1 Hz, 1H), 6.68 (dd, *J* = 8.5, 1 Hz, 1H), 6.63 (m, 5H), 6.53 (dd, *J* = 8.5, 2 Hz, 2H), 6.50 (td, *J* = 8.5, 2.5 Hz, 1H), 6.35 (d, *J* = 10, 3 Hz, 1H), 6.07 (s, 1H), 4.00 (bs, 2H); ¹³C NMR ((CD₃)₂CO, 125 MHz): δ 155.6, 154.5, 150.4, 143.2, 136.3, 134.8, 132.0, 130.1, 127.9, 127.2, 124.5, 122.8, 117.2, 116.4, 115.6, 111.6, 111.4, 110.2, 106.6, 103.5, 33.2; HR-ESI-MS: *m/z* calcd for C₂₉H₂₂FN₃NaO₃: 502.1543 [M + Na]⁺; found: 502.1544.

2-(4-Chloro-2-(di(1H-indol-3-yl)methyl)phenoxy)-4-fluoroaniline (4i)

¹H NMR ((CD₃)₂CO, 500 MHz): δ 10.11 (bs, 2H), 7.41 (d, *J* = 8 Hz, 2H), 7.38 (d, *J* = 8 Hz, 2H), 7.26 (d, *J* = 3 Hz, 1H), 7.21 (dd, *J* = 7.5, 2.5 Hz, 1H), 7.08 (t, *J* = 7.5 Hz, 2H), 6.92 (t, *J* = 7.5 Hz, 2H), 6.92 (s, 2H), 6.83 (d, *J* = 8.5 Hz, 1H), 6.77 (dd, *J* = 8.5, 6.5 Hz, 1H), 6.67 (td, *J* = 8.5, 3 Hz, 1H), 6.50 (dd, *J* = 9.5, 2.5 Hz, 1H), 6.40 (s, 1H), 4.15 (bs, 2H); ¹³C NMR (CDCl₃, 125 MHz): δ 156.6, 152.6, 143.6, 143.5, 136.7, 136.3, 134.2, 130.0, 128.6, 127.6, 126.8, 123.7, 122.2, 119.6, 119.5, 118.4, 118.1, 116.5, 116.5, 111.1, 110.8, 106.7, 106.5, 33.2; HR-ESI-MS: *m/z* calcd for C₂₉H₂₀ClFN₃O⁺: 480.1273 [M - H]⁺; found: 480.1295.

2-(2-(Bis(1-methyl-1H-indol-3-yl)methyl)-4-chlorophenoxy)-4-fluoroaniline (4j)

¹H NMR ((CD₃)₂CO, 500 MHz): δ 7.36 (m, 4H), 7.25 (d, *J* = 2.5 Hz, 1H), 7.22 (dd, *J* = 8.5, 2.5 Hz, 1H), 7.14 (t, *J* = 7.5 Hz, 2H), 6.93 (d, *J* = 7.5 Hz, 2H), 6.83 (m, 2H), 6.74 (m, 2H), 6.65 (td, *J* = 8.5, 2.5 Hz, 1H), 6.43 (dd, *J* = 9.5, 2.5 Hz, 1H), 6.35 (s, 1H), 4.13 (bs, 2H), 3.76 (s, 6H); ¹³C NMR ((CD₃)₂CO, 125 MHz): δ 137.6, 137.2, 129.4, 128.4, 128.3, 127.2, 121.4, 121.2, 119.4, 119.2, 118.6, 118.4, 116.3, 115.7, 110.6, 110.5, 109.4, 106.5, 33.1, 31.9; HR-ESI-MS: *m/z* calcd for C₃₁H₂₅ClFN₃NaO: 532.1568 [M + Na]⁺; found: 532.1574.

2-(2-(Bis(5-methyl-1H-indol-3-yl)methyl)-4-chlorophenoxy)-4-fluoroaniline (4k)

¹H NMR ((CD₃)₂CO, 500 MHz): δ 9.93 (bs, 2H), 7.24 (m, 3H), 7.20 (m, 3H), 6.81 (m, 3H), 6.75 (m, 3H), 6.68 (td, *J* = 8.5, 3 Hz, 1H), 6.51 (dd, *J* = 9.5, 3 Hz, 1H), 6.33 (s, 1H), 4.14 (bs, 2H), 2.37 (s, 6H); ¹³C NMR ((CD₃)₂CO, 125 MHz): δ 155.6, 153.7, 153.4, 142.7, 137.7, 136.4, 130.8, 129.5, 127.4, 127.1, 124.9, 123.4, 120.4, 118.9, 117.9, 117.2,

115.9, 111.3, 110.8, 106.8, 33.3, 20.9; HR-ESI-MS: m/z calcd for $C_{31}H_{25}ClFN_3NaO$: 532.1568 $[M + Na]^+$; found: 532.1570.

2-(2-(Bis(6-methyl-1*H*-indol-3-yl)methyl)-4-chlorophenoxy)-4-fluoroaniline (4l)

1H NMR ($(CD_3)_2CO$, 500 MHz): δ 9.96 (bs, 2H), 7.28 (m, 3H), 7.22 (m, 3H), 6.91 (m, 3H), 6.84 (m, 3H), 6.68 (td, $J = 8.5$, 3 Hz, 1H), 6.52 (dd, $J = 9.5$, 3 Hz, 1H), 6.33 (s, 1H), 2.29 (s, 6H); ^{13}C NMR ($(CD_3)_2CO$, 125 MHz): δ 155.5, 153.7, 153.2, 149.7, 137.6, 136.2, 135.6, 129.6, 127.6, 127.4, 127.2, 124.1, 123.1, 118.7, 118.5, 116.9, 115.9, 111.2, 110.6, 106.4, 32.9, 20.7; HR-ESI-MS: m/z calcd for $C_{31}H_{25}ClFN_3NaO$: 532.1568 $[M + Na]^+$; found: 532.1565.

2-(2-(Bis(5-methoxy-1*H*-indol-3-yl)methyl)-4-chlorophenoxy)-4-fluoroaniline (4m)

1H NMR ($(CD_3)_2CO$, 500 MHz): δ 9.98 (bs, 2H), 7.30 (d, $J = 9$ Hz, 2H), 7.29 (s, 1H), 7.23 (dd, $J = 9$, 3 Hz, 1H), 6.92 (s, 1H), 6.91 (s, 1H), 6.87 (d, $J = 8.5$ Hz, 1H), 6.85 (s, 1H), 6.84 (s, 1H), 6.79 (dd, $J = 8.5$, 5.5 Hz, 1H), 6.75 (dd, $J = 8.5$, 2.5 Hz, 2H), 6.68 (td, $J = 8.5$, 3 Hz, 1H), 6.50 (dd, $J = 9.5$, 2.5 Hz, 1H), 6.27 (s, 1H), 4.17 (bs, 2H), 3.64 (s, 6H); ^{13}C NMR ($(CD_3)_2CO$, 125 MHz): δ 155.6, 153.7, 153.7, 153.2, 143.0, 137.4, 136.2, 132.3, 129.6, 127.7, 127.3, 127.2, 124.8, 118.6, 116.8, 115.9, 112.1, 111.5, 110.6, 106.2, 101.0, 54.8, 33.4; HR-ESI-MS: m/z calcd for $C_{31}H_{25}ClFN_3NaO_3$: 564.1466 $[M + Na]^+$; found: 564.1479.

2-(2-(Bis(5-fluoro-1*H*-indol-3-yl)methyl)-4-chlorophenoxy)-4-fluoroaniline (4n)

1H NMR ($(CD_3)_2CO$, 500 MHz): δ 10.25 (bs, 2H), 7.41 (dd, $J = 9$, 4.5 Hz, 2H), 7.24 (m, 2H), 7.03 (m, 4H), 6.87 (m, 3H), 6.78 (dd, $J = 8.5$, 6 Hz, 1H), 6.66 (td, $J = 8.5$, 3 Hz, 1H), 6.45 (dd, $J = 9.5$, 2.5 Hz, 1H), 6.31 (s, 1H), 4.22 (bs, 2H); ^{13}C NMR ($(CD_3)_2CO$, 125 MHz): δ 158.2, 156.4, 153.4, 136.5, 136.3, 133.8, 129.5, 129.3, 127.5, 127.4, 127.3, 127.2, 127.1, 126.6, 126.1, 118.7, 118.3, 117.2, 117.1, 115.9, 115.8, 112.5, 112.4, 110.9, 110.8, 110.7, 109.6, 109.4, 106.7, 103.8, 103.6, 103.5, 33.2; HR-ESI-MS: m/z calcd for $C_{29}H_{18}ClF_3N_3O^+$: 516.1085 $[M - H]^+$; found: 516.1075.

2-(2-(Bis(6-chloro-1*H*-indol-3-yl)methyl)phenoxy)-4-fluoroaniline (4o)

1H NMR ($(CD_3)_2CO$, 500 MHz): δ 10.30 (bs, 2H), 7.46 (s, 2H), 7.34 (d, $J = 8.5$ Hz, 2H), 7.23 (dd, $J = 8.5$, 2.5 Hz, 1H), 7.20 (d, $J = 2.5$ Hz, 1H), 6.97 (s, 2H), 6.93 (dd, $J = 8.5$, 1.5

Hz, 2H), 6.84 (d, $J = 8.5$ Hz, 1H), 6.77 (dd, $J = 8.5, 5.5$ Hz, 1H), 6.67 (td, $J = 8.5, 2.5$ Hz, 1H), 6.46 (dd, $J = 9, 2.5$ Hz, 1H), 6.37 (s, 1H), 4.19 (bs, 2H); ^{13}C NMR ($(\text{CD}_3)_2\text{CO}$, 125 MHz): δ 155.6, 153.7, 153.4, 142.6, 137.6, 136.4, 136.3, 129.3, 127.6, 127.5, 126.9, 125.6, 125.2, 120.3, 119.2, 118.2, 117.3, 115.9, 111.3, 110.9, 106.6, 33.0; HR-ESI-MS: m/z calcd for $\text{C}_{29}\text{H}_{18}\text{Cl}_3\text{FN}_3\text{O}^+$: 548.0494 $[\text{M} - \text{H}]^+$; found: 548.0496.

3,3'-((2-(2-Amino-5-fluorophenoxy)-5-chlorophenyl)methylene)bis(1H-indol-5-ol)
(4p)

^1H NMR ($(\text{CD}_3)_2\text{CO}$, 500 MHz): δ 9.84 (bs, 2H), 7.57(m, 2H), 7.21 (m, 4H), 6.78 (m, 6H), 6.68 (m, 3H), 6.52 (dd, $J = 8.5, 3$ Hz, 1H), 6.20 (s, 1H), 4.13 (s, 1H); ^{13}C NMR ($(\text{CD}_3)_2\text{CO}$, 125 MHz): δ 153.7, 153.6, 150.7, 136.9, 136.5, 132.0, 129.5, 127.7, 127.2, 127.0, 124.6, 117.5, 116.4, 116.0, 115.9, 111.8, 111.6, 111.4, 111.4, 111.0, 110.8, 107.2, 107.0, 103.3, 33.3; HR-ESI-MS: m/z calcd for $\text{C}_{29}\text{H}_{20}\text{ClFN}_3\text{O}_3^+$: 512.1172 $[\text{M} - \text{H}]^+$; found: 512.0988.

4.6. References

- (1) (a) Sharma, V.; Kumar, P.; Pathak, D. Biological importance of the indole nucleus in recent years: A comprehensive review. *J. Heterocycl. Chem.* **2010**, *47*, 491–502. (b) Lalit, K.; Shashi, B.; Kamal, J. The diverse pharmacological importance of indole derivatives : A review. *Int. J. Res. Pharm. Sci.* **2012**, *2*, 23–33. (c) Naim, M. J.; Alam, O.; Alam, J.; Bano, F.; Alam, P.; Shrivastava, N. Recent review on indole: A privileged scaffold structure. *Int. J. Pharma Sci. Res.* **2016**, *7*, 51–62. (d) Patil, R.; Patil, S. A.; Beaman, K. D.; Patil, S. A. Indole molecules as inhibitors of tubulin polymerization: potential new anticancer agents, an update (2013–2015). *Future Med. Chem.* **2016**, *8*, 1291–1316. (e) Sulthana, S.; Pandian, P. A review on indole and benzothiazole derivatives its importance. *J. Drug Deliv. Ther.* **2019**, *9*, 505–509.
- (2) (a) Aggarwal, B. B.; Ichikawa, H. Molecular targets and anticancer potential of indole-3-carbinol and its derivatives. *Cell Cycle* **2005**, *4*, 1201–1215. (b) Maruthanila, V. L.; Poornima, J.; Mirunalini, S. Attenuation of carcinogenesis and the mechanism underlying by the influence of indole-3-carbinol and its metabolite 3,3'-diindolylmethane: a therapeutic marvel. *Adv. Pharmacol. Sci.* **2014**, *2014*, 1–7. (c) Thomson, C. A.; Ho, E.; Strom, M. B. Chemopreventive properties of 3,3'-

- diindolylmethane in breast cancer: evidence from experimental and human studies. *Nutr. Rev.* **2016**, *74*, 432–443. (d) Kim, S. Cellular and molecular mechanisms of 3,3'-diindolylmethane in gastrointestinal cancer. *Int. J. Mol. Sci.* **2016**, *17*, 1155–1167. (e) Weiben, W.; Feng, Z.; Narod, S. A. Multiple therapeutic and preventive effects of 3,3'-diindolylmethane on cancers including prostate cancer and high grade prostatic intraepithelial neoplasia. *J. Biomed. Res.* **2014**, *28*, 339–348. (f) Weng, J.-R.; Tsai, C.-H.; Kulp, S. K.; Chen, C.-S. Indole-3-carbinol as a chemopreventive and anti-cancer agent. *Cancer Lett.* **2008**, *262*, 153–163. (g) Bradlow, H. L. Indole-3-carbinol as a chemoprotective agent in breast and prostate cancer. *in vivo.* **2008**, *22*, 441–445. (h) Fujioka, N.; Fritz, V.; Upadhyaya, P.; Kassie, F.; Hecht, S. S. Research on cruciferous vegetables, indole-3-carbinol, and cancer prevention: a tribute to Lee W. Wattenberg. *Mol. Nutr. Food Res.* **2016**, *60*, 1228–1238.
- (3) (a) Murillo, G.; Mehta, R. G. Cruciferous vegetables and cancer prevention. *Nutr. Cancer* **2001**, *41*, 17–28. (b) Higdon, J. V.; Delage, B.; Williams, D. E.; Dashwood, R. H. Cruciferous vegetables and human cancer risk: epidemiologic evidence and mechanistic basis. *Pharmacol. Res.* **2007**, *55*, 224–236. (c) Royston, K. J.; Tollefsbol, T. O. The epigenetic impact of cruciferous vegetables on cancer prevention. *Curr. Pharmacol. Reports* **2015**, *1*, 46–51.
- (4) Wattenberg, L. W. Inhibition of polycyclic aromatic hydrocarbon-induced neoplasia by naturally occurring indoles. *Cancer Res.* **1978**, *38*, 1410–1413.
- (5) <https://www.diindolylmethane-dim.com>.
- (6) (a) Kassouf, W.; Chintharlapalli, S.; Abdelrahim, M.; Nelkin, G.; Safe, S.; Kamat, A. M. Inhibition of bladder tumor growth by 1,1-bis(3'-indolyl)-1-(*p*-substitutedphenyl) methanes: a new class of peroxisome proliferator-activated receptor γ agonists. *Cancer Res.* **2006**, *66*, 412–419. (b) Chintharlapalli, S.; Smith, R.; Samudio, I.; Zhang, W.; Safe, S. 1,1-Bis(3'-indolyl)-1-(*p*-substitutedphenyl)methanes induce peroxisome proliferator-activated receptor γ -mediated growth inhibition, transactivation, and differentiation markers in colon cancer cells. *Cancer Res.* **2004**, *64*, 5994–6001. (c) Qin, C.; Morrow, D.; Stewart, J.; Spencer, K.; Porter, W.; Smith, R.; Phillips, T.; Abdelrahim, M.; Samudio, I.;

- Safe, S. A new class of peroxisome proliferator-activated receptor γ (PPAR γ) agonists that inhibit growth of breast cancer cells: 1,1-bis(3'-indolyl)-1-(*p*-substituted phenyl) methanes. *Mol. Cancer Ther.* **2004**, *3*, 247–260.
- (7) Pal, C.; Dey, S.; Mahato, S. K.; Vinayagam, J.; Pradhan, P. K.; Giri, V. S.; Jaisankar, P.; Hossain, T.; Baruri, S.; Ray, D.; Biswas, S. M. Eco-friendly synthesis and study of new plant growth promoters: 3,3'-diindolylmethane and its derivatives. *Bioorganic Med. Chem. Lett.* **2007**, *17*, 4924–4928.
- (8) Roy, A.; Chowdhury, S.; Sengupta, S.; Mandal, M.; Jaisankar, P.; D'Annessa, I.; Desideri, A.; Majumder, H. K. Development of derivatives of 3,3'-diindolylmethane as potent *Leishmania donovani* bi-subunit topoisomerase IB poisons. *PLoS One* **2011**, *6*, e28493.
- (9) (a) Roy, S.; Gajbhiye, R.; Mandal, M.; Pal, C.; Meyyapan, A.; Mukherjee, J.; Jaisankar, P. Synthesis and antibacterial evaluation of 3,3'-diindolylmethane derivatives. *Med. Chem. Res.* **2014**, *23*, 1371–1377. (b) Sung, W. S.; Lee, D. G. *In vitro* antimicrobial activity and the mode of action of indole-3-carbinol against human pathogenic microorganisms. *Biol. Pharm. Bull.* **2007**, *30*, 1865–1869. (c) Ko, M.-O.; Kim, M.-B.; Lim, S.-B. Relationship between chemical structure and antimicrobial activities of isothiocyanates from cruciferous vegetables against oral pathogens. *J. Microbiol. Biotechnol.* **2016**, *26*, 2036–2042. (d) Kumar, G. S. S.; Kumaresan, S.; Prabhu, A. A. M.; Bhuvanesh, N.; Seethalakshmi, P. G. An efficient one pot syntheses of aryl-3,3'-bis(indolyl)methanes and studies on their spectral characteristics, DPPH radical scavenging-, antimicrobial-, cytotoxicity-, and antituberculosis activity. *Spectrochim. Acta - Part A Mol. Biomol. Spectrosc.* **2013**, *101*, 254–263.
- (10) (a) Bhowmik, A.; Das, N.; Pal, U.; Mandal, M.; Bhattacharya, S.; Sarkar, M.; Jaisankar, P.; Maiti, N. C.; Ghosh, M. K. 2,2'-Diphenyl-3,3'-diindolylmethane: A potent compound induces apoptosis in breast cancer cells by inhibiting EGFR pathway. *PLoS One* **2013**, *8*, e59798. (b) Andey, T.; Patel, A.; Jackson, T.; Safe, S.; Singh, M. 1,1-Bis(3'-indolyl)-1-(*p*-substitutedphenyl)methane compounds inhibit lung cancer cell and tumor growth in a metastasis model. *Eur. J. Pharm. Sci.* **2013**, *50*, 227–241. (c) Ichite, N.; Chougule, M.; Patel, A. R.; Jackson, T.; Safe, S.; Singh, M. Inhalation delivery of a novel diindolylmethane derivative for

- the treatment of lung cancer. *Mol. Cancer Ther.* **2010**, *9*, 3003–3015.
- (11) (a) Bringmann, G.; Menche, D.; Bezabih, M.; Abegaz, B. M.; Kaminsky, R. Antiplasmodial activity of knipholone and related natural phenylanthraquinones. *Planta Med.* **1999**, *65*, 757–758. (b) Goa, K. L.; Wagstaff, A. J. Losartan potassium a review of its pharmacology, clinical efficacy and tolerability in the management of hypertension. *Drugs* **1996**, *51*, 820–845. (c) Bringmann, G.; Gulder, T.; Gulder, T. A. M.; Breuning, M. Atroposelective total synthesis of axially chiral biaryl natural products. *Chem. Rev.* **2011**, *111*, 563–639.
- (12) Santoshi, S.; Manchukonda, N. K.; Suri, C.; Sharma, M.; Sridhar, B.; Joseph, S.; Lopus, M.; Kantevari, S.; Baitharu, I.; Naik, P. K. Rational design of biaryl pharmacophore inserted noscapine derivatives as potent tubulin binding anticancer agents. *J. Comput. Aided. Mol. Des.* **2015**, *29*, 249–270.
- (13) McNulty, J.; van den Berg, S.; Ma, D.; Tarade, D.; Joshi, S.; Church, J.; Pandey, S. Antimitotic activity of structurally simplified biaryl analogs of the anticancer agents colchicine and combretastatin A4. *Bioorg. Med. Chem. Lett.* **2015**, *25*, 117–121.
- (14) Challa, C.; Vellekkatt, J.; Ravindran, J.; Lankalapalli, R. S. A metal-free one-pot cascade synthesis of highly functionalized biaryl-2-carbaldehydes. *Org. Biomol. Chem.* **2014**, *12*, 8588–8592.
- (15) (a) Patel, A. R.; Doddapaneni, R.; Andey, T.; Wilson, H.; Safe, S.; Singh, M. Evaluation of self-emulsified DIM-14 in dogs for oral bioavailability and in Nu/Nu mice bearing stem cell lung tumor models for anticancer activity. *J. Control. Release* **2015**, *213*, 18–26. (b) Goldberg, A. A.; Draz, H.; Montes-Grajales, D.; Olivero-Verbél, J.; Safe, S. H.; Sanderson, J. T. 3,3'-Diindolylmethane (DIM) and its ring-substituted halogenated analogs (ring-DIMs) induce differential mechanisms of survival and death in androgen-dependent and -independent prostate cancer cells. *Genes Cancer* **2015**, *6*, 265–280. (c) Draz, H.; Goldberg, A. A.; Titorenko, V. I.; Tomlinson, E. S.; Safe, S. H.; Sanderson, J. T. Diindolylmethane and its halogenated derivatives induce protective autophagy in human prostate cancer cells *via* induction of the oncogenic protein AEG-1 and activation of AMP-dependent kinase (AMPK). *Cell. Signal.* **2017**, *40*, 172–182. (d)

- Godugu, C.; Doddapaneni, R.; Safe, S. H.; Singh, M. Novel diindolylmethane derivatives based NLC formulations to improve the oral bioavailability and anticancer effects in triple negative breast cancer. *Eur. J. Pharm. Biopharm.* **2016**, *108*, 168–179. (e) Afzali, M. F.; Popichak, K. A.; Burton, L. H.; Klochak, A. L.; Wilson, W. J.; Safe, S.; Tjalkens, R. B.; Legare, M. E. A novel diindolylmethane analog, 1,1-bis(3'-indolyl)-1-(p-chlorophenyl)methane, inhibits the tumor necrosis factor-induced inflammatory response in primary murine synovial fibroblasts through a Nurr1-dependent mechanism. *Mol. Immunol.* **2018**, *101*, 46–54. (f) Kim, K.; Li, X.; Lee, S. NR4A orphan receptors and cancer. *Nucl. Recept. Signal.* **2011**, *9*, e002. (g) Abdelrahim, M.; Newman, K.; Vanderlaag, K.; Samudio, I.; Safe, S. 3,3'-Diindolylmethane (DIM) and its derivatives induce apoptosis in pancreatic cancer cells through endoplasmic reticulum stress-dependent upregulation of DR5. *Carcinogenesis* **2006**, *27*, 717–728. (h) Lee, S.; Li, X.; Khan, S.; Safe, S. Targeting NR4A1 (TR3) in cancer cells and tumors. *Expert Opin. Ther. Targets* **2011**, *15*, 195–206. (i) Shin, J.; Shim, J.; Choi, E.; Leem, D.; Han, K.; Lee, S.; Safe, S.; Cho, N.; Cho, S. Chemopreventive effects of synthetic C-substituted diindolylmethanes originating from cruciferous vegetables in human oral cancer cells. *Eur. J. Cancer Prev.* **2011**, *20*, 417–425. (j) Safe, S.; Papineni, S.; Chintharlapalli, S. Cancer chemotherapy with indole-3-carbinol, bis(3'-indolyl)methane and synthetic analogs. *Cancer Lett.* **2008**, *269*, 326–338.
- (16) (a) Calabrò, P.; Samudio, I.; Safe, S. H.; Willerson, J. T.; Yeh, E. T. H. Inhibition of tumor-necrosis- α induced endothelial cell activation by a new class of PPAR- γ agonists. *J. Vasc. Res.* **2005**, *42*, 509–516. (b) Praveen, C.; DheenKumar, P.; Muralidharan, D.; Perumal, P. T. Synthesis, antimicrobial and antioxidant evaluation of quinolines and bis(indolyl)methanes. *Bioorg. Med. Chem. Lett.* **2010**, *20*, 7292–7296.
- (17) Torre, L. A.; Islami, F.; Siegel, R. L.; Ward, E. M.; Jemal, A. Global cancer in women: burden and trends. *Cancer Epidemiol. Biomarkers Prev.* **2017**, *26*, 444–457.
- (18) Bray, F.; Ferlay, J.; Soerjomataram, I.; Siegel, R. L.; Torre, L. A.; Jemal, A. Global cancer statistics 2018: GLOBOCAN estimates of incidence and mortality worldwide for 36 cancers in 185 countries. *CA. Cancer J. Clin.* **2018**, *68*, 394–424.

- (19) (a) Jhan, J.; Andrechek, E. R. Triple-negative breast cancer and the potential for targeted therapy. *Pharmacogenomics* **2017**, *18*, 1595–1609. (b) Mayer, E. L.; Burstein, H. J. Chemotherapy for triple-negative breast cancer: is more better? *J. Clin. Oncol.* **2016**, *34*, 3369–3371. (c) O'Toole, S. A.; Beith, J. M.; Millar, E. K. A.; West, R.; McLean, A.; Cazet, A.; Swarbrick, A.; Oakes, S. R. Therapeutic targets in triple negative breast cancer. *J. Clin. Pathol.* **2013**, *66*, 530–542. (d) Marotti, J. D.; de Abreu, F. B.; Wells, W. A.; Tsongalis, G. J. Triple negative breast cancer: next generation sequencing for target identification. *Am. J. Pathol.* **2017**, *187*, 2133–2138.
- (20) Chakraborty, S.; Ghosh, S.; Banerjee, B.; Santra, A.; Adhikary, A.; Misra, A. K.; Sen, P. C. Phemindole, a synthetic di-indole derivative maneuvers the store operated calcium entry (SOCE) to induce potent anti-carcinogenic activity in human triple negative breast cancer cells. *Front. Pharmacol.* **2016**, *7*, 1–21.
- (21) (a) Gillis, E. P.; Eastman, K. J.; Hill, M. D.; Donnelly, D. J.; Meanwell, N. A. Applications of fluorine in medicinal chemistry. *J. Med. Chem.* **2015**, *58*, 8315–8359. (b) Purser, S.; Moore, P. R.; Swallow, S.; Gouverneur, V. Fluorine in medicinal chemistry. *Chem. Soc. Rev.* **2008**, *37*, 320–330. (c) Maienfisch, P.; Hall, R. G. The importance of fluorine in the life science industry. *Chimia.* **2004**, *58*, 93–99. (d) Shah, P.; Westwell, A. D. The role of fluorine in medicinal chemistry. *J. Enzyme Inhib. Med. Chem.* **2007**, *22*, 527–540.
- (22) Jamsheena, V.; Mahesha, C. K.; Joy, M. N.; Lankalapalli, R. S. Metal-free diaryl etherification of tertiary amines by *ortho* -C(sp²)-H functionalization for synthesis of dibenzoxazepines and -ones. *Org. Lett.* **2017**, *19*, 6614–6617.
- (23) Pradhan, P. K.; Dey, S.; Giri, V. S.; Jaisankar, P. InCl₃-HMTA as a methylene donor: one-pot synthesis of diindolylmethane (DIM) and its derivatives. *Synthesis.* **2005**, *2005*, 1779–1782.
- (24) Mosmann, T. Rapid colorimetric assay for cellular growth and survival: application to proliferation and cytotoxicity assays. *J. Immunol. Methods* **1983**, *65*, 55–63.

Summary and conclusion

Chapter 1 gives an overview of heterocycles and their importance in drug discovery along with a brief history of 1,2-dihydropyridines (DHPs), dibenzoxazepines and diindolylmethanes (DIMs). 1,2-DHPs are widely used as precursor scaffold for the preparation of many biologically active compounds. Cyclization reactions (Hantzsch ring closure), reduction or nucleophilic addition of pyridinium ions and pericyclic reactions are commonly employed for the synthesis of 1,2-DHPs. Dibenzoxazepine and dibenzoxazepinones belong to a class of seven-member heterocyclic compounds fused with two benzene rings. They possess a broad range of biological activities such as anti-HIV, antitumor, antioxidant, oral contraceptive, TRPA1 agonist, sodium channel blocker, CNS depressant, etc. Researchers have extensively studied the pharmacological properties of various dibenzoxazepine derivatives and over the years, various approaches have been developed for the synthesis of dibenzoxazepine core skeleton. Base promoted nucleophilic aromatic substitution (S_NAr) is a classical method employed for the construction of the seven-membered ring via Smiles rearrangement of suitable substrates by a domino C-O and C-N bond formation. 3,3'-Diindolylmethane (DIM) is an active metabolite of indole-3-carbinol, a glucosinolate conjugate present in various *Brassica* vegetables such as cabbage, broccoli, brussels, sprouts, etc. DIM compounds have been reported extensively as promising anticancer agents due to its low toxicity and cytotoxic ability to inhibit the growth of a multitude of cancer cell types both *in vitro* and *in vivo*. They have garnered considerable medicinal interest due to their potential therapeutic effect against different cancers.

Chapter 2 comprise design, synthesis and application of new 1,2-dihydropyridine (1,2-DHP) based fluorophores. Small molecule based organic fluorophores are of primary interest which can be used for sensing and bio-imaging due to their selectivity, high sensitivity, fast response and the validity of quantitative information on the subcellular distribution for the molecules of interest. Even though a number of fluorophores, particularly heterocyclic scaffolds are reported, only a few exhibit optimal performance while majority of them suffer from various limitations for advanced applications in biology. A four-component condensation reaction using dienaminodioxide, aldehyde, an *in situ* generated hydrazone in presence of trifluoroacetic acid, modification of our previous report, was employed for the synthesis. The design offers various sites for appendage to bioactives or functionalities required for conjugation. The photophysical properties of

1,2-DHPs were studied in detail, which led to the design of 1,2-DHP **2h** as an optimal fluorophore suitable for its potential application as a small-molecule probe in aqueous medium. 1,2-DHP **2h** exhibited six fold enhanced emission intensity than its phosphorylated analogue **2h'** in long wavelength region ($\lambda_{em} \sim 600$ nm) which makes 1,2-DHP **2h'** meet the requirement as a bioprobe for protein tyrosine phosphatases (Figure 2.1).

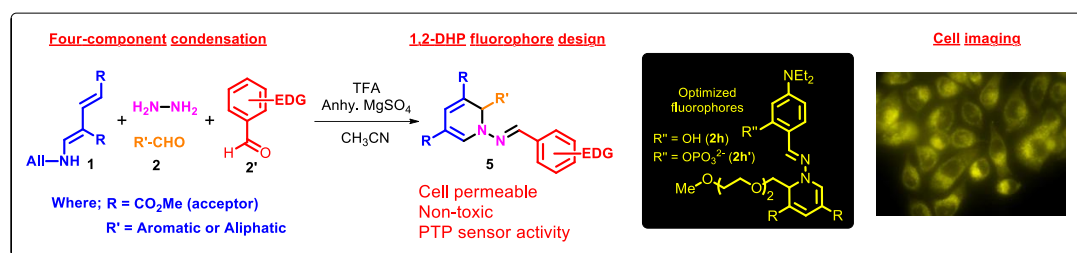


Figure 2.1 Design and synthesis of new 1,2-DHP fluorophores

Chapter 3 focuses on the development of an unprecedented one-pot method for the synthesis of dibenzoxazepines from tertiary amines mediated by HIR. Dibenzoxazepines and dibenzoxazepinones are privileged structural motifs of pharmaceutical relevance. Owing to its wide pharmaceutical significance, many synthetic approaches have been developed for the preparation of dibenzoxazepine skeleton. Base-promoted nucleophilic aromatic substitution (S_NAr) is a classic method to construct the seven-membered ring of dibenzoxazepines via Smiles rearrangement. Apart from this, several metal catalyzed and metal-free reaction methodologies were also reported. Dibenzoxazepines have also been used as valuable synthetic intermediates in development of more complex heterocyclic structures. Hypervalent iodine reagents (HIR) have been considered as a mild alternative to toxic metal oxidants for the construction of several C–C and C–heteroatom bonds. In this chapter, a phenyliodine(III) diacetate mediated umpolung reactivity of the tertiary amines with suitably substituted *ortho*-hydroxybenzyl and phenyl groups is exploited to facilitate *ortho*-C(sp²)-H functionalization to afford diaryl ethers. The presence of an *ortho*-CHO and secondary amine functionalities in the resulting diaryl ether, generated *in situ*, were utilized for synthesis of dibenzoxazepines and dibenzoxazepinones (Figure 3.1). Mild conditions and relative broad substrate scope, and potential for further diversification of the diaryl ethers are highlights of this methodology.

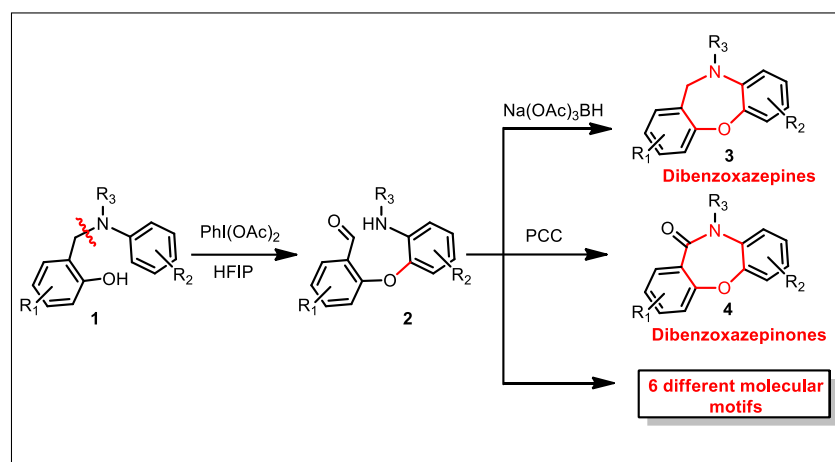


Figure 3.1 One-pot synthesis of dibenzoxazepine and dibenzoxazepinone.

Chapter 4 deals with structure activity relationship study of diindolylmethane derivatives. The design and synthesis of three libraries of DIM was based on the conjugation of DIM with biaryl and diaryl ethers. (Figure 4.1) The synthesized compounds were explored for their preliminary anticancer (HeLa, MDA MB 231) and antimicrobial properties. Our interest was mainly focused on the identification of the effect of substituents both on the indole moiety and biaryl, and the DIM conjugates (biaryl or diaryl ether), which would support biological activity and whose substructure optimization would efficiently produce molecules with better activity. The incorporation of biaryl or diaryl ether, a known pharmacophore, in a single molecule enhanced the biological activity of the DIM. The compound with primary amine in its structure DIM **3aa** showed a better cytotoxicity when compared to simple DIM.

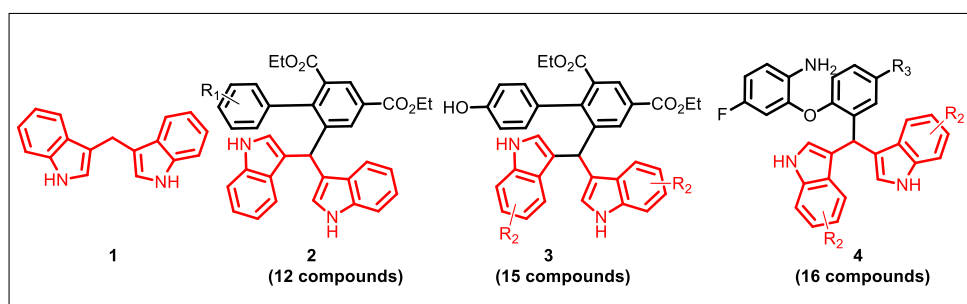


Figure 4.1 Library of DIM derivatives

List of publications

1. Cytotoxicity studies of semi-synthetic derivatives of the side chain derived from the aqueous extract of leaves of 'suicide tree' *Cerbera odollam* — *Nat. Prod. Res.* **2014**, 28, 1507-1512.
Jaggiah N. Gorantla, **Jamsheena Vellekkatt**, Lekshmi R. Nath, Ruby John Anto, Ravi S. Lankalapalli*
2. A metal-free one-pot cascade synthesis of highly functionalized biaryl-2-carbaldehydes — *Org. Biomol. Chem.* **2014**, 12, 8588-8592.
Chandrasekhar Challa, **Jamsheena Vellekkatt**, Jaice Ravindran, Ravi S. Lankalapalli*
3. Anticancer activity of synthetic bis(indolyl)methane-ortho-biaryls against human cervical cancer (HeLa) cells. *Chem. Biol. Interact.* **2016**, 247, 11-21.
Vellekkatt Jamsheena, Ganesan Shilpa, Jayaram Saranya, Nissy Ann Harry, Ravi S. Lankalapalli,* Sulochana Priya*
4. Anti-microbial activity of chrysomycin A produced by *Streptomyces* sp. against *Mycobacterium tuberculosis*. *RSC Advances* **2017**, 7, 36335-36339. Balaji Muralikrishnan, Vipin Mohan Dan, Vinodh J S, **Vellekkatt Jamsheena**, Ranjit Ramachandran, Sabu Thomas, Syed G Dastegar, K Santhosh Kumar, Ravi S. Lankalapalli, Ramakrishnan Ajay Kumar*
5. Metal-free diaryl etherification of tertiary amines by ortho-C(sp²)-H functionalization for synthesis of dibenzoxazepines and -ones. *Org. Lett.* **2017**, 19, 6614-6617.
Vellekkatt Jamsheena, Chikkagundagal K. Mahesha, M. Nibin Joy, Ravi S. Lankalapalli*
6. New 1,2-dihydropyridine based fluorophores and their applications as fluorescent probes. *ACS Omega* **2018**, 3, 856–862.
Vellekkatt Jamsheena, Rakesh K. Mishra, Kollery S. Veena, Suresh Sini, Purushothaman Jayamurthy* and Ravi S. Lankalapalli*

Contributions to academic conferences

1. New 1,2-Dihydropyridine Based Fluorophores for Bio-imaging Application.
Poster Presentation at 8th East Asia Symposium on Functional Dyes and

Advanced Materials, organized by CSIR-NIIST, Trivandrum, Kerala, September 20-22, 2017.

Vellekkatt Jamsheena, Rakesh K. Mishra, C. K. Mahesha, Ravi Shankar Lankalapalli and Ayyappanpillai Ajayaghosh.

2. A Metal-Free Method for One-Pot Synthesis of Dibenz[*b,f*][1,4]oxazepines and oxazepinones. **Oral presentation at XIII J-NOST Conference for Research Scholars, BHU Varanasi, November 9-12, 2017.**

3. Metal-free diaryl etherification of tertiary amines by *ortho*-C(sp²)-H functionalization for synthesis of dibenzoxazepines and dibenzoxazepinones. **Poster Presentation at 30th Kerala Science Congress at Govt. Brennen College, Thalassery, Kerala, January 28-30, 2018.**

Vellekkatt Jamsheena and Ravi S. Lankalapalli.

4. Attended **National Workshop** on ‘Applications of High-field NMR spectrometers in Drug Discovery’, *organized by CSIR-Central Drug Research Institute, Lucknow, August 24-26, 2016.*